



GRAY INSTITUTE FOR
RADIATION ONCOLOGY
& BIOLOGY

Gray Institute for Radiation Oncology and Biology, Department of Oncology, University of Oxford

Identification and Characterisation of Determinants of Genome Stability in Response to a Double-Strand Break

Hilary Term 2013

A thesis presented for the degree of Doctor of Philosophy

By Torben Kasparek

Supervisor: Dr. Timothy Humphrey





Acknowledgements

First of all, I would like to thank Cancer Research UK and the Medical Research Council for supporting my work. I would also like to thank past and present members of the Humphrey group, and Tim for his patience, support and guidance.

Outside of science I would like to thank my family, especially my parents for boosting my morale with their constant support and encouragement, even when times were rough.

Special shout-out to all my friends I have made during my time in Oxford (you know who you are). You guys made all the difference during this roller coaster ride of the last 4 years. I am leaving this place very grateful having met you and with a lifetime of stories to tell (which would certainly make for a funnier read than this thesis).

Identification and Characterisation of Determinants of Genome Stability in Response to a Double-Strand Break

Torben Kasparek
Christ Church
Medical Science Division

Doctor of Philosophy
University of Oxford
Hilary 2013

Chromosomal rearrangements can lead to loss of heterozygosity (LOH) and oncogene activation, both of which represent possible causative events in cancer development. Such outcomes can result from the misrepair of DNA damage arising from a variety of events including DNA double-strand breaks (DSBs), collapsed replication forks, and dysfunctional telomeres. In response to a DSB, chromosomal stability is principally maintained through the two major DNA repair pathways; non- homologous DNA end-joining (NHEJ) and homologous recombination (HR).

The objective of this thesis was to identify novel factors functioning in prevention of chromosomal instability in response to a DSB in *Schizosaccharomyces pombe*. To achieve this, a central aim was to identify the genes mutated in a number of radiation-sensitive mutants in fission yeast, previously isolated by the laboratory. These include the '*loh*' mutants *loh-2, loh-5, loh-6* and *loh-7*, which were found to harbour mutations in known DNA repair genes *rad3*, *rad17*, and *rad57*.

Further, a pan-genomic screen for novel HR repair factors was carried out. The Bioneer Version 2 deletion-library, consisting of 3308 haploid deletion strains, was screened for strains displaying hypersensitivity to the DNA damaging agents MMS, bleomycin and camptothecin. This screen yielded 209 hits which were further characterised, utilising a set of non-essential Ch^{16} minichromosomes . The minichromosome Ch^{16}-*LMYAU* harbours an HO endonuclease recognition sequence and a centromere-distal *ade6*-M216 heteroallele. Following break-induction, failed repair of the DSB leads to loss of the *ade6* allele, indicated by pink sectoring on low adenine plates. 39 sectoring hits were identified and further characterised to quantify levels of gene conversion via HR in response to a DSB, utilising Ch^{16}-*RMYAH*. As a result of this study, a group of novel genes functioning in HR repair were identified.

Finally, one of these hits, putative RNA metabolism protein Nrl1, was subjected to further characterisation, associating this protein with DNA damage repair for the first time.

The work presented here, documents the approaches taken to successfully identify novel DNA repair factors in fission yeast.

Declaration

I declare:

The work presented in this thesis is my own, with the exception of initial Ch^{16}-*RMGAH* DSB assays of *loh-2*, *loh-5*, *loh-6*, and *loh-7*, which have been carried out by Dr. Helen Tinline-Purvis. Pin-plating to screen for sensitive deletion strains in the Bioneer deletion library V2 plates 1-17 (out of 54) was carried out by Carol Walker.

No portion of this work has been previously submitted for another qualification at this, or any other university.

Signed ……..……

Torben Kasparek

List of Tables

Table 1.1	List of DSB repair genes associated with human genetic disease and tumour suppressors	3
Table 1.2	HR factors in *S.pombe*, *S.cerevisiae*, and humans	20
Table 1.3	Conserved checkpoint proteins in *S.pombe*, *S.cerevisiae*, and humans	30
Table 2.1	Non-minichromosome strains used in this study	47
Table 2.2	Minichromosome strains used in this study	59
Table 2.3	Outcomes of the colony-sectoring assay	70
Table 2.4	Outcomes of DSB assay and the marker loss linked with each event	71
Table 2.5	Antibodies used in the study	75
Table 3.1	Genotype and associated repair events of DSB assay	79
Table 3.2	Summary of identified mutants	97
Table 4.1	Summary of all confirmed sensitive hits	109
Table 5.1	List of all sectoring deletion mutants	129
Table 6.1	Predicted interaction partners of Nrl1 based on *Krogan Lab Interactome Database*	186

List of Figures

Figure 1.1	The DNA damage response	5
Figure 1.2	DNA damaging agents	9
Figure 1.3	End joining in eukaryotic cells	14
Figure 1.4	Homologous recombination repair of a double-strand break	18
Figure 1.5	Misrepair of DSBs	25
Figure 1.6	The S. *pombe* checkpoint response	28
Figure 1.7	DSB repair assay Ch^{16}-*RMYAH*	33
Figure 1.8	The S.pombe siRNA pathway	36
Figure 3.1	The minichromosome Ch^{16}-*RMGAH*	78
Figure 3.2	Schematic of the '*cut*' phenotype assay	80
Figure 3.3	Schematic of the complementation assay	82
Figure 3.4	*loh-2* displays severe DNA damage repair defects	83
Figure 3.5	*loh-5* displays severe DNA damage repair defects	86
Figure 3.6	*loh-7* displays severe DNA damage repair defects	87
Figure 3.7	*loh-6* displays severe DNA damage repair defects	89
Figure 3.8	Proposed model	91
Figure 3.9	The Ch^{16}-*L5-RMGAH* DSB assay	94
Figure 4.1	Outline of the screen	99
Figure 4.2	The Bioneer deletion library	103
Figure 4.3	Confirmation by spot-dilution exemplified with a selection of hits	105
Figure 4.4	Cluster enrichment and distribution of sensitivities	108
Figure 4.5	GO Network of enriched clusters	116

Figure 4.6	Selection of hits identified as part of the genome-wide DNA-damage sensitivity screen	119
Figure 5.1	Schematic of the colony sectoring assay	125
Figure 5.2	Overview of screen and Ch^{16}-*LMYAU* colony sectoring phenotypes	128
Figure 5.3	DSB repair assays of sectoring mutants	133
Figure 5.4	4-set Venn diagram of sectoring cohort of genes	134
Figure 5.5	Linear regression analysis of Ch^{16}-*RMYAH* repair outcomes	136
Figure 5.6	Ago1 is a novel factor in HR	139
Figure 5.7	Arb2 is a novel factor in HR	140
Figure 5.8	Examination of the siRNA pathway	142
Figure 5.9	Fkh2 is conferring resistance to DNA damaging agents and facilitates efficient HR repair	144
Figure 5.10	SPAC664.03 is a novel factor in HR	146
Figure 5.11	Est1 is required for efficient HR	148
Figure 5.12	Fbh1 is a Rad51 disruptase	150
Figure 5.13	Atd1 is a novel factor in HR	152
Figure 6.1	Nrl1 confers resistance to DNA damaging agents and is localised to the nucleus	162
Figure 6.2	Nrl1 is evolutionary highly conserved	164
Figure 6.3	Proposed functions for Nrl1 at the interface of RNAi and DNA damage repair	165
Figure 6.4	Further characterisation of Nrl1 in DNA double-strand break repair	167
Figure 6.5	Nrl1 is not required for cell cycle arrest following replication stress	170
Figure 6.6	Nrl1 is required for efficient unloading of RPA following IR treatment	172
Figure 6.7	Nrl1 displays Rad11-GFP foci 5 h after irradiation	174

Figure 6.8	Defective loading of Rad51 in Nrl1-deficient cells	176
Figure 6.9	Efficient H3K9 methylation in *nrl1*Δ cells	178
Figure 6.10	*nrl1*Δ exhibits silencing defects at centromeric regions	178
Figure 6.11	*nrl1*Δ exhibits silencing defects at subtelomeric regions	179
Figure 6.12	Epistasis analysis of Nrl1 and Rad2	182
Figure 6.13	Epistasis analysis with Ku70 and Rad3	183
Figure 6.14	Epistasis analysis of Nrl1 and Sen1	188
Figure 6.15	Model	194

Nomenclature

S. pombe

Genes are denoted by lower-case letters in italics. Genes in the wild-type locus given the +suffix e.g. *rad51+*, deletion/null mutants are indicated by Δ e.g. *rad51Δ*. A double colon (::) designates an insertion into the genome disrupting the gene in question e.g. *rad51::ura4* signifies the *rad51* gene disrupted by *ura4*. Letters and numbers following the gene name identify mutant alleles e.g. *ade6*-M210. Names of proteins are denoted by non-italics letters with a capitalised first letter e.g. Rad51.

S. cerevisiae

Genes are denoted by capital letters in italics e.g. *RAD51*. Deletion/null mutants are signified by lower-case italics e.g. *mec1* with a suffix designating the allele where necessary e.g. *rad51*-D65N. Names of proteins are denoted by non-italics letters with a capitalised first letter e.g. RAD51.

Mammalian/human

Genes are denoted by capital letters in italics e.g. *RAD51*. Homozygous/heterozygous knockouts are shown as -/- or +/- respectively e.g. *RAD51 -/-* and *RAD51 +/-*. Protein names are denoted by capital letters in non-italics e.g. RAD51. Designated suffixes are used:

Sp = Schizosaccharomyces pombe

Sc = Saccharomyces cerevisiae

Hs = Homo sapiens

e.g. $Rad51^{Sp}$

Abbreviations

Δ	gene deletion
°C	degree Celsius
9-1-1 complex	Rad9-Rad1-Hus1
ATM	Ataxia telangiectasia mutated
ATR	ATM and Rad3-related protein
BER	base excision repair
BIR	break-induced replication
Bp	base pair
BSA	bovine serum albumin
CFP	cyan fluorescent protein
Ch	Chromosome
Ch16	minichromosome 16
DAPI	6'-diamidino-2-phenylindole
DDC	DNA damage checkpoint
DDR	DNA damage response
D-loop	displacement-loop
DMSO	dimethyl sulphoxide
DNA	deoxyribonucleic acid
dNTP	deoxyribonucleotide triphosphate (A,C,G,T)
DSB	double-strand break
dsDNA	double-stranded DNA
E.coli	*Escherichia coli*
EDTA	Ethylenediamine tetra-acetic acid
EMM	Edinburgh minimal medium
EtBr	ethidium bromide
G	relative centrifugal force
G	Gram
G418	Geneticin
GC	gene conversion
GCR	gross chromosomal rearrangement
GFP	green fluorescent protein
HCl	hydrochloric acid
HJ	Holliday junction
HO	Homothallic endonuclease
HR	homologous recombination
HU	Hydroxyurea
Hyg	Hygromycin
IR	ionising radiation
kb	Kilobase
l	Litre
LB	Luria-Bertani medium
LOH	loss of heterozygosity
M	Molar
Mb	Megabase
mg	Milligram
ml	Millilitre
mM	Millimolar
MMS	methylmethane sulphonate
MQ	milli Q water
MRN complex	Mre11/Rad32-Rad50-Nbs1 complex
NaCl	sodium chloride

NaOH	sodium hydroxide
ng	Nanogram
NHEJ	non-homologous end-joining
nm	Nanometer
nmt	no message in thiamine
O/N	Overnight
PBS	phosphate-buffered saline
PCR	polymerase chain reaction
rpm	revolutions per minute
RNase A	ribonuclease A
S. cerevisiae	*Saccharomyces cerevisiae*
S. pombe	*Schizosaccharomyces pombe*
SCC	sister chromatid conversion
SDS	sodium lauryl sulphate
ssDNA	single-stranded DNA
TAE	tris acetate EDTA
TCA	trichloracetic acid
TE	tris EDTA
Tris	N,N,N'N'-tetramethylethylenediamine
UV	Ultraviolet
V	volts/volume
v/v	volume per volume
w/v	weight per volume
wt	wild type
YE6S	yeast extract 6 supplements
µg	Microgram
µl	Microliter
µM	Micromolar

Table of Contents

ACKNOWLEDGEMENTS ..... **I**

ABSTRACT ..... **II**

DECLARATION ..... **III**

LIST OF TABLES ..... **IV**

LIST OF FIGURES ..... **V**

NOMENCLATURE ..... **VIII**

ABBREVIATIONS ..... **IX**

CHAPTER I **1**

INTRODUCTION **1**

1.1 GENOME INSTABILITY AND CANCER 1
1.2 THE DNA DAMAGE RESPONSE (DDR) 4
1.3 DNA DOUBLE-STRAND BREAK (DSB) FORMATION 7
1.3.1 DNA damaging agents *7*
1.3.2 Enzymatically induced DSBs *10*
1.4 MECHANISMS OF DSB REPAIR 10
1.4.1 Canonical Non-homologous end-joining (NHEJ) *10*
1.4.1.1 Disrupting Non-Homologous End-Joining 12
1.4.1.2 Alternative NHEJ pathways 12
1.4.1.3 C-NHEJ vs HR 15
1.4.2 Homologous recombinational repair *15*
1.4.2.1 Chromosomal rearrangements associated with HR repair 21
1.4.2.1.1 Single-strand annealing. 21
1.4.2.1.2 Gene conversion 22
1.4.2.1.3 Crossovers 22
1.4.1.2.4 Break-induced replication 23
1.5 DNA INTEGRITY CHECKPOINTS 26
1.5.1 Sensing the damage *26*
1.5.2 Signal transduction *28*
1.5.3 Arresting the cell cycle *29*
1.5.4 Non-canonical roles of checkpoint proteins *30*
1.6 A SYSTEM FOR ANALYSING DSB REPAIR IN *S. POMBE* 30
1.7 RNA METABOLISM AND GENOME STABILITY 33
1.7.1 The siRNA machinery *33*
1.7.2 A role for non-coding RNAs in DNA repair and genome stability *37*
1.7.3 RNA:DNA hybrids and genome stability *38*
1.8 AIMS OF THIS WORK 39

CHAPTER II **40**

2.1 GENERAL LABORATORY SUPPLIES 40
2.2 BUFFERS AND SOLUTIONS 41
2.3 MEDIA 43

2.3.1 Escherichia coli (E. coli) media ... *43*
2.3.2 Schizosaccharomyces pombe (S. pombe) media ... *43*
2.4 STRAINS ... 45
2.4.1 E. coli ... *45*
2.4.2 S. pombe ... *45*
2.5 PLASMIDS ... 61
2.6 STORAGE AND GROWTH CONDITIONS ... 61
2.6.1 Growth and storage of E. coli strains ... *61*
2.6.2 Growth and storage of S. pombe strains ... *61*
2.6.5 Genetic crosses, tetrad and free spore analysis ... *62*
2.6.6 Analysis of cell growth and viability ... *62*
2.6.6.1 Serial dilution assay ... 62
2.6.7 Losing the minichromsome from S. pombe strains ... *63*
2.7 TRANSFORMATION OF CELLS ... 63
2.7.1 Transformation of E. coli ... *63*
2.7.1.1 Preparation of competent bacteria ... 63
2.7.2 Transformation of S. pombe ... *64*
2.7.2.1 Transformation by electroporation ... 64
2.7.2.2 Transformation by LiAc method ... 64
2.7.2.3 PLATE method ... 65
2.8 DNA ISOLATION ... 65
2.8.1 Isolation of plasmid DNA from E. coli (Miniprep and Maxiprep) ... *65*
2.8.2 Isolation of S. pombe genomic DNA ... *65*
2.8.3 Isolation of DNA from agarose gels ... *65*
2.8.4 PCR purification ... *66*
2.9 MANIPULATION AND ANALYSIS OF DNA ... 66
2.9.1 Restriction digestion and dephosphorylation of DNA ... *66*
2.9.2 DNA ligation ... *66*
2.9.3 Polymerase Chain Reaction (PCR) ... *66*
2.9.4 Quantification of DNA samples ... *68*
2.9.5 DNA sequencing ... *68*
2.9.6 Analysis of DNA by gel electrophoresis ... *68*
2.9.6.1 Agarose gel electrophoresis ... 68
2.10 DNA DSB REPAIR ASSAYS ... 68
2.10.1 The sectoring assay ... *68*
2.10.2 The DSB assay ... *69*
2.11 MICROSCOPY ... 70
2.11.1 Light microscopy ... *70*
2.11.2 Fluorescence microscopy ... *71*
2.12 PROTEIN EXTRACTION, MANIPULATION, AND ANALYSIS ... 71
2.12.1 TCA protein extraction ... *71*
2.12.2 Histone preparation ... *72*
2.12.3 SDS-polyacrylamide gel-electrophoresis (SDS-PAGE) ... *72*

2.12.4 Western blotting *73*

CHAPTER III **75**

3.1 INTRODUCTION 75
3.2 RESULTS 76
3.2.1 Identification of 'loh' mutants *76*
3.2.1.1 Strategy to identify and characterise '*loh*' mutants 76
3.2.1.2 *'loh-2'* harbours missense mutation K106N in *rad57* 83
3.2.1.3 *'loh-5'* and *'loh-7'* carry truncating mutations in *rad3* 87
3.2.1.4 *'loh-6'* harbours a truncating mutation in *rad17* 89
3.2.2 An additional role for checkpoint proteins in resection *91*
3.3 DISCUSSION 94
3.3.1 Rad3, Rad17 and Rad57 are known suppressors of LOH *94*
3.3.2 Summary *96*

CHAPTER IV **97**

4.1 INTRODUCTION 97
4.2 RESULTS 100
4.2.1 The Bioneer Version 2 deletion library *100*
4.2.2 Identification of MMS, bleomycin or camptothecin sensitive mutants *100*
4.2.3 Results Overview *105*
4.2.4 Novel genes in chromatin dynamics *113*
4.2.5 Novel genes in transcription regulation *116*
4.2.6 DNA damage repair and telomere maintenance *116*
4.2.7 DNA damage and ribosomal proteins *119*
4.2.8 DNA damage and the siRNA machinery in fission yeast *119*
4.2.9 Other genes *119*
4.3 DISCUSSION 120
4.3.1 Further analysis *120*
4.3.2 General Discussion *121*
4.3.3 Summary *121*

CHAPTER V **122**

5.1 INTRODUCTION 122
5.2 RESULTS 122
5.2.1 Ch^{16}-LMYAU Sectoring Assay *122*
5.2.2 Sectoring mutants and sensitivities *126*
5.2.3 The Ch^{16}-RMYAH DSB Assay *130*
5.2.4. Global analysis of DSB repair profiles of HR mutants *134*
5.2.5 Novel factors in HR; A selection of hits *136*
5.2.5.1 Ago1, Arb2, and the siRNA machinery 136
5.2.5.1.1 RNAi proteins Ago1 and Arb2 136
5.2.5.1.2 The siRNA machinery and DNA damage repair 142
5.2.5.2 Transcription factor Fkh2 144
5.2.5.3 RNA biogenesis protein SPAC664.03 (Paf1 complex) 146

5.2.5.4 Telomere maintenance protein Est1 148
5.2.5.5 Anti-recombinogenic helicase Fbh1 151
5.2.5.6 Cell metabolism protein Atd1 153
5.3 DISCUSSION 155
5.3.1 Colony sectoring is an intermediate predictor of DSB repair efficiency *155*
5.3.2 DNA damage sensitivities and HR proficiency *156*
5.3.3 HR genes suppress Ch^{16} loss and LOH in response to a DSB *156*
5.3.3 Novel HR factors *157*
5.3.3.1 Ago1 and Arb2 157
5.3.3.2 Fkh2 158
5.3.3.3 SPAC664.03 (Paf1 complex) 159
5.3.3.4 Est1 159
5.3.3.5 Fbh1 160
5.3.3.6 Atd1 161
5.4 SUMMARY 161
CHAPTER VI 162
6.1 INTRODUCTION 162
6.2 RESULTS 163
6.2.1 Phenotypic characterisation of Nrl1 ..... *163*
6.2.1.1 Nrl1 confers resistance to DNA damaging agents and is localised to the nucleus 163
6.2.1.2 Nrl1 harbours evolutionary conserved functional domains 165
6.2.1.3 Proposed functions for Nrl1 in fission yeast 169
6.2.1.4 Nrl1 is required for efficient homologous recombinational repair of DSBs 170
6.2.1.5 Nrl1 is dispensable for checkpoint arrest following replication stress 173
6.2.1.6 Nrl1 displays defects in RPA unloading following IR 175
6.2.1.7 Nrl1 is required for efficient Rad51 loading following IR 178
6.2.1.8 *nrl1*Δ displays mild silencing defects 180
6.2.2 Genetic characterisation of Nrl1 ..... *183*
6.2.2.1 *nrl1*Δ is not synthetically lethal with *rad2*Δ 183
6.2.2.2 *nrl1*Δ is synthetically sick with Ku70 and Rad3 deletions when challenged with DNA damaging agents
6.2.2.3 Nrl1 interacts negatively with Sen1 189
6.3 DISCUSSION 193
6.3.1 Nrl1 is a novel determinant of genome stability *193*
6.3.2 Nrl1 physically interacts with splicing factors and is required for splicing of Swi5 and RPA *195*
6.3.3 RNA-DNA hybrids *196*
6.3.4 Predicted model *197*
6.4 SUMMARY 200
CHAPTER VII 201
7.1 A ROLE FOR RAD17 IN RESECTION 201
7.2 GENOME-WIDE SENSITIVITY SCREENS IN *S. POMBE* 202
7.3 RNA METABOLISM AND DNA DAMAGE REPAIR 204
REFERENCES 206
APPENDIX I: PLASMIDS USED IN THIS STUDY 230

APPENDIX II OLIGONUCLEOTIDE PRIMERS USED IN THIS STUDY 233
APPENDIX III: GENETIC DETERMINANTS OF SITE-SPECIFIC DSB-INDUCED MARKER LOSS 234
APPENDIX IV: CONFIRMATION OF DELETION LIBRARY MUTANT IDENTITIES 236
APPENDIX V: NRL1 EPISTASIS ANALYSIS 237
APPENDIX VI: LIST OF PUBLICATIONS 238

CHAPTER I

Introduction

1.1 Genome Instability and Cancer

Chromosomal rearrangements are a hallmark of cancer cells, which can lead to oncogene activation and tumour suppressor loss, both of which represent possible causative events in tumour development. Such outcomes can result from both the repair and misrepair of DNA ends which arise from a variety of events including DNA double-strand breaks (DSBs), collapsed replication forks, and dysfunctional telomeres. DSBs are considered the most toxic DNA lesion and can, if misrepaired, lead to loss of heterozygosity (LOH) of tumour suppressor genes, thus resulting in tumorigenesis.

The DNA of every cell in the human body is exposed to damaging agents on a daily basis, leading to DSBs, single-strand breaks (SSBs), DNA adducts and inter-strand cross linking; all being potential causes for tumorigenesis (Pfeiffer et al. 2000; Shrivastav et al. 2008). The insults are different in nature and consist of both endogenous and exogenous agents. Examples for endogenous factors are reactive oxygen species (ROS) being produced during metabolic processes, replication fork stalling, topoisomerase failures, and RAG/AID recombination during immunoglobulin gene (Ig) diversification (Pfeiffer et al. 2000; Mahowald et al. 2008; Shrivastav et al. 2008). External agents include ionising radiation (IR), UV and various chemical carcinogens internalised through food or air (Friedberg et al. 2006). DSBs represent the most detrimental class of DNA lesions with even one unrepaired DSB being enough to kill the harbouring cell (Rich et al. 2000). It is

therefore of vital importance for the cell to possess adequate repair mechanisms to deal with such damage.

In response to DSBs, genome stability is maintained principally through the two highly conserved major DNA repair pathways, non-homologous DNA end-joining (NHEJ) and homologous recombination (HR) (Heyer et al. 2010; Lieber 2010). Misregulation or failure to repair by these major pathways is known to result in increased levels of cell death or in chromosomal rearrangements and mutations, potentially leading to loss of heterozygosity (LOH) and subsequently to cancer. Genes involved in these pathways are potential tumour-suppressor genes, and a number of HR genes are implicated in human genetic diseases (Heyer et al. 2010; Kasparek and Humphrey 2011) (**Table 1.1**).

Loss of heterozygosity (LOH) refers to the functional loss of one allele of a gene in which the other allele is already inactivated (Knudson 1971). Studies from the Humphrey lab and those of others support a model in which extensive end-processing associated with failed homologous recombination can lead to a range of chromosomal rearrangements and/or chromosome loss (Tinline-Purvis et al. 2009; Kasparek and Humphrey 2011). A variety of mechanisms, such as translocations, deletions, *de-novo* telomere addition, break-induced replication, isochromosome formation and gene conversion (GC) can lead to extensive LOH in response to a break, depending on which stage of the pathway is affected (Jasin 2000).

The fission yeast *Schizosaccharomyces pombe* (*S. pombe*) shares many genetic and biochemical features with higher eukaryotic cells. Since *S. pombe* (*Sp*) can be rapidly grown and manipulated with a range of genetic, molecular and biochemical techniques, it is particularly useful in investigating evolutionary highly conserved cellular processes such as DNA damage response and cell cycle control.

Table 1.1

Gene	Inheritance	Chromosome location	Disease association	Cancer predisposition
Ku70	AR	22q11-13		T-cell lymphomas
Ku80	AR	2q35		Pro-B cell lymphomas
Artemis	AR	10p	Severe combined immunodeficiency	EBV-associated lymphomas
DNA ligase IV	AR	13q22-24	Ligase IV (LIG4) syndrome	Lymphoid malignancies
Cernunnos (XLF)	AR	2q35	Severe combined immunodeficiency	
BRCA1	AD	17q21	Hereditary breast cancer	Breast and ovarian cancer
BRCA2 (FANCD1)	AD (AR)	13q12.3	Hereditary breast cancer (Fanconi anaemia)	Breast and ovarian cancer
Mre11	AR	11q21	Ataxia telangiectasia-like disorder	
Rad50	AR	5q31		Slightly elevated breast cancer risk
Nbs1	AR	8q21	Nijmegen breakage syndrome	Haematologic malignancies
ATM	AR	11q22.3	Ataxia telangiectasia	Haematologic malignancies
ATR	AR	3q22-24	Seckel syndrome	
FANCD2	AR	3p25.3	Fanconi anaemia	Acute myeloid leukaemia, squamous cell carcinoma
BLM	AR	15q26.1	Bloom's syndrome	Broad spectrum (leukaemia, lymphoma, carcinoma)
PALB2 (FANCN)	AR	16p12	Fanconi anaemia	Breast and ovarian cancer
BRIP1 (BACH1/FANCJ)	AR	17q22	Fanconi anaemia	Breast cancer
CHEK2	AR	22q12.1	Li–Fraumeni syndrome 2	Breast cancer, sarcomas, brain tumours
WRN	AR	8p12-11.2	Werner's syndrome	Sarcomas
RAD51C	AR	17q25.1	Hereditary breast cancer (Fanconi anaemia)	Breast and ovarian cancer
RAD51D	AR	17q12	Hereditary ovarian cancer	Ovarian cancer

Table 1.1 List of DSB repair genes associated with human genetic disease and tumour suppressors. AD=autosomal dominant; AR=autosomal recessive (Kasparek and Humphrey 2011).

1.2 The DNA damage response (DDR)

In response to threats to DNA integrity, cells have evolved a complex network of pathways to detect DNA lesions, signal their presence, and promote repair (Rouse and Jackson 2002; Harrison and Haber 2006; Harper and Elledge 2007). All the mechanisms mobilised in response to DNA damage are collectively termed "DNA damage response" (DDR) (Ljungman 2010). A multitude of distinct, yet collectively operating pathways fall under the umbrella term DDR, such as cell cycle arrest, transcription, DNA repair, apoptosis, autophagy, replication, RNA metabolism, and chromatin remodelling (**Figure 1.1**) (Jackson and Bartek 2009). The wide spectrum of different DNA lesions necessitate numerous, largely distinct repair pathways within the cell, each one dealing with a specific type of lesion (Christmann et al. 2003; Ciccia and Elledge 2010). However, the initiation of the signal cascade, coordinating a plethora of cellular responses (Matsuoka et al. 2007), is mainly orchestrated by two major phosphatidylinositol 3-kinase-like kinases (PI3KK): $Tel1^{Sp}/ATM^{Hs}$, and $Rad3^{Sp}/ATR^{Hs}$ (Lee and Paull 2004; Lavin 2007). In addition, there is accumulating evidence that the DDR is also targeted by a number of DNA and RNA viruses (Lilley et al. 2007; Chaurushiya and Weitzman 2009) and is closely linked to polyomavirus infections (Jiang et al. 2012).

The significance of the DDR in human disease is emphasised by the wide range of human malignancies that can emerge when any part of the highly coordinated response is disrupted (Jackson and Bartek 2009). Finally, the high evolutionary conservation of the DDR from yeast to humans further illustrates the vital importance of the DDR in regard to genome stability and cell survival.

Figure 1.1

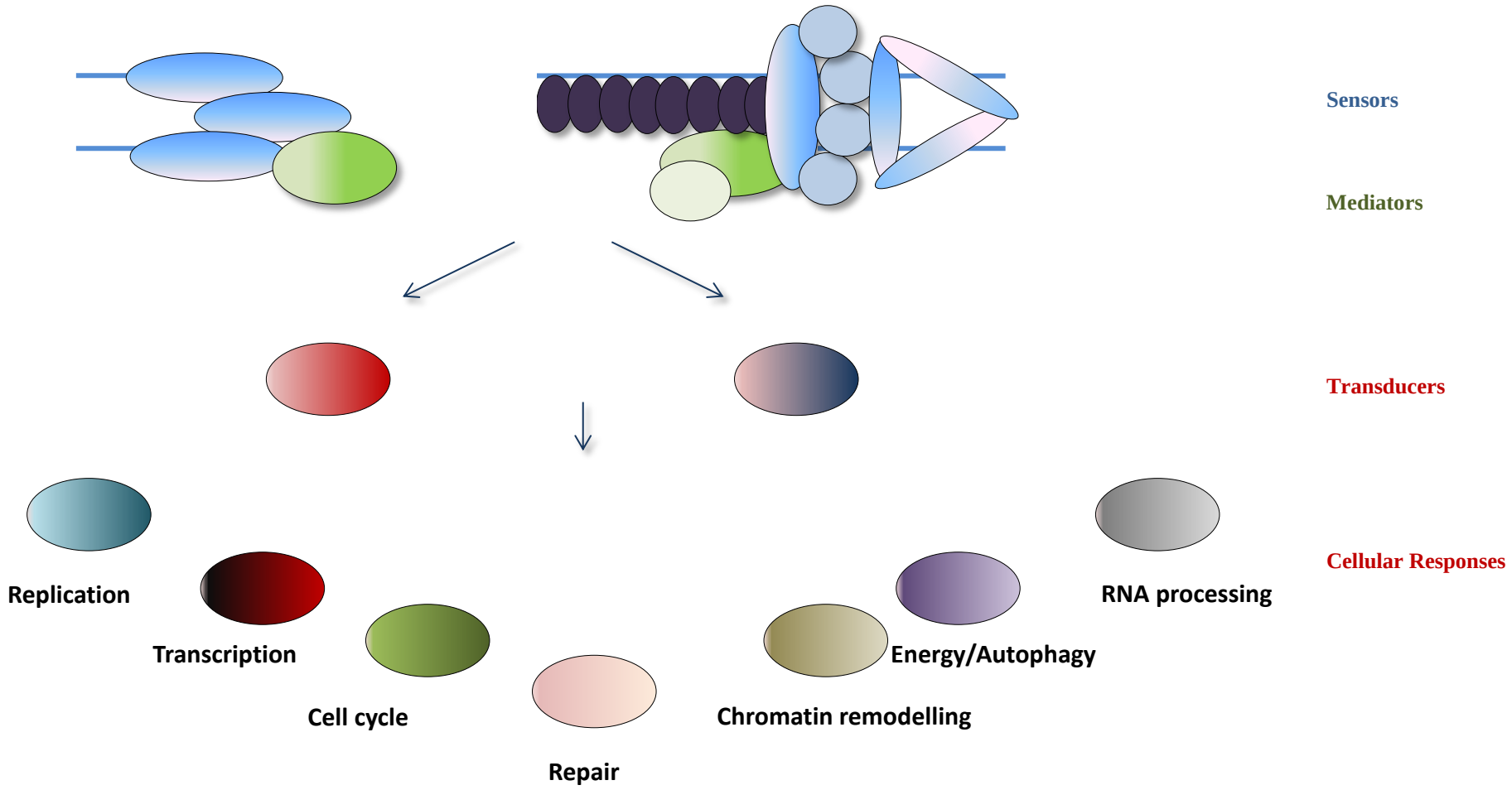

Sensors
Mediators
Transducers
Cellular Responses
Replication
Transcription
Cell cycle
Repair
Chromatin remodelling
Energy/Autophagy
RNA processing

Figure 1.1: The DNA damage response.
Following detection of DNA lesions, a variety of cellular responses is activated to deal with the genotoxic threat; involved modulated pathways include: replication, transcription, cell cycle, repair, chromatin remodelling, energy/autophagy, and RNA processing. (Adapted from Jackson and Bartek 2009)

1.3 DNA double-strand break (DSB) formation

1.3.1 DNA damaging agents

In this study, a variety of DNA damaging agents were used. Methyl methanesulfonate (MMS) is an alkylating agent inducing DNA damage and mutagenesis (**Figure 1.2**). MMS causes base damage, single-strand breaks, and replication fork stalling by methylation of N7-deoxyguanine, and N3-deoxyadenine (Lee et al. 1989). Genes typically conferring resistance to MMS function in base excision repair (BER) (Peterson and Cote 2004), but also mutations of genes of the *RAD52* epistasis group were found to be sensitive to MMS (Krogh and Symington 2004); this might be due to the formation of replication-associated DSBs (Sobol et al. 2003).

Ionising radiation (IR) inflicts different types of DNA damage such as DSBs, SSBs, and interstrand crosslinks (Jeggo and Lobrich 2006). The damage is caused either directly, leading to ionisation and breakage of the DNA by energy deposition, or indirectly, via emerging hydroxyl radicals. In case of two opposing SSBs in proximity, DSBs with overhangs are known to form (Mahaney et al. 2009). Bleomycin and bleocin function as radiomimetic drugs, whose action introduces DSBs and SSBs at random locations as a result of free radicals attacking the DNA (Povirk 1996). Genes conferring resistance to bleomycin treatment typically act in DSBR and DDR.

Camptothecin is a poison of the enzyme topoisomerase I (TopoI) (Hsiang and Liu 1988). TopoI catalyses the removal of DNA supercoils, that can emerge during transcription, replication or recombination by introducing a nick into the sugar-phosphate backbone, allowing rotation and release of the torsional strand. Camptothecin specifically interferes with the DNA re-ligation step of the nicked strand, blocking the release of the enzyme, ultimately leading to an S-phase dependent DSB once the replication fork collides with the

complex (Svejstrup et al. 1991). Genes involved in replication, DSBR and DDC function to suppress CPT-induced DNA damage. Hydroxyurea (HU) is a metal-binding hydroxamic acid, used to deplete deoxyribonucleotide triphosphate (dNTP) pools (Moore and Hurlbert 1985). By its mechanism of action, it can quench the tyrosil free radical the active site of the M2 protein subunit of ribonucleotide reductase (RNR), inactivating the enzyme and attenuating DNA synthesis (Yarbro 1992). Administration of HU gives rise to stalled and collapsed replication forks within the cell, thus triggering DSB formation at or near replication sites (Petermann et al. 2010).

Figure 1.2

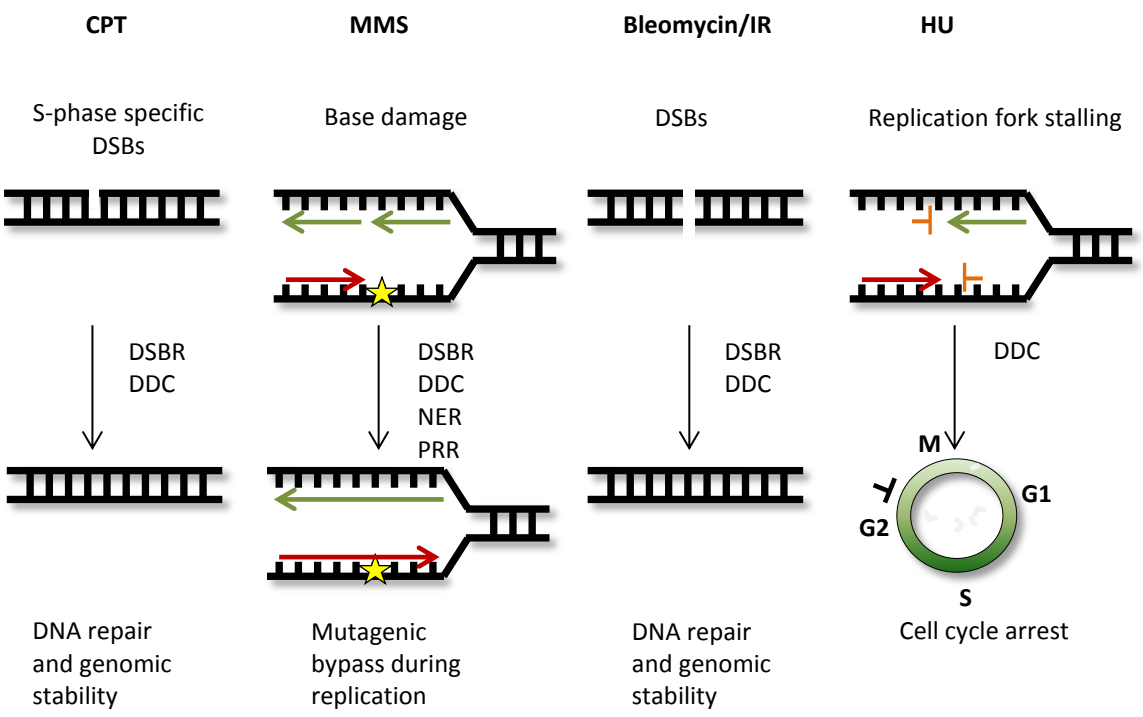


Figure 1.2: DNA damaging agents. Depiction of inflicted damage and resistance-conferring pathways for a variety of DNA damage inducing agents used in this study. DSBR (Double-strand break repair), DDC (DNA damage checkpoint), NER (Nucleotide excision repair), PRR (Post transcriptional repair).

1.3.2 Enzymatically induced DSBs

While treatment with DNA damaging agents lead to DNA lesions at random locations across the whole genome, site-specific restriction enzymes can be utilised to induce DSBs at specific loci, in a time-controlled manner. In this study, the *S. cerevisiae* homothallic (HO) endonuclease was used to introduce a single DSB into the non-essential minichromosome Ch^{16}. Expression of either an exogenous (*pREP81X*), or endogenous (Ch^{16}) copy of the HO endonuclease was controlled with a 'no-message in thiamine' (*nmt*) promoter (Prudden et al. 2003; Cullen et al. 2007; Tinline-Purvis et al. 2009; Moss et al. 2010.). The 22 bp target site (*MAT* locus; (Nickoloff et al. 1990)) is cleaved by the HO endonuclease to give rise to a 4 bp staggered cut with 3'-OH overhangs (Paques and Haber 1999). A single DSB can be induced at this location 20-24 hours following removal of thiamine from the media (Prudden et al. 2003).

1.4 Mechanisms of DSB repair

1.4.1 Canonical Non-homologous end-joining (NHEJ)

In mammalian cells, NHEJ is the predominant DSB repair mechanism and is active throughout the cell cycle, while NHEJ in yeast appears to be restricted to the G1 phase (Moore and Haber 1996; Guirouilh-Barbat et al. 2004). In vertebrates, the 'classical' NHEJ pathway (C-NHEJ) requires several core factors, DNA-PK, Ku70-80, Artemis, Lig4, XRCC4, XLF, and Pol μ to repair a DSB (Lieber 2010) (**Figure 1.3**). During NHEJ, DNA ends are bound by the highly abundant end-protecting Ku protein, which functions as a 'docking station' for loading of the other NHEJ components. While NHEJ repair of perfectly compatible overhangs is generally considered error-free, repair of IR-induced lesions is error-prone (Boulton and Jackson 1996; Moore and Haber 1996; Budman and

Chu 2005). In addition to repair of pathological breaks, C-NHEJ is essential for the rejoining of physiological breaks during V(D)J recombination and class switch recombination (CSR) mediated by the RAG complex (RAG1 and -2) and activation-induced deaminase (AID) (Soulas-Sprauel et al. 2007).

The oncogenic capacity of C-NHEJ lies in its ability to inappropriately join non-contiguous sequences if there is more than one DSB, resulting in deletions, insertions or translocations. A classic example of this is the generation of dicentric chromosomes by telomeric fusions leading to chromosomal rearrangements through the breakage-fusion-bridge (BFB) cycle (McClintock 1941). Furthermore, translocations can generate novel gene fusions with potential to initiate neoplastic cell growth. More than 358 known gene fusions, involving 337 different genes that have been found across all the main subtypes of human neoplasia and account for ~20% of human cancer morbidity, have been documented (Mitelman et al. 2007). Prominent examples of oncogenic gene fusions in humans include BCR-ABL, arising from a fusion of chromosome 9 and 22 into the Philadelphia chromosome (Nowell and Hungerford 1960) and c-myc–Igh translocations, associated with B-cell malignancies, such as Burkitt's lymphoma (Taub et al. 1982). In addition to such "driver mutations" promoting cancer progression, recent evidence has emerged in which a single catastrophic event, termed "chromothripsis" induces multiple breaks that are randomly joined by NHEJ and microhomology-mediated end joining (MMEJ), thus resulting in a chaotic genomic structure (Stephens et al. 2011). However, such events may also result from replication mechanisms (Liu et al. 2011).

NHEJ-mediated translocations and telomere fusions are influenced by spatial considerations. Ku70 is required to positionally stabilise DSB ends, which can undergo illegitimate joining with chromosomes in their spatial proximity (Soutoglou et al. 2007). However, 53BP1 promotes end-joining of DSBs in a distance-dependent manner, and

supports end-joining of dysfunctional telomeres by facilitating chromatin mobility (Dimitrova et al. 2008; Bothmer et al. 2010). Multiple pathways also function to suppress NHEJ leading to translocations and telomere fusions, indicating that such events are highly regulated (Lee et al. 2008).

While C-NHEJ has the capacity to induce chromosomal rearrangements, the consequences of disrupting this pathway on genome stability will be considered now.

1.4.1.1 Disrupting Non-Homologous End-Joining

Disruption of C-NHEJ not only results in loss of V(D)J and class switch recombination (CSR) in lymphoid cells, therefore causing severe immunodeficiencies in humans, but also in acute sensitivity to DNA damaging agents including ionising radiation (Lieber 2010). Additionally, disrupting C-NHEJ increases levels of abnormal joining and translocations mediated by 'alternative' NHEJ (A-NHEJ) pathways, and also increases HR repair (Kass and Jasin 2010; Nussenzweig and Nussenzweig 2010).

1.4.1.2 Alternative NHEJ pathways

Alternative NHEJ pathways (A-NHEJ) were first discovered in mammalian cells (Kabotyanski et al. 1998) and are conserved in yeast (McVey and Lee 2008). The A-NHEJ pathways display a bias towards microhomology-mediated joins (Haber et al., 2008) and follow slower kinetics than classical NHEJ (Han et al., 2008). Although the specific mechanisms of alternative end-joining and their regulation with regard to C-NHEJ are currently unclear, several factors including the MRN complex (MRE11, RAD50, NBS1), CtIP, XRCC1, PARP, Lig1 and Lig3 have been proposed to participate (**Figure 1.3**) (Lieber 2010). A-NHEJ is implicated in many human hematologic and mesenchymal malignancies, harbouring reciprocal translocations (Kuppers and Dalla-Favera 2001) as

well as stimulating breakage-fusion-bridge induced translocations in B cell lymphomas in mice with a C-NHEJ/p53 double deficiency background (Difilippantonio et al. 2002). In accordance with a role for C-NHEJ suppressing A-NHEJ, it has been shown that 'NHEJ-derived' chromosomal translocations do not require Ku70 (Weinstock et al. 2007) and fibroblasts deficient in Ku80 and Lig4 even display highly elevated frequencies of spontaneous DSBs and translocations (Difilippantonio et al. 2000; Ferguson et al. 2000); thus components of the classical NHEJ pathway have an additional important role as tumour suppressors (**Table 1.1**) (Hartlerode and Scully 2009).

Two studies examining the genesis of translocations in B lymphocytes, utilising novel sequencing techniques, revealed transcriptional activity and physical proximity of DSBs as major determinants of the nature of chromosomal translocations. Additionally, the majority of translocational junctions were fused via end-joining mechanisms exploiting short microhomologies, consistent with misrepair by translocation-prone A-NHEJ pathways (Chiarle et al. 2011; Klein et al. 2011).

Figure 1.3

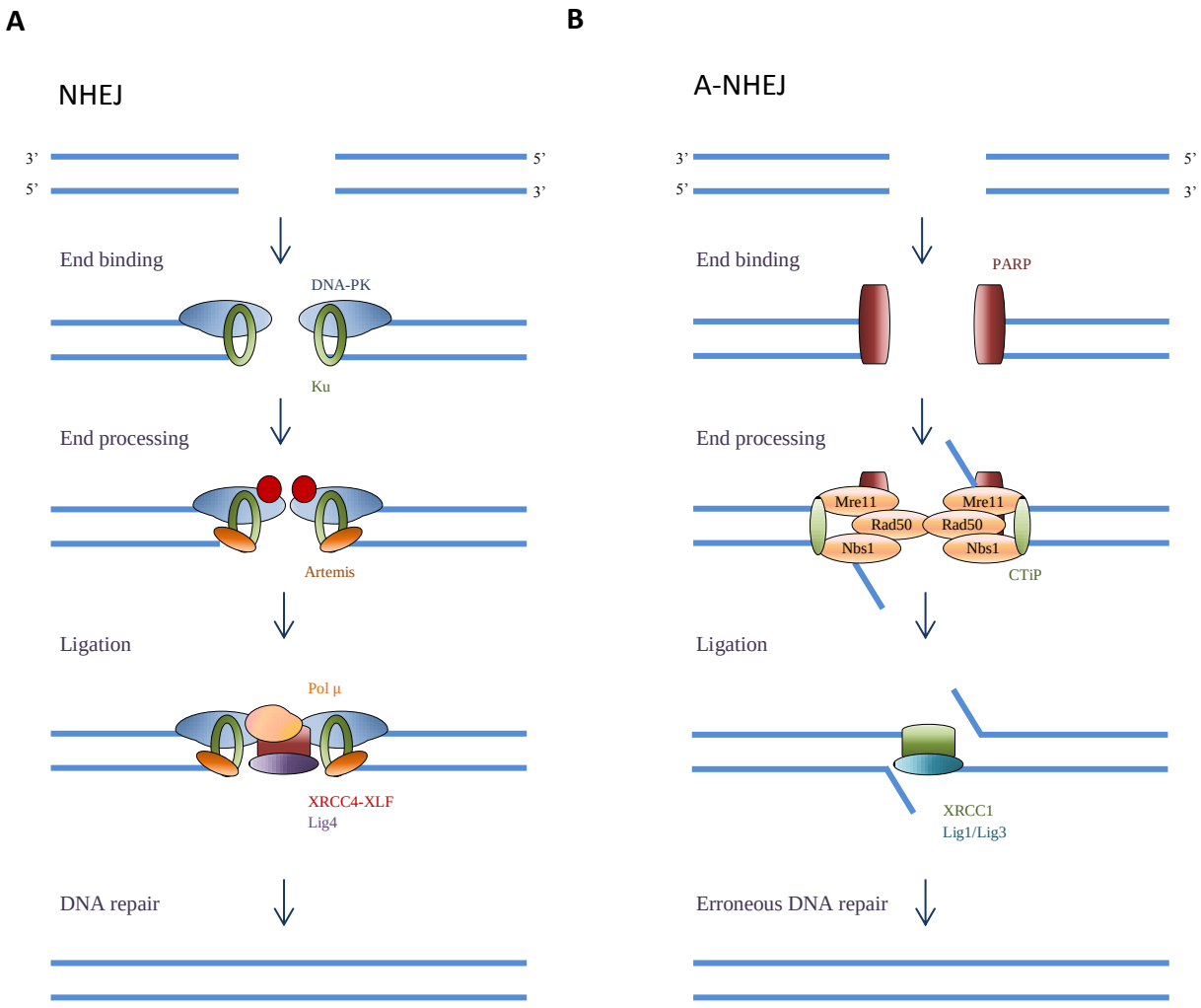


Figure 1.3: End joining in eukaryotic cells. (A) Classical non-homologous end joining (C-NHEJ). DNA ends are bound by the highly abundant end-protecting Ku protein and DNA-PK. More repair factors like Artemis, Pol μ, XRCC4-XLF, and Lig4 are recruited to the break-site, and repair the DSB by re-joining of the DNA ends. (B) Alternative non-homologous end joining (A-NHEJ). Ends are bound by PARP and MRN-CtIP dependent short-range resection occurs. Ligation of micro-homologous complementary DNA strands is mediated by XRCC1, and Lig1/Lig3. See text for further details.

1.4.1.3 C-NHEJ vs HR

C-NHEJ also exhibits a competitive relationship with HR such that disrupting C-NHEJ can also lead to increased HR repair (Paques and Haber 1999). While utilising HR may result in error free repair, utilising HR during G1 promotes use of a homologous chromosome as a template, resulting in localised loss of heterozygosity (LOH) and potentially reciprocal translocations if associated with crossovers. Such competition between NHEJ and HR can be exploited as disrupting NHEJ can lead to enhanced gene targeting through reduced random integration and possibly increased target integration by homologous recombination (Iiizumi et al. 2008).

1.4.2 Homologous recombinational repair

Homologous recombination not only promotes genetic recombination during meiosis, an important step to drive evolution (Holliday 2007), HR has also emerged as a key pathway in DNA repair during the last decades. Many of the known HR genes were originally identified in *S. cerevisiae* (*Sc*) as radiation-sensitive mutants ("rad" mutants) and constitute the core HR machinery in eukaryotes. This set of genes, termed the *RAD52* epistasis group, includes $RAD51^{Sc}/rad51^{Sp}$, $RAD52^{Sc}/rad22^{Sp}$, $RAD54^{Sc}/rad54^{Sp}$, $RAD55^{Sc}/rad55^{Sp}$, $RAD57^{Sc}/rad57^{Sp}$, $MRE11^{Sc}/rad32^{Sp}$, $RAD50^{Sc}/rad50^{Sp}$, and $XRS2^{Sc}/nbs1^{Sp}$ (Krogh and Symington 2004), and is evolutionary highly conserved (**Table 1.2**)

Substrates include not only DSBs and stalled replication forks (Aguilera and Gomez-Gonzalez 2008), but also DNA interstrand crosslinks (ICLs) (Long et al. 2011), and DSBs within heterochromatin (Goodarzi et al. 2010); in addition HR plays a role in telomere maintenance (Verdun and Karlseder 2006), and centrosome stabilisation (Cappelli et al. 2011). It functions during late S phase to G2 phase of the cell cycle, since it requires a DNA template for precise repair, *i.e.* a sister chromatid or homologous chromosome.

The first step of HR repair involves sensing of the break by the Mre11-Rad50-Nbs1 (MRN)-complex, followed by initial 5'-3' resection with $Ctp1^{Sp}$/$CtIP^{Hs}$, and subsequent extensive resection either by exodeoxyribonuclease 1 (Exo1), or unwinding of the DNA duplex by helicase $Rqh1^{Sp}$/BLM^{Hs} together with a nuclease like Dna2 to digest the 5' strand. In yeast, resection is tightly controlled by cell cycle proteins such as Cdc28/Cdk1 (Aylon et al. 2004; Ira et al. 2004). It has been demonstrated that Cdk1 phosphorylates Dna2, thus controlling DNA double-strand break end resection and repair pathway choice (Chen et al. 2011).

Additionally, MRN recruits replication protein A (RPA) to bind the uncovered stretches of single-stranded DNA (ssDNA), to prevent formation of secondary structures, detrimental for the establishment of Rad51 filaments (Wold 1997; Iftode et al. 1999). Rad51 is the eukaryotic homolog of *E. coli* RecA and the central recombinase of the HR pathway, and thus essential for genome stability (Shinohara et al. 1992). Rad51 catalyses strand exchange, during which Rad51-coated ssDNA invades the homologous double-stranded template DNA, and forms a displacement loop (D-loop) (Kowalczykowski et al. 1994; San Filippo et al. 2008). Loading of Rad51 is achieved by recombination mediator proteins, such as Swi5-Sfr1, Rad55-Rad57 ($Rad55^{Hs}$-$Rad57^{Hs}$), and $Rad22^{Sp}$/$Rad52^{Hs}$ (Liu et al. 2011). Swi5 facilitates efficient mating type switching in fission yeast (Egel et al. 1984), Further, it forms a heterocomplex with Sfr1 to displace RPA from ssDNA and thus mediating Rad51-DNA nucleofilament formation (Haruta et al. 2006; Akamatsu et al. 2007). Similarly, the Rad55-Rad57 heterodimer has been described as a recombination mediator, assisting loading of Rad51 onto ssDNA, by displacement of RPA (Sung 1997).

$Rad22^{Sp}$/$Rad52^{Hs}$ has not only been found to facilitate Rad51-ssDNA nucleoprotein filament assembly by overcoming the competition posed by RPA for binding to ssDNA in the context of strand-exchange (Sung 1997; Song and Sung 2000). In addition, Rad52 also

mediates pairing for complementary stretches of ssDNA (Mortensen et al. 1996), consistent with a role in single-strand annealing (SSA) repair, as well as the second end capture step of HR (Ivanov et al. 1996).

After the active HR intermediate ssDNA-Rad51 forms and strand invasion occurs, repair-dependent DNA synthesis ensues, copying the genetic information from the donor template, utilising $Pcn1^{Sp}$/$PCNA^{Hs}$, and Polδ (Li et al. 2009). One potential outcome is the synthesis-dependent strand annealing (SDSA) pathway, in which the newly-synthesised strand is displaced by the $Srs2^{Sp}$/$RTel1^{Hs}$ helicase and anneals back to the second end in a Rad52-dependent manner, resulting in a non-crossover (Sung and Klein 2006). Alternatively, the second DNA end is captured, giving rise to a double Holliday junction (dHJ) (Nimonkar and Kowalczykowski 2009). This intermediate can either be processed via dissolution, for example by BLM-TOP3-RMI1 in humans (Rqh1-Top3 in *S. pombe*), resulting in a non-crossover, or via resolution (Ashton et al. 2011). Resolution can cause both crossovers, and non-crossovers, dependent on the plane in which the dHJ is cut. Enzymes associated with resolution include Mus81-Eme1, Slx1-4, and Yen1 (Svendsen and Harper 2010). While crossovers during meiosis ensure genetic diversity, non-crossovers are the preferred outcome during mitotic homologous recombination (**Figure 1.4**).

Figure 1.4

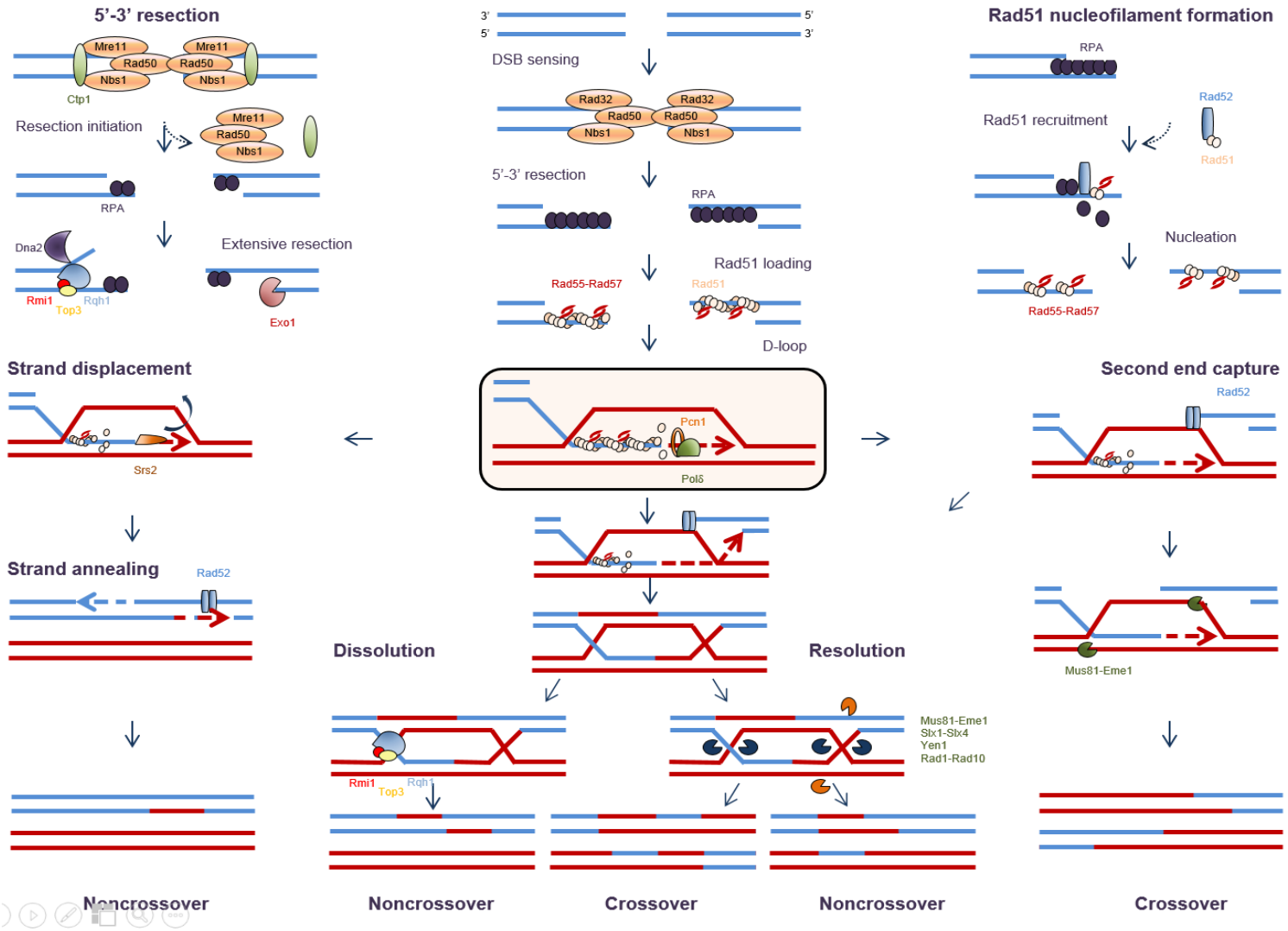

5'-3' resection
Mre11
Rad50
Nbs1
Ctp1
Resection initiation
RPA
Dna2
Rmi1
Top3
Rqh1
Extensive resection
Exo1
DSB sensing
Rad32
5'-3' resection
Rad55-Rad57
Rad51 loading
Rad51
D-loop
Rad51 nucleofilament formation
Rad51 recruitment
Rad52
Nucleation
Strand displacement
Srs2
Strand annealing
Pcn1
Polδ
Second end capture
Dissolution
Resolution
Mus81-Eme1
Slx1-Slx4
Yen1
Rad1-Rad10
Noncrossover
Noncrossover
Crossover
Noncrossover
Crossover

Figure 1.4: Homologous recombinational repair of a double-strand break. The DSB is sensed and processed by the MRN complex in conjunction with CtIP. Following initial short-term resection, extensive resection is carried out either by Exo1, or Dna2 with the Rmi1-Top3-Rqh1 complex. The emerging stretches of ssDNA are coated with RPA. RPA is then displaced with Rad51 by Rad55-Rad57, Rad22, or the Swi5-Sfr1 complexes. The Rad51-DNA nucleofilament invades, and copies the homologous template DNA forming a D-loop, facilitated by Pcn1, and Polδ. The newly synthesised strand is then either displaced, leading to synthesis-dependent strand annealing, or the second end is captured, giving rise to double Holliday junctions which are either resolved, or dissolved, ultimately leading to crossover or non-crossover end-products. Adapted, (Mazon et al. 2010).

Table 1.2

Function	*S. pombe*	*S. cerevisiae*	Humans
Resection	Mre11-Rad50-Nbs1	Mre11-Rad50-Xrs2	MRE11-RAD50-NBS1
	Ctp1	Sae2	CtIP
	Exo1	Exo1	EXO1
	Rqh1	Sgs1	BLM1
	Dna2	Dna2	DNA2
ssDNA binding	RPA (large subunit Rad11)	RPA (large subunit Rfa1)	RPA (large subunit RPA70)
Filament formation	Rad51	Rad51	RAD51
	Rad22	Rad52	RAD52
	Rad54	Rad54	RAD54
	Rad55-Rad57	Rad55-Rad57	RAD51B-RAD51C-RAD51D-XRCC2
			RAD51C-XRCC3
	Swi5-Sfr1	Sea3-Mei5	SWI5-MEI5
Anti-recombinases	Fbh1	?	FBH1
	Srs2	Srs2	RTEL
DNA synthesis	Pcn1, Polδ, Polε	PCNA, Polδ, Polε	PCNA, Polδ, Polε
HJ dissolution	Rqh1-Top3	Sgs1-Top3	BLM-TOPIIIa-RMI1
HJ resolution	Mus81-Eme1	Mus81-Mms4	MUS81-EME1
	?	YEN1	GEN1
	Slx1-4	Slx1-4	SLX1-4

Table 1.2: HR factors in *S. pombe*, *S. cerevisiae*, and humans.

1.4.2.1 Chromosomal rearrangements associated with HR repair

While HR is generally considered to be error-free, in contrast to NHEJ, sub-variants of HR repair can give rise to gross chromosomal rearrangements (GCRs) and loss of genetic information. This can occur both in HR mutants as well as in wild-type. Some sub-variants are considered below.

1.4.2.1.1 Single-strand annealing.

Single strand annealing (SSA) is a minor form of HR repair. Following resection of the DSB site, the chromosome is reconstituted without strand invasion of a homolog template strand. Stretches of complementary single-stranded sequences on either end of the DSB are utilised for annealing of exposed homologous regions in a $Rad22^{Sp}/Rad52^{Sc/Hs}$ -dependent manner, leaving non-homologous ssDNA flaps on either side, which are cleaved by the nuclease $Rad16^{Sp}/Rad1^{Sc}/XPF^{Hs}$ in complex with $Swi10^{Sp}/Rad10^{Sc}/ERCC1^{Hs}$ (**Figure 1.5**) (Ivanov et al. 1996). Emerging gaps/nicks are filled by the DNA synthesis and ligation machinery (Paques and Haber 1999; Raji and Hartsuiker 2006), resulting in additional deletions (Krogh and Symington 2004). While components of SSA overlap heavily with those of other HR models, including factors promoting for end resection and annealing, it does not require the canonical recombinase Rad51 (Ivanov et al. 1996). Further, SSA always generates deletions of varying size, depending on the distance separating two regions of sequence homology, thus causing a loss of genetic information, in contrast to other HR variations (Schildkraut et al. 2005). If two or more DSBs are present in the same nucleus, interchromosomal translocations can occur when sequence homology on two different chromosomes is utilised (Manthey and Bailis 2010). SSA is also distinct from A-NHEJ (MMEJ) in that resection appears to be unlimited until homologous regions are exposed. Following telomere loss, SSA can act as a mechanism giving rise to

chromosomal fusions (Wang and Baumann 2008). Despite its highly mutagenic nature, SSA competes with GC, even in a wild-type genetic background (Fishman-Lobell et al. 1992)

1.4.2.1.2 Gene conversion

Gene conversion (GC) refers to the unidirectional, thus non-reciprocal transfer of genetic information from a 'donor' to an 'acceptor' DNA molecule as part of homologous recombination (Chen et al. 2007). It frequently occurs between tandemly-linked homologous sequences, and can result in localised LOH when the homologous sequences are non-identical, with potentially pathogenic consequences. In mammals, the extent of GC typically does not exceed a few hundred bp up to 1 kb (Bosch et al. 2004; Jeffreys et al. 2004). In yeast, mitotic gene-conversion has been found to span over regions larger than 4 kb (Judd and Petes 1988). In addition to potential sequelea caused by LOH, GC can also exert a significant mutagenic effect when both strands of DNA are newly synthesised due to microhomology-mediated template switches (Verdin et al. 2013).

1.4.2.1.3 Crossovers

Meiotic homologous recombination is a major driver of evolution by providing genetic variation. This is achieved by crossovers between homologous chromosomes during prophase I (Creighton and McClintock 1931). While recombination during meiosis is considered desirable, crossovers produced during mitotic HR repair bear the potential to cause translocations or LOH, depending on cell cycle phase and genetic background. Crossovers can emerge through resolution of double-Holliday junctions (HJs) by the nucleolytic action of GEN1, YEN1, SLX1-SLX4, and MUS81-EME1, acting on different planes, or early D-loop cleavage following second-end capture, before a double Holliday

junction is formed (Ip et al. 2008). A number of antagonistically acting mechanisms exist in the cell to prevent crossovers. Following strand invasion, anti-recombinogenic helicases $Srs2^{Sc,Sp}$/$RTEL1^{Hs}$, $Fbh1^{Sp}$/$FBH1^{Hs}$ $Mph1^{Sc}$/Fml^{Sp}/$FANCM^{Hs}$, $Sgs1^{Sc}$/$Rqh1^{Sp}$/BLM^{Hs} prevent D-loop and subsequent dHJ formation by strand displacement of the invading strand, during synthesis-dependent strand annealing (SDSA) (Wu and Hickson 2006). If a double Holliday junction has already been formed, dissolution leading to non-crossovers is promoted by the BLM-TOP3-RMI1 complex (Cejka et al. 2010). LOH through mitotic recombination has been implicated with tumorigenesis in initial studies on the retinoblastoma susceptibility gene (Rb) locus (Cavenee et al. 1985).

1.4.1.2.4 Break-induced replication

Break-induced replication (BIR) is a sub-variant of HR, in which strand invasion of a homologous duplex DNA molecule occurs, followed by replication to the chromosome end **Figure 1.5** (Malkova et al. 1996; Bosco and Haber 1998; Llorente et al. 2008). This pathway is utilised when only one end of a broken chromosome is present, *e.g.* at uncapped telomeres or collapsed replication forks (Krogh and Symington 2004). While BIR maintains chromosome integrity, a loss of genetic information by LOH is possible when the invaded homologous donor DNA is non-identical to the locus in which the break occurred. Further, BIR-associated DNA synthesis has been found to be intrinsically inaccurate, giving rise to frame-shift mutations (Deem et al. 2011), and to result in conservative inheritance of the new genetic material (Saini et al. 2013). The genetic requirements of BIR include HR genes involved in initial processing of the nucleofilament, as well as strand invasion; *rad51*, *rad52*, *rad55*, and *rad54* (Llorente et al. 2008). However, instances of Rad51-independent BIR have also been reported, potentially including recombinases such as Rad52 (Malkova et al. 1996; Tinline-Purvis et al. 2009).

In addition to its oncogenic potential due to LOH, BIR has also been associated with emergence of complex phenotypes due to error-prone template switching, thus generating genomic instability (Myung et al. 2001; Smith et al. 2007). Microhomology-mediated break-induced replication (MMBIR) has also been found to be the general underlying mechanism of a replication-based event of fork stalling and template switching (FoSTeS), associated with complex genomic rearrangements in dysmyelinating central nervous system disorders in humans (Zhang et al. 2009). In this context, MMBIR/FoSTeS has been demonstrated to bear the potential to generate copy number variations of individual genes and rearrangements of single exons.

Figure 1.5

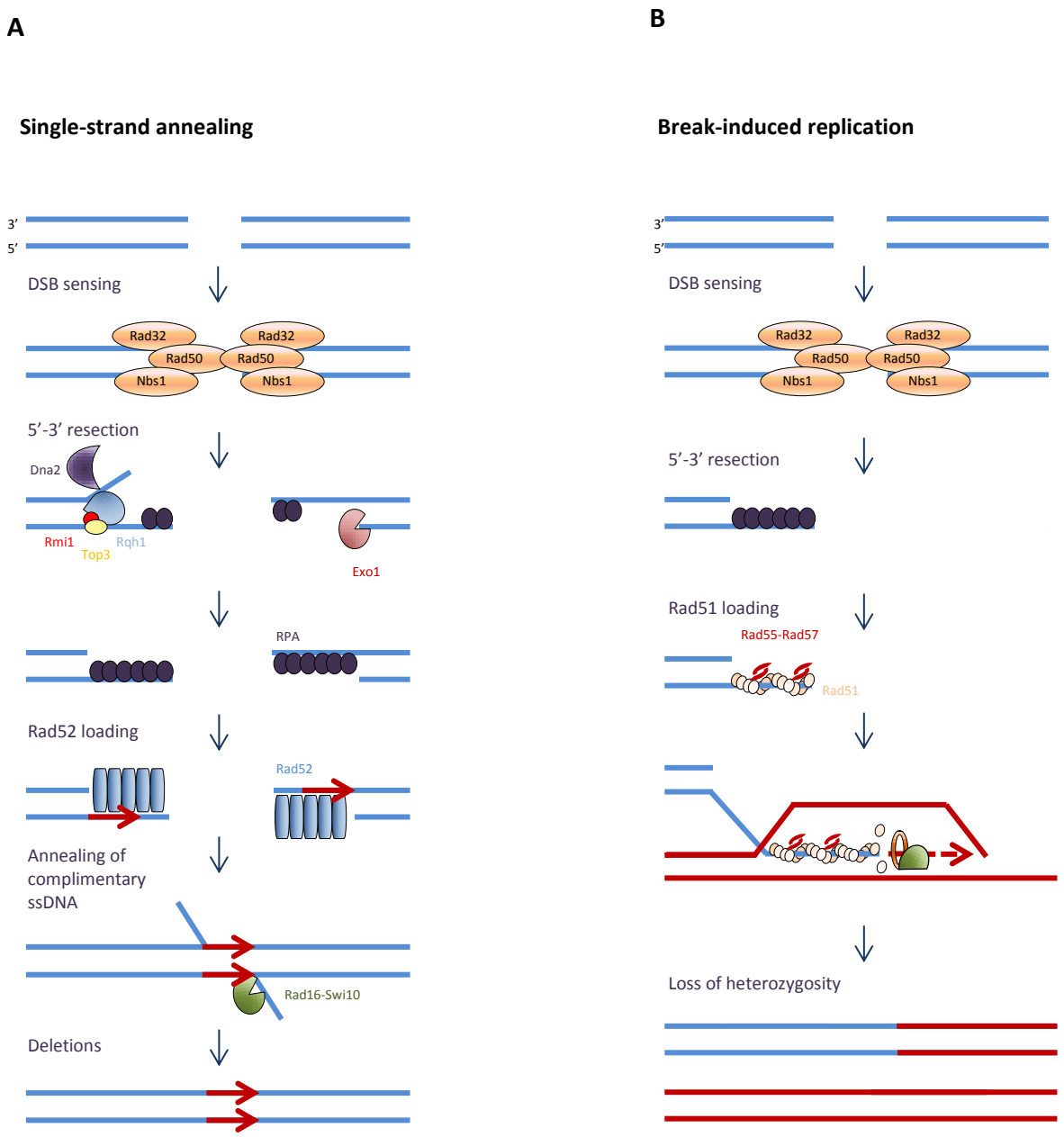


Figure 1.5: Misrepair of DSBs. (A) Single-strand annealing (SSA). In response to a DSB, the lesion is recognised by the MRN complex and Exo1- or Dna2-dependent resection occurs. If the cell fails to displace RPA with Rad51, Rad52-dependent annealing of complimentary ssDNA stretches gives rise to overhangs which are subsequently cleaved by the Rad16-Swi10 nuclease complex, leading to loss of genetic information. (B) During break-induced replication (BIR), failure of strand displacement of the newly-synthesised strand leads to replication of the invaded template DNA, causing potential loss of heterozyogsity.

1.5 DNA Integrity checkpoints

The DNA repair pathways described above function in concert with cell cycle checkpoints, which augment efficient repair not only by sensing DNA lesions, but also by promotion of appropriate cellular responses; *i.e.* arresting the cell cycle to provide time for repair, regulation of transcription, chromatin remodelling, and triggering cell senescence or apoptosis (Bartek et al. 2004; Su 2006).

Disruption of the checkpoint machinery often gives rise to genome instability. Thus, many checkpoint participants are considered tumour suppressor genes (Zhou and Elledge 2000). The vital importance of the cell cycle machinery for the genome's integrity of the cell is also reflected in the high degree of evolutionary conservation from yeast to humans (**Table 1.3**). In *S. pombe*, the DNA damage checkpoint, and the DNA replication checkpoint, collectively coined the DNA integrity checkpoints, are safeguarding genome integrity.

1.5.1 Sensing the damage

In response to a diverse range of genotoxic stress-inducing agents, DNA lesions are typically recognised by the damage sensory machinery, consisting of the highly conserved proteins: Rad9, Rad1, and Hus1, dubbed the 9-1-1 complex (Kemp and Sancar 2009). The 9-1-1 complex is a heterotrimeric complex resembling the doughnut shape of PCNA. It is loaded onto chromatin by the clamp loader Rad17 (You et al. 2002; Zou et al. 2002), in conjunction with Rfc2, Rfc3, Rfc4, Rfc5 clamp-loader subunits (Bermudez et al. 2003), and activates two distinct, yet cross-talking pathways (Abraham 2001). Replication stress and other substrates, including ssDNA-RPA stretches, activate the Chk1 protein kinase via phosphorylation by $Rad3^{Sp}/ATR^{Hs}$, and its binding partner $Rad26^{Sp}/ATRIP^{Hs}$ (**Figure 1.6**) (Zhao and Piwnica-Worms 2001; Weiss et al. 2002; Roos-Mattjus et al. 2003; Smith et al. 2010). Rad3 is one of the major phosphatidylinositol 3 (PI3) kinase-like kinases.

Figure 1.6

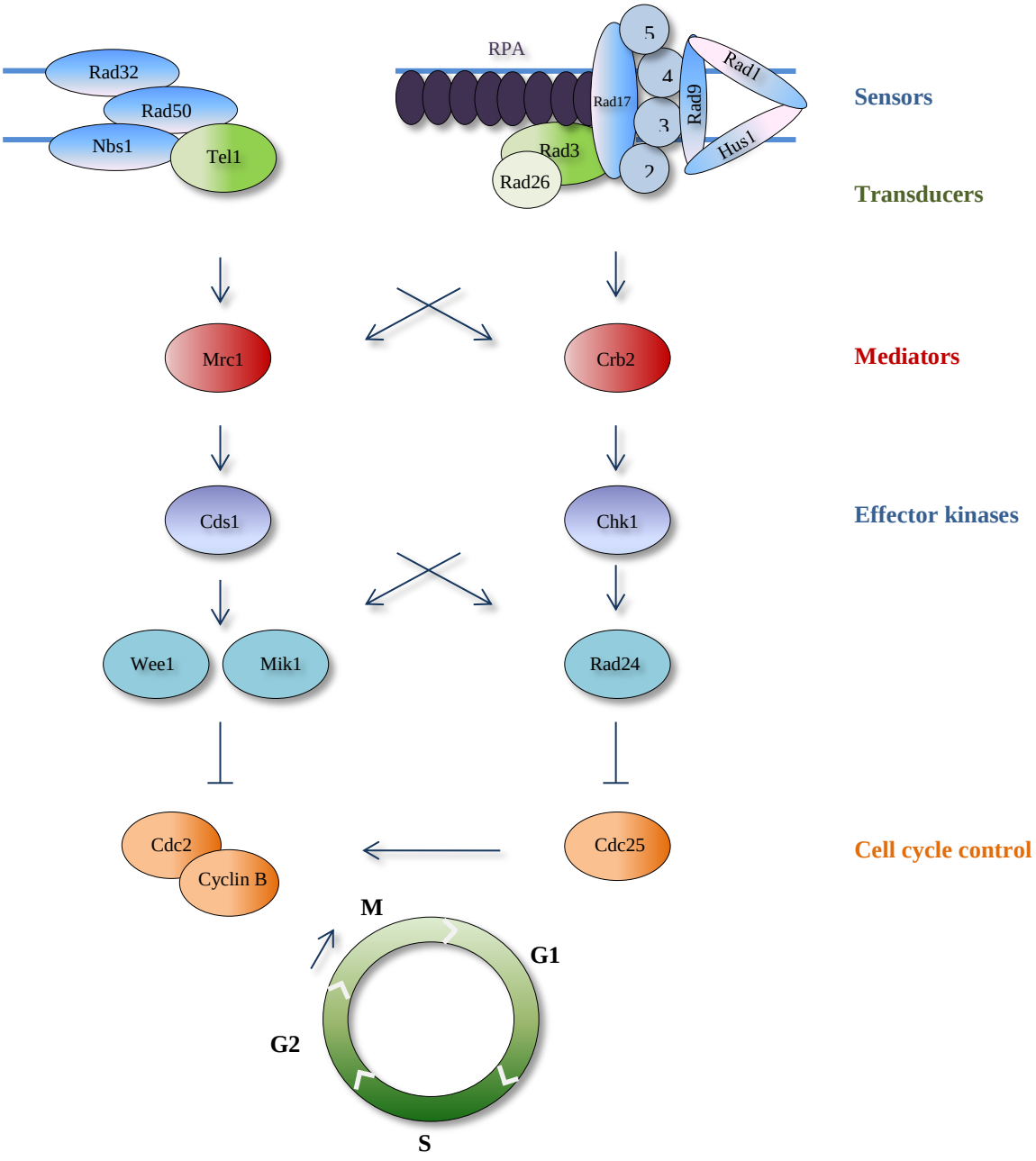


Figure 1.6: The *S. pombe* checkpoint response. DSBs are recognised by the sensors MRN (Mre11-Rad50-Nbs1) complex or by the 9-1-1 (Rad9-Rad1-Hus1) complex which is loaded by the PCNA like clamp-loader complex Rad17-Rfc2-Rfc3-Rfc4-Rfc5. Signal transduction is modulated by the PI3K kinases Tel1 or the Rad3-Rad26 complex, and relayed by either Mrc1 or Crb2, depending on the type of genotoxic stress. Effector kinases include Cds1 and Chk1, which phosphorylate Wee1, Mik1, and Rad24, ultimately leading to cell cycle arrest by inhibition of the Cdc2-CyclinB complex and phosphatase Cdc25. See text for further details.

Another early responder to DSBs is the MRN complex, which activates the second major PI3KK ATM, which further modulates the checkpoint response via phosphorylation of downstream targets, including Chk2 (Uziel et al. 2003). While resistance to DNA damage in humans is conferred by both ATM^{Hs}/$Tel1^{Sp}$ and ATR^{Hs}/$Rad3^{Sp}$ (Cuadrado et al. 2006; Toczyski 2006), *S. pombe* and *S. cerevisiae* rely mainly on $Rad3^{Sp}$/$Mec1^{Sc}$; Tel1 is only a minor participant in checkpoint activation.

Rad3 and 9-1-1 complex recruitment can occur independently from each other, but both factors are indispensable for full checkpoint activation (Caspari and Carr 2002).

1.5.2 Signal transduction

Subsequent to DNA damage sensing by the 9-1-1 and MRN complex and initiation of the checkpoint signals by the two PI3KK $Tel1^{Sp}$/ATM^{Hs}, and $Rad3^{Sp}$/ATR^{Hs}, the signal is amplified and transduced. At this stage, the replication checkpoint and DNA damage checkpoint diverge. For activation of the replication checkpoint, mediator protein $Mrc1^{Sp/Sc}$ is required for signal transduction via Cds1 phosphorylation (Alcasabas et al. 2001). In humans, replication stress causes phosphorylation of Mrc1 homolog Claspin, and thus signal transduction via CHK1 is achieved (Kumagai and Dunphy 2000; Chini and Chen 2003; Kumagai and Dunphy 2003; Chini and Chen 2004). For the DNA damage checkpoint, signal transduction is initiated by $Crb2^{Sp}$/$53BP1^{Hs}$, resulting in phosphorylation of Chk1 in *S. pombe* (Saka et al. 1997).

Table 1.3

Protein function	*S. pombe*	*S. cerevisiae*	Humans
9-1-1 complex	Rad9	Ddc1	Rad9
	Rad1	Rad17	Rad1
	Hus1	Mec3	Hus1
RFC-like clamp-loader	Rad17	Rad24	Rad17
ATR kinase	Rad3	Mec1	ATR
ATM kinase	Tel1	Tel1	ATM
ATR interacting protein	Rad26	Ddc2	ATRIP
Damage checkpoint transducer	Crb2	Rad9	53BP1
S-phase checkpoint transducer	Mrc1	Mrc1	Claspin
	Rad4/Cut5	Dpb11	TopBP1
Effector kinase	Cds1	Rad53	Chk2
	Chk1	Chk1	Chk1

Table 1.3: Conserved checkpoint proteins in *S. pombe, S. cerev*isiae, and humans.

1.5.3 Arresting the cell cycle

S. pombe spends extended periods of time in G2 phase of the cell cycle. Consequently, G2/M transition is tightly controlled by both the DNA damage and the replication checkpoint. Following signal transduction, Cds1 and Chk1 activate effector kinases Wee1 and Mik1, as well as 14-3-3 protein Rad24 (Rhind and Russell 2000). Wee1 and Mik1 exert cell cycle arrest at the G2/M boundary by inhibitory phosphorylation of mitotic driver $Cdc2^{Sp}/CDK1^{Hs}$ a cyclin-dependent kinase (CDK) (Rhind et al. 1997), which acts in concert with Cyclin B, driving mitotic entry. The phosphatase Cdc25 acts antagonistically to this cascade. Following checkpoint activation, Cdc25 is inactivated two-fold; by direct inhibitory phosphorylation by Chk1 and Cds1, and by binding to Rad24, which acts by sequestration of Cdc25 to the cytoplasm (Furnari et al. 1997; Zeng et al. 1998; Lopez-Girona et al. 1999; Zeng and Piwnica-Worms 1999; Rhind and Russell 2000). Ultimately, cell cycle progression is halted by inhibition of the Cdc2-CyclinB complex. Regulation of

the G2/M checkpoint in humans is controlled by similar mechanisms (Niida and Nakanishi 2006).

1.5.4 Non-canonical roles of checkpoint proteins

There is accumulating evidence for additional roles for the checkpoint machinery in non-canonical processes. The 9-1-1 complex has been associated with telomere maintenance, template switching at stalled replication forks, meiotic homologous recombination, and cancer progression (Shinohara et al. 2003; Pandita et al. 2006; Grandin and Charbonneau 2007; Broustas et al. 2012; Karras et al. 2013).

Regulation of transcription, as well as phosphorylation and localisation of DNA repair factors by cell cycle proteins have also been reported (Aylon and Kupiec 2004). In addition, direct roles in HR repair have been postulated, as *S. cerevisiae* mutants depleted of $Rad17^{Sc}/Rad1^{Sp}$, $Rad24^{Sc}/Rad17^{Sp}$ have been found to be defective in ssDNA production around enzymatically induced DSB as well as exposed telomeres (Aylon and Kupiec 2003), indicative of participation of checkpoint proteins in resection. Direct evidence for a role in resection has been presented (Jia et al. 2004), but remains controversial.

1.6 A system for analysing DSB repair in *S. pombe*

In this study, a range of non-essential minichromosomes Ch^{16} were used to obtain quantifiable DSB repair profiles. Ch^{16} was originally derived from chromosome III (Niwa et al. 1989), but has been modified by introduction of an *S. cerevisiae* MATa break-site, inducible by expression of the HO endonuclease, which was present either ectopically (pREP81X), or endogenously, depending on the specific DSB assay (Prudden et al. 2003; Moss et al. 2010). In addition, to differentiate repair events following break-induction, a

variety of markers have been introduced. A kanamycin or hygromycin resistance cassette was present adjacently to the break-site, while auxotrophic markers (Leu2, His, Ade6, Arg2, Ura4) were placed onto different arms of the chromosome. Following DSB repair, the underlying repair event could be deduced based on marker loss or retention (**Figure 1.7**) (Cullen et al. 2007; Tinline-Purvis et al. 2009). In total, four different repair events can be monitored; *i.e.* NHEJ/Uncut/sister chromatid conversion (SCC), homologous recombination (HR), utilising homologous chromosome III as repair template, loss of heterozygosity (LOH), and Ch^{16} loss. The former two outcomes were considered beneficial repair events, while the latter two events emerge due to failed repair. Mechanisms of LOH were found to be isochromosome formation, during which the right arm of the minichromosome is lost due to extensive resection, and the left arm subsequently invaded and copied, *de-novo* telomere addition, and break-induced replication (Cullen et al. 2007; Tinline-Purvis et al. 2009). The system is described in greater detail in **Chapter II**.

Figure 1.7

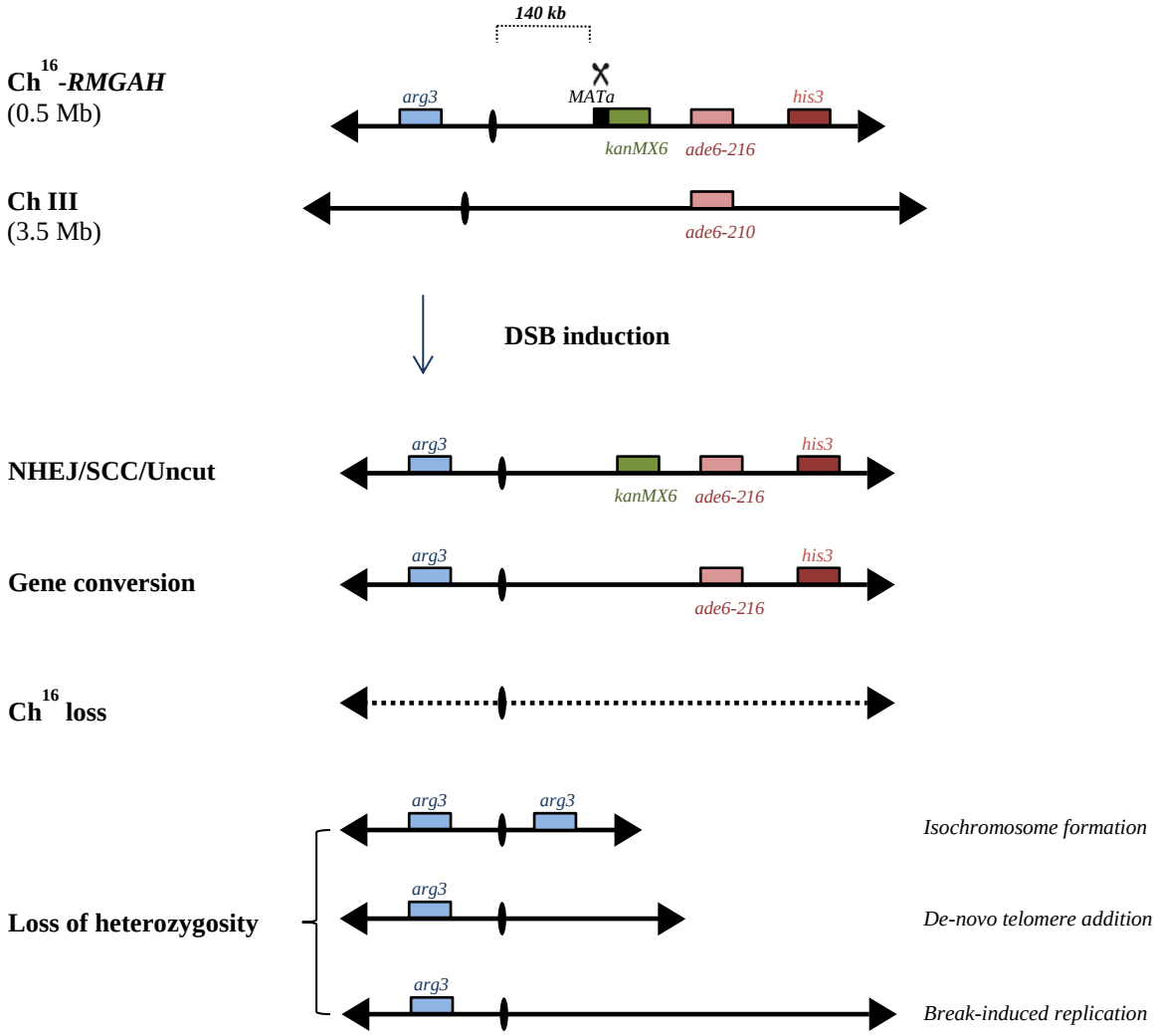


Figure 1.7: DSB repair assay Ch^{16}-*RMGAH*. Depiction of the DSB assay Ch^{16}-*RMGAH*. A non-essential minichromosome, derived from ChrIII was utilised to study DSB repair in *S. pombe*. Ch^{16}-*RMGAH* harbours an inducible HO-endonuclease recognition site MATa with an adjacent selection marker (*kanMX6*). In addition, auxotrophic markers were placed on the left (*arg3*), and the right arm of the chromosome (*ade6*-M216, *his3*). Following break-induction by expression of HO-endonuclease, four different repair events can be differentiated based on marker profile of surviving colonies: NHEJ (*arg3*, *kanMX6*, *ade6*, *his3*), GC (*arg3*, *ade6*, *his3*), Ch^{16} loss (loss of all markers), and Loss of heterozygosity (*arg3*). LOH includes three different events; isochromosome formation in which the left arm of the chromosome is invaded and copied following extensive resection, *de-novo* telomere addition, and break-induced replication. See text and **Chapter II** for details.

1.7 RNA metabolism and genome stability

1.7.1 The siRNA machinery

RNA interference (RNAi) was first discovered as a post-transcriptional mechanism of gene silencing, based on double-stranded RNA (dsRNA) (Fire et al. 1998). dsRNA products are thought to preserve genome integrity against endogenous transposons, and viruses. Later it became apparent, that RNAi also participates in organisation of chromatin structure, such as RNA-directed DNA methylation, as well as transcriptional gene silencing in a number of organisms, including yeast (Moazed 2009). In *S. pombe*, RNA-based modification of chromatin is thought to function via recruitment of silencing proteins to nascent RNA polymerase II (RNAPII) transcripts and their corresponding genomic region (Buhler and Moazed 2007; Lejeune and Allshire 2011). Establishment and maintenance of centromeric heteterochromatin in fission yeast requires RNAi factors Dicer (Dcr1), a dsRNA nuclease, Argonaute protein Ago1, and RNA-directed RNA polymerase (Rdp1) (Volpe et al. 2002). Ago1 has been found to be part of the RNA-induced transcriptional silencing (RITS) complex, and interacts directly with short single-stranded siRNAs, targeting this complex to nuclear heterochromatised loci, like the centromere (Verdel et al. 2004). The RITS complex triggers transcriptional down-regulation of this region by mediating H3K9 methylation, thus targeting the locus for heterochromatin formation. Guidance relies on the complementary sequence of the siRNA to nascent transcripts and their corresponding genomic site. Subsequently, the RNA-dependent RNA polymerase complex (RDRC), including Rdp1, and Dcr1, is recruited to the nascent transcript and double-stranded RNA is produced, which in turn is processed into dsRNA molecules of 20-25 nucleotides (nt) in size, binding Ago1. Both RITS and RDRC are necessary for initiation and spreading of H3K9 methylation, which is thought to be promoted by recruitment of the CLRC (Clr4-

Rik1-Cul4) complex, which in turn mediates methylation by the Clr4 methyltransferase (Buker et al. 2007) (**Figure 1.8**).

Figure 1.8

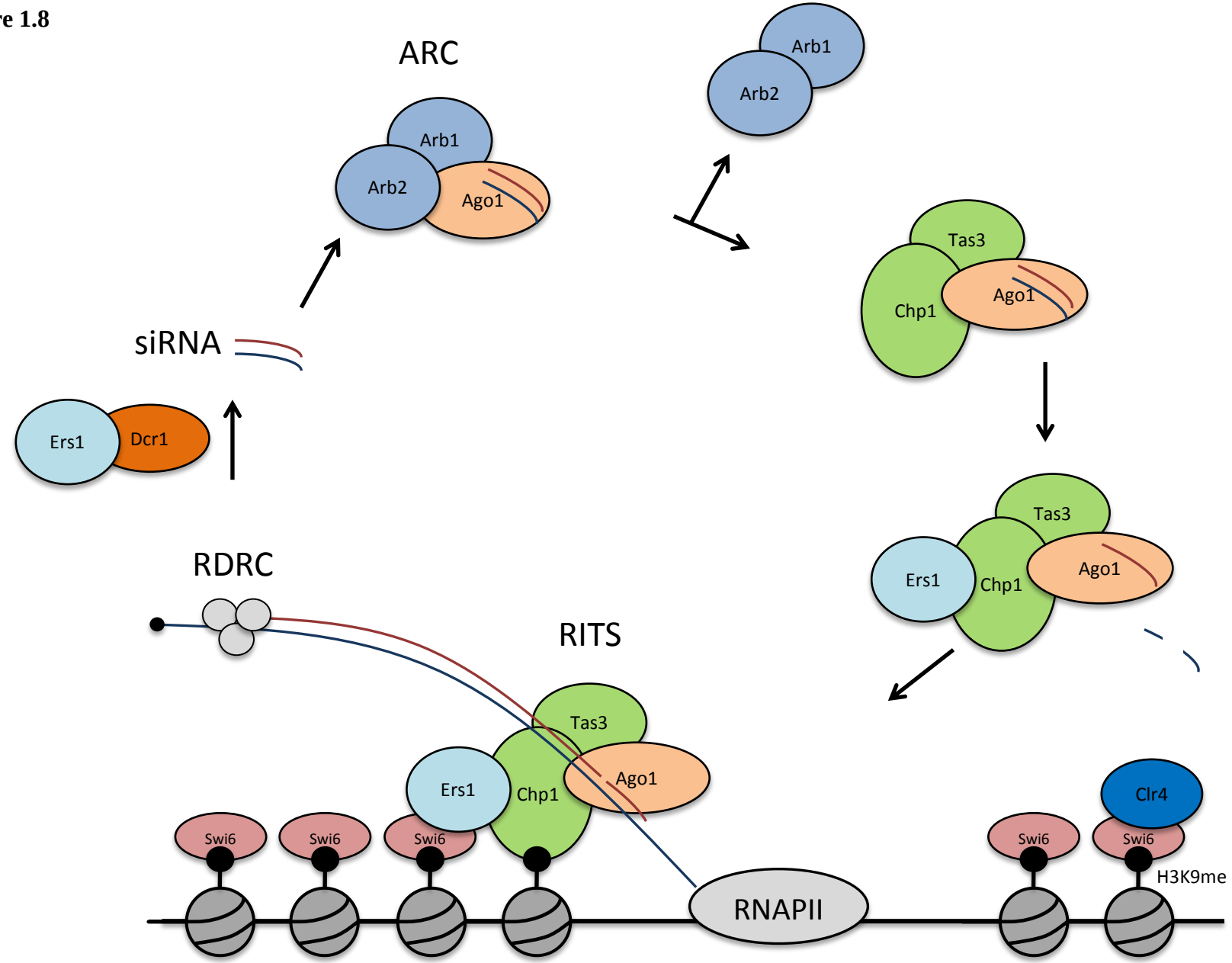

ARC
Arb1
Arb2
Ago1
Arb1
Arb2
Tas3
Chp1
Ago1
siRNA
Ers1
Dcr1
Tas3
Ers1
Chp1
Ago1
RDRC
RITS
Tas3
Ers1
Chp1
Ago1
Clr4
Swi6
Swi6
Swi6
Swi6
Swi6
H3K9me
RNAPII

Figure 1.8: The *S. pombe* siRNA pathway. Nascent transcripts of RNAPII are bound by the RITS complex, which is targeted to sequence-specific locations based on interaction of Ago1 and single-stranded siRNA molecules. RITS interacts both with RNA transcripts and the methylated histones at the corresponding genomic region. RITS is also believed to recruit the CLRC complex, thus promoting H3K9 methylation, and thus heterochromatin formation. The RDRC complex produces double-stranded RNA out of the nascent transcript which is further processed by Dicer protein Dcr1, and the ARC complex. See text for details. Adapted from (Buker et al. 2007).

1.7.2 A role for non-coding RNAs in DNA repair and genome stability

Intriguingly, in recent years, evidence accumulated for crosstalk of the RNAi machinery and DNA repair in humans. It was reported that non-coding RNAs (ncRNAs) processed by DICER and DROSHA ribonucleases were found to be required for activation of the DNA damage response, monitored by fluorescence microscopy of DDR foci, upon oncogene-induced genotoxic stress, ionising radiation, and site-specific endonucleases. Site-specific small RNAs were shown to be produced locally around the damages sites, and were coined damage-dependent RNAs (ddRNAs) (Francia et al. 2012). Further, it was demonstrated that ddRNAs act in an MRN-complex dependent manner. A different study uncovered that in *Arabidopsis thaliana* and human cells, 21-nucleotide small RNAs are synthesised in direct vicinity of the DSB sites, and were termed DSB-induced RNAs (diRNAs) (Wei et al. 2012). They further reported that diRNA production in *Arabidopsis* relies on PI3K ATR, a key protein functioning in checkpoints and DSB repair. It is hypothesised that these sequence-specific diRNAs facilitate DSB repair by providing targeting templates, directing either chromatin modifiers, or repair factors to DSB sites. Furthermore, studies in mice unveiled Dicer to be a haploinsufficient tumour suppressor; a conditional deletion of a single copy of Dicer led to reduced survival and elevated tumorigenesis (Kumar et al. 2007). The authors propose this effect was due to disturbed biogenesis of micro RNAs (miRNAs). Micro RNAs are short, single-stranded, non-coding stretches of RNA, involved in post-transcriptional inhibition of expression by disruption of translation, and are hypothesised to possess both oncogenic and tumour suppressor functions (Plasterk 2006; Ventura and Jacks 2009). In contrast to siRNAs, miRNAs are single-stranded and are expressed by genes whose only purpose is the production of miRNAs. miRNAs are not 100% complementary to their target mRNA; thus, one miRNA molecule may target up to hundreds of mRNAs (Mack 2007).

Taken together, these findings underline an emerging role for RNA biogenesis, in particular ncRNAs, including siRNAs, miRNAs, ddRNAs, and diRNAs, as a new leg in the DNA damage response (Liu and Lu 2012).

1.7.3 RNA:DNA hybrids and genome stability

Another recently appreciated group of genes maintaining genome stability are factors involved in transcription and RNA processing of protein-coding genes. When RNA biogenesis is disrupted at sites of transcription initiation, repression, elongation, splicing, degradation, or export, occurrences of genome instability increase by a common mechanism (Huertas and Aguilera 2003; Wahba et al. 2011; Stirling et al. 2012; Wahba et al. 2013; Wahba and Koshland 2013). Mutations in RNA biogenesis genes give rise to persistent, transcription-associated RNA:DNA hybrids (R-loops). These structures destabilise the integrity of the genome by exposing damage-prone ssDNA of the complementary strand, and by acting as a block for DNA replication, potentially causing replication fork collisions (Prado and Aguilera 2005; Gomez-Gonzalez et al. 2009; Gan et al. 2011). However, many important aspects about the underlying mechanics, as well as contributing factors to R-loop-based genome instability, remain opaque. Since many RNA processing and transcription factors bind the nascent RNA molecule at sites of transcription, it has been speculated that they function to prevent RNA:DNA hybrid formation at spatially close complementary genomic loci (Aguilera and Garcia-Muse 2012). Further, it has been demonstrated that two endogenous RNAse H enzymes, and Sen1 function to resolve RNA:DNA hybrids after formation, and mutations in Sen1 give rise to accumulation of these fragile sites, causing genome instability (Mischo et al. 2011; Wahba et al. 2011). A recent report demonstrated the requirement of recombination proteins Rad51 and Rad52 for RNA:DNA hybrid formation in yeast mutants defective for

transcription repression and RNA degradation (Wahba et al. 2013). It is suggested that HR factors facilitate RNA:DNA strand exchange both in *cis*, and in *trans*, further amplifying the genome-destabilising potential of these hybrid structures. Finally, anti-recombinase Srs2 has been shown to antagonise hybrid formation, representing a novel counter-mechanisms to these sequelae.

1.8 Aims of this work

In this study, efforts are described to identify and characterise novel factors facilitating efficient DSB repair, thereby preventing genome instability. For this purpose, a number of mutant *S. pombe* strains derived from a previous genetic screen of the lab, carrying randomly introduced point mutations, were identified and characterised preliminarily. Further, a commercially available *S. pombe* deletion library was utilised to screen for novel genes conferring resistance to a range of DNA damaging agents; subsequently, a potential involvement in homologous recombinational repair of DSBs was investigated, in an effort to uncover the complex network of pathways governing the DDR.

CHAPTER II

Materials and Methods

2.1 General laboratory supplies

General commercially available laboratory chemicals of analytical grade were purchased from Sigma-Aldrich, Fisher Scientific, BDH Laboratory Supplies and Invitrogen. Bacto-agar and Bacto-tryptone were acquired from Scientific Laboratory Supplies. EZmix™ yeast extract was obtained from Sigma-Aldrich. Gensieve LE agarose was bought from Flowgen. All DNA ladders, restriction endonucleases, ligases, phosphatases, *Taq* DNA polymerase and Phusion High Fidelity DNA polymerase were purchased from New England Biolabs. dNTPs were ordered from ABgene and oligonucleotides from Sigma-Aldrich.

As part of this study, the following kits were used:

- QIAGEN: Maxiprep, Miniprep, Gel extraction and PCR purification kits.
- Epicentre: MasterPure™ Yeast DNA Purification kit.

During the research, following centrifuges were used:

- Jouan CR4.12
- Beckman Coulter Avanti J-26 XP
- Beckman Coulter Optima L-100 XP Ultracentrifuge
- Eppendorf microcentrifuge 5415D

2.2 Buffers and solutions

Buffers provided with commercially obtained enzymes were used according to specifications of the manufacturer. Non-commercial buffers and solutions used are presented below. All were prepared with purified water (MQ; Millipore system) and autoclaved or filter-sterilised.

- **Phosphate buffered saline (PBS)**

  1 PBS tablet (Oxoid) per 100 ml MQ water.

- **PLATE solution**

  50% polyethylene glycol, 100 mM lithium acetate, 10 mM Tris-HCl (pH 4.2), 1 mM EDTA.

- **Lithium acetate/TE buffer (LiAc/TE)**

  100 mM lithium acetate, 10 mM Tris-HCl (pH 8.0), 1 mM EDTA (pH 8.0).

- **Polyethylene glycol/lithium acetate/TE buffer (PEG/LiAc/TE)**

  40% polyethylene glycol (PEG), 100 mM lithium acetate (pH 8.0), 10 mM Tris-HCl (pH 8.0), 1 mM EDTA (pH 8.0).

- **Tris-EDTA (TE) buffer**

  10 mM Tris-HCl (pH 8.0), 1 mM EDTA (pH 8.0).

- **10x loading dye**

  0.25% (w/v) bromophenol blue, 0.25% (w/v) xylene cyanole, 15% (w/v) ficoll.

- **50x Tris-Acetate EDTA (TAE) buffer**

  2 M Tris-HCl, 0.1 M EDTA (pH 8.0), 1 M acetic acid. Adjusted to pH 8.0 with acetic acid.

- **Laemmli buffer**

  125 mM Tris-Cl pH 6.8, 100 mM dithiothreitol (DTT), 2% (w/v) sodium dodecyl sulphate (SDS), 0.1% (w/v) bromophenol blue, 10% (w/v) glycerol.

- **1x Running buffer**

  10 g/l SDS, 30 g/l Tris-Cl, 144 g/l glycine.

- **1x Transfer buffer**

  48 mM Tris-Cl, 39 mM glycine, 0.04% SDS, 20% methanol.

- **Lysis buffer**

  18% ficoll 400, 20 mM potassium phosphate pH 6.5, 1 mM $MgCl_2$, 0.5 M EDTA pH 8.0, 1 mM PMSF, 1 µg/ml leupeptin, 1 µg/ml pepstatin, 1x phosphate inhibitor cocktail, 2 µg/ml aprotinin.

- **DTT / Tris Buffer**

  0.1 mM Tris-HCl, pH 9.4, 10 mM DTT.

- **Buffer 2**

  1.2 M Sorbitol, 20 mM Hepes, pH 7.4.

- **Buffer 3**

  1.2 M Sorbitol, 20 mM Pipes, pH 6.8, 1 mM $MgCl_2$.

- **NIB Buffer**

  0.25 M Sucrose, 60 mM KCl, 15 mM NaCl, 5 mM $MgCl_2$, 1 mM $CaCl_2$, 15 mM MES, pH 6.6, 1 mM PMSF, 0.8% Triton X-100.

- **A Wash**

  10 mM Tris-HCl, pH 8.0, 0.5 % NP-40, 75 mM NaCl, 30 mM Sodium Butyrate, 1 mM PMSF.

- **B Wash**

  10 mM Tris-HCl, pH 8.0, 0.4 M NaCl, 30 mM Sodium Butyrate, 1 mM PMSF.

2.3 Media

Media and additive solutions were dissolved in MQ water and autoclaved. For solid media, Bacto-agar was added prior to autoclaving.

2.3.1 Escherichia coli (E. coli) media

- **Luria-Bertani (LB) medium**

  10 g/l Bacto-tryptone, 5 g/l Bacto-yeast extract, 10 g/l NaCl. 2% Bacto-agar added for solid media. Ampicillin was added to a final concentration of 50-100 µg/ml, post autoclaving.

2.3.2 *Schizosaccharomyces pombe* (*S. pombe*) media

- **Edinburgh Minimal Medium (EMM)**

  14.7 mM potassium hydrogen phthalate, 15.5 mM disodium hydrogen orthophosphate, 93.5 mM ammonium chloride, 2% glucose, 1x salt stock, 1x vitamin stock, 1x mineral stock. Supplements of adenine (A), leucine (L), uracil (U), histidine (H) and arginine (R) were added to a final concentration of 150 mg/l. When appropriate, thiamine was added to a final concentration of 2 µM or 8 µM. 2% Bacto-agar added for solid media. When used as an alternative nitrogen source, phenylalanine and tryptophan were added to a final concentration of 20 mM.

- **50x Salt stock**

  260 mM magnesium chloride, 5 mM calcium chloride, 670 mM potassium chloride, 14.1 mM disodium phosphate.

- **1000x Vitamin stock**

  4.2 mM pantothenic acid, 81.2 mM nicotinic acid, 55.5 mM inositol, 40.8 µM biotin.

- **10,000x Mineral stock**

80.9 mM boric acid, 23.7 mM manganese sulphate, 13.9 mM zinc sulphate, 7.4 mM iron chloride, 2.47 mM molybdic acid, 6.02 mM potassium iodide, 1.6 mM copper sulphate, 47.6 mM citric acid.

- **SPAS6S**

  10 g/l glucose, 1 g/l KH_2PO_4, 1 ml/l vitamins, 45 mg/l supplements. 2% Bacto-agar added for solid media.

- **YE6S (Yeast Extract and 6 supplements)**

  3% glucose, 0.5% EZmix™ yeast extract (Sigma), 1.31 mM adenine, 1.45 mM L-histidine, 1.71 mM L-leucine, 2.01 mM uracil, 1.29 mM arginine, 1.23 mM L-lycine, 2% Bacto-agar added for solid media.

  - YE6S and G418: 500 μg/ml Geneticin (G418) added post sterilisation.
  - YE6S and HygB: 180-240 μg/ml Hygromycin B (Hyg) added post sterilisation.
  - YE6S and clonNAT: 100 μg/ml clonNAT added post sterilisation

- ***S. pombe* minimal glutamate (PMG)**

  2% glucose, 14.7 mM potassium hydrogen phthalate, 15.5 mM Na_2HPO_4, 22 mM L-glutamic acid, 1x salt stock, 1x vitamin stock, 1x mineral stock. 2% Bacto-agar added for solid media. Required supplements were then added, as with EMM. PMG is compatible for selection with G418 and Hygromycin B. G418 was added to agar media at 500 μg/ml post sterilisation. Hygromycin B was added to liquid culture at 20 μg/ml.

- **Yeast freezing mix (YFM)**

  Mix of YE6S and glycerol (1:1).

- **5-Fluoroorotic acid (5-FOA)**

To 400 ml sterilised EMM, 20 mg of uracil, 90 mg of adenine, leucine, histidine and arginine(as required), 2 μM thiamine and 0.8 g 5-FOA were added.

2.4 Strains

2.4.1 *E. coli*

DH5α (*supE44, Δlac*U169, (*φ80lac*ZDM15), *hsdR*17, *rec*A1, *end*A1, *gyr*A96, *thi-1, rel*A1*)* was purchased from Invitrogen.

2.4.2 *S. pombe*

Non-minichromosome *S. pombe* strains used during this study are listed in Table **2.1.** Minichromosome containing *S. pombe* strains used during this study are listed in **Table 2.2.**

Table 2.1 Non-minichromosome strains used in this study

Strain	Genotype	Source
TH2093/2094	*leu1-32 arg3-D4 ade6-M210 ura4-D18 his3-D1 h⁻/ h⁺*	Lab stock
loh-2	*arg3-D4, ade6-D1, ura4-D18, leu1-32, his3-D1, rhp57K106N h-*	Lab stock
loh-5	*arg3-D4, ade6-D1, ura4-D18, leu1-32, his3-D1, rad3 W1701X h-*	Lab stock
loh-6	*arg3-D4, ade6-D1, ura4-D18, leu1-32, his3-D1, rad17 W72X h-*	Lab stock
loh-7	*arg3-D4, ade6-D1, ura4-D18, leu1-32, his3-D1, rad3 W253X h-*	Lab stock
TH675	***rad32::Ura4**, arg3-D4, ade6-D1, ura4-D18, leu1-32, his3-D1 h-*	Lab stock
TH395	***rad32::Ura4**, arg3-D4, ade6-D1, ura4-D18, leu1-32, his3-D1 h-*	Lab stock
TH315	***rad9::ura4,** arg3-D4, ade6-D1, ura4-D18, leu1-32, his3-D1 h-*	Lab stock
TH316	***rad1::ura4,** arg3-D4, ade6-D1, ura4-D18, leu1-32, his3-D1 h-*	Lab stock
TH308	***hus1::leu2**, arg3-D4, ade6-D1, ura4-D18, leu1-32, his3-D1 h-*	Lab stock
TH589	***rad17::ura4**, arg3-D4, ade6-D1, ura4-D18, leu1-32, his3-D1 h-*	Lab stock
V2-27-B10	***SPAC56E4.07:: kanMX4**, ade6-M210, ura4-D18, leu1-32 h+*	Bioneer
V2-26-G10	***SPAC1039.08::kanMX4,** ade6-M210, ura4-D18, leu1-32 h+*	Bioneer
V2-13-B09	***atg22::kanMX4**, ade6-M210, ura4-D18, leu1-32 h+*	Bioneer
V2-24-F04	***SPBC83.18c::kanMX4**, ade6-M210, ura4-D18, leu1-32 h+*	Bioneer
V2-27-D04	***SPCC645.07::kanMX4**, ade6-M210, ura4-D18, leu1-32 h+*	Bioneer
V2-06-D11	***rad24::kanMX4**, ade6-M210, ura4-D18, leu1-32 h+*	Bioneer
V2-16-G12	***cdt2::kanMX4**, ade6-M210, ura4-D18, leu1-32 h+*	Bioneer
V2-30-G09	***mik1::kanMX4**, ade6-M210, ura4-D18, leu1-32 h+*	Bioneer
V2-54-D08	***rad3::kanMX4**, ade6-M210, ura4-D18, leu1-32 h+*	Bioneer
V2-55-F2	***csk1::kanMX4**, ade6-M210, ura4-D18, leu1-32 h+*	Bioneer

Strain	Genotype	Source
V2-03-E08	***rad26::kanMX4***, *ade6-M210, ura4-D18, leu1-32 h+*	Bioneer
V2-05-B05	***rad1::kanMX4***, *ade6-M210, ura4-D18, leu1-32 h+*	Bioneer
V2-18-C07	***rad9::kanMX4***, *ade6-M210, ura4-D18, leu1-32 h+*	Bioneer
V2-19-C02	***hus1::kanMX4***, *ade6-M210, ura4-D18, leu1-32 h+*	Bioneer
V2-30-G05	***rad17::kanMX4***, *ade6-M210, ura4-D18, leu1-32 h+*	Bioneer
V2-10-A07	***mrc1::kanMX4***, *ade6-M210, ura4-D18, leu1-32 h+*	Bioneer
V2-15-C11	***cds1::kanMX4***, *ade6-M210, ura4-D18, leu1-32 h+*	Bioneer
V2-15-G08	***SPCC126.04c::kanMX4***, *ade6-M210, ura4-D18, leu1-32 h+*	Bioneer
V2-28-H04	***mst2::kanMX4***, *ade6-M210, ura4-D18, leu1-32 h+*	Bioneer
V2-10-H06	***hat1::kanMX4***, *ade6-M210, ura4-D18, leu1-32 h+*	Bioneer
V2-29-D08	***rsc1::kanMX4***, *ade6-M210, ura4-D18, leu1-32 h+*	Bioneer
V2-30-E11	***rsc4::kanMX***, *ade6-M210, ura4-D18, leu1-32 h+*	Bioneer
V2-44-D1	***arp42::kanMX***, *ade6-M210, ura4-D18, leu1-32 h+*	Bioneer
V2-24-F09	***nht1::kanMX***, *ade6-M210, ura4-D18, leu1-32 h+*	Bioneer
V2-23-H10	***cph2::kanMX4***, *ade6-M210, ura4-D18, leu1-32 h+*	Bioneer
V2-25-E12	***pht1::kanMX***, *ade6-M210, ura4-D18, leu1-32 h+*	Bioneer
V2-44-H10	***rtt109::kanMX4***, *ade6-M210, ura4-D18, leu1-32 h+*	Bioneer
V2-45-F3	***cph1::kanMX***, *ade6-M210, ura4-D18, leu1-32 h+*	Bioneer
V2-03-E06	***SPAC25A8.01c::kanMX4***, *ade6-M210, ura4-D18, leu1-32 h+*	Bioneer
V2-09-G05	***hip3::kanMX4***, *ade6-M210, ura4-D18, leu1-32 h+*	Bioneer
V2-44-H05	***arp5::kanMX4***, *ade6-M210, ura4-D18, leu1-32 h+*	Bioneer
V2-01-C02	***shg1::kanMX4***, *ade6-M210, ura4-D18, leu1-32 h+*	Bioneer

Strain	Genotype	Source
V2-02-D02	***SPAC6F6.09::kanMX4***, *ade6-M210, ura4-D18, leu1-32 h+*	Bioneer
V2-03-C11	***SPBC28F2.11::kanMX4***, *ade6-M210, ura4-D18, leu1-32 h+*	Bioneer
V2-10-F09	***msc1::kanMX4***, *ade6-M210, ura4-D18, leu1-32 h+*	Bioneer
V2-26-F11	***dad5::kanMX4***, *ade6-M210, ura4-D18, leu1-32 h+*	Bioneer
V2-01-C08	***dad3::kanMX4***, *ade6-M210, ura4-D18, leu1-32 h+*	Bioneer
V2-03-B02	***spc19::kanMX4***, *ade6-M210, ura4-D18, leu1-32 h+*	Bioneer
V2-32-H01	***dad2::kanMX4***, *ade6-M210, ura4-D18, leu1-32 h+*	Bioneer
V2-26-C06	***SPAC16E8.01::kanMX4***, *ade6-M210, ura4-D18, leu1-32 h+*	Bioneer
V2-47-D12	***rad2::kanMX4***, *ade6-M210, ura4-D18, leu1-32 h+*	Bioneer
V2-03-F12	***apn2::kanMX4***, *ade6-M210, ura4-D18, leu1-32 h+*	Bioneer
V2-13-C04	***rad13::kanMX4***, *ade6-M210, ura4-D18, leu1-32 h+*	Bioneer
V2-18-E08	***nth1::kanMX4***, *ade6-M210, ura4-D18, leu1-32 h+*	Bioneer
V2-22-B11	***exo1::kanMX4***, *ade6-M210, ura4-D18, leu1-32 h+*	Bioneer
V2-13-B05	***eme1::kanMX4***, *ade6-M210, ura4-D18, leu1-32 h+*	Bioneer
V2-20-F04	***SPBC18H10.19::kanMX4***, *ade6-M210, ura4-D18, leu1-32 h+*	Bioneer
V2-44-C4	***rad32::kanMX4***, *ade6-M210, ura4-D18, leu1-32 h+*	Bioneer
V2-44-E01	***rad51::kanMX4***, *ade6-M210, ura4-D18, leu1-32 h+*	Bioneer
V2-46-C5	***rad50::kanMX4***, *ade6-M210, ura4-D18, leu1-32 h+*	Bioneer
V2-46-D6	***rad22::kanMX4***, *ade6-M210, ura4-D18, leu1-32 h+*	Bioneer
V2-51-D10	***rad57::kanMX4***, *ade6-M210, ura4-D18, leu1-32 h+*	Bioneer
V2-21-F10	***ctp1::kanMX4***, *ade6-M210, ura4-D18, leu1-32 h+*	Bioneer
V2-54-G7	***rqh1::kanMX4***, *ade6-M210, ura4-D18, leu1-32 h+*	Bioneer

Strain	Genotype	Source
V2-44-H4	***crb2::kanMX***, *ade6-M210, ura4-D18, leu1-32 h+*	Bioneer
V2-03-A08	***mus7::kanMX***, *ade6-M210, ura4-D18, leu1-32 h+*	Bioneer
V2-30-A02	***rdl1::kanMX***, *ade6-M210, ura4-D18, leu1-32 h+*	Bioneer
V2-45-A7	***fbh1::kanMX4***, *ade6-M210, ura4-D18, leu1-32 h+*	Bioneer
V2-04-F06	***rlp1::kanMX***, *ade6-M210, ura4-D18, leu1-32 h+*	Bioneer
V2-11-G12	***ddb1::kanMX4***, *ade6-M210, ura4-D18, leu1-32 h+*	Bioneer
V2-12-G12	***rhp26::kanMX***, *ade6-M210, ura4-D18, leu1-32 h+*	Bioneer
V2-02-B04	***csn2::kanMX4***, *ade6-M210, ura4-D18, leu1-32 h+*	Bioneer
V2-26-C01	***csn1::kanMX4***, *ade6-M210, ura4-D18, leu1-32 h+*	Bioneer
V2-16-E10	***ubc13::kanMX4***, *ade6-M210, ura4-D18, leu1-32 h+*	Bioneer
V2-04-D02	***SPCC126.07c::kanMX4***, *ade6-M210, ura4-D18, leu1-32 h+*	Bioneer
V2-52-F11	***brl1::kanMX4***, *ade6-M210, ura4-D18, leu1-32 h+*	Bioneer
V2-29-A01	***pep3::kanMX4***, *ade6-M210, ura4-D18, leu1-32 h+*	Bioneer
V2-44-B6	***pub1::kanMX4***, *ade6-M210, ura4-D18, leu1-32 h+*	Bioneer
V2-10-B04	***SPBC21D10.09c::kanMX4***, *ade6-M210, ura4-D18, leu1-32 h+*	Bioneer
V2-11-F11	***rad8::kanMX4***, *ade6-M210, ura4-D18, leu1-32 h+*	Bioneer
V2-22-G11	***alg6::kanMX4***, *ade6-M210, ura4-D18, leu1-32 h+*	Bioneer
V2-10-F05	***vgl1::kanMX4***, *ade6-M210, ura4-D18, leu1-32 h+*	Bioneer
V2-21-G07	***SPBC887.15c::kanMX4***, *ade6-M210, ura4-D18, leu1-32 h+*	Bioneer
V2-03-A02	***wtf10::kanMX4***, *ade6-M210, ura4-D18, leu1-32 h+*	Bioneer
V2-48-B6	***SPAC1B3.01c::kanMX4***, *ade6-M210, ura4-D18, leu1-32 h+*	Bioneer
V2-52-G2	***SPAC17G8.06c::kanMX4***, *ade6-M210, ura4-D18, leu1-32 h+*	Bioneer

Strain	Genotype	Source
V2-52-E11	***SPAC15E1.04::kanMX4***, *ade6-M210, ura4-D18, leu1-32 h+*	Bioneer
V2-23-D05	***SPAC9E9.09c::kanMX4***, *ade6-M210, ura4-D18, leu1-32 h+*	Bioneer
V2-24-E07	***atp14::kanMX4***, *ade6-M210, ura4-D18, leu1-32 h+*	Bioneer
V2-25-F07	***SPAC1F12.07::kanMX4***, *ade6-M210, ura4-D18, leu1-32 h+*	Bioneer
V2-52-D3	***SPAC11D3.08c::kanMX4***, *ade6-M210, ura4-D18, leu1-32 h+*	Bioneer
V2-53-B4	***arf3::kanMX4***, *ade6-M210, ura4-D18, leu1-32 h+*	Bioneer
V2-22-E11	***hmt2::kanMX4***, *ade6-M210, ura4-D18, leu1-32 h+*	Bioneer
V2-24-F03	***coq7::kanMX4***, *ade6-M210, ura4-D18, leu1-32 h+*	Bioneer
V2-27-A03	***atp15::kanMX4***, *ade6-M210, ura4-D18, leu1-32 h+*	Bioneer
V2-32-F05	***atl1::kanMX4***, *ade6-M210, ura4-D18, leu1-32 h+*	Bioneer
V2-20-D10	***ctr5::kanMX4***, *ade6-M210, ura4-D18, leu1-32 h+*	Bioneer
V2-25-A08	***snz1::kanMX***, *ade6-M210, ura4-D18, leu1-32 h+*	Bioneer
V2-49-H1	***lcf1::kanMX***, *ade6-M210, ura4-D18, leu1-32 h+*	Bioneer
V2-10-C07	***SPAC521.04c::kanMX***, *ade6-M210, ura4-D18, leu1-32 h+*	Bioneer
V2-21-E04	***ogm4::kanMX4***, *ade6-M210, ura4-D18, leu1-32 h+*	Bioneer
V2-23-H01	***SPCC1450.03::kanMX***, *ade6-M210, ura4-D18, leu1-32 h+*	Bioneer
V2-44-E7	***png1::kanMX4***, *ade6-M210, ura4-D18, leu1-32 h+*	Bioneer
V2-54-B6	***psd1::kanMX***, *ade6-M210, ura4-D18, leu1-32 h+*	Bioneer
V2-18-C11	***sts1::kanMX4***, *ade6-M210, ura4-D18, leu1-32 h+*	Bioneer
V2-21-A08	***SPBC947.15c::kanMX4***, *ade6-M210, ura4-D18, leu1-32 h+*	Bioneer
V2-48-F01	***SPBC1A4.09::kanMX4***, *ade6-M210, ura4-D18, leu1-32 h+*	Bioneer
V2-03-B01	***SPBP8B7.31::kanMX4***, *ade6-M210, ura4-D18, leu1-32 h+*	Bioneer

Strain	Genotype	Source
V2-16-B10	***SPAC1071.05::kanMX4***, *ade6-M210, ura4-D18, leu1-32 h+*	Bioneer
V2-23-C02	***SPCC1739.06c::kanMX4***, *ade6-M210, ura4-D18, leu1-32 h+*	Bioneer
V2-15-D11	***mto1::kanMX4***, *ade6-M210, ura4-D18, leu1-32 h+*	Bioneer
V2-01-E11	***SPAC29A4.17c::kanMX4***, *ade6-M210, ura4-D18, leu1-32 h+*	Bioneer
V2-11-B04	***rad8::kanMX4***, *ade6-M210, ura4-D18, leu1-32 h+*	Bioneer
V2-53-E2	***mcp2::kanMX4***, *ade6-M210, ura4-D18, leu1-32 h+*	Bioneer
V2-20-D11	***ulp2::kanMX4***, *ade6-M210, ura4-D18, leu1-32 h+*	Bioneer
V2-22-E09	***mcl1::kanMX4***, *ade6-M210, ura4-D18, leu1-32 h+*	Bioneer
V2-01-H09	***ctf8::kanMX4***, *ade6-M210, ura4-D18, leu1-32 h+*	Bioneer
V2-27-B11	***ssb3::kanMX4***, *ade6-M210, ura4-D18, leu1-32 h+*	Bioneer
V2-31-C04	***swi3::kanMX4***, *ade6-M210, ura4-D18, leu1-32 h+*	Bioneer
V2-22-F07	***rpl1101::kanMX4***, *ade6-M210, ura4-D18, leu1-32 h+*	Bioneer
V2-27-B01	***rps23::kanMX4***, *ade6-M210, ura4-D18, leu1-32 h+*	Bioneer
V2-49-C12	***rpl1702:kanMX4***, *ade6-M210, ura4-D18, leu1-32 h+*	Bioneer
V2-10-G11	***rpl3001::kanMX4***, *ade6-M210, ura4-D18, leu1-32 h+*	Bioneer
V2-24-C11	***rpl2002::kanMX4***, *ade6-M210, ura4-D18, leu1-32 h+*	Bioneer
V2-28-A05	***rpl801::kanMX4***, *ade6-M210, ura4-D18, leu1-32 h+*	Bioneer
V2-28-E04	***cgr1::kanMX4***, *ade6-M210, ura4-D18, leu1-32 h+*	Bioneer
V2-27-D12	***rpl3202::kanMX4***, *ade6-M210, ura4-D18, leu1-32 h+*	Bioneer
V2-28-B12	***rpl2101::kanMX4***, *ade6-M210, ura4-D18, leu1-32 h+*	Bioneer
V2-25-A06	***rps801::kanMX4***, *ade6-M210, ura4-D18, leu1-32 h+*	Bioneer
V2-25-E07	***SPAC8C9.07::kanMX4***, *ade6-M210, ura4-D18, leu1-32 h+*	Bioneer

Strain	Genotype	Source
V2-26-A06	***SPAC1610.02c::kanMX***, *ade6-M210, ura4-D18, leu1-32 h+*	Bioneer
V2-02-C04	***rpl3703::kanMX***, *ade6-M210, ura4-D18, leu1-32 h+*	Bioneer
V2-02-F05	***rpl1801::kanMX***, *ade6-M210, ura4-D18, leu1-32 h+*	Bioneer
V2-31-C12	***arb1::kanMX4***, *ade6-M210, ura4-D18, leu1-32 h+*	Bioneer
V2-9-D04	***ago1::kanMX***, *ade6-M210, ura4-D18, leu1-32 h+*	Bioneer
V2-01-H07	***arb2::kanMX4***, *ade6-M210, ura4-D18, leu1-32 h+*	Bioneer
V2-28-H8	***nrl1::kanMX***, *ade6-M210, ura4-D18, leu1-32 h+*	Bioneer
V2-28-G06	***ers1::kanMX4***, *ade6-M210, ura4-D18, leu1-32 h+*	Bioneer
V2-27-G06	***cid14::kanMX4***, *ade6-M210, ura4-D18, leu1-32 h+*	Bioneer
V2-13-E09	***nab3::kanMX4***, *ade6-M210, ura4-D18, leu1-32 h+*	Bioneer
V2-27-H04	***SPBP8B7.28c::kanMX4***, *ade6-M210, ura4-D18, leu1-32 h+*	Bioneer
V2-02-G09	***SPBC2D10.16::kanMX4***, *ade6-M210, ura4-D18, leu1-32 h+*	Bioneer
V2-26-E06	***SPAC17C9.15c::kanMX4***, *ade6-M210, ura4-D18, leu1-32 h+*	Bioneer
V2-30-D01	***SPCC16C4.20c::kanMX4***, *ade6-M210, ura4-D18, leu1-32 h+*	Bioneer
V2-02-A03	***SPAC8C9.19::kanMX4***, *ade6-M210, ura4-D18, leu1-32 h+*	Bioneer
V2-03-D03	***mug42::kanMX4***, *ade6-M210, ura4-D18, leu1-32 h+*	Bioneer
V2-11-A07	***SPAC3H8.05c::kanMX4***, *ade6-M210, ura4-D18, leu1-32 h+*	Bioneer
V2-25-E05	***mhf2::kanMX4***, *ade6-M210, ura4-D18, leu1-32 h+*	Bioneer
V2-01-G08	***SPAC16E8.08::kanMX4***, *ade6-M210, ura4-D18, leu1-32 h+*	Bioneer
V2-02-A05	***SPAPB21F2.03::kanMX4***, *ade6-M210, ura4-D18, leu1-32 h+*	Bioneer
V2-02-G08	***SPBC21D10.08c::kanMX4***, *ade6-M210, ura4-D18, leu1-32 h+*	Bioneer
V2-03-A01	***SPBP8B7.26::kanMX4***, *ade6-M210, ura4-D18, leu1-32 h+*	Bioneer

Strain	Genotype	Source
V2-14-A09	***SPAC4H3.02c::kanMX4***, *ade6-M210, ura4-D18, leu1-32 h+*	Bioneer
V2-30-F10	***pmk1::kanMX4***, *ade6-M210, ura4-D18, leu1-32 h+*	Bioneer
V2-31-D07	***apm1::kanMX4***, *ade6-M210, ura4-D18, leu1-32 h+*	Bioneer
V2-44-C8	***sst2::kanMX4***, *ade6-M210, ura4-D18, leu1-32 h+*	Bioneer
V2-14-H10	***sin1::kanMX4***, *ade6-M210, ura4-D18, leu1-32 h+*	Bioneer
V2-53-C6	***ryh1::kanMX4***, *ade6-M210, ura4-D18, leu1-32 h+*	Bioneer
V2-03-A11	***SPBC26H8.05c::kanMX4***, *ade6-M210, ura4-D18, leu1-32 h+*	Bioneer
V2-29-B11	***dcn1::kanMX4***, *ade6-M210, ura4-D18, leu1-32 h+*	Bioneer
V2-03-C04	***SPAC1071.04c::kanMX4***, *ade6-M210, ura4-D18, leu1-32 h+*	Bioneer
V2-04-D05	***alp14::kanMX4***, *ade6-M210, ura4-D18, leu1-32 h+*	Bioneer
V2-11-G01	***stg1::kanMX4***, *ade6-M210, ura4-D18, leu1-32 h+*	Bioneer
V2-15-E02	***rga7::kanMX***, *ade6-M210, ura4-D18, leu1-32 h+*	Bioneer
V2-31-F11	***rap1::kanMX***, *ade6-M210, ura4-D18, leu1-32 h+*	Bioneer
V2-46-G12	***ccq1::kanMX***, *ade6-M210, ura4-D18, leu1-32 h+*	Bioneer
V2-31-A10	***est1::kanMX4***, *ade6-M210, ura4-D18, leu1-32 h+*	Bioneer
V2-11-B08	***trt1::kanMX***, *ade6-M210, ura4-D18, leu1-32 h+*	Bioneer
V2-03-H09	***SPBC16A3.08c::kanMX4***, *ade6-M210, ura4-D18, leu1-32 h+*	Bioneer
V2-01-G10	***php3::kanMX***, *ade6-M210, ura4-D18, leu1-32 h+*	Bioneer
V2-15-C12	***SPCC74.02c::kanMX4***, *ade6-M210, ura4-D18, leu1-32 h+*	Bioneer
V2-52-D4	***pap1::kanMX4***, *ade6-M210, ura4-D18, leu1-32 h+*	Bioneer
V2-04-D11	***SPAC144.02::kanMX4***, *ade6-M210, ura4-D18, leu1-32 h+*	Bioneer
V2-27-B02	***SPBC13E7.08c::kanMX4***, *ade6-M210, ura4-D18, leu1-32 h+*	Bioneer

Strain	Genotype	Source
V2-33-C11	***smd3::kanMX4***, *ade6-M210, ura4-D18, leu1-32 h+*	Bioneer
V2-50-A09	***ker1::kanMX4***, *ade6-M210, ura4-D18, leu1-32 h+*	Bioneer
V2-31-D10	***SPAC664.03::kanMX4***, *ade6-M210, ura4-D18, leu1-32 h+*	Bioneer
V2-20-A05	***cuf1::kanMX4***, *ade6-M210, ura4-D18, leu1-32 h+*	Bioneer
V2-51-F5	***pabp::kanMX4***, *ade6-M210, ura4-D18, leu1-32 h+*	Bioneer
V2-21-F04	***fkh2::kanMX4***, *ade6-M210, ura4-D18, leu1-32 h+*	Bioneer
V2-30-C02	***res2::kanMX4***, *ade6-M210, ura4-D18, leu1-32 h+*	Bioneer
V2-31-C02	***pob3::kanMX4***, *ade6-M210, ura4-D18, leu1-32 h+*	Bioneer
V2-44-F5	***nut2::kanMX4***, *ade6-M210, ura4-D18, leu1-32 h+*	Bioneer
V2-52-E01	***ssn6::kanMX4***, *ade6-M210, ura4-D18, leu1-32 h+*	Bioneer
V2-04-A08	***SPAC1071.02::kanMX4***, *ade6-M210, ura4-D18, leu1-32 h+*	Bioneer
V2-19-B05	***sep11::kanMX4***, *ade6-M210, ura4-D18, leu1-32 h+*	Bioneer
V2-30-A10	***SPAP14E8.02::kanMX4***, *ade6-M210, ura4-D18, leu1-32 h+*	Bioneer
V2-02-B07	***nrm11::kanMX4***, *ade6-M210, ura4-D18, leu1-32 h+*	Bioneer
V2-02-C11	***Sep1::kanMX4***, *ade6-M210, ura4-D18, leu1-32 h+*	Bioneer
V2-03-B06	***srb10::kanMX4***, *ade6-M210, ura4-D18, leu1-32 h+*	Bioneer
V2-16-B03	***SPBC21C3.02c::kanMX4***, *ade6-M210, ura4-D18, leu1-32 h+*	Bioneer
V2-20-E01	***SPCC4F11.04c::kanMX4***, *ade6-M210, ura4-D18, leu1-32 h+*	Bioneer
V2-23-H09	***SPAC17G8.11c::kanMX4***, *ade6-M210, ura4-D18, leu1-32 h+*	Bioneer
V2-02-G06	***SPBC15D4.06::kanMX4***, *ade6-M210, ura4-D18, leu1-32 h+*	Bioneer
V2-26-B10	***SPAC3A12.13c::kanMX4***, *ade6-M210, ura4-D18, leu1-32 h+*	Bioneer
V2-02-C07	***SPBC16C6.05::kanMX4***, *ade6-M210, ura4-D18, leu1-32 h+*	Bioneer

Strain	Genotype	Source
V2-28-D12	***tom13::kanMX***, *ade6-M210, ura4-D18, leu1-32 h+*	Bioneer
V2-24-C03	***SPBC27B12.08::kanMX***, *ade6-M210, ura4-D18, leu1-32 h+*	Bioneer
V2-43-E09	***vps1302::kanMX***, *ade6-M210, ura4-D18, leu1-32 h+*	Bioneer
V2-23-F12	***tlg2::kanMX4***, *ade6-M210, ura4-D18, leu1-32 h+*	Bioneer
V2-27-D10	***vps901::kanMX***, *ade6-M210, ura4-D18, leu1-32 h+*	Bioneer
V2-20-E10	***vps32::kanMX4***, *ade6-M210, ura4-D18, leu1-32 h+*	Bioneer
V2-25-C11	***sft1::kanMX***, *ade6-M210, ura4-D18, leu1-32 h+*	Bioneer
V2-28-B09	***sbh1::kanMX4***, *ade6-M210, ura4-D18, leu1-32 h+*	Bioneer
V2-02-D06	***arf6::kanMX4***, *ade6-M210, ura4-D18, leu1-32 h+*	Bioneer
V2-11-C08	***SPBC359.03c::kanMX4***, *ade6-M210, ura4-D18, leu1-32 h+*	Bioneer
V2-01-E03	***trm112::kanMX4***, *ade6-M210, ura4-D18, leu1-32 h+*	Bioneer
V2-53-D01	***pof12::kanMX4***, *ade6-M210, ura4-D18, leu1-32 h+*	Bioneer
V2-28-C10	***SPAC1F3.03::kanMX4***, *ade6-M210, ura4-D18, leu1-32 h+*	Bioneer
V2-25-F08	***mug176::kanMX4***, *ade6-M210, ura4-D18, leu1-32 h+*	Bioneer
V2-53-C11	***duf953::kanMX4***, *ade6-M210, ura4-D18, leu1-32 h+*	Bioneer
V2-44-D08	***SPAC31G5.19::kanMX4***, *ade6-M210, ura4-D18, leu1-32 h+*	Bioneer
V2-30-C11	***fkh2::kanMX4***, *ade6-M210, ura4-D18, leu1-32 h+*	Bioneer
V2-53-G06	***SPBC660.09::kanMX4***, *ade6-M210, ura4-D18, leu1-32 h+*	Bioneer
V2-02-F07	***SPBC1703.11::kanMX4***, *ade6-M210, ura4-D18, leu1-32 h+*	Bioneer
V2-03-E12	***swd3::kanMX4***, *ade6-M210, ura4-D18, leu1-32 h+*	Bioneer
V2-04-D04	***btb1::kanMX4***, *ade6-M210, ura4-D18, leu1-32 h+*	Bioneer
V2-13-G12	***SPCC4B3.03c::kanMX4***, *ade6-M210, ura4-D18, leu1-32 h+*	Bioneer

Strain	Genotype	Source
V2-33-D09	***SPCC1739.01::kanMX4****, ade6-M210, ura4-D18, leu1-32 h+*	Bioneer
V2-47-G-2	***clr4::kanMX4****, ade6-M210, ura4-D18, leu1-32 h+*	Bioneer
V2-06-D08	***swi6::kanMX4****, ade6-M210, ura4-D18, leu1-32 h+*	Bioneer
TH8121	***arb2::kanMX4, rad51::ura4-rad51-eCFP*** *ade6-M210, ura4-D18, leu1-32*	This study
TH8122	***ago1::kanMX4, rad51::ura4-rad51-eCFP*** *ade6-M210, ura4-D18, leu1-32*	This study
TH8123	***nrl1::kanMX4, rad51::ura4-rad51-eCFP*** *ade6-M210, ura4-D18, leu1-32*	This study
TH8124	***est1::kanMX4, rad51::ura4-rad51-eCFP*** *ade6-M210, ura4-D18, leu1-32*	This study
TH3607	***rad51::ura4-rad51-eCFP*** *ade6-M210, ura4-D18, leu1-32*	Lab stock
TH8104	***nrl1::kanMX4 -nrl1-YFP*** *ade6-M210, ura4-D18, leu1-32*	This study
TH8125	***nrl1::kanMX4, rad11::kanMX4-rad11-GFP*** *ade6-M210, ura4-D18, leu1-32*	This study
TH2151	***rad11::kanMX4-rad11-GFP*** *ade6-M210, ura4-D18, leu1-32*	Lab stock
TH8143	***nrl1::kanMX4, tlh1::ura4****, ade6-M210, ura4-D18, leu1-32*	This study
TH8142	***nrl1::kanMX4, otr1::ura4,*** *ade6-M210, ura4-D18, leu1-32*	This study
TH4970	***tlh1::ura4****, ade6-M210, ura4-D18, leu1-32*	Lab stock
TH6150	***otr1::ura4,*** *ade6-M210, ura4-D18, leu1-32*	Lab stock
TH584	***rad2 ::ura4****, ade6-M210, ura4-D18, leu1-32*	Lab stock
TH8126	***nrl1::kanMX4, rad2::ura4****, ade6-M210, ura4-D18, leu1-32*	This study
TH558	***ku70::ura4*** *leu1-32 ade6 216 or 210 ura4-D18 his3-DI h+*	Lab stock
TH8140	***nrl1::kanMX4,ku70::ura4*** *leu1-32 ade6 216 or 210 ura4-D18 his3-DI h+*	This study
TH585	***rad3::ura4****, leu1-32, ade6M216*	Lab stock
TH8127	***nrl1::kanMX4, rad3::ura4****, leu1-32, ade6M216*	This study
V2-12-C05	***sen1::kanMX4****, ade6-M210, ura4-D18, leu1-32 h+*	Bioneer

Strain	Genotype	Source
TH8110	***nrl1::kanMX4, sen1::kanMX4****, ade6-M210, ura4-D18, leu1-32 h+*	This study
TH8107	***nrl1::kanMX4***, ***mrc1::kanMX4****, ade6-M210, ura4-D18, leu1-32 h+*	This study
V2-10-A07	***mrc1::kanMX4****, ade6-M210, ura4-D18, leu1-32 h+*	Bioneer
V2-20-D07	***sty1::kanMX4****, ade6-M210, ura4-D18, leu1-32 h+*	Bioneer
TH8114	***nrl1::kanMX4, sty1::kanMX4****, ade6-M210, ura4-D18, leu1-32 h+*	This study
V2-45-F4	***cph1::kanMX4****, ade6-M210, ura4-D18, leu1-32 h+*	Bioneer
TH8111	***nrl1::kanMX4****, cph1****::kanMX4****, ade6-M210, ura4-D18, leu1-32 h+*	This study
V2-45-B05	***rtt109::kanMX4****, ade6-M210, ura4-D18, leu1-32 h+*	Bioneer
TH8112	***nrl1::kanMX4, rtt109::kanMX4, ade6-M210, ura4-D18, leu1-32 h+***	This study
V2-15-C11	***cds1::kanMX4****, ade6-M210, ura4-D18, leu1-32 h+*	Bioneer
TH8106	***nrl1::kanMX4, cds1::kanMX4****, ade6-M210, ura4-D18, leu1-32 h+*	This study
V2-19-B01	***duf1716::kanMX4****, ade6-M210, ura4-D18, leu1-32 h+*	Bioneer
TH8113	***nrl1::kanMX4***, ***duf1716::kanMX4****, ade6-M210, ura4-D18, leu1-32 h+*	This study
V2-10-E9	***SPAC23H4.08::kanMX4****, ade6-M210, ura4-D18, leu1-32 h+*	Bioneer
TH8109	***nrl1::kanMX4, SPAC23H4.08::kanMX4****, ade6-M210, ura4-D18, leu1-32 h+*	This study
V2-19-G11	***sdh4::kanMX4****, ade6-M210, ura4-D18, leu1-32 h+*	Bioneer
TH8108	***nrl1::kanMX4, sdh4::kanMX4****, ade6-M210, ura4-D18, leu1-32 h+*	This study
TH8128	***dcr1::kanMX4, rad51::ura4-rad51-eCFP*** *ade6-M210, ura4-D18, leu1-32*	This study
TH8129	***arb1::kanMX4, rad51::ura4-rad51-eCFP*** *ade6-M210, ura4-D18, leu1-32*	This study
TH8130	***clr4::kanMX4, rad51::ura4-rad51-eCFP*** *ade6-M210, ura4-D18, leu1-32*	This study
TH8131	***swi6::kanMX4, rad51::ura4-rad51-eCFP*** *ade6-M210, ura4-D18, leu1-32*	This study

Table 2.2 Minichromosome strains used in this study

Strain	Genotype	pREP81X-HO	pREP81X
TH2125/6	*leu1-32 arg3-D4 ade6-M210 ura4-D18 his3-D1* **Ch^{16}-RMGAH**	TH2130-2	TH2357
TH2654/3165	*leu1-32 arg3-D4 ade6-M210 ura4-D18 his3-D1* **Ch^{16}-RMYAH**	TH4104, 4121-2 (6815 pREP82X-HO)	TH4125
TH4252	*leu1-32 arg3-D4 ade6-M210 ura4-D18 his3-D1 mat1_m-cyhS, smt0; rpl42::cyhR* (sP56Q) *h-* **Ch^{16}-LMYAU**	(-)	(-)
OC64-65	***atg22::kanMX4,*** *ade6-210 arg3-D4 his3-D1 leu1-32 ura4-D18* **Ch^{16}-RMYAH**	OC178-180	OC181-183
OC42	***mik1::kanMX4,*** *ade6-210 arg3-D4 his3-D1 leu1-32 ura4-D18* **Ch^{16}-RMYAH**	OC102-104	OC105
OC66/67	***csk1::kanMX4,*** *ade6-210 arg3-D4 his3-D1 leu1-32 ura4-D18* **Ch^{16}-RMYAH**	OC160-162	OC163-165
OC87	***pht1::kanMX4,*** *ade6-210 arg3-D4 his3-D1 leu1-32 ura4-D18* **Ch^{16}-RMYAH**	OC320-322	O238-240
OC65	***cph1::kanMX4,*** *ade6-210 arg3-D4 his3-D1 leu1-32 ura4-D18* **Ch^{16}-RMYAH**	OC117-119	OC351
OC74/75	***exo1::kanMX4,*** *ade6-210 arg3-D4 his3-D1 leu1-32 ura4-D18* **Ch^{16}-RMYAH**	OC207-209	OC210-212
OC319	***apn2::kanMX4,*** *ade6-210 arg3-D4 his3-D1 leu1-32 ura4-D18* **Ch^{16}-RMYAH**	OC315-317	OC318
OC352	***rad13::kanMX4,*** *ade6-210 arg3-D4 his3-D1 leu1-32 ura4-D18* **Ch^{16}-RMYAH**	OC 297-299	OC300
OC72/73	***rad50::kanMX4,*** *ade6-210 arg3-D4 his3-D1 leu1-32 ura4-D18* **Ch^{16}-RMYAH**	OC196-198	OC199-200
OC52/53	***rad22::kanMX4,*** *ade6-210 arg3-D4 his3-D1 leu1-32 ura4-D18* **Ch^{16}-RMYAH**	OC172-174	OC157-177
OC68/69	***rqh1::kanMX4,*** *ade6-210 arg3-D4 his3-D1 leu1-32 ura4-D18* **Ch^{16}-RMYAH**	OC166-168	OC169-171
OC287	***fbh1::kanMX4,*** *ade6-210 arg3-D4 his3-D1 leu1-32 ura4-D18* **Ch^{16}-RMYAH**	OC288-290	OC291
OC41	***csn1::kanMX4,*** *ade6-210 arg3-D4 his3-D1 leu1-32 ura4-D18* **Ch^{16}-RMYAH**	OC96-98	OC99-100
OC62/63	***SPCC126.07c::kanMX4,*** *ade6-210 arg3-D4 his3-D1 leu1-32 ura4-D18* **Ch^{16}-RMYAH**	OC202-204	OC204-206
OC353	***alg6::kanMX4,*** *ade6-210 arg3-D4 his3-D1 leu1-32 ura4-D18* **Ch^{16}-RMYAH**	OC154-156	OC157-159
OC259-261	***atd1::kanMX4,*** *ade6-210 arg3-D4 his3-D1 leu1-32 ura4-D18* **Ch^{16}-RMYAH**	OC274-276	OC277-279

Strain	Genotype	pREP81X-HO	pREP81X
OC58-59	***SPAC521.04c::kanMX4,*** *ade6-210 arg3-D4 his3-D1 leu1-32 ura4-D18* **Ch^{16}-RMYAH**	OC213-215	OC216-217
OC78-79	***swi3::kanMX4,*** *ade6-210 arg3-D4 his3-D1 leu1-32 ura4-D18* **Ch^{16}-RMYAH**	OC137-139	OC140-141
OC50/51	***rps23::kanMX4,*** *ade6-210 arg3-D4 his3-D1 leu1-32 ura4-D18* **Ch^{16}-RMYAH**	OC24-26	OC250-252
OC82/83	***cgr1::kanMX4,*** *ade6-210 arg3-D4 his3-D1 leu1-32 ura4-D18* **Ch^{16}-RMYAH**	OC106-108	OC109-111
OC292	***arb2::kanMX4,*** *ade6-210 arg3-D4 his3-D1 leu1-32 ura4-D18* **Ch^{16}-RMYAH**	OC293-295	OC296
OC70/71	***nrl1::kanMX4,*** *ade6-210 arg3-D4 his3-D1 leu1-32 ura4-D18* **Ch^{16}-RMYAH**	OC184-186	OC187-189
OC303	***ago1::kanMX4,*** *ade6-210 arg3-D4 his3-D1 leu1-32 ura4-D18* **Ch^{16}-RMYAH**	OC327-329	OC330-332
OC43/44	***est1::kanMX4,*** *ade6-210 arg3-D4 his3-D1 leu1-32 ura4-D18* **Ch^{16}-RMYAH**	OC101	OC324,326
OC262-264	***fkh2::kanMX4,*** *ade6-210 arg3-D4 his3-D1 leu1-32 ura4-D18* **Ch^{16}-RMYAH**	OC280-282	OC283-285
OC85/86	***res2::kanMX4,*** *ade6-210 arg3-D4 his3-D1 leu1-32 ura4-D18* **Ch^{16}-RMYAH**	OC112-113	OC114-116
OC304	***paf1::kanMX4,*** *ade6-210 arg3-D4 his3-D1 leu1-32 ura4-D18* **Ch^{16}-RMYAH**	OC305-307	OC308
OC314	***pmk1::kanMX4,*** *ade6-210 arg3-D4 his3-D1 leu1-32 ura4-D18* **Ch^{16}-RMYAH**	OC311-313	OC310
OC325	***rtt109::kanMX4,*** *ade6-210 arg3-D4 his3-D1 leu1-32 ura4-D18* **Ch^{16}-RMYAH**	OC133	OC134-136
TH8144	***loh-2,*** *ade6-210 arg3-D4 his3-D1 leu1-32 ura4-D18* **Ch^{16}-RMGAH**	TH8145-8147	TH8148
LOH330	***loh-5,*** *ade6-210 arg3-D4 his3-D1 leu1-32 ura4-D18* **Ch^{16}-RMGAH**	TH8150/8151	TH8152
LOH333	***loh-6,*** *ade6-210 arg3-D4 his3-D1 leu1-32 ura4-D18* **Ch^{16}-RMGAH**	TH8115/8116	TH8117
LOH334	***loh-7,*** *ade6-210 arg3-D4 his3-D1 leu1-32 ura4-D18* **Ch^{16}-RMGAH**	TH8118/8119	TH8120
TH3226	***rad17::kanMX4,*** *ade6-210 arg3-D4 his3-D1 leu1-32 ura4-D18* **Ch^{16}-RMGAH**	TH3245-3247	TH3246
TH6406-6408	***rad17::kanMX4,*** *ade6-210 arg3-D4 his3-D1 leu1-32 ura4-D18* **Ch^{16}-L5-RMGAH**	TH6451-6453	TH6454-6456

Strain	Genotype	pREP81X-HO	pREP81X
TH5805-5807	*ade6-210 arg3-D4 his3-D1 leu1-32 ura4-D18* **Ch^{16}-L5-RMGAH**	TH5854	TH5856
OC301	***swi6::kanMX4,*** *ade6-210 arg3-D4 his3-D1 leu1-32 ura4-D18* **Ch^{16}-RMYAH**	OC333-335	OC336-338
OC302	***dcr1::kanMX4,*** *ade6-210 arg3-D4 his3-D1 leu1-32 ura4-D18* **Ch^{16}-RMYAH**	TH7775-7777	TH7774
OC303	***arb1::kanMX4,*** *ade6-210 arg3-D4 his3-D1 leu1-32 ura4-D18* **Ch^{16}-RMYAH**	OC345-347	OC348-350

OC: Orange Cap collection; TH: Tim Humphrey group collection; LOH: LOH collection.

[1]: made by Dr. Lydia Hulme; [2]: made by Dr. Helen Tinline-Purvis; [3]: made by Dr. Jason Cullen.

Mating types are shown where possible; mating type is not shown where multiple isolates were constructed and consequently $h^+$and h^- strains exist.

Minichromosome genotypes:

Ch^{16}-*RMGAH* (Ch^{16} *yps1::arg3*$^+$*ert1::MAT*a-*kanMX ade6-M216 cid2::his3*$^+$)

Ch^{16}-*RMYAH* (Ch^{16} *yps1::arg3*$^+$*ert1::MAT*a-*hph ade6-M216 cid2::his3*$^+$)

2.5 Plasmids

Plasmids used during this study are described in **Appendix I**.

2.6 Storage and Growth conditions

2.6.1 Growth and storage of *E. coli* strains

E.coli transformed with plasmid DNA were plated onto LB + ampicillin, and incubated O/N at 37°C to obtain single bacterial colonies. For small-scale plasmid DNA preparation (Miniprep), single *E. coli* colonies were picked from LB + ampicillin plates, inoculated into 2 ml LB + ampicillin media and cultured O/N at 37°C with shaking (300 rpm). For large-scale plasmid DNA preparations (Maxiprep), a 3 ml culture from a single colony was grown for 6-8 hours and used to prepare a 500 ml culture. This was subsequently cultured O/N at 37°C with agitation (300 rpm). Stocks of *E. coli* strains were stored in Nunc cryo-tubes containing 0.5 ml of prepared culture and 0.5 ml of glycerol at -80°C.

2.6.2 Growth and storage of *S. pombe* strains

Yeast strains were cultured and stored as published in Moreno *et al.*, 1991. Cells were cultured in either non-selective, nutrient rich media (YE6S), Edinburgh minimal media (EMM), or minimal glutamate (PMG) media with appropriate amino acid supplements. Strains were grown at 32°C for 2-3 days and then stored at room temperature. Liquid cultures were prepared by inoculation of a single colony or a loop of cells, taken from a fresh agar plate, into liquid YE6S, EMM, or PMG media. Cultures were grown overnight with agitation (220 rpm) at 32°C. The absorbance at 595 nm (optical density OD_{595}) in a Pharmacia Biotech Ultraspec 2000 was used to measure the concentration of the cells; an OD_{595} of 0.1 being ~2 x 10^6 cells/ml. Unless stated, cultures were maintained in mid-

exponential growth between 2 x 10^6 and 1 x 10^7 cells/ml (OD_{595} between 0.1 to 0.5). Permanent stocks of yeast strains were stored in Nunc cryo-tubes in 0.5 ml YE6S and 0.5 ml YFM at -80°C.

2.6.5 Genetic crosses, tetrad and free spore analysis

Yeast strains of opposite mating types (h^- and h^+) were mixed on SPAS6 agar plates with 10 µl MQ water, and incubated at 25°C for 48 h. Light microscopy was used to confirm asci formation. Selection of desired genotype occurred by either free spore analysis or tetrad dissection. For free spore analysis, a 1 µl loop of cells was suspended in a 1:200 dilution of β-glucoronidase and incubated at 25°C for 24 h, or 37°C for 4 h with agitation. 150 µl of a 1:100 dilution was plated onto YE6S and grown at 32°C for 4-5 days. Subsequently, colonies were replica-plated on selective plates.

For tetrad analysis, a 1 µl loop of the mating mix was suspended in 500 ml MQ water and 1 µl of the suspension was streaked onto one side on a flat YE6S plate. The asci were micromanipulated onto a virtual grid on the plate using a Singer Instruments MSM tetrad system. Following tetrad separation, the plate was incubated at 17°C overnight, to allow the asci walls to break down. The released spores were placed onto separate grid-points and allowed to grow into individual colonies at 32°C. The colonies were replica-plated onto selective plates to allow selection for desired genotype.

2.6.6 Analysis of cell growth and viability

2.6.6.1 Serial dilution assay

Viability of strains on selective plates, *i.e*. CPT, MMS, Bleomycin/Bleocin as well as 5-FOA was tested using spot-dilutions. Log-phase cells were diluted to a cell density of 2 x

10^6 cells/ml (OD_{595} 0.2) and subsequently diluted 5-fold before being spotted (8 µl) onto YE6S and selective plates. The plates were then incubated at 32°C for 2-3 days. Damaging agents were used at indicated concentrations.

2.6.7 Losing the minichromsome from *S. pombe* strains

10 ml medium was inoculated with cells and grown at 32°C for 3 days, maintaining the cells in logarithmic growth phase (OD_{595} 0.1-0.5). An appropriate amount of the culture was plated onto YE6S plates, and replicated-plated when colonies were visible, to detect minichromosome loss.

2.7 Transformation of cells

2.7.1 Transformation of *E. coli*

2.7.1.1 Preparation of competent bacteria

A 5 ml LB culture was started by inoculation of a single DH5α colony and was grown overnight at 37°C with agitation (300 rpm). A 1:100 dilution of the overnight culture was subsequently grown for 1-2 hours at 37°C until OD_{595} reached 0.6. Cells were incubated on ice for 15 minutes and then centrifuged at 1730 *g* for 15 minutes at 4°C. The pellet was resuspended in 20 ml cold 50 mM $CaCl_2$ and chilled on ice for 15 minutes. The cells were then centrifuged at 1730 *g* for 10 minutes at 4°C, the pellet resuspended in 1 ml cold 50 mM $CaCl_2$ and left on ice for 15 minutes. Cells were immediately frozen and stored at -80°C.

2.7.1.2 Transformation of *E. coli*

150 ml CaCl2 competent DH5aTM cells were incubated on ice with 50 ng of plasmid DNA for 10 min, then heat-shocked at 42°C for 45 sec and returned to ice for 2 min. 1 ml

LB broth was added and the mixture incubated at 37°C for 30 min. Subsequently, the suspension was harvested by brief centrifugation and resuspended in 150 µl LB medium. Transformants were selected on LB + Amp plates following overnight incubation at 37°C.

2.7.2 Transformation of *S. pombe*

2.7.2.1 Transformation by electroporation

50 ml culture was incubated at 32°C until OD_{595} reached 0.3-0.5, and was cooled on ice for 10 min. Subsequently, cells were centrifuged at 1000 *g* for 2 min, washed once with MQ water, once with 1 M sorbitol, and then resuspended in 1 ml 1 M sorbitol. The cell suspension was sedimented at 15700 *g* for 10 sec and the pellet resuspended in 1 M sorbitol at a 1:1 ratio. 45 µl of cells were mixed with 1 µg DNA in a chilled electroporation cuvette (0.1 cm gap), and electroporation was carried out at:

- Field strength, 0.66 kV/cm
- Resistance 200 Ω
- Capacitance, 25 µF.

600 µl 1 M sorbitol was immediately added to the cells and 150 µl was plated onto selective media and grown at 32°C for 4 days.

2.7.2.2 Transformation by LiAc method

Cells from 50 ml log-phase cultures were harvested by centrifugation at 2000 rpm for 2 min, washed in 25 ml MQ, and resuspended in 1 ml 100 mM LiAc. A 50 ml sample was subjected to centrifugation at 2000 rpm for 2 min and resuspended in transformation mixture:

- 36 µl 1M LiAc
- 100 µl DNA (in MQ water)

- 10 µl ssDNA (boiled salmon sperm)
- 240 µl 50 % PEG

The suspension was incubated for at 30°C 2-5 h and subsequently heat-shocked at 42°C for 30 min. The transformation mixture was sedimented by centrifugation (2000 rpm, 2 min), resuspended in 500 ml MQ and 150 ml were spread onto three selective plates, respectively.

2.7.2.3 PLATE method

A loop of cells were suspended in 500 µl of PLATE solution, with 10 µl ssDNA (boiled salmon sperm DNA), and 1 µg of plasmid DNA. The solution was incubated at room temperature for at least 2 d. Cells were harvested by centrifugation at 17,000 g for 30 sec, resuspended in 200 µl MQ water, and plated onto appropriate selective media plates.

2.8 DNA isolation

2.8.1 Isolation of plasmid DNA from *E. coli* (Miniprep and Maxiprep)

An overnight LB culture was inoculated with a single colony. Mini- and Maxi-preparations were carried out according to manufacturer's instructions (QIAGEN), based on rapid alkaline lysis. DNA was stored at -20°C.

2.8.2 Isolation of *S. pombe* genomic DNA

Genomic DNA was isolated and purified using the MasterPure™ Yeast DNA Purification Kit (Epicentre), as per manufacturer's instructions. Genomic DNA was stored at -20°C.

2.8.3 Isolation of DNA from agarose gels

DNA was first separated by agarose gel electrophoresis (0.8% agarose gel). The desired band was excised and the DNA extraced using a QIAGEN Gel Extraction Kit, according to manufacturer's instructions.

2.8.4 PCR purification

DNA from PCR was purified using QIAGEN PCR Purification Kit, according to manufacturer's instructions.

2.9 Manipulation and analysis of DNA

2.9.1 Restriction digestion and dephosphorylation of DNA

Restriction digests were carried out in 10 µl reactions with 1x buffer (NEB), 1x BSA, 50 ng DNA and 10 U restriction enzyme. Digests were incubated at appropriate temperatures for at least 2 hours, and enzymes inactivated accordingly to manufacturer's instructinos. If required, DNA was dephosphorylated by adding 10 U calf-intestinal alkaline phosphatase (CIP) and incubating at 37°C for 30 mins.

2.9.2 DNA ligation

A typical ligation reaction consisted of 50 ng de-phosphorylated linear DNA, a 3-5 fold molar excess of insert, 1x Quick ligation buffer and 10 U Quick ligase™ (NEB), incubated at room temperature for 5 min. This step has been applied in numerous variations, when appropriate.

2.9.3 Polymerase Chain Reaction (PCR)

The polymerases used to amplify DNA were Phusion™ or Taq (both from NEB). For Phusion PCR, a typical reaction consisted of:

- 1x Phusion GC buffer
- 800 µM dNTP mix
- 0.5 µM forward and reverse primers
- 50 ng template DNA
- 3% DMSO and 1 U Phusion polymerase

For Taq PCR, a typical reaction consisted of:

- x Taq buffer
- 800 M dNTP mix
- 0.5 µM forward and reverse primers
- 50 ng template DNA
- 1 U Taq polymerase.

For colony PCR, Megamix Blue was used. In this case, one loop of cells was incubated in water for 15 min at 95°C. 2 µl of the suspension were added to 18 µl Megamix Blue, and primers added to 0.5 µM. Oligonucleotides used in this study are shown in **Appendix II**.

Standard PCR conditions used:

- 94°C for 5 minutes
- 30 cycles (94°C for 20 seconds, X°C for 30 seconds, 68°C for Y minutes)
- 68°C for 7 minutes.

The extension time (Y) was determined by size of PCR product and processivity of polymerase (Phusion^{TM} 15-30 sec/kb; Taq 1 min/kb). The annealing temperature (X), was generally set at 4°C below the lowest melting temperature of the forward and reverse primers.

2.9.4 Quantification of DNA samples

DNA concentration was determined using a Nanodrop 1000 spectrophotometer (Thermo Scientific). Samples were diluted in MQ or TE buffer to appropriate concentrations and absorbance was measured at 260 nm and 280 nm. An A_{260}/A_{280} ratio of 1.8 signifies a pure DNA solution, with low levels of salt/protein contamination. Concentration was calculated in μg/μl.

2.9.5 DNA sequencing

Purified plasmid or PCR DNA was sequenced by Source BioScience LifeSciences (Oxford). Whole genome sequencing was carried out at Wellcome Trust Centre for Human Genetics (Oxford).

2.9.6 Analysis of DNA by gel electrophoresis

2.9.6.1 Agarose gel electrophoresis

Linear DNA was resolved using 1 % TAE agarose gel containing 5 μg ethidium bromide and run at 80 V for 1 hour, and visualised using an UV transilluminator (BioRad).

2.10 DNA DSB repair assays

2.10.1 The sectoring assay

Strains from the Bioneer V2-deletion library were transformed with the non-essential minichromosome Ch^{16}-*LMYAU* (Leu2, MATa, HygB, Ade-m216, Uracil), carrying an endogenous copy of the HO-endonuclease gene under an 'nmt' (no message in thiamin) promoter. Following growth on selective media, containing 2 μM of thiamine, cells were diluted in MQ water and plated onto sectoring plates, which contained EMM+

- $LRHUA_L$+/- T to identify break-dependent, and independent Ch^{16} loss

- $RHUA_L$+/- T to identify break-dependent, and independent LOH.

Plates were incubated at 32°C for 2-3 d, and subsequently kept at 4°C for 2 d prior to analysis.

Sectoring strains were confirmed by reproduction of the assay for 2 further times.

Table 2.3 Outcomes of the colony-sectoring assay

	$LRHUA_LT$	**$LRHUA_L$**	**$RHUA_LT$**	**$RHUA_L$**
Break-dependent Ch^{16} loss	Sectored	Sectored	White	White
Break-independent Ch^{16} loss	White	Sectored	White	White
Break-dependent LOH	Sectored	Sectored	Sectored	Sectored
Break-independent LOH	White	Sectored	White	Sectored

2.10.2 The DSB assay

Three isolates of Ch^{16}-*RMGAH* or Ch^{16}-*RMYAH* strains for each mutant background were transformed with pREP81X-HO plasmid (p28), or a blank plasmid, pREP81X (p40). A wild-type strain was analysed alongside as a control. Transformed strains were grown and kept on selective media to ensure maintenance of the minichromosome under non-inducing conditions (-T). For break-induction, 20 mL of selectively grown over-night cultures were diluted to OD_{595} 0.1 in the morning and grown for 3 h at 32°C. Subsequently, cells were harvested (3000 g, 5 min), and washed twice with PBS. Pellets were resuspendend in EMM+RAHU (-T; DSB on), diluted and cultures were incubated for 48 h at 32°C with agitation. Cultures were maintained in logarithmic growth phase by dilution. Following break-induction, cells were harvested (3000 g, 5 min), and resuspended in YE6S media. The equivalent of 20 µl of an OD_{595} 0.2 culture was inoculated into 10 ml YE6S, and 150 µl were plated onto three YE6S solid plates, yielding approximately 200 colonies per plate. When colonies were visible, plates were replica-plated onto selective plates to

determine the genotypes of the colonies. Based on loss or retention of markers following break-induction, a DNA repair profile could be deduced, see **Table 2.4**. Utilising this assay, following repair events can be differentiated, based on the genotype of the colonies:

- Non-homologous end-joining (NHEJ)/sister chromatid conversion (SCC)
- Interchromosomal gene conversion (GC)
- Minichromosome loss (Ch^{16} loss)
- Loss of heterozygosity (LOH)

Spontaneous levels of Ch^{16} loss, GC or LOH, calculated from the blank plasmid controls, were subtracted from the levels observed following break induction to give final levels of break-dependent outcomes and control for leakage.

Table 2.4 Outcomes of the DSB assay and the marker loss linked with each event

Ch^{16}	Replica plating	Outcome			
		NHEJ/SCC	GC	Ch^{16} loss	LOH
RMYAH	EMM+ AHULT (arg-)	arg^+	arg^+	arg^-	arg^+
	EMM+ RHULT (ade-)	ade^+	ade^+	ade^-	ade^-
	EMM+ RAULT (his-)	his^+	his^+	his^-	his-
	YE6S + hyg	hyg^R	hyg^S	hyg^S	hyg^S
RMGAH	EMM+ AHULT (arg-)	arg^+	arg^+	arg^-	arg^+
	EMM+ RHULT (ade-)	ade^+	ade^+	ade^-	ade^-
	EMM+ RAULT (ura-)	his^+	his^+	his^-	his-
	YE6S + G418	$G418^R$	$G418^S$	$G418^S$	$G418^S$

2.11 Microscopy

2.11.1 Light microscopy

Cells were visualised via light microscopy utilising a Nikon microscope-Eclipse E-E400 with a 10x/20x, or 50x objective lens. Cells growing on agar plates were visualised by

streaking out using a sterile toothpick. Cells growing in culture were visualised by adding 8 µl culture to a microscope slide with coverslip.

2.11.2 Fluorescence microscopy

To monitor foci formation of DNA repair proteins following break-induction, asynchronous cultures were treated with 50 Gy of ionising radiation (IR) using a ^{137}Cs source with a dose rate of 2.8 Gy per minute, or left untreated. 5 ml aliquots were harvested (3000 g, 5 min), washed with MQ water, fixed by incubation on ice in 100% methanol, and stored in 100% acetone at -20°C. Samples were rehydrated and stained with 6'-diamidino-2-phenylindole (DAPI) and mounted (ProLong® Gold antifade rearent with DAPI; Invitrogen), and examined with a Zeiss Axioplan 2ei microscope, Hamamatsu Orca ER camera and micromanager software.

2.12 Protein extraction, manipulation, and analysis

2.12.1 TCA protein extraction

Per sample, approximately $1x10^8$ cells were harvested by centrifugation (3000 g, 2 min), and the pellet was resuspended in 1 ml 1.2 M sorbitol. The suspension was harvested at 16100g, for 30 sec, and the pellet resuspended in 100 µl 20% trichloroacetic acid (TCA), and agitated by vortex. Glass beads were added to 0.5 ml volume, and the tubes vortexed for 5-10 min at 4°C. 900 µl of 5% TCA was added and the tube was vortexted for 1 min. The solution was separated from the glass beads and centrifuged at 800 g for 10 min; the protein pellet was resuspended in 250 µl 1 x Laemmli buffer, and boiled for 3 min. The extract was centrifuged at 800 g for 10 minutes, the supernatant was stored at -20°C.

2.12.2 Histone preparation

A 1 l culture of non-selectively grown cells in logarithmic growth phase were harvested by centrifugation (3000 g, 5 min) at 4°C, washed with 400 ml MQ water, and centrifuged again. Cells were resuspended in 50 ml DTT (added freshly)/Tris-HCl, pH 9.5 and incubated at 30°C for 15 min, with shaking, and spun as above. Pellet was resuspended in 50 ml Sorbitol/Hepes buffer (Buffer 2), and centrifuged. Sediment was resuspended in 50 ml Buffer 2, and 1-2 ml zymolase (10 mg/ml) was added. Solution was incubated at 30°C, for 45-60 min. Subsequently, 100 ml ice-cold Buffer 3 (Sorbitol/Pipes/MgCl2) was added and centrifuged at 3.5K (JA10 rotor) for 5 min at 4°C. Pellet was resuspended in 50 ml ice-cold NIB buffer, held on ice for 20 min, and spun at 4K (JA10 rotor) for 5 min at 4°C. The wash with NIB buffer was repeated twice, holding the solution on ice for 20 min each time. Harvest was resuspended in 50 ml Buffer A, and held on ice for 15 min, and centrifuged as above for 5 mins. Buffer A wash was repeated. Pellet was resuspended in 50 ml Buffer B, held on ice for 5 min, and centrifuged as above for 5 minutes. Pellet was resuspended in 25 ml B wash and spun immediately. Pellet was resuspended in 10 ml cold 0.8M H_2SO_4 to extract histones, and held on ice for 30 min, with occasional agitation. Histones were spun at 10K for 10 min, supernatant saved. 100% TCA were added to a final concentration of 20%, and held on ice for 30 min. Histones were spun at 12K for 30 min, and washed with 10 ml acid acetone (acetone + 0.1% concentrated HCl), and spun for 5 min at 10K. Pellet was washed in cold acetone and centrifuged at 10K for 5 min. Acetone was decanted, and the pellet air-dried. Pellets were resuspended in a total of 1 ml of 10 mM Tris-Hcl, pH 8.0. Histones were stored at -20°C.

2.12.3 SDS-polyacrylamide gel-electrophoresis (SDS-PAGE)

Protein extracts were separated on commercially available SDS-PAGE mini-gels of appropriate concentration. The gel was placed into an electrophoresis chamber containing 1x Running Buffer. Protein samples were boiled for 3 min, and 10 – 30 µl were added to each lane. Gels were run at 180 V for 1 h.

2.12.4 Western blotting

Linearised and separated proteins were transferred from the SDS gel to a nitrocellulose Immobilon-P membrane (Milipore) by semi-dry Western blotting procedure. Six pieces (9 cm x 6 cm) of 3M chromatography paper were soaked in 1x Transfer Buffer, along with a nitrocellulose membrane, to activate its positive charge. The blotting stack was assembled, with the gel placed on top of the membrance, sandwiched in between two triple layers of wet 3M paper. Transfer occurred at 100 V for 1 h. After transfer, the membrane was blocked in PBS+5% milk powder. Antibodies used in this studies are listed in **Table 2.5**. All antibodies were diluted in PBS+ milk powder. The secondary antibodies were HRP-labelled; Supersignal West Dura (Pierce) was used for chemiluminescence detection as per manufacturer's instructions. Washing steps in between incubation with primary and secondary antibody was carried out with PBS+Tween (0.1%), for 3 x 10 min.

Table 2.5 Antibodies used in this study

Antibody	Source	Dilution	Conditions
Peroxidase anti-peroxidase (PAP)	Sigma, P1291	1:1000	4°C overnight/ 2 hours, room temperature
α-tubulin	Sigma, T5168	1:10000	1 hour, room temperature
α-GFP	Roche, 11814460001	1:500	4°C overnight/ 3 hours, room temperature
α-H3K9me2	Abcam, ab9050	1:500	4°C overnight/ 3 hours, room temperature
α-H3	Abcam, ab1791	1:500	4°C overnight/ 3 hours, room temperature
Peroxidase labelled anti-mouse IgG	Vector Laboratories, PI-2000	1:10000	1 hour, room temperature
Peroxidase labelled anti-rabbit IgG	GE Healthcare, RPN2108	1:8000-1:10000	1 hour, room temperature

CHAPTER III

Identification and characterisation of *'loh'* mutants

3.1 Introduction

Chromosomal rearrangements are a hallmark of cancer cells, which can lead to oncogene activation and tumour suppressor loss. Such outcomes can result from both the repair and misrepair of DNA ends which arise from a variety of events including DSBs, collapsed replication forks and dysfunctional telomeres. DSBs are considered the most detrimental DNA lesions. Even one single DSB can, if misrepaired, lead to loss of genetic information via heterozygosity (LOH) of tumour suppressor genes. Alternatively, inaccurate mending of DSBs can also lead to gross chromosomal rearrangements and oncogene amplification, thus resulting in cancer (Kasparek and Humphrey 2011).

To identify suppressors of break-induced LOH, a genetic screen in *Schizosaccharomyces pombe* was performed by Helen Tinline-Purvis. For this purpose, random mutations were introduced into fission yeast strains by ethyl methanesulfonate (EMS), an agent that produces nucleotide substitutions, thus creating a library of strains with point-mutations (Bokel 2008). This library was further subjected to a screening for mutant strains which display erroneous repair of DSBs, leading to high levels of LOH, a potentially tumourigenic event in human cells. The non-essential minichromsome Ch^{16}-*RMGAH* (*arg3*$^{+}$, *MATa, G418R, ade*M216, *his2*$^{+}$) (**Figure 3.1**) was utilised to isolate 'sectoring' mutants on low-adenine plates, exhibiting elevated levels of DSB-induced extensive LOH (Tinline-Purvis et al. 2009).

3.2 Results

3.2.1 Identification of *'loh'* mutants

3.2.1.1 Strategy to identify and characterise '*loh*' mutants

Four of the derived mutants, referred to in this study as *loh-2*, *loh-5*, *loh-6*, and *loh-7* displayed a significant increase in break-induced LOH but remained yet to be identified. For further characterisation, a number of assays were carried out. In a first instance, a spot-dilution assay was conducted (as described in **Chapter 2.6.6.1**), in which the strains were challenged with the DNA-damaging agents methyl methanesulfonate (MMS), bleomycin and camptothecin. The alkylating agent MMS causes stalling of replication forks and DNA adducts, ultimately leading to single-stranded and double-stranded DNA lesions (Sikora et al. 2010). Bleomycin is a radiomimetic cancer drug, which induces DSBs (Povirk 1996). Camptothecin is a topoisomerase inhibitor, causing replication-dependent DSBs (Hsiang et al. 1985). Typically, hypersensitivity of strains to these agents, are indicative of defects in genes essential for DNA damage repair.

To gain a better and quantifiable understanding of the repair deficiencies, DSB repair assays of the respective mutants were analysed. In this respect, the non-essential minichromsome Ch^{16}-*RMGAH* (*arg*$^{+}$, *MATa*, *G418R*, *ade*M216, *his*$^{+}$) was utilised. This minichromosome has been experimentally derived from chromosome III. Truncations of both ends make its size smaller (0.5 MB) compared to parental chromosome III (3.5 MB) and markers have been introduced onto both arms (**Figure 3.1**). An inducible *Saccharomyces cerevisiae* MAT*a* break-site with an adjacent G418-resistance cassette was placed onto the right arm of Ch^{16} (Cullen et al. 2007).

Figure 3.1

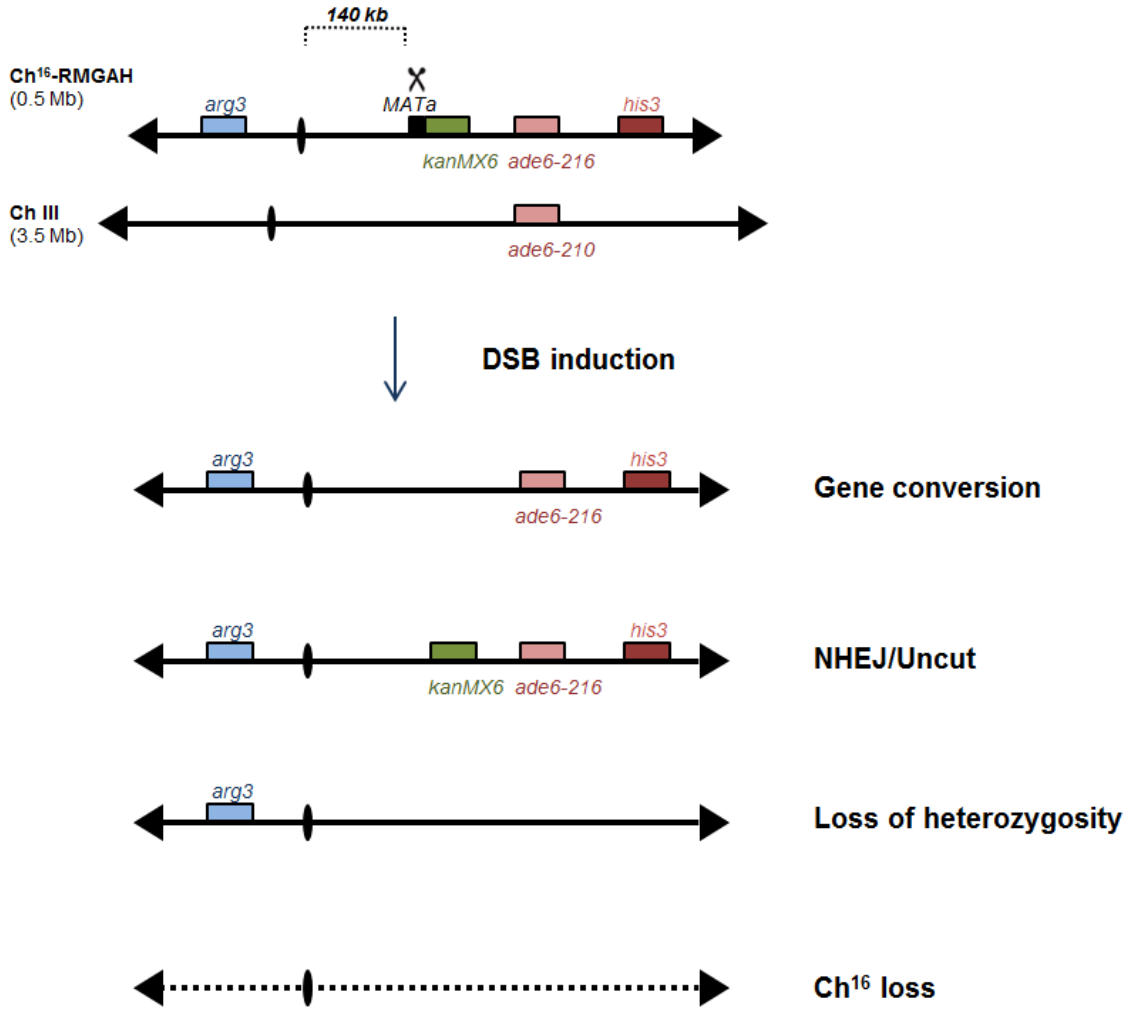


Figure 3.1: The minichromsome Ch^{16}-*RMGAH*: Schematic drawing of the minichromosome Ch^{16} *RMGAH* (*arg+, MATa, G418R, adeM216, his+*). Following break induction, a number of different repair events can occur. The genotype of the resulting colonies as indicated by growth on selective plates, gives information about the associated repair event (see also **Table 3.1**)

Table 3.1

Ch^{16}	Replica plating	Outcome			
		NHEJ/SCC	GC	Ch^{16} loss	LOH
RMGAH	EMM+ AHULT (arg-)	arg^+	arg^+	arg^-	arg^+
	EMM+ RHULT (ade-)	ade^+	ade^+	ade^-	ade^-
	EMM+ RAULT (ura-)	his^+	his^+	his^-	his-
	YE6S + G418	$G418^R$	$G418^S$	$G418^S$	$G418^S$

Table 3.1: Genotype and associated repair events of DSB assay. Following break-induction, cells are incubated until colonies form on non-selective plates. Replica-plating onto indicated selective plates reveals genotype of the colonies, on which upon repair events non-homologous end-joining (NHEJ)/sister chromatid conversion (SCC)/Uncut, gene conversion (GC), minichromosome loss (Ch^{16} loss), and loss of heterozygosity (LOH) can be deduced and scored.

Upon transformation with HO-endonuclease under an *nmt*-promoter on a plasmid and subsequent ectopic expression, a single localised DSB can be introduced at the MAT*a* site and repair events deduced, based on marker loss after 48 h of incubation. Using this assay, several repair events, *i.e.* gene conversion (GC), non-homologous end-joining (NHEJ)/sister chromatid conversion (SCC), loss of heterozygosity (LOH) and chromosome loss (Ch^{16} loss) can be differentiated upon break-induction based on genotype of the surviving colonies (**Table 3.1**). To investigate potential defects in cell cycle checkpoints, the strains were challenged with hydroxyurea (HU). HU is an agent that is thought to deplete nucleotide levels by ribonucleotide reductase inhibition, thus causing replication fork stalling. In wild-type cells, this leads to activation of the replication checkpoint, which ensures full replication of the DNA before the cells divide to prevent mitotic catastrophe.

Figure 3.2

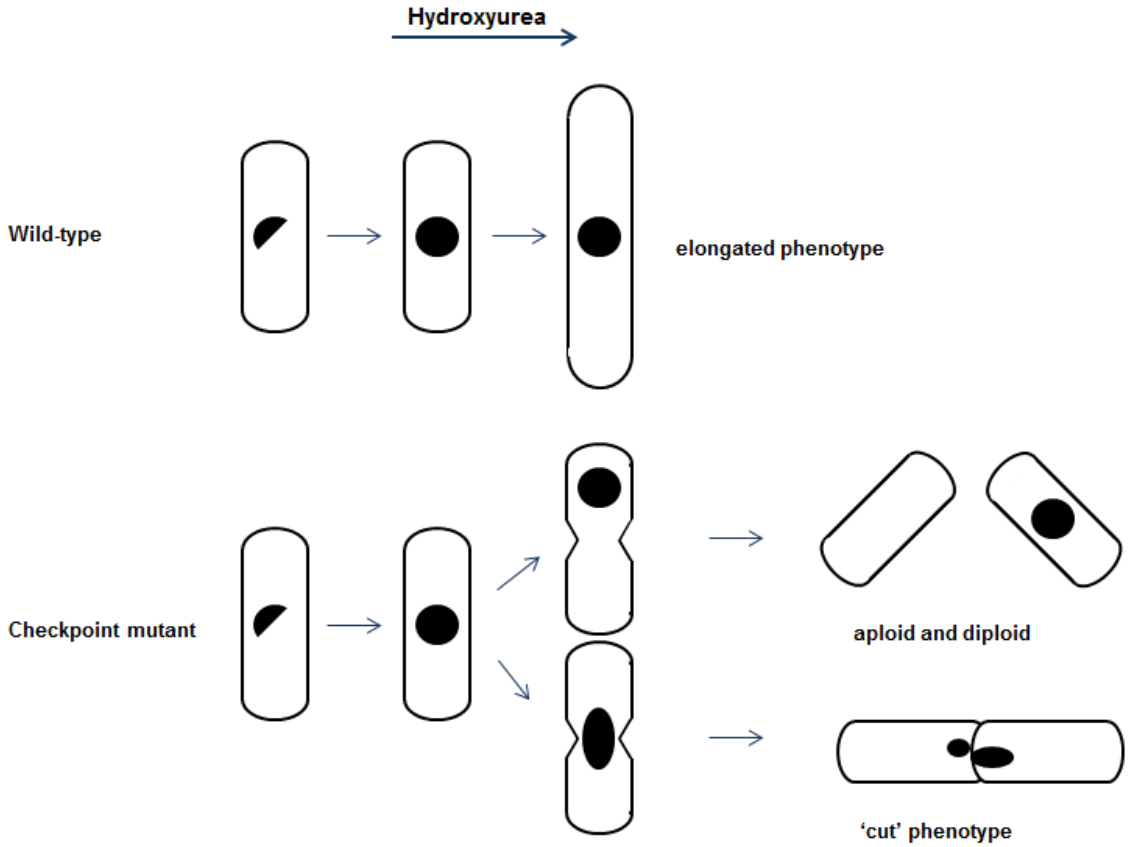


Figure 3.2: Schematic of the '*cut*' phenotype assay. Cells are challenged with HU, depleting dNTP pools and thus leading to activation of the S-phase checkpoint. In wild type, cell cycle arrest can be visually detected by an elongated phenotype after 6 h of HU treatment. Mutation strains with defective checkpoint control will enter mitosis without a full round of replication, causing aploid and diploid cell pairs, as well as the '*cut*' phenotype. Visualisation is achieved by DAPI stain and microscopy.

Activation of the checkpoint can be monitored by an elongated phenotype of checkpoint-proficient cells, since the cells continue to grow but will not divide.

Checkpoint-deficient cells will display the '*cut*' (cell untimely torn) phenotype, arising through cell division without complete replication, observable by DAPI-staining of the DNA (**Figure 3.2**).

Finally, in an effort to identify the affected genes of the mutants, a functional complementation analysis was carried out, as depicted in **Figure 3.3**. Deletion strains, lacking candidate genes *rad9*$^{+}$, *rad1*$^{+}$, *hus1*$^{+}$ and *rad17*$^{+}$, were crossed with the *'loh'* mutants and free spores were plated onto selective MMS plates. No growth on selective plates is indicative of disruption of the same gene in both the *'loh'* strain and the deletion strain, while complementation suggests a mutation in different genes.

For strains which could not be identified using classical complementation, whole-genome sequencing was applied. Since these mutants were generated by random EMS mutagenesis, the strains were backcrossed to wild type 6-8 times to eliminate background mutations and then subjected to whole-genome sequencing by Illumina paired-end technique and bioinformatics analysis was performed to identify the underlying point-mutations.

Figure 3.3

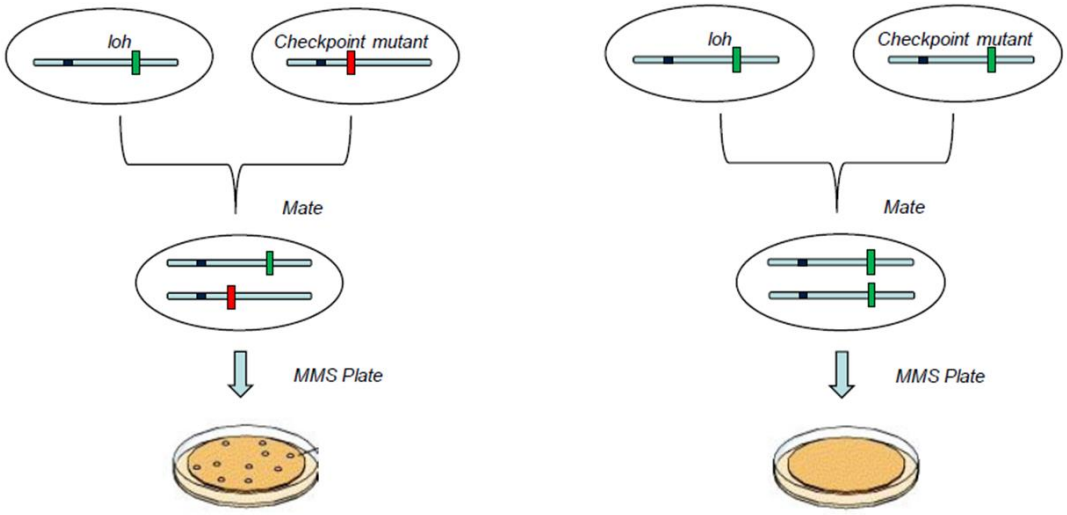


Figure 3.3: Schematic drawing of the complementation assay. All mutants were crossed with strains harbouring deletions of candidate genes *i.e.* *rad9*$^{+}$, *rad1*$^{+}$, *hus1*$^{+}$ and *rad17*$^{+}$. Following mating, the spores were spread onto selective MMS plates. Growing cells indicate complementation of the *loh*-strain with the deletion strain and hence disruption of different genes. No growth on the selective plates suggests that the random mutation could not be complemented by the known deletion strain; hence the same gene is affected.

Figure 3.4

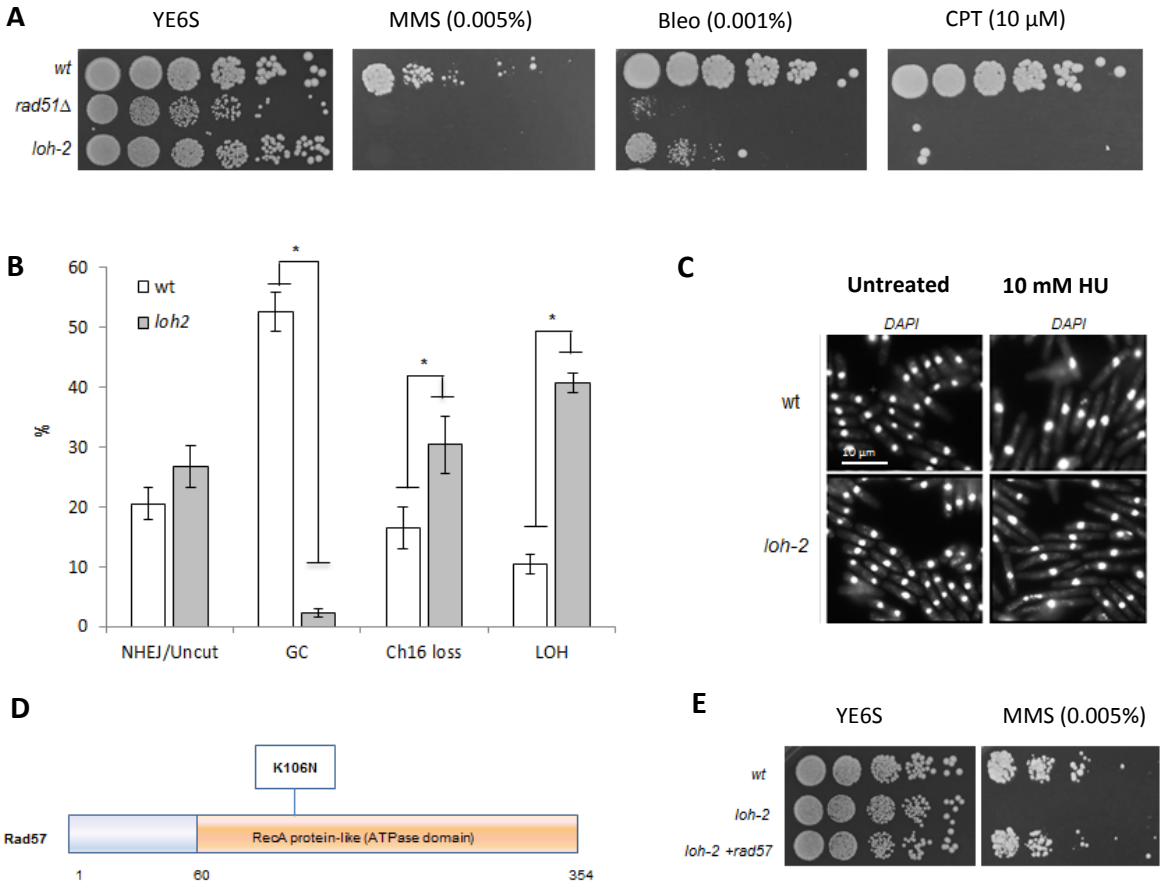


Figure 3.4: *loh-2* displays severe DNA damage repair defects. (A) *loh-2* was hypersensitive to MMS, bleomycin and camptothecin. Spot dilution assay was carried out at a five-fold dilution and indicated concentrations of clastogens were used. (B) Ch^{16}- *RMYAH* DSB assay revealed a significant decrease in GC with a concomitant increase in both Ch^{16} loss and LOH. Error bars represent standard deviation of the mean of three experiments. **(p<0.05)* (C) Cells displayed a functional S-phase checkpoint after treatment with 10 mM HU. (D) Whole-genome sequencing of *loh-2* confirmed a *rad57* K106N point mutation. Schematic of Rad57 and site of point mutation (E) Complementation of MMS sensitivity of *loh-2* by ectopic expression of *rad57*.

3.2.1.2 *'loh-2'* harbours missense mutation K106N in *rad57*

The mutation strain *loh-2* displayed distinct hypersensitivity to all of the DNA damaging agents MMS, bleomycin, and camptothecin, typically suggestive of a defect in DSB repair (**Figure 3.4A**).

The DSB assay with Ch^{16}-*RMGAH* revealed a DSB repair profile, strikingly different to a wild-type profile. NHEJ levels were slightly, but not significantly (p=0.08) elevated: *loh-2:* 27%; wt: 21%. Repair by GC was almost entirely absent in the mutant (2%) in comparison to wt (53%). The events Ch^{16} loss *(loh-2*: 28%; wt: 16%) and LOH (*loh-2*: 40%; wt: 10%), considered failed repair, were concomitantly increased, consistent with a repair defect in HR (**Figure 3.4B**). Failure to utilise HR for DSB repair, leads to hyper-resection of Ch^{16} and subsequent chromosome removal or LOH either by isochromosome formation or *de-novo* telomere formation (Tinline-Purvis et al. 2009).

To investigate a potential checkpoint defect, cells were treated with HU. Like wild type, *loh-2* cells elongated following challenge, indicative of cell cycle arrest caused by the insult, thus excluding a disruptive mutation in a checkpoint gene (**Figure 3.4C**).

After back-crossing and subjecting to whole-genome sequencing, it was discovered using bioinformatics, that *loh-2* contains a point mutation in *rad57 ($XRCC3^{Hu}$)*, causing a lysine to asparagine amino acid substitution at position 106 of the polypeptide (**Figure 3.4D**). Both the predictive algorithms SIFT and PolyPhen that have been utilised to analyse a potential functional disruption of Rad57, classified the K106N substitution as deleterious in regard to protein function (data not shown). The mutation was subsequently confirmed by complementation by ectopic expression of *rad57* (**Figure 3.4E**). Rad57 forms a heterodimer with Rad55 *in-vivo* to promote homologous recombinational repair by loading

Rad51 onto stretches of ssDNA-RPA (Liu et al. 2011). Rad57 has been identified previously by the lab as suppressor of break-induced LOH (Tinline-Purvis et al. 2009).

Figure 3.5

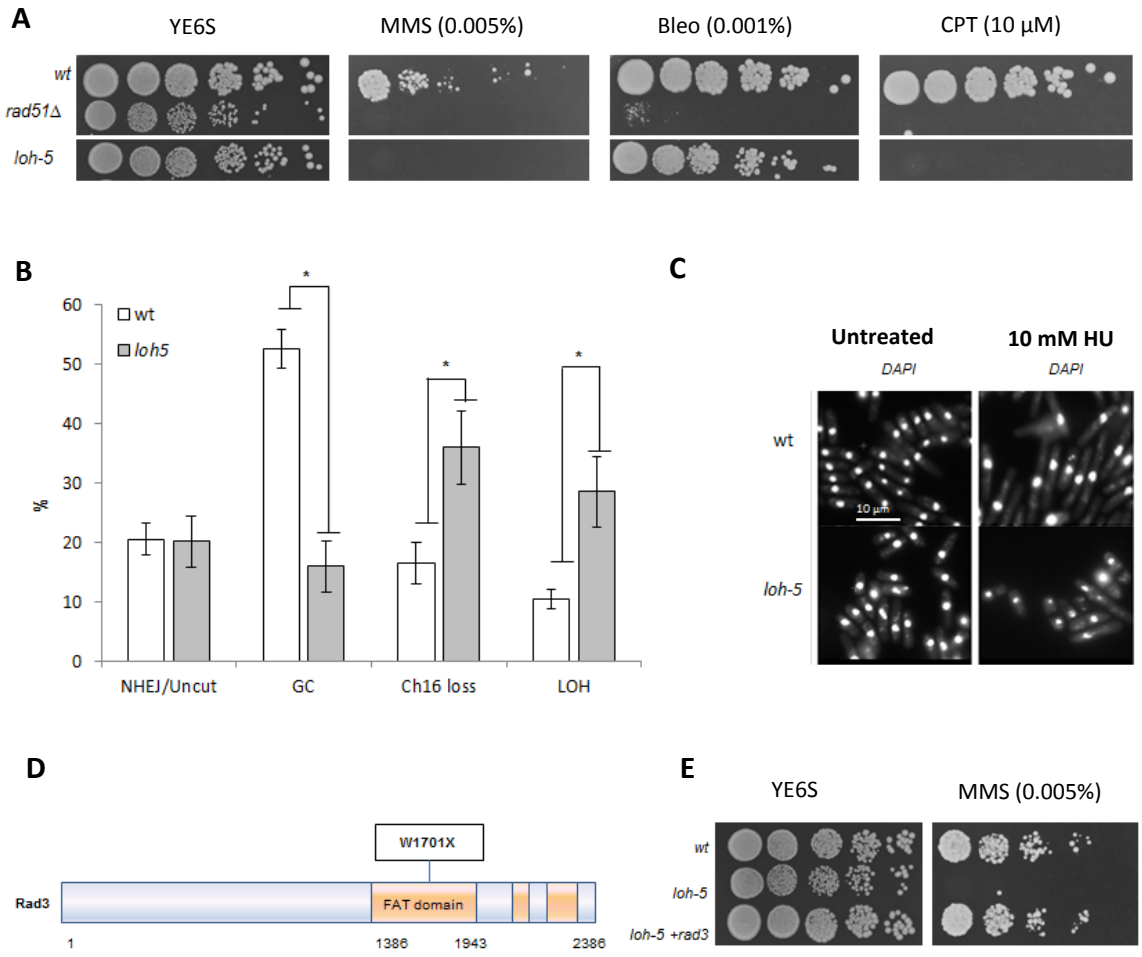


Figure 3.5: *loh-5* displays severe DNA damage repair defects. (A) *loh-5* was hypersensitive to MMS, bleomycin and camptothecin. Spot dilution assay was carried out at a five-fold dilution and indicated concentrations of clastogens are used. (B) Ch^{16}-*RMYAH* DSB assay revealed a significant decrease in GC with a concomitant increase in both Ch^{16} loss and LOH. Error bars represent standard deviation of the mean of three experiments. **(p<0.05)* (C) Cells displayed a functional S-phase checkpoint after treatment with 10 mM HU. (D) Sequencing of *loh-5* confirmed a *rad3* W1701X nonsense mutation. Schematic of Rad3 and site of point mutation (E) Complementation of MMS sensitivity of *loh-5* by ectopic expression of *rad3*. **(P<0.05)*

Figure 3.6

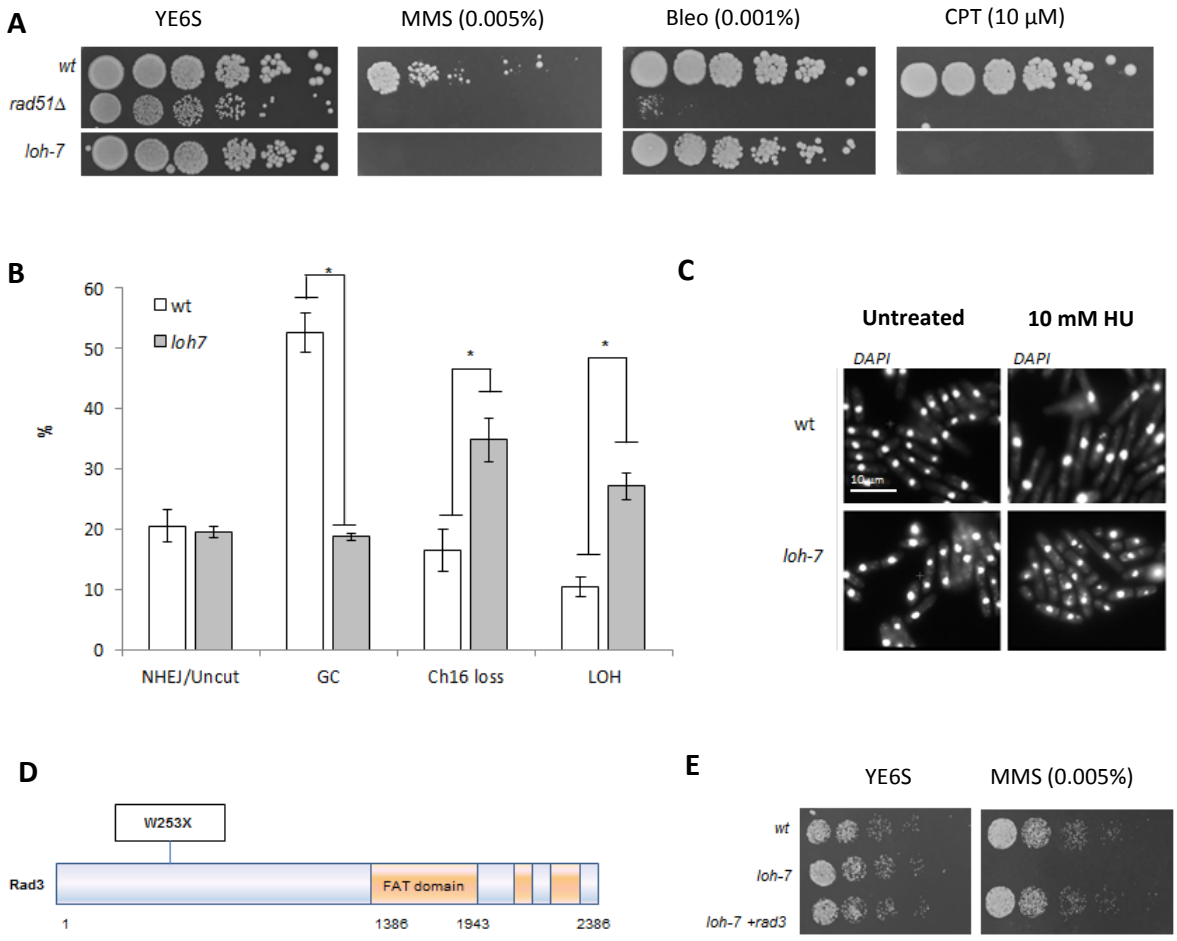


Figure 3.6: *loh-7* displays severe DNA damage repair defects. (A) *loh-7* was hypersensitive to MMS, bleomycin and camptothecin. Spot dilution assay was carried out at a five-fold dilution and indicated concentrations of clastogens are used. (B) Ch^{16}-*RMYAH* DSB assay revealed a significant decrease in GC with a concomitant increase in both Ch^{16} loss and LOH. Error bars represent standard deviation of the mean of three experiments. **(p<0.05)* (C) Cells displayed a functional S-phase checkpoint after treatment with 10 mM HU. (D) Sequencing of *loh-7* confirmed a *rad3* W253X nonsense mutation. Schematic of Rad3 and site of point mutation. (E) Complementation of MMS sensitivity of *loh-7* by ectopic expression of *rad3*. **(P<0.05)*

3.2.1.3 *'loh-5'* and *'loh-7'* carry truncating mutations in *rad3*

The other '*loh*' mutants, *loh-5* and *loh-7* displayed similar phenotypes. Both mutation strains were hypersensitive to MMS and camptothecin, but not bleomycin at indicated concentrations. (**Figures 3.5A, 3.6A**) The DSB repair profile obtained by the Ch^{16}-*RMGAH* assay, revealed comparable DSB-induced repair outcomes. While NHEJ levels were not significantly different to wild-type levels (*wt*: 21%, *loh-5*: 22% *loh-7*: 20%), GC levels dropped down to 13% for *loh-5* and 19% for *loh-7*, significantly ($p<0.01$) lower than wild-type levels with 53%. Correspondingly, the adverse outcomes LOH and Ch^{16} levels were significantly increased (Ch^{16} loss; *loh-5*: 36%, *loh-7*: 31%, wt: 16% and LOH; *loh-5*: 28%, *loh-7*: 29%, wt: 10%) (**Figures 3.5B, 3.6B**).

Strikingly, when challenged with HU, both mutant strains displayed the '*cut*' phenotype, which formation is typically associated with defects in the checkpoint machinery (**Figures 3.5C, 3.6C**). Using classical candidate-approach complementation, *loh-5* and *loh-7* both failed to be complemented with a *rad3*Δ strain, strongly suggesting an underlying disruption in this gene for both mutation strains. Utilising Sanger sequencing, truncating mutations in *rad3 (ATR^{Hu})* were found in both *loh-5* (W1701X) and *loh-7* (W253X) **(Figures 3.5D, 3.6D)**. For confirmation purposes, the hypersensitive phenotype was rescued by ectopic expression of *rad3* (**Figures 3.5E, 3.6E**). Rad3 (ATR^{Hu}) is a checkpoint kinase, which activates checkpoint signalling upon genotoxic stress via phosphorylation of Chk1 and Rad17 (Bentley et al. 1996). Rad3 is a central player in homologous recombination repair of DNA lesions and its role in suppression of break-induced LOH aligns well with the literature and is congruent with prior data of the lab.

Figure 3.7

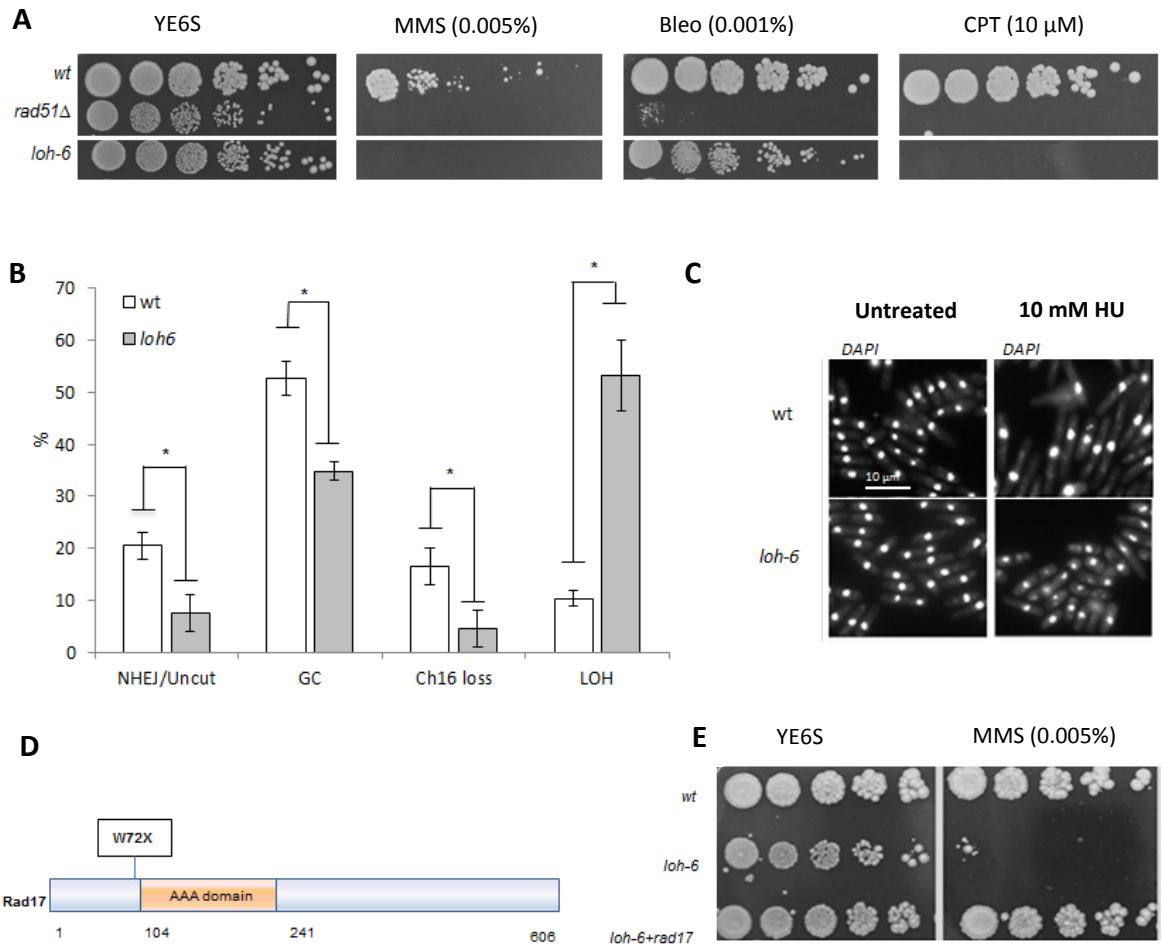


Figure 3.7: *loh-6* displays severe DNA damage repair defects. (A) *loh-6* was hypersensitive to MMS, bleomycin and camptothecin. Spot dilution assay was carried out at a five-fold dilution and indicated concentrations of clastogens are used. (B) Ch^{16}-*RMYAH* DSB assay revealed a significant decrease in GC with a concomitant increase in both Ch^{16} loss and LOH. Error bars represent standard deviation of the mean of three experiments. **(p<0.05)* (C) Cells displayed a functional S-phase checkpoint after treatment with 10 mM hydroxyurea HU. (D) Sanger sequencing of *rad17* confirmed a W72X nonsense mutation. Schematic of Rad17 and site of point mutation. (E) Complementation of MMS sensitivity of *loh-6* by ectopic expression of *rad17*. **(P<0.05)*

3.2.1.4 *'loh-6'* harbours a truncating mutation in *rad17*

Mutant strain *loh-6* displayed high sensitivity to MMS, and camptothecin, but only mild sensitivity to bleomycin (**Figure 3.7A**). The DSB assay with Ch^{16}-*RMGAH* revealed a distinct DSB repair profile. While NHEJ levels of the mutant were only slightly decreased compared to wild type, GC levels dropped by 19% to 34% (wt: 53%). Strikingly, LOH levels were over 53% while Ch^{16} loss was lower (*loh-6*: 4%) than in wild type (16%). This profile indicated a genetic disruption in a gene not only required for efficient GC, but intriguingly also for efficient chromosome removal following a DSB. After a 6 h treatment with HU, *loh-6* cells displayed the '*cut*' phenotype, suggesting defective cell cycle arrest (**Figure 3.7C**). Performing the complementation assay, the mutant *loh-6* was unable to complement a *rad17*Δ checkpoint mutant, which is consistent with the '*cut*' phenotype of the strain when exposed to hydroxyurea. Further, sequence analysis confirmed, that *loh-6* encodes a nonsense mutation (W72X) in *rad17 (*$Rad17^{Hu}$*)*, leading to an early truncation (**Figure 3.7D**). Finally, *loh-6* was then transformed with a wild-type copy of *rad17* on an expression plasmid and challenged with MMS to check for complementation (**Figure 3.7E**).

Rad17 is a protein involved in cell cycle checkpoint response to DNA damage with high similarity to DNA replication factor C (RFC). It binds chromatin and is phosphorylated by Rad3, following DNA damage, subsequently recruiting the 9-1-1 complex (Rad9-Rad1-Hus1) to the damaged site to promote cell cycle arrest (as described in **Chapter 1.5**) (Yang and Zou 2006). Its identification as suppressor of break-induced LOH is consistent with prior data from the lab. Components of its pathway, *i.e.* 9-1-1 complex, display strikingly similar DSB repair profiles when subjected to the DSB repair assay (data not shown). Rad17 is evolutionary highly conserved and the human homolog is functionally analogous (Beretta et al. 2008).

Figure 3.8

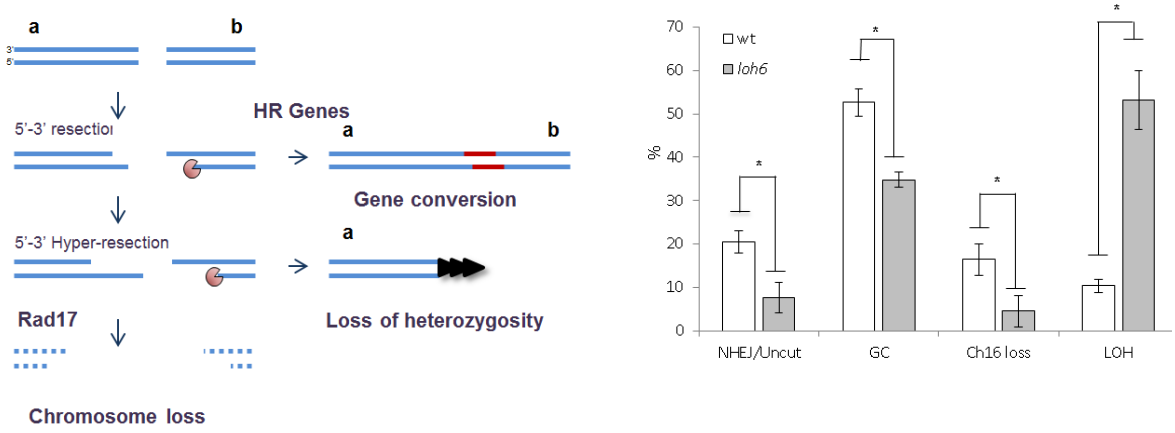


Figure 3.8: Proposed model. Data from this study and prior data from the lab suggest a mechanism by which HR genes promote GC following a DSB. Failure to repair leads to hyper-resection of the minichromosome causing either LOH or Ch^{16} loss. An additional role for Rad17 in Ch^{16} removal is proposed based on the Ch^{16}-*RMGAH* DSB assay. Error bars represent standard deviation of the mean of three experiments. **(p<0.05)*

3.2.2 An additional role for checkpoint proteins in resection

While the importance of functional checkpoints in the DNA damage response is well understood, our data are suggesting an additional role for Rad17 in DSB repair. While cells devoid of Rad17 display an expected drop in GC levels, chromosome removal after break-induction was also impaired. It was therefore hypothesised that Rad17, along with its interactors of the 9-1-1 complex, are required for efficient removal of the minichromosome following break-induction, thus driving cells into death under physiological conditions, as a potential mean to prevent LOH.

The underlying mechanism of Ch^{16} removal following break-induction is hypothesised to be hyper-resection through the centromeric region (**Figure 3.8**). Rad17 is involved in loading of the 9-1-1 ring structure onto DNA. It was hypothesised that this ring structure provides physical stability and facilitates efficient resection, required to remove the minichromosome, by opening up heterochromatised regions or secondary structure. Strains lacking activation of the 9-1-1 complex therefore resect inefficiently, which leads to an increase in LOH, for example by stabilisation of the end by either *de-novo* telomere addition or isochromosome formation.

To test this hypothesis, a modified version of the Ch^{16}-*RMGAH* minichromosome was applied. The modified version, *L5-RMGAH*, contains a centromere-proximal L5 element, adjacent to the MAT*a* break-site (**Figure 3.9A)**. This genetic L5 element nucleates *de-novo* heterochromatin domains flanking the sequence (Wheeler et al. 2009). In order to perform efficient GC, the heterochromatised regions flanking the break-site must be resected to promote strand invasion and second-end capture.

According to our hypothesis, cells lacking a functional copy of *rad17*, should display a decrease in GC in comparison with the parental minichromosome, since resection through heterochromatin is thought to be impaired.

However, when performing DSB assays of wild type and *rad17*Δ, no significant difference was measured when comparing the DSB repair profiles in the L5 system with the parental minichromosome Ch^{16}-*RMGAH*, for each of the respective genetic backgrounds (**Figure 3.9B**).

Figure 3.9

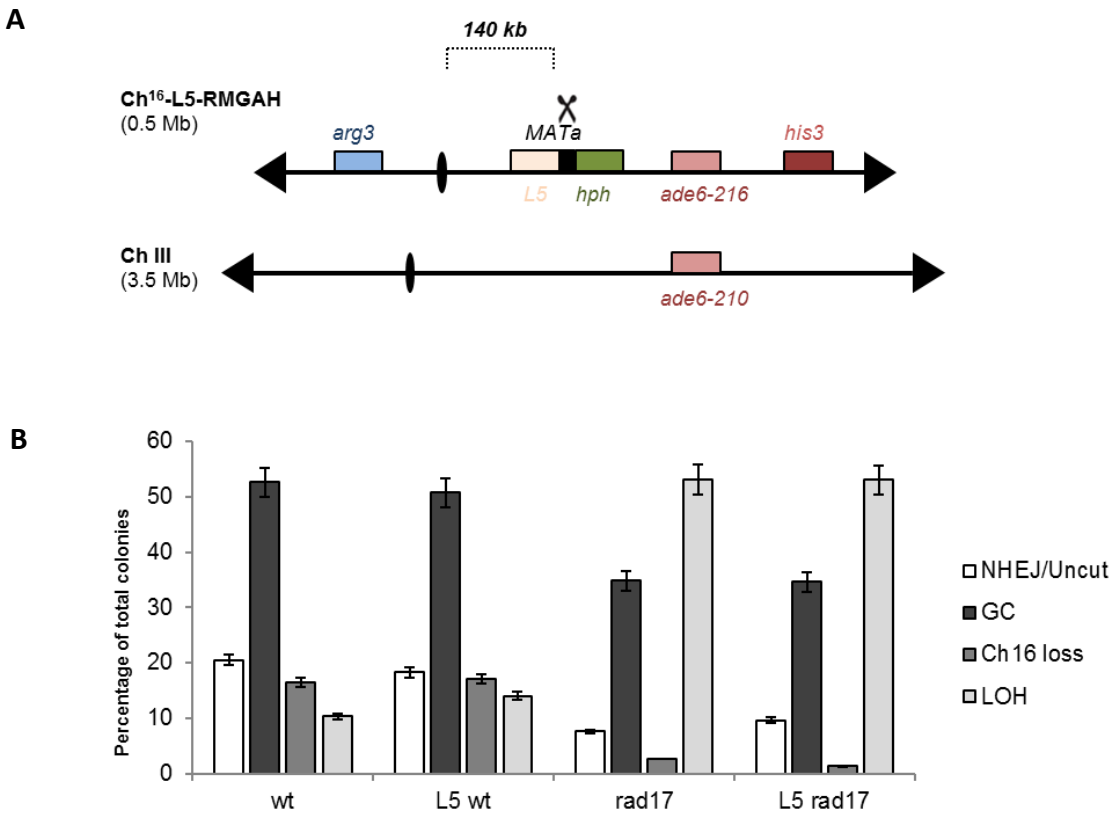


Figure 3.9: The Ch^{16}-*L5-RMGAH* DSB assay. (A) Schematic drawing of Ch^{16}-*L5-RMGAH*. Deduction of repair events is carried out analogously to Ch^{16}-*RMGAH* (Figure 3.1). (B) DSB assays of wild type and *rad17*Δ in Ch^{16}-*RMGAH* and Ch^{16}-*L5-RMGAH* background. Error bars represent standard deviation of the mean of three experiments. **(p<0.05)*

3.3 Discussion

3.3.1 Rad3, Rad17 and Rad57 are known suppressors of LOH

The crosstalk of cell cycle checkpoints and the DDR has been well characterised (Niida and Nakanishi 2006). Following DNA lesions, checkpoints are activated to provide time for cellular repair before entering mitosis. With a dysfunctional checkpoint, unrepaired lesion can lead to mitotic catastrophe or breakage-fusion-bridge cycles, ultimately leading to gross chromosomal rearrangements or cell death. Rad3 is an upstream checkpoint kinase, recruited to DSBs by the Rad17 and the 9-1-1 complex and essential for activation of the DNA damage checkpoint, ultimately halting the cell cycle (Bermudez et al. 2003). Impairment of this cascade is known to interrupt the cell cycle arrest and cells are generally hypersensitive to a wide array of DNA damaging agents. In this study we could confirm a role for Rad3 and Rad17 for suppression of break-induced LOH, which aligns well with the literature and prior data from the lab rendering these factors tumour-suppressor genes.

While Rad57 is not involved in the DNA damage checkpoint, its role in loading of Rad51 onto RPA-coated single-stranded DNA in a heteroduplex with Rad55 is well established (Sung 1997). Cells devoid of either Rad55 or Rad57 display similar phenotypes, typically entailing hypersensitivity to many clastogens, since efficient facilitation of HR is disturbed in the absence of these loading factors. The Ch^{16}-*RMGAH* DSB assay of *rad57*Δ is consistent with the predictions, and indicates a stark decrease in GC, with a concomitant increase in Ch^{16} loss and LOH; the latter outcomes are considered adverse repair events.

Strikingly, the DSB repair profile of Rad17 is different to those of HR mutants, since no Ch^{16} loss following a DSB occurs. While we do not know the exact mechanisms of Ch^{16} removal, it is tempting to speculate on hyperresection through the centromere as the

underlying causal action. A deficiency for this removal in *rad17*Δ background would thus suggest a role for Rad17 in resection, along with the 9-1-1 complex, which deletion strains display a similar phenotype (data not shown). However, a direct role for the checkpoint machinery in resection could not be established in this study, utilising the L5-*RMGAH* assay to test this hypothesis. Notably, introduction of the L5 genetic element, presenting the challenge of extra non-homologous DNA sequence adjacent to the break-site as well as heterochromatin, has not affected the DSB repair profile of either *rad17*Δ or wt.

This could either mean that the employed assay is not sensitive enough to monitor subtle differences in resection kinetics, or our hypothesis is false and chromosome loss is realised by different means.

The data generated from this study, complements a prior study carried out by Helen Tinline-Purvis and is used towards a manuscript currently in preparation, illuminating a potential role of checkpoint proteins in resection. However, further research in this regard was out of the scope of this study.

Table 3.2

Strain	Affected gene	Mutation	Gene function	Human homolog
loh-2	*rad57*	K106N	RecA family ATPase	*XRCC3*
loh-5	*rad3*	W1701X	Checkpoint kinase	*ATR*
loh-6	*rad17*	W72X	Cell cycle checkpoint	*RAD17*
loh-7	*rad3*	W253X	Checkpoint kinase	*ATR*

Table 3.2: Summary of identified mutants. All four '*loh*' mutants could be identified as part of this study. The underlying mutations, gene functions, and human homologs are presented.

3.3.3 Summary

In this chapter, the efforts are described to identify four unknown mutants, previously derived from a screen for suppressors of break-induced LOH. All four mutant strains carry disruptive point mutations in known genes, associated with HR repair and cell cycle checkpoints respectively, as summarised in **Table 3.2**. Strikingly, two different DSB repair profiles were observed for deletions of the two affected checkpoint genes *rad3* and *rad17*, indicating distinct roles for these factors of the checkpoint machinery in DNA repair in fission yeast. Further investigation could not confirm the hypothesis for a role of Rad17 (and the 9-1-1 complex) in resection following DSB. The data generated are used towards complementation of a study characterising a role of checkpoint proteins in resection.

CHAPTER IV

A pan-genomic screen for novel factors of the DNA damage response in fission yeast

4.1 Introduction

Maintenance of genome stability in response to various kinds of DNA damage is an essential cellular feature to avoid cell death and, in higher eukaryotes, cancer. Genetically amenable model organisms, such as *Schizosaccharomyces pombe,* have been utilised in the past to identify and functionally elucidate causal genetic variants and elements associated with DNA damage repair and cancer. *S. pombe* share an estimated 3,038 genes with humans (Kim et al. 2010). Due to the high evolutionary conservation of ancient mechanisms like DNA repair and cell cycle control, a high number of human tumour suppressor genes have previously been identified in *S. pombe,* rendering fission yeast an excellent model organism. However, these screens have not been collectively exhaustive and many novel factors remain to be identified. Therefore, a genome-wide deletion library of *S. pombe* was screened in a four-step process for novel genes involved in DNA damage repair, utilising a range of genotoxins and non-essential minichromosomes for further characterisation (**Figure 4.1**).

Throughout evolution, cells have developed a wide range of specialised repair pathways and cellular responses to deal with genotoxic insults, ultimately ensuring maintenance of genome stability. Different types of DNA lesions require different repair pathways.

Figure 4.1

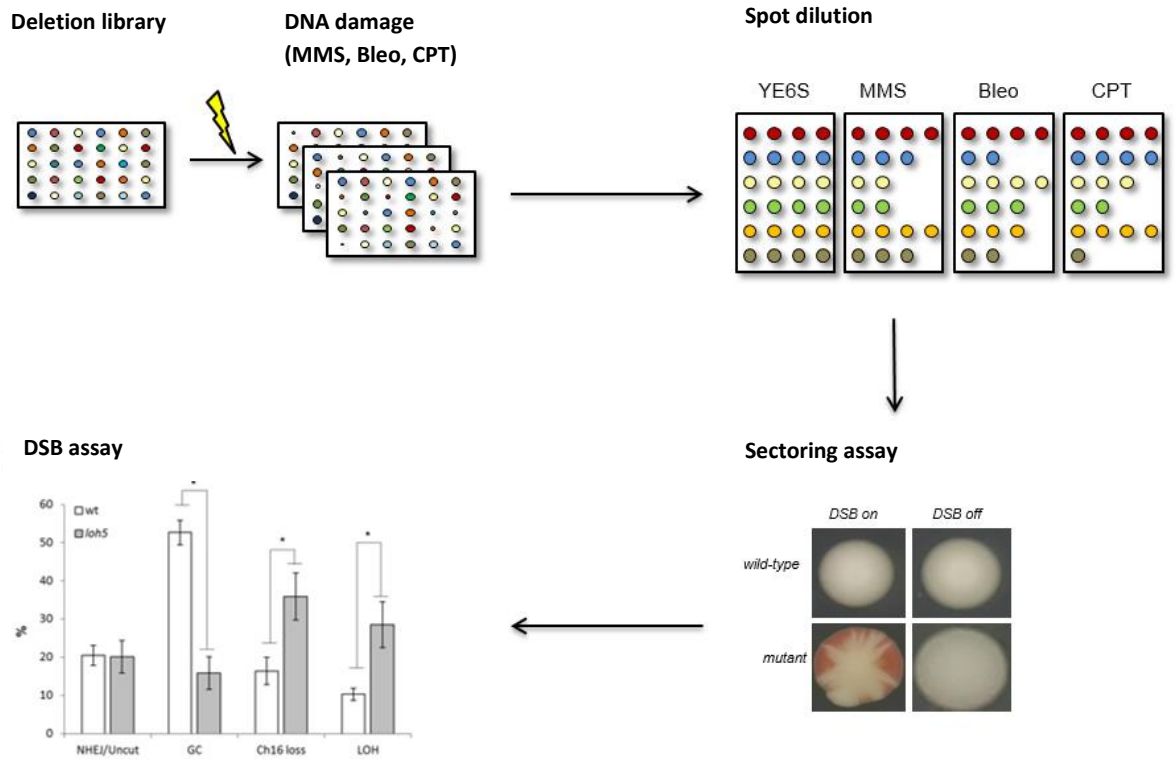


Figure 4.1: Outline of the screen. The Bioneer deletion libraries Version2, Version2-Upgrade and Version 2-Replacement, containing 3308 single haploid deletion strains were screened for deletion strains displaying hypersensitivity to DNA damaging agent MMS, bleomycin (Bleo) and camptothecin (CPT). The library in 96-well format was replica-plated onto plates containing the DNA damaging drugs, as well as non-selective media as a control. Strains (325) with a reduction in colony size on DNA challenging plates were selected and sensitivity was confirmed and quantified utilising five-fold spot dilution on drug-containing plates. Sensitivity for 209 strains was confirmed and further subjected to a sectoring assay, utilising a non-essential minichromosome. Finally, levels of DNA repair events in response to a single DSB were quantified using a different minichromosome, yielding 29 strains with a significant reduction in GC.

Base lesions, including damaged bases, mismatches and bulky adducts, are typically repaired by excision and re-filling of the gap utilising DNA nucleases, polymerases, and ligases. Notable pathways in this regard are base excision repair (BER), nucleotide excision repair (NER), as well as mismatch repair (MMR) (Costa et al. 2003; Fortini and Dogliotti 2007; Li 2008).

A different set of repair factors is employed when the DNA backbone is compromised. While DNA single-strand breaks (SSBs) are repaired by a subgroup of BER factors (Pascucci et al. 2005), DSBs are mainly repaired by virtue of one of the two major DSB repair pathways: NHEJ and HR (Jackson 2002).

DSBs are the most detrimental genomic lesion, with a single DSB bearing the potential to drive the cell into death or loss of genetic information, a potentially oncogenic event (Kasparek and Humphrey 2011). While DSBs can arise spontaneously as result of replication errors, DNA damaging agents as ionising radiation (IR), oxidative metabolites, or dysfunctional topoisomerase action are also threats to DNA integrity. In humans, scheduled physiological events such as class-switch recombination (CSR) and V(D)J recombination can also yield DSBs (Heyer et al. 2010; Lieber 2010). A detailed description of NHEJ and HR in DSB repair is given in **Chapter I**.

If a DNA lesion is not resolved in a timely manner and cells enter mitosis, potential sequelae including mitotic catastrophe, breakage-fusion-bridge cycles and GCRs can occur. To provide time for DNA damage repair, cells have evolved complex cell cycle control mechanisms, including the DNA damage checkpoints, effectively arresting the cell cycle before mitosis is entered.

As a result, cells maintain a complex network of interdependent DNA repair and cell cycle checkpoint pathways, whose importance is reflected in the high degree of evolutionary conservation.

Cancer, among other human genetic diseases, has been associated with disruption of DNA repair/cell cycle genes. Modern cancer therapy still relies on inflicting DNA damage to cancer cells, either via irradiation or various chemical DNA damaging agents. Thus, a deep understanding of the physiology of DNA repair will ultimately improve therapeutic efficiency in regard to cancer.

4.2 Results

4.2.1 The Bioneer Version 2 deletion library

The Version 2 *S. pombe* Bioneer deletion-library consists of over 3308 haploid strains with single deletions. Each strain of the deletion library carries a deletion cassette with a KanMX4 resistance marker, flanked by unique up- and downtags for identification purposes (**Figure 4.2A**). To our knowledge, comparable DNA damage sensitivity screens of earlier versions have already been performed, however Bioneer deletion-library Version 1 is notoriously unreliable, which warranted the screening of Version 2, along with the extensions of this library,Version 2 Upgrade and Version 2 Replacements, including over 5500 strains due to redundancy. The cluster of screened genes as part of this study represents 92.8% of the non-essential genome of fission yeast (http://us.bioneer.com/).

4.2.1 Identification of MMS, bleomycin or camptothecin sensitive mutants

Genes involved in maintenance of genome stability often confer resistance to clastogens. Thus, screening for DNA damage sensitive deletion strains was predicted to yield a cluster

of hits, highly enriched with factors functioning in DNA damage repair and genome stability. The selection of DNA damaging agents MMS, bleomycin, and camptothecin, used for this screen was unique at the time and challenges the DNA of the cells in distinct ways.

MMS is an alkylating agent with use in cancer treatment. MMS causes methylation of N7-deoxyguanine and N3-deoxyadenine (Shrivastav et al. 2010). These adducts are believed to lead to single-strand DNA breaks and stalling of replication forks. The cluster of MMS-hypersensitive strains are typically enriched for deletions of genes involved in multiple repair pathways, *i.e.* nucleotide excision repair (NER), double-strand break repair (DSBR), post-replication repair (PRR) as well as DNA damage checkpoint genes (DDC) (Fujiwara 1975; Tercero and Diffley 2001; Costa et al. 2003; Pascucci et al. 2005).

Figure 4.2

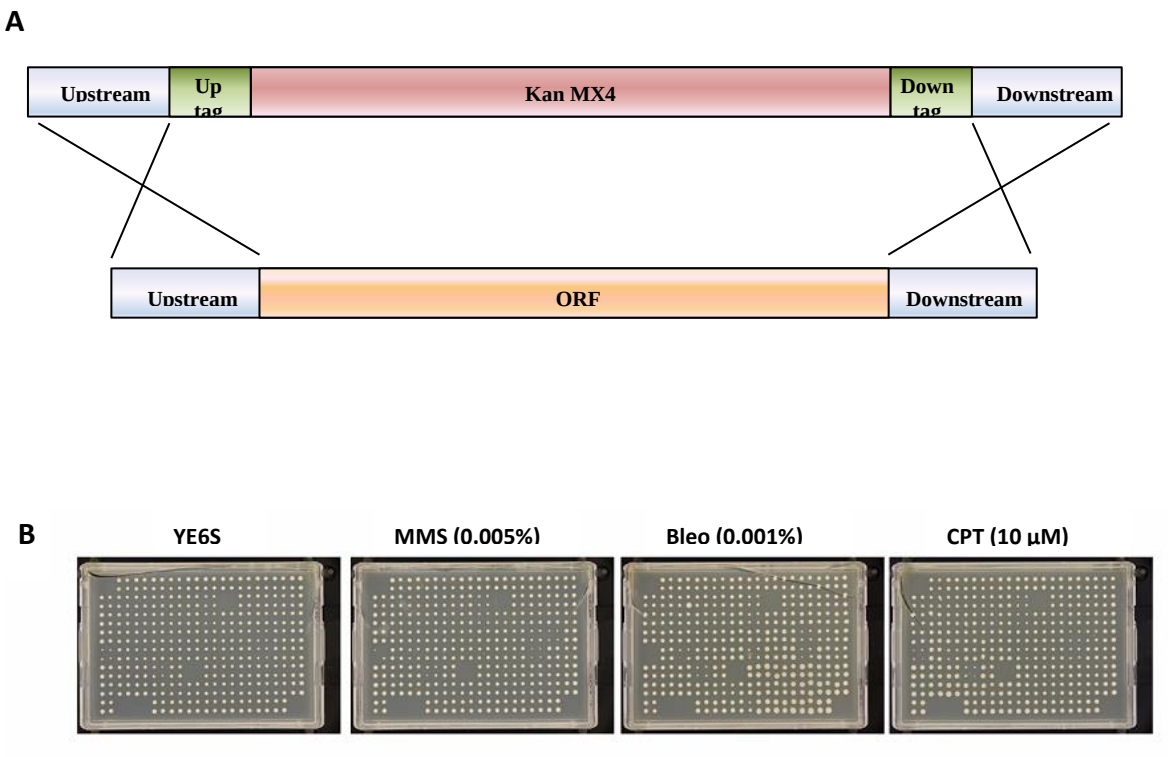


Figure 4.2: The Bioneer deletion library. (A) ORFs of >90% of all non-essential genes were deleted using depicted gene-deletion cassette. Gene loci were targeted by homologous up- and downstream regions, flanking a KanMX4 resistance element as well as unique up- and downtags for identification purposes. (B) In the first instance of the screen, the library in 96-well format was woken up, and pin-plated in 384 format onto non-selective YE6S plates, every strain was present in quadruple spots. Subsequently, colonies were replica-plated onto plates containing indicated DNA-damaging agents. A reduction in colony size on the drug plate was considered a hit, and selected for further confirmation.

Bleomycin functions as a radiomimetic drug (Povirk 1996), whose action introduces DSBs into DNA at random locations. Genes conferring resistance to DSBs typically act in DSBR and DDR (Jackson and Bartek 2009).

Camptothecin is an inhibitor of the enzyme topoisomerase I (TopoI). TopoI catalyses the removal of DNA supercoils, that can emerge during transcription, replication or recombination by introducing a nick into the sugar-phosphate backbone, allowing rotation and release of the torsional strand (Hsiang and Liu 1988). Upon inhibition by camptothecin, DNA re-ligation of the nicked strand is prevented and release of the enzyme is blocked, ultimately leading to a DSB once the replication fork collides with the complex. Genes involved in replication, DSBR and DDC function to suppress CPT-induced DNA damage (Wan et al. 1999; Jacob et al. 2005; Saleh-Gohari et al. 2005).

To screen for novel genes implicated in the DDR, the deletion strains in 96-well format were grown on solid YE6S medium plates and subsequently replica-plated onto the respective drug plates in quadruple spots. Following concentrations were used: 0.005% MMS, 10 μM CPT, 0.001% bleomycin. This was performed in duplicates. Sensitive strains were identified by reduced colony-size on the drug plates after 48 hours of incubation at 32°C (**Figure 4.2**). For confirmation, sensitive strains were subjected to a semi-quantitative spot dilution assay, as exemplified with a selection of hits in **Figure 4.3.**

Figure 4.3



Figure 4.3: Confirmation by spot-dilution exemplified with a selection of hits. A selection of hits used to exemplify confirmation process. Cells were diluted five-fold and incubated for 48 h on non-selective YE6S media and challenging plates (MMS, bleomycin, camptothecin). Deletion strains displaying at least one missing spots on any of the drug plates were considered positive hits.

4.2.2 Results Overview

A total of over 280 strains were selected based on the first round of screening using replica-plating with a Singer ROTOR HDA© robot. After confirmation via five-fold spot-dilution, 209 strains could be confirmed as hypersensitive to at least one of the DNA damaging agents, yielding a comprehensive list of deletion mutants conferring resistance to specific types of DNA damage. (**Table 4.1, Figure 4.4**). The majority of genes fulfilling core function in homologous recombination (*e.g. rad51, rad52, rad32, rad57*) and DNA damage checkpoint pathways (*rad3, rad26, rad9, rad1, hus1, rad17, crb2*) were pulled out, and their respective deletion strains were sensitive to most DNA damaging agents. Gene ontology (GO) terms from the Gene Ontology Consortium (http://www.geneontology.org) were assigned to each gene and for simplification, (subjectively) allocated into functionally related groups. Statistical analysis was performed to investigate over-representation of specific GO terms in the list of sensitive mutants when compared to their genome-wide representation and placed in an interaction network using BiNGO/Cytoscape (**Figure 4.5**). The most enriched GO terms are "Chromatin Dynamics", "DNA DSB Repair & Replication", "DNA Damage Response and Cell Cycle Regulation", "Telomere Maintenance", "Transcription Regulation", "RNA Interference", and "Stress Response & Cell Metabolism" ($p<0.0005$). As predicted, GO groups associated with "DNA DSB Repair & Replication", "DNA Damage Response and Cell Cycle Regulation" were strongly over-represented. In recent years, very strong ties emerged between DNA repair and genes associated with "Chromatin Dynamics", since these genes regulate chromatin accessibility of DNA repair factors, DNA repair pathway choice, and are also involved in transcription regulation. Similarly, crosstalk of many factors of the "Telomere Maintenance" (*rap1, ccq1, est1, trt1*) machinery with DNA repair has been demonstrated, and their role in genome stability is well established.

Transcription-related annotations, as well as factors involved in RNA interference were also found to be over-represented.

Figure 4.4

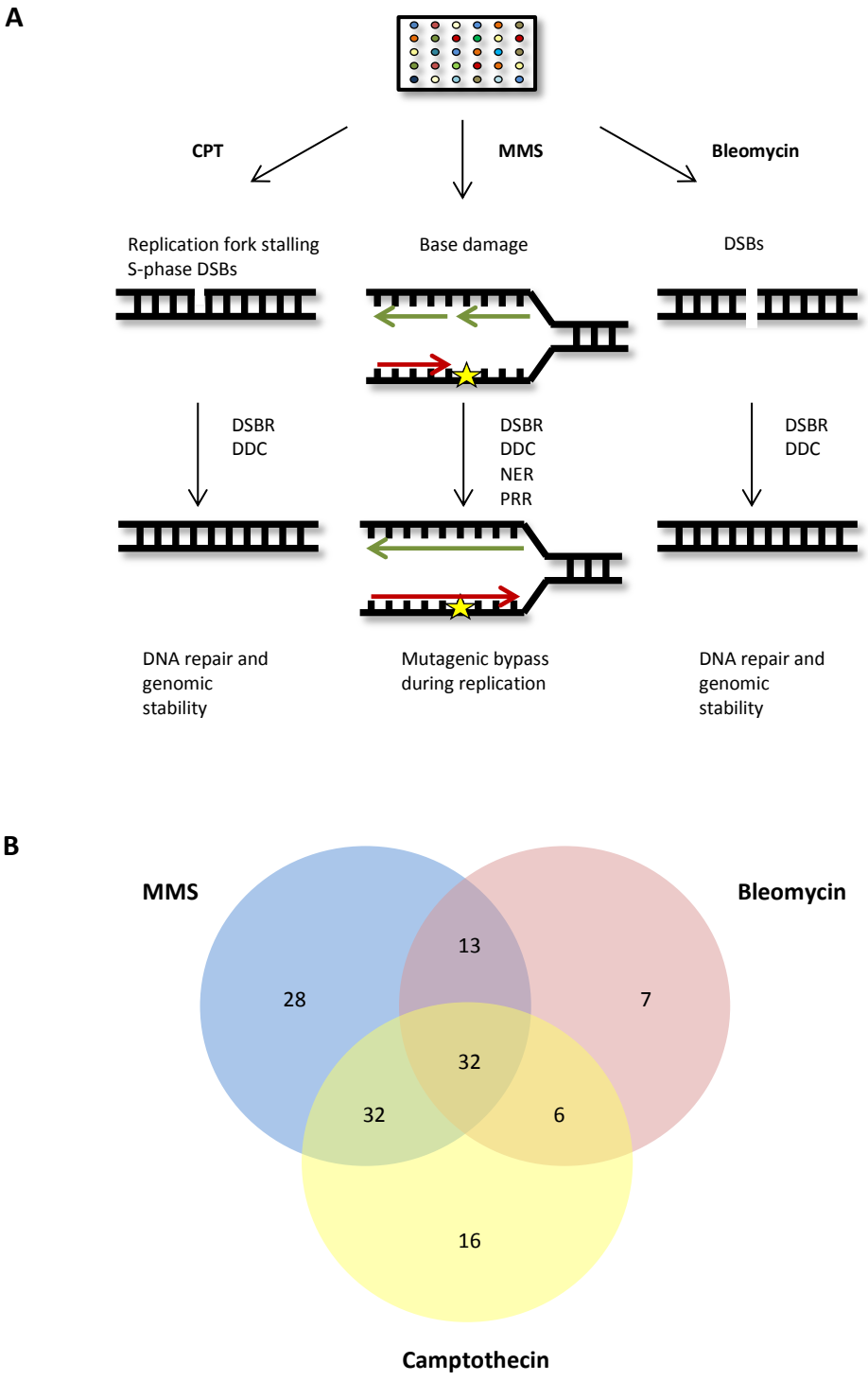


Figure 4.4: Cluster Enrichment and sensitivity distribution. (A) Schematic depicting the inflicted damage by the various agents and cellular pathways required to resolve caused lesions. Abbreviations: Double-Strand Break Repair (DSBR), DNA Damage Checkpoint (DDC), Nucleotide Excision Repair (NER), Post Replication Repair (PRR). (B) Venn diagram of the sensitivity distribution of hits. Most hits were sensitive to MMS, consistent with a number of pathways involved in mending inflicted damage by this clastogen. Most genes functioning in DSB repair (DSBR) and DNA damage checkpoints (DDC) were found in the subgroup sensitive to all three agents MMS, bleomycin and camptothecin.

Table 4.1

Strain	Gene Name	Sensitivities	GO Term	Human homolog
SPAC56E4.07		CPT	Acetyltransferase	-
SPAC1039.08		MMS, CPT	Acetyltransferase	-
SPAC2G11.13	*atg22*	CPT	Autophagy	-
SPBC83.18c		Bleo	Cell cycle	-
SPCC645.07	*rgf1*	MMS, Bleo, CPT	Cell wall synthesis	*ARHGEF3*
SPAC8E11.02c	*rad24*	Bleo	Checkpoint	*14-3-3 Protein*
SPAC17H9.19c	*cdt2*	CPT	Checkpoint	*DTL*
SPBC660.14	*mik1*	MMS	Checkpoint	*Wee1 Kinase*
SPBC216.05	*rad3*	MMS, Bleo, CPT	Checkpoint	*ATR*
SPAC1D4.06c	*csk1*	MMS, Bleo, CPT	Checkpoint	*CAKAK*
SPAC9E9.08	*rad26*	MMS, Bleo, CPT	Checkpoint	*ATRIP*
SPAC1952.07	*rad1*	MMS, Bleo, CPT	Checkpoint	*RAD1*
SPAC664.07c	*rad9*	MMS, Bleo, CPT	Checkpoint	*RAD9*
SPAC20G4.04c	*hus1*	MMS, Bleo, CPT	Checkpoint	*HUS1*
SPAC14C4.13	*rad17*	MMS, Bleo, CPT	Checkpoint	*RAD17*
SPAC694.06c	*mrc1*	MMS, CPT	Checkpoint	-
SPCC18B5.11c	*cds1*	MMS	Checkpoint	*CHK2*
SPCC126.04c		CPT	Chromatin remodeling	*ATXN7*
SPAC17G8.13c	*mst2*	CPT	Chromatin remodeling	*MYST1*
SPAC139.06	*hat1*	MMS	Chromatin remodeling	*HAT1*
SPBC4B4.03	*rsc1*	MMS	Chromatin remodeling	*hPB1*
SPBC1734.15	*rsc4*	MMS	Chromatin remodeling	*hPB1*
SPAC23D3.09	*arp42*	MMS, Bleo	Chromatin remodeling	*ACTL6A*
SPAC10F6.08c	*nht1*	MMS, Bleo	Chromatin remodeling	-
SPAC2F7.07c	*cph2*	MMS, Bleo, CPT	Chromatin remodeling	*PHD-finger*
SPBC11B10.10c	*pht1*	MMS, Bleo, CPT	Chromatin remodeling	*H2A*
SPBC342.06c	*rtt109*	MMS, CPT	Chromatin remodeling	*p300-CBP*
SPAC16C9.05	*cph1*	MMS, CPT	Chromatin remodeling	*PHD-finger*
SPAC25A8.01c		MMS, CPT	Chromatin remodeling	*SMARCAD1*
SPBC31F10.14c	*hip3*	MMS, CPT	Chromatin remodeling	-
SPBC365.10	*arp5*	MMS, Bleo	Chromatin remodeling	*FLJ12785*
SPAC17G8.09	*shg1*	MMS	Chromatin remodeling	-
SPAC6F6.09		MMS, Bleo	Chromatin remodeling	*FLJ11730*
SPBC28F2.11		MMS	Chromatin remodeling	*HMGB2*
SPAC343.11c	*msc1*	Bleo	Chromatin remodeling	*SMCX*
SPCC417.02	*dad5*	MMS, Bleo, CPT	Chromosome segregation	-
SPAC14C4.16	*dad3*	MMS, CPT	Chromosome segregation	-
SPCC1223.15c	*spc19*	MMS, CPT	Chromosome segregation	-
SPAC1805.07c	*dad2*	MMS, CPT	Chromosome segregation	-
SPAC16E8.01		MMS	Cytoskeleton	*La protein*
SPAC3G6.06c	*rad2*	MMS	DNA Nuclease	*FEN-1*
SPBC3D6.10	*apn2*	MMS	DNA Nuclease	*APEX1*

SPBC3E7.08c	*rad13*	MMS	DNA Nuclease	*XPGC*
SPAC30D11.07	*nth1*	MMS	DNA Nuclease	*NTHL1*
SPBC29A10.05	*exo1*	MMS	DNA Nuclease	*EXO1*
SPAPB1E7.06c	*eme1*	MMS, Bleo	DNA Nuclease	*Eme1*
SPBC18H10.19		MMS	DNA Repair	*UVRAG*
SPAC13C5.07	*rad32*	MMS, Bleo, CPT	DNA Repair	*MRE11*
SPAC644.14c	*rhp51*	MMS, Bleo, CPT	DNA Repair	*RAD51D*
SPAC1556.01c	*rad50*	MMS, Bleo, CPT	DNA Repair	*RAD50*
SPBC119.14	*rad22*	MMS, Bleo, CPT	DNA Repair	*RAD52*
SPAC20H4.07	*rhp57*	MMS, Bleo, CPT	DNA Repair	*XRCC3*
SPCC338.08	*ctp1*	MMS, Bleo, CPT	DNA Repair	*CtIP*
SPAC2G11.12	*rqh1*	MMS, Bleo, CPT	DNA Repair	*BLM*
SPBC342.05	*crb2*	MMS, CPT	DNA Repair	*53BP1*
SPAC6B12.02c	*mus7*	MMS, CPT	DNA Repair	-
SPAC17H9.03c	*rdl1*	MMS, CPT	DNA Repair	*RAD51D*
SPBC336.01	*fbh1*	MMS, CPT	DNA Repair	*FLJ14590*
SPBC1685.11	*rlp1*	MMS	DNA Repair	-
SPAC17H9.10c	*ddb1*	MMS	DNA Repair	*DDB1*
SPCP25A2.02c	*rhp26*	MMS	DNA Repair	*ATRIP*
SPAPB17E12.04c	*csn2*	MMS, Bleo, CPT	dNTP metabolism	*CSN2*
SPBC215.03c	*csn1*	MMS, Bleo, CPT	dNTP metabolism	*GPS1*
SPAC11E3.04c	*ubc13*	MMS	E2 Ligase	*UBE2*
SPCC126.07c		CPT	E3 Ligase	*SCAF1*
SPCC1919.15	*brl1*	MMS, Bleo	E3 Ligase	*RNF40*
SPCC790.02	*pep3*	MMS, Bleo	E3 Ligase	*VPS18*
SPAC11G7.02	*pub1*	MMS, CPT	E3 Ligase	*SMURF2*
SPBC21D10.09c		MMS, Bleo	E3 Ligase	*ZNF294*
SPAC13G6.01c	*rad8*	MMS	E3 Ligase	*HLTF*
SPBC342.01c	*alg6*	Bleo	Lipid metabolism	*ALG6*
SPCC550.14	*vgl1*	CPT	Lipid metabolism	*HDLBP*
SPBC887.15c		MMS, Bleo, CPT	Lipid metabolism	-
SPCC1183.10	*wtf10*	MMS	Membrane	-
SPAC1B3.01c	-	Bleo	Metabolism	*UCK1*
SPAC17G8.06c	-	Bleo	Metabolism	-
SPAC15E1.04	-	Bleo, CPT	Metabolism	*TYMS*
SPAC9E9.09c		Bleo, CPT	Metabolism	*ALDH1A2*
SPBC29A3.10c	*atp14*	CPT	Metabolism	-
SPAC1F12.07		CPT	Metabolism	*PSAT1*
SPAC11D3.08c	-	MMS	Metabolism	-
SPBC776.06c	*Arf3/6*	MMS	Metabolism	-
SPBC2G5.06c	*hmt2*	MMS	Metabolism	*SQRDL*
SPBC337.15c	*coq7*	MMS	Metabolism	*COQ7*
SPBC31F10.15c	*atp15*	MMS	Metabolism	*ATP5E*
SPAC1250.04c	*atl1*	MMS	Metabolism	*MGMT*
SPAC1142.05	*ctr5*	MMS, Bleo	Metabolism	*SLC31A1*

SPAC29B12.04	*snz1*	MMS, Bleo	Metabolism	-
SPBC18H10.02	*lcf1*	MMS, Bleo, CPT	Metabolism	*ACSL4*
SPAC521.04c		MMS, Bleo, CPT	Metabolism	-
SPBC16C6.09	*ogm4*	MMs, Bleo, CPT	Metabolism	*OGM4*
SPCC1450.03		MMS, Bleo, CPT	Metabolism	*KIAA0007*
SPBC354.12	*png1*	MMS, CPT	Metabolism	*GADPH*
SPBC16E9.18	*psd1*	MMS, CPT	Metabolism	*PISD*
SPAC20G4.07c	*sts1*	MMS, CPT	Metabolism	*DHCR7*
SPBC947.15c		MMS, CPT	Metabolism	-
SPBC1A4.09	-	MMS, CPT	Metabolism	*FLJ20485*
SPBP8B7.31		MMS, Bleo	Metabolism	*BC009495*
SPAC1071.05		CPT	Methyltransferase	*C1orf156*
SPCC1739.06c		CPT	Methyltransferase	-
SPCC417.07c	*mto1*	CPT	Microtubule	-
SPAC29A4.17c		MMS	Mitochondrium	-
SPAC823.10c		MMS	Mitochondrium	*SLC25A38*
SPBC582.06c	*mcp6*	MMS, CPT	Movement	-
SPAC17A5.07c	*ulp2*	MMS, Bleo, CPT	Protease	*SENP7*
SPAPB1E7.02c	*mcl1*	Bleo	Replication	*WDHD1*
SPAC19D5.11c	*ctf8*	Bleo, CPT	Replication	*CTF8*
SPCC23B6.05c	*ssb3*	MMS, CPT	Replication	*RPA3*
SPBC30D10.04	*swi3*	MMS, CPT	Replication	*TIPIN*
SPAC26A3.07c	*rpl1101*	Bleo, CPT	Ribosomal protein	*RPL11*
SPAC23C11.02c	*rps23*	Bleo, CPT	Ribosomal protein	*RPS23*
SPCC364.03	*rpl1702*	CPT	Ribosomal protein	*RPL17*
SPAC9G1.03c	*rpl3001*	MMS, Bleo	Ribosomal protein	*RPL30*
SPAC26A3.04	*rpl2002*	MMS, Bleo	Ribosomal protein	*RPL20*
SPAC1F7.13c	*rpl801*	MMS, Bleo	Ribosomal protein	*RPL8*
SPAC1556.05c	*cgr1*	MMS, Bleo	Ribosomal protein	-
SPAC3H5.10	*rpl3202*	MMS, Bleo, CPT	Ribosomal protein	*RPL32*
SPBC365.03c	*rpl2101*	MMS, Bleo, CPT	Ribosomal protein	*RPL21*
SPAC521.05	*rps802*	MMS, CPT	Ribosomal protein	*RPS8*
SPAC8C9.07		MMS, CPT	Ribosomal protein	-
SPAC1610.02c		MMS, CPT	Ribosomal protein	*MRPL1*
SPAPB17E12.05	*rpl3703*	MMS, Bleo	Ribosomal protein	*RPL37*
SPBC11C11.07	*rpl1801*	MMS, Bleo	Ribosomal protein	*RPL18*
SPAC140.03	*arb1*	MMS, Bleo	RNA interference	-
SPCC736.11	*ago1*	MMS, Bleo, CPT	RNA interference	*EIF2C1*
SPAC13G7.07	*arb2*	MMS, Bleo, CPT	RNA interference	-
SPBC20F10.05	*nrl1*	MMS, Bleo, CPT	RNA interference	*C14orf102*
SPCC1393.05	*ers1*	MMS, Bleo, CPT	RNA interference	-
SPAC12G12.13c	*cid14*	MMS, Bleo, CPT	RNA processing	*PAPD7*
SPAC3H8.09c	*nab3*	MMS	RNA processing	*HNRPC*
SPBP8B7.28c		Bleo	sequence orphan	-
SPBC2D10.16		MMS	Sequence orphan	-
SPAC17C9.15c		MMS	Sequence orphan	-

SPCC16C4.20c		MMS, Bleo	Sequence orphan	-
SPAC8C9.19		MMS, Bleo, CPT	Sequence orphan	-
SPCC584.12	*mug42*	MMS, CPT	Sequence orphan	-
SPAC3H8.05c		MMS, CPT	Sequence orphan	-
SPCC576.12c	*Mhf2*	MMS	Sequence orphan	-
SPAC16E8.08		Bleo	Sequence orphan	-
SPAPB21F2.03		MMS, Bleo	Sequence orphan	-
SPBC21D10.08c		MMS	Sequence orphan	-
SPBP8B7.26		Bleo	Sequence orphan	-
SPAC4H3.02c		Bleo	Sequence orphan	-
SPBC119.08	*pmk1*	Bleo, CPT	Signaling	*MAPK6*
SPBP16F5.07	*apm1*	Bleo, CPT	Signaling	*AP1M1*
SPAC19B12.10	*sst2*	CPT	Signaling	*STAMBP*
SPAPYUG7.02c	*sin1*	CPT	Signaling	*MAPKAP1*
SPAC4C5.02c	*ryh1*	MMS, Bleo, CPT	Signaling	*RAB36*
SPBC26H8.05c		MMS, CPT	Signaling	*PPP4C*
SPBC839.03c	*Dcn1*	MMS, CPT	Signaling	*RP42*
SPAC1071.04c		Bleo	Signaling	-
SPCC895.07	*alp14*	Bleo	Signaling	-
SPAC4F8.10c	*stg1*	MMS	Signaling	*SM22*
SPBC23G7.08c	*rga7*	MMS	Signaling	*ARHGAP9*
SPBC1778.02	*rap1*	MMS	Telomere maintenance	*TERF2IP*
SPCC188.07	*ccq1*	MMS, Bleo	Telomere maintenance	-
SPBC2D10.13	*est1*	MMS, Bleo	Telomere maintenance	*EST1*
SPBC29A3.14c	*trt1*	MMS, CPT	Telomere maintenance	*TERT*
SPBC16A3.08c		MMS, Bleo	Telomere maintenance	-
SPAC23C11.08	*php3*	Bleo	Transcription	*NFYB*
SPCC74.02c		CPT	Transcription	-
SPAC1783.07c	*pap1*	MMS	Transcription	-
SPAC144.02		MMS	Transcription	*ZNF*
SPBC13E7.08c		MMS	Transcription	*LEO1*
SPBC19C2.14	*smd3*	MMS	Transcription	*SNRPD3*
SPBC1718.03	*ker1*	MMS, Bleo	Transcription	-
SPAC664.03		MMS, Bleo	Transcription	*PD2*
SPAC31A2.11c	*cuf1*	MMS, Bleo	Transcription	-
SPAC57A7.04c	*pabp*	MMS, Bleo, CPT	Transcription	*PABP3*
SPBC16G5.15c	*fkh2*	MMS, Bleo, CPT	Transcription	*FOXO*
SPAC22F3.09c	*res2*	MMS, Bleo, CPT	Transcription	-
SPBC609.05	*pob3*	MMS, Bleo, CPT	Transcription	*SSRP1*
SPBC31F10.09c	*nut2*	MMS, CPT	Transcription	*MGC5309*
SPBC23E6.09	*ssn6*	MMS, CPT	Transcription	*UTX*
SPAC1071.02		MMS, CPT	Transcription	*MMS19L*
SPAC5D6.05	*sep11*	MMS, CPT	Transcription	-
SPAP14E8.02		MMS, CPT	Transcription	-
SPBC16A3.07c	*nrm1*	MMS, Bleo	Transcription	-
SPBC4C3.12	*Sep1*	MMS, Bleo	Transcription	*FOXO*

SPAC23H4.17c	*srb10*	Bleo	Transcription	*CDK8*
SPBC21C3.02c		MMS	Transcription	-
SPCC4F11.04c		MMS	Transferase	-
SPAC17G8.11c		MMS, Bleo, CPT	Transferase	-
SPBC15D4.06		MMS	Transferase	*NAT8*
SPAC3A12.13c		MMS, Bleo	Translation	*eIF3*
SPBC16C6.05		MMS	Translation	*DRP1*
SPBC713.08	*tom13*	MMS	Translocation	-
SPBC27B12.08		Bleo	Transport	*C13F10.4.p*
SPBC16C6.02c	*vps1302*	Bleo, CPT	Transport	*VPS13A*
SPAC823.05c	*tlg2*	Bleo, CPT	Transport	*STX16*
SPBC4F6.10	*vps901*	CPT	Transport	*RABGEF1*
SPAC1142.07c	*vps32*	MMS	Transport	*Snf7*
SPAC31A2.13c	*sft1*	MMS, Bleo, CPT	Transport	*SPAC31A2.13c*
SPBC2G2.03c	*sbh1*	MMS, Bleo, CPT	Transport	*SEC61B*
SPBC1539.08	*arf6*	MMS, Bleo	Transport	*ARF6*
SPBC359.03c		Bleo	Transport	*KIAA1613*
SPAC31A2.02	*trm112*	MMS	tRNA metabolism	*HSPC152*
SPBC56F2.01	*pof12*	MMS	Ubiquitination	-
SPAC1F3.03		Bleo	Unknown	*KIAA1006*
SPBC3H7.14	*mug176*	CPT	Unknown	-
SPBC21C3.12c	*Duf953*	MMS	Unknown	*TXNL5*
SPAC31G5.19	-	MMS	Unknown	*KIAA1240*
SPCC1442.02		MMS, CPT	Unknown	-
SPBC660.09		MMS, CPT	Unknown	-
SPBC1703.11		MMS, Bleo	Unknown	*OPA3*
SPBC354.03	*swd3*	MMS, Bleo	Unknown	*WDR71*
SPCC330.11	*btb1*	MMS	Unknown	-
SPCC4B3.03c		MMS	Unknown	*CNNM1*
SPCC1739.01		CPT	Zinc finger	-

Table 4.1: Summary of all confirmed sensitive hits. Sensitive deletion strains with Gene Name, Sensitivites, Gene Ontology (GO) term, and Human homolog.

4.2.3 Novel genes in chromatin dynamics

Mutants of three members of the Chromatin Structure Remodeling (RSC) complex (*rsc1*, *rsc4*, *arp42*) were found to be sensitive to MMS, while *arp42Δ* also displayed hypersensitivity to bleomycin. Chromatin remodeling activities are known to enable efficient DSB repair. Rsc1 has previously been implicated in conferring resistance to DNA damaging agents (Shim et al. 2005; Kent et al. 2007), and its role in remodeling chromatin around a DNA DSB as a mean to contribute to DNA repair was recently further elucidated (Chambers and Downs 2012). However, Arp42's role in DNA repair remains to be more elusive. It is not only part of the RSC complex, but also a functional subunit of the (SWItch/Sucrose NonFermentable) SWI/SNF complex (Monahan et al. 2008). SWI/SNF functions in nucleosome remodelling, the complex is highly conserved in eukaryotes, and members have been implicated in a wide range of human clinical malignancies (Kosho et al. 2013), including tumour-supressing activities (Khursheed et al. 2013). While sensitivity of *arp42* mutants in yeast has been reported to the antimicrotubular drug thiabendazole and depolymerising drugs (Han et al. 2010), its MMS and bleomycin sensitivity has, to our knowledge, not been reported yet. The human ortholog of *arp42* is Actin-like protein 6A (*ACTL6A*), part of the BAF (BRG1/brm-associated factor) complex, which is the mammalian functional analogue to SWI/SNF in yeast. A direct involvement neither of Arp42 nor of its human counterpart ACTL6A in DNA damage repair has so far been identified (Bao et al. 2013).

In addition, the Clr6 histone deacetylation proteins Cph1 and Cph2 were found to be required for resistance to MMS and CPT, while *cph2Δ* also displays sensitivity to bleomycin. According to PomBase (http://www.PomBase.org) hypersensitivity of *cph*-mutants to DNA damaging agents has not been reported. The genes function in the same pathway as Clr6, which is involved in H3-K9 specific deacetylation (Nicolas et al. 2007).

Furthermore, Sgf73, which is part of the SAGA complex (Lee et al. 2009), another histone acetylation complex, was found to confer resistance to camptothecin. In addition, deletion of Nht1, a widely uncharacterised protein, sensitised the strain to MMS and bleomycin. Nht1 contains a high mobility box (HMB) domain, which is known to mediate chromatin-associated DNA-binding. HMG-box domains have been found in various types of proteins, including transcription factors, chromatin remodelling factors, as well as proteins involved in replication and DNA repair (Stros et al. 2007). Nht1 is related to the mammalian and *S. cerevisiae* INO80 complex, which is an ATP-dependent nucleosome remodelling complex, acting at DSBs (Morrison et al. 2004; Tsukuda et al. 2005; van Attikum and Gasser 2005).

Figure 4.5

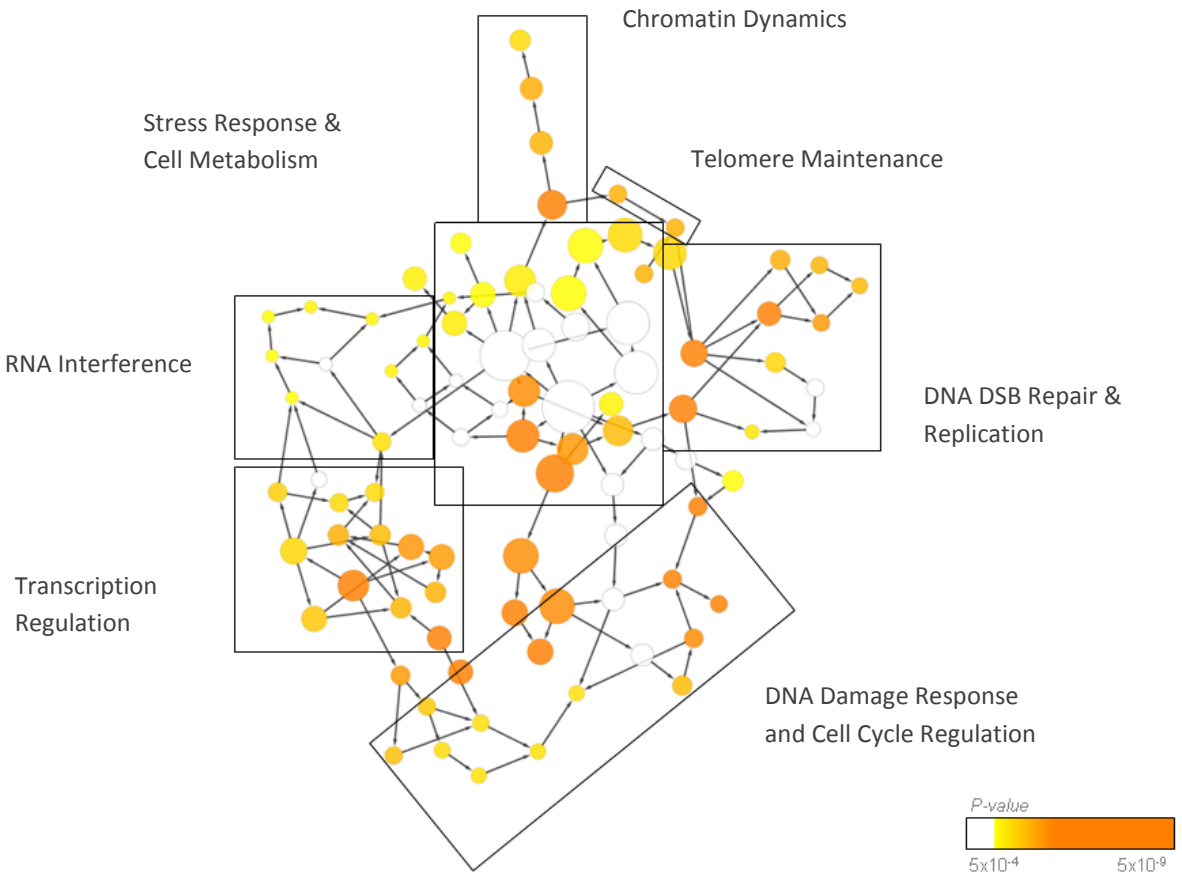


Figure 4.5 GO Network of enriched clusters. Every sensitive hit of the screen was annotated with a Gene Ontology term and placed into functionally related super-groups utilising Cytoscape/BiNGO. Statistical analysis was carried out and groups displaying an enrichment of $p<10^{-4}$ in the sensitive list when compared with the genome-wide distribution, were placed into an interaction network.

4.2.3 Novel genes in transcription regulation

Another over-represented group contained genes involved in regulation of transcription. Notably, the yeast forkhead transcription factor Fkh2, homologous to human forkhead box O (FOXO) transcription factors, displayed sensitivity to all agents, MMS, bleomycin and CPT, indicative of an essential function in DNA repair. Recent data suggest a role for the yeast forkhead transcription factors Fkh1 and Fkh2 as evolutionary conserved regulators of lifespan by interaction with the Anaphase-Promoting Complex (APC), potentially through interdependent regulation of genome stability, cell cycle regulation and stress response (Postnikoff et al. 2012). Furthermore, fission yeast Start-specific transcription factor Res2 was found to be sensitive to all of the used clastogens. Its role in regulation of meiotic as well as mitotic cell cycle progression as transcriptional activator subunit of the Res2-Cdc10 complex is firmly established (Zhu et al. 1997; Whitehall et al. 1999), a direct involvement in DNA damage repair remains uncharacterised. Since cell cycle pathways are known to augment DNA damage repair pathways, it is tempting to speculate on a function of Res2 in this regard.

4.2.4 DNA damage repair and telomere maintenance

The complex interdependencies of telomere maintenance and DNA damage repair factors are reviewed here (Ribeyre and Shore 2013). Since telomeres are technically a form of a DSB, a delicate balance in maintaining these entities at the end of the chromosomes has evolved, since DNA repair mechanisms and checkpoint activation have to be avoided. While some interplay of DNA repair factors in telomere maintenance is known, such as ‘capping’ of telomeric ends by NHEJ proteins, such as the Ku70/80 complex, the involvement of telomeric proteins at non-telomeric DSBs remains widely elusive. However, limited 5’ to 3’ exonucleolytic resection of DSBs, was found to increase *de-novo* telomere addition at non-telomeric break-sites, indicative of a presence of telomeric

maintenance factors, especially when long-range resection is defective (Chung et al. 2010; Lydeard et al. 2010). In this study, the telomere factors Rap1, Ccq1, Trt1, and Est1 were found to confer resistance to DNA damaging agents. All mutants of these genes displayed sensitivity to MMS, *ccq1*Δ and *est1*Δ were also sensitive to bleomycin, while *trt1*Δ was sensitive to MMS and CPT.

While dysfunctional telomeres *per se* naturally pose a serious threat to genome stability, an Mre11-dependent recruitment of the telomerase Est1 (along with Est2) at non-telomeric DSBs was previously reported (Negrini et al. 2007; Ribaud et al. 2012), leaving room for conjecture on a direct function of telomeric factors in HR repair. Bleomycin-sensitivity of the *est1*Δ strain is consistent with such a hypothesis.

Figure 4.6

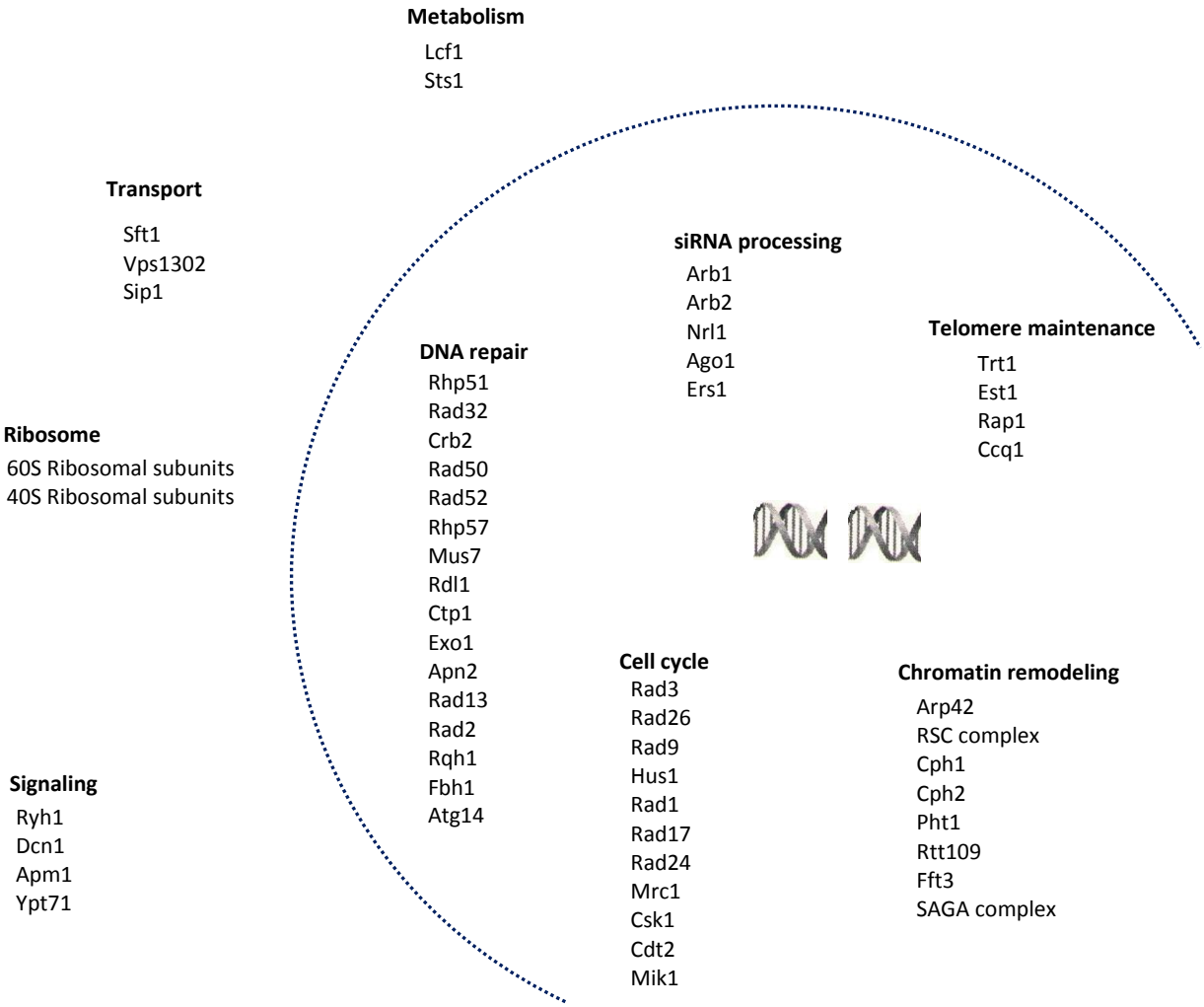


Figure 4.6: Selection of hits identified as part of the genome-wide DNA-damage sensitivity screen. Most known DNA repair and cell cycle factors in fission yeast were confirmed as hits as part of this pan-genomic DNA repair screen, validating the chosen methodology of the screen. A number of interesting hits, functioning in a variety of pathways were identified.

4.2.5 DNA damage and ribosomal proteins

Intriguingly, a number of ribosomal genes (*rpl1101, rps23, rpl1702, rpl3001, rpl2002, rpl801, rpl3202, rpl2101, rps802, cgr1*) were identified in this study as conferring resistance to DNA damaging agents. While a direct effect of the ribosome in DNA repair has not been established, it is tempting to speculate on indirect effects such as translation levels of DNA damage or cell cycle factors. Misregulation of the DDR or general stress responses would leave the cell vulnerable to clastogens.

4.2.6 DNA damage and the siRNA machinery in fission yeast

Notably, deletion mutants of several core components (*arb2, ago1, ers1*), along with one putative novel member (*nrl1*), of the siRNA machinery were found to be hypersensitive to damaging agents. While preliminary accounts of crosstalk of the RNAi pathway and the DNA damage response have recently emerged in humans (Francia et al. 2012; Wei et al. 2012), a role for the *S. pombe* RNAi machinery remains enigmatic and has not been established to this date. siRNA genes in fission yeast function mainly in establishing heterochromatic silencing via H3K9 methylation at telomeres, centromeres, rDNA loci, and the mating type locus; a direct involvement in DNA repair remains speculative (Buhler and Moazed 2007). Since chromatin remodeling is strongly associated with DNA repair, a direct role of the siRNA machinery in DNA damage repair represents an intriguing corollary. A more detailed account of a potential role of this pathway in homologous recombinational repair is presented in **Chapter V**.

4.2.7 Other genes

Interestingly, a strain harbouring a deletion of *rdl1*, homolog of human *RAD51D*, was found to be sensitive to MMS and camptothecin. In fission yeast, *rdl1* is not characterised, and sensitivity to DNA damaging agents has not been reported yet. In humans, *RAD51D*, being one of the five *RAD51* paralogues (*RAD51B, RAD51C, RAD51D, XRCC2, XRCC3*),

functions in a complex with Rad51B, Rad51C, and Xrcc2 to promote homologous pairing between double- and single-stranded DNA, upstream of Rad51 filament formation (Chun et al. 2013), and germline mutations of *RAD51D* have been associated with increased risk for ovarian carcinoma (Loveday et al. 2011).

Remarkably, one over-represented sub-group was associated with microtubule maintenance and chromosome segregation. Four members of the DASH complex (*dad2, dad3, dad5, spc19*) came out as hits as part of this screen. The DASH complex is involved in attachment of spindle microtubules to the kinetochore. While previous studies could establish roles for microtubule organising centres (spindle pole bodies and centrosomes) and genome stability, the mechanisms behind this interaction are elusive; a role for the DASH complex in this regard has not been characterised yet (Kobayashi et al. 2007).

4.3 Discussion

4.3.1 Further analysis

Confirmed hits were subsequently transformed with the mini-chromosome Ch^{16}-*LMYAU* (*L*eu2 *M*ATa H*y*gromycin *A*denine *U*racil), carrying an inducible HO-recognition-site as well as an endogenous copy of HO endonuclease under an *nmt*-promoter. The minichromosome harbours an *ade6*-M216 heteroallele, centromere-distal to the break-site. After break-induction on minus thiamine plates, failed repair can lead to loss of the *ade6* allele by loss of heterozygosity or loss of the whole chromosome, indicated by pink sectoring on low-adenine plates.

For further characterisation, the hypersensitive sectoring mutants were back-crossed to wild type to lose endogenous markers and the minichromosome Ch^{16}-*RMYAH* was

introduced, along with an ectopic, inducible HO endonuclease. Ch^{16}-*RMYAH* allows for a quantifiable DSB repair assay, in which different repair events, *i.e.* gene conversion, non-homologous end-joining or failure of repair, *i.e.* chromosome loss or loss of heterozygosity can be deduced based on marker loss following break-induction. A detailed account of the further characterisation is given in **Chapter V**.

4.3.2 General Discussion

In this chapter, efforts are described to compile a list of genes involved in the fission yeast DNA damage response. For this purpose, the three DNA damaging agents MMS, bleomycin, and camptothecin were utilised. As predicted, most known DNA damage and cell cycle control factors could be identified as part of this screen, providing confirmation of the validity of the chosen methodology. Additionally, a number of new factors in DNA repair were identified and associated with functions in this regard for the first time (**Figure 4.6**). To enrich the cluster of DNA damage resistance-conferring genes for novel factors functioning in HR, two assays utilising different non-essential minichromosomes were employed.

4.3.3 Summary

A total of 209 mutants were hypersensitive to at least one of the DNA damaging agents MMS, bleomycin and camptothecin. Well-defined DNA damage factors were removed from further characterisation to enrich the final list of hits for novel DNA damage repair factors, while a *rad22* deletion strain was kept as internal control.

CHAPTER V

Screening for novel factors in HR

5.1 Introduction

This chapter describes the second half of the genome-wide screen for novel HR factors. Having compiled a comprehensive list of genes conferring resistance to DNA damaging agents in fission yeast, as described in **Chapter IV**, the objective of this chapter was the identification of novel DNA damage repair factors functioning in HR. For this purpose, two different minichromosomes Ch^{16}-*LMYAU*, and Ch^{16}-*RMYAH* were utilised to investigate potential disruptions in DSB repair, and derive quantifiable DNA repair profiles of hypersensitive null mutants.

5.2 Results

5.2.1 Ch^{16}-*LMYAU* Sectoring Assay

To test the cohort of confirmed sensitive mutant strains from the DNA damage screen for their ability to repair DSBs, the deletion strains were subjected to the Ch^{16}-*LMYAU* colony sectoring assay. Since the objective of this part of the study was the identification of novel HR factors, well defined DNA damage genes were excluded before the sectoring step of the screen. For this purpose, the deletion strains were transformed with the mini-chromosome Ch^{16}-*LMYAU* (*L*eu2 *M*ATa H*y*gromycin *A*denine *U*racil), carrying an inducible HO recognition-site as well as an endogenous copy of HO endonuclease under

an *nmt*-promoter (**Figure 5.1; Chapter 2.10.1**). The minichromosome harbours an *ade6*-M216 heteroallele, centromere-distal to the break-site. After break-induction on minus-thiamine plates, failed repair can lead to loss of the *ade6* allele by loss of heterozygosity or loss of the whole chromosome. Ade^- cells accumulate a pink metabolite when growing under limiting conditions, causing sectoring or striations of colonies (Fisher 1969) on low-adenine plates, thus visualising failed repair events in this assay.

Figure 5.1

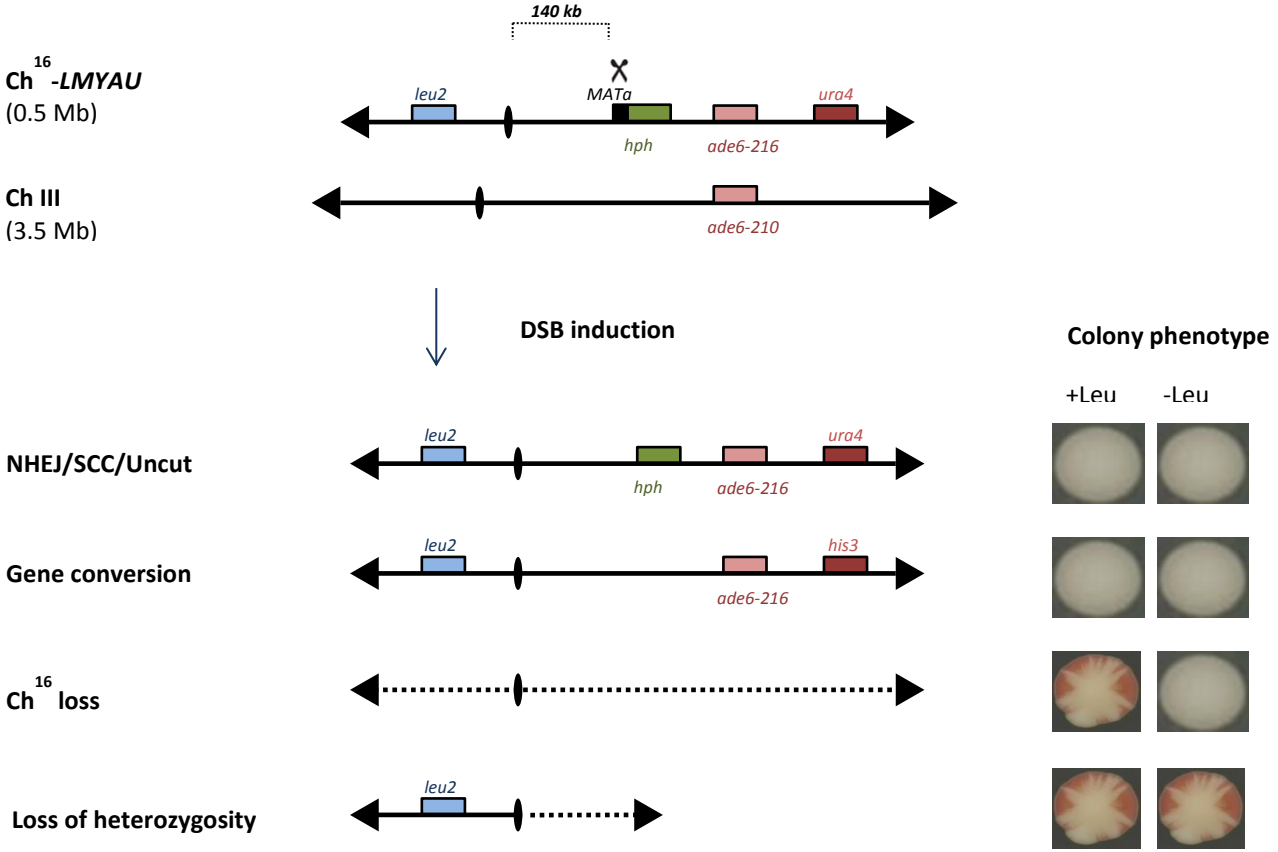

140 kb
Ch 16 -LMYAU
(0.5 Mb)
leu2
MATa
ura4
hph
ade6-216
Ch III
(3.5 Mb)
ade6-210
DSB induction
Colony phenotype
+Leu
-Leu
NHEJ/SCC/Uncut
leu2
ura4
hph
ade6-216
Gene conversion
leu2
his3
ade6-216
Ch 16 loss
Loss of heterozygosity
leu2

Figure 5.1: Schematic of the colony sectoring assay. Under thiamine-limiting conditions, expression of the endogenous HO endonuclease on the left arm of Ch^{16}-*LMYAU* is induced and results in a DSB at the *MATa* site, illustrated by scissors. Repair events NHEJ/SCC and GC lead to retention of the *ade6*-M216 allele on the minichromosome. Consequently, white colony phenotypes are present on both EMM + $RHUTA_L$L, and EMM+ $RHUTA_L$ media plates. If the cells fail to repair, the *ade6*-M216 allele is lost, causing accumulation of a pink pigment under low-adenine conditions. Failed repair events Ch^{16} loss and LOH can be differentiated by retention of the *leu2* marker on the left arm of the minichromsome, as only LOH cells are viable on EMM+$RHUTA_L$ plates.

5.2.2 Sectoring mutants and sensitivities

Of the 209 hypersensitive hits derived from the DNA damage screen (**Chapter IV**), 141 strains could be successfully crossed with the Ch^{16}-*LMYAU* harbouring strain, and were subjected to the colony sectoring assay. Growth of this set of mutants occurred on selective media, under break-repressing conditions (2 μM thiamine). Subsequently, cells were diluted and streaked onto 4 different sectoring plates: EMM+$HRUA_L$, EMM+$HRUA_L$T, EMM+$HRUA_L$L, and EMM+$HRUA_L$LT. Spontaneous and break-induced minichromosome loss, as well as LOH could be detected by pink sectoring of respective colonies (**Figure 5.1**). Of the 141 strains, 39 mutants displayed break-induced sectoring on at least one of the sectoring plates, indicative of defective genome stability (**Table 5.1**). Confirmation of correct deletions was obtained with PCR analysis for the cohort of sectoring deletion strains; all but one strain (V2-30-F10; *pmk1*Δ) harboured the deletion cassette at the appropriate locus (**Appendix IV**). While the sectoring colony phenotype was mainly observed on break-inducing (no thiamine) plates, some deletion strains exhibited spontaneous minichromosome loss (**Figure 5.2**). Well defined DNA damage genes were excluded before the sectoring step of the screen. However, some deletion strains of known DNA repair factors were retained, either as internal control (*rad22*Δ, *rqh1*Δ), or when DSB assays of the respective strains have not yet been carried out by the lab (*rad50*Δ, *fbh1*Δ).

Figure 5.2

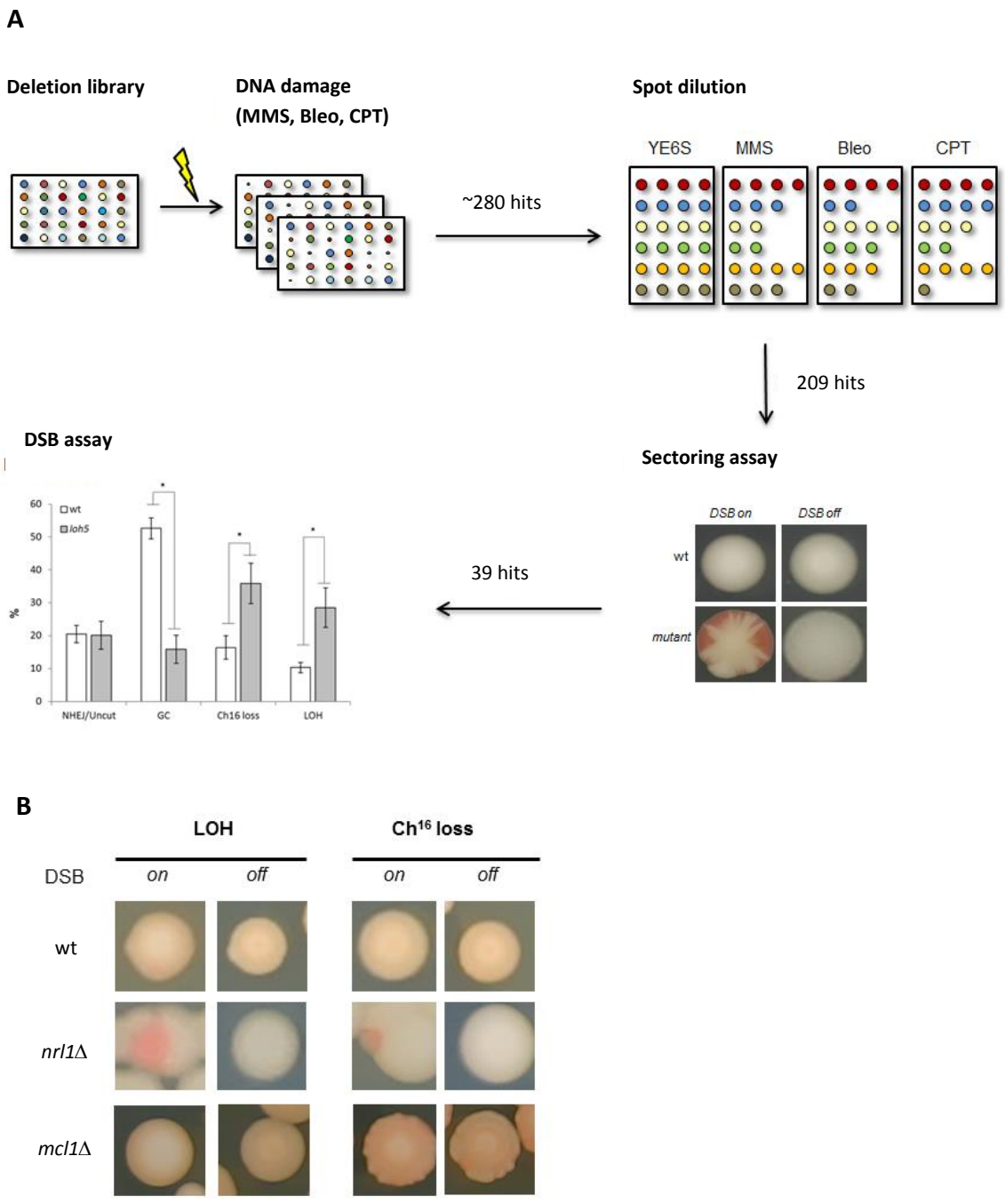


Figure 5.2: Overview of screen and Ch^{16}-*LMYAU* colony sectoring phenotypes. (A) Overview of genome-wide screen. Following screening and confirmation of deletion-library for sensitivity to DNA damaging agents, the colony sectoring assay was carried out as described. (B) A selection of mutants (*nrl1*Δ, *mcl1*Δ) is shown to exemplify different colony phenotypes as a result of differential repair of a DSB. While induction of a DSB in an *nrl1*-mutant leads to both increased LOH, and Ch^{16} loss, an *mcl1*Δ strain exhibits spontaneous and break-induced Ch^{16} loss, as illustrated by sectoring colonies.

Table 5.1

Strain	Gene Name	GO Term	Human homolog	Sensitivities
SPAC2G11.13	*atg22*	Autophagy		CPT
SPBC660.14	*mik1*	Checkpoint	*Wee1 Kinase*	MMS
SPAC1D4.06c	*csk1*	Checkpoint	*CAKAK*	MMS, Bleo, CPT
SPBC11B10.10c	*pht1*	Chromatin remodelling	*H2A*	MMS, Bleo, CPT
SPBC342.06c	*rtt109*	Chromatin remodelling	*P300-CBP*	MMS, CPT
SPAC16C9.05	*cph1*	Chromatin remodelling	*PHD-finger*	MMS, CPT
SPBC29A10.05	*exo1*	DNA Nuclease	*EXO1*	MMS
SPBC3D6.10	*apn2*	DNA Nuclease	*APEX1*	MMS
SPBC3E7.08c	*rad13*	DNA Nuclease	*XPGC*	MMS
SPAC1556.01c	*rad50*	DNA Repair	*RAD50*	MMS, Bleo, CPT
SPBC119.14	*rad22*	DNA Repair	*RAD52*	MMS, Bleo, CPT
SPAC2G11.12	*rqh1*	DNA Repair	*BLM*	MMS, Bleo, CPT
SPBC336.01	*fbh1*	DNA Repair	*FLJ14590*	MMS, CPT
SPBC18H10.19	*atg14*	DNA Repair	*UVRAG*	MMS
SPBC215.03c	*csn1*	dNTP metabolism	*GPS1*	MMS, Bleo, CPT
SPAPB17E12.04c	*csn2*	dNTP metabolism	*CSN2*	MMS, Bleo, CPT
SPCC1919.15	*brl1*	E3 Ligase	*RNF40*	MMS, Bleo, CPT
SPCC126.07c		E3 Ligase	*SCAF1*	CPT
SPBC342.01c	*alg6*	Lipid metabolism	*ALG6*	Bleo
SPAC9E9.09c	*atd1*	Metabolism	*ALDH1A2*	MMS, Bleo, CPT
SPAC521.04c		Metabolism		MMS, Bleo, CPT
SPBC30D10.04	*swi3*	Replication	*TIPIN*	MMS, CPT
SPAPB1E7.02c	*mcl1*	Replication		Bleo
SPAC23C11.02c	*rps23*	Ribosomal protein	*RPS23*	Bleo, CPT
SPAC1556.05c	*cgr1*	Ribosomal protein		MMS, Bleo
SPAC13G7.07	*arb2*	RNA interference		MMS, Bleo, CPT
SPBC20F10.05	*nrl1*	RNA interference	C14Orf102	MMS, Bleo, CPT
SPCC736.11	*ago1*	RNA interference	*AGO1*	Bleo, CPT
SPBC660.09	*mug168*	Sequence orphan		MMS, CPT

Strain	Gene Name	GO Term	Human homolog	Sensitivities
SPBC119.08	*pmk1*	Signaling	*MAPK6*	Bleo, CPT
SPBC2D10.13	*est1*	Telomere maintenance	*EST1*	MMS, Bleo, CPT
SPBC1778.02	*rap1*	Telomere maintenance	*TERF2IP*	MMS
SPBC16G5.15c	*fkh2*	Transcription	*FOXO*	MMS, Bleo, CPT
SPAC22F3.09c	*res2*	Transcription		MMS, Bleo, CPT
SPAC664.03	*paf1*	Transcription	*PD2*	MMS, Bleo, CPT
SPBC23E6.09	*ssn6*	Transcription		MMS, CPT
SPBC16C6.02c	*vps1302*	Transport	*VPS13A*	Bleo, CPT
SPAC57A7.04c	*pabp*	Transport		MMS, Bleo, CPT
SPBC2G2.03c	*sbh1*	Transport		MMS, Bleo, CPT

Table 5.1 Table of all sectoring mutants. Systematic name, gene name, GO term, human homolog, and sensitivity to DNA damaging agents are shown.

5.2.3 The Ch^{16}-*RMYAH* DSB Assay

Having characterised the derived mutants in a semi-quantitative manner with the serial-dilution assay and the colony sectoring assay, the DNA repair proficiency in this set of genes was then quantified. For this purpose, the hypersensitive sectoring mutants were back-crossed to lose endogenous markers and the minichromosome Ch^{16}-*RMYAH* was introduced, along with an ectopic, inducible HO endonuclease. Ch^{16}-*RMYAH* allows for a quantifiable DSB repair assay, in which different repair events, *i.e.* gene conversion, non-homologous end-joining or failure of repair, *i.e.* chromosome loss or loss of heterozygosity can be deduced based on marker loss following break-induction (**Chapter 2.10.2**). The DSB assays were carried out for 31 out of the 39 sectoring strains; the other 8 strains would either not retain Ch^{16}-*RMYAH* stably enough, or a marker-negative strain could not be derived. Out of the 31 assayed, sectoring mutants, 20 exhibited at least a mild reduction in GC with a concomitant increase in failed repair events Ch^{16} loss and LOH (**Figure 5.3**). Since most known HR factors were excluded from the list, only 9 deletion strains, including controls, exhibited an intermediate (*SPAC664.03*Δ, *est1*Δ, *atd1*Δ, *ago1*Δ, *nrl1*Δ, *arb2*Δ) or strong (*rad22*Δ, *rqh1*Δ, *fkh2*Δ) decrease in GC (subjectively assigned categories).

To examine the relationship between an intermediate or strong reduction in GC and sensitivity to DNA damaging agents, a 4-set Venn diagram was created (**Figure 5.4**). Over 40% (9 out of 21) of the mutants displaying hypersensitivity to the DSB-inducing radiomimetic bleomycin revealed accompanying attenuation of GC, while all strains with at least an intermediate reduction GC levels exhibited sensitivity to bleomycin. 8 of the 9 deletion strains with decreased GC levels were sensitive to all DNA damaging agents, while *ago1*Δ was only sensitive to bleomycin and CPT. Approximately half (16 out of 31) of all sectoring mutants were sensitive to all DNA damaging agents, and half of those

hypersensitive mutants (8 out of 16) exhibited an attenuation in GC. In conclusion, combined sensitivity of deletion-mutants to the DNA damaging agents MMS, bleomycin, and CPT is the best predictor for a role in facilitating HR-dependent GC.

Figure 5.3

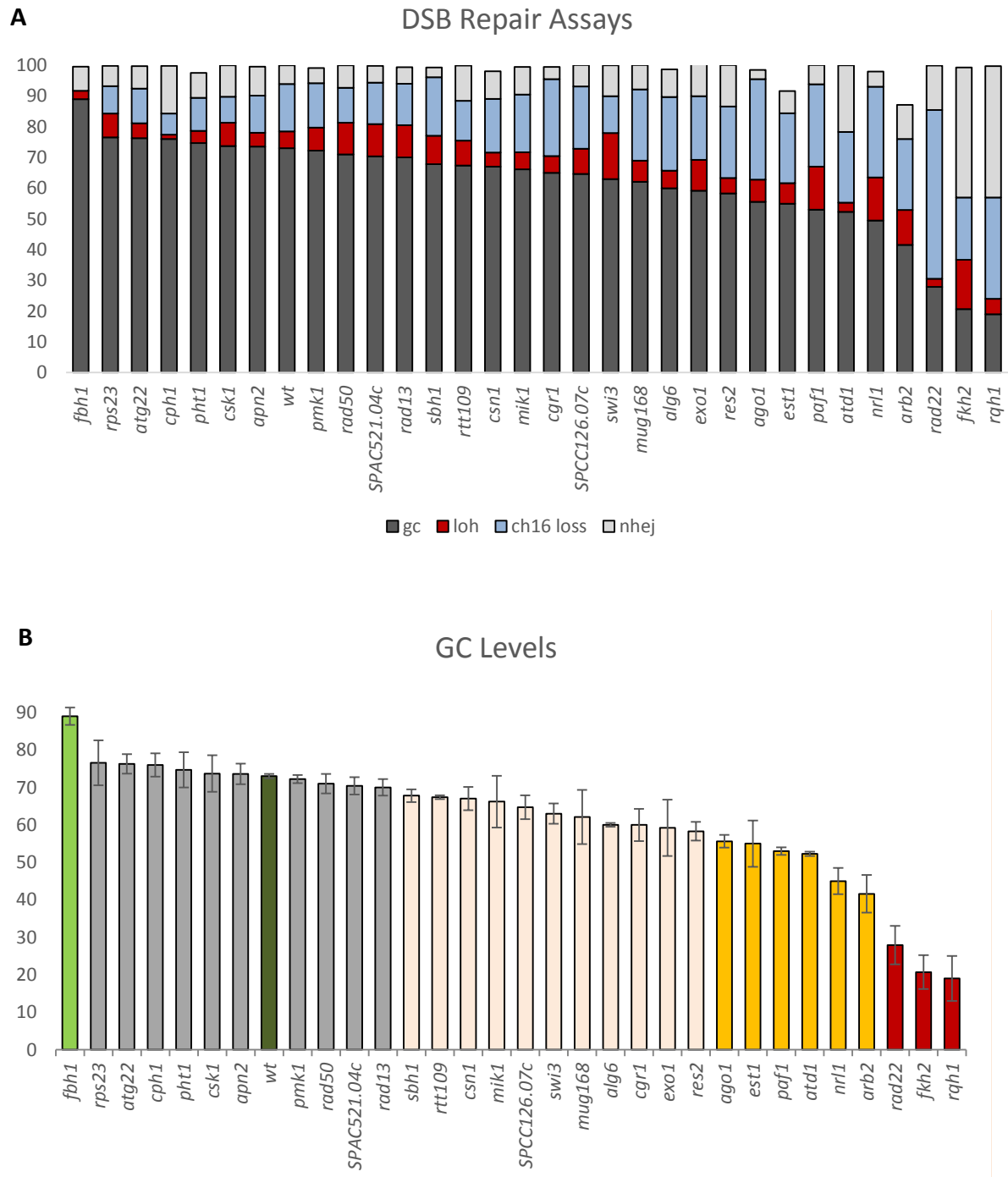


Figure 5.3: DSB repair assays of sectoring mutants. (A) Ch^{16}-*RMYAH* DNA repair profiles of set of sectoring mutants; light gray box: NHEJ/SCC/Uncut, blue box: Ch^{16}loss, red box: LOH, black box: gene conversion (GC). Spontaneous Ch^{16} loss explains accumulated values below 100%. (B) Plot of GC levels. Red indicates strong decrease in GC; orange indicates intermediate decrease in GC; light yellow indicates mild decrease in GC; dark green, wild type; light green indicates enhanced GC. Error bars represent standard deviation of the mean of three experiments.

Figure 5.4

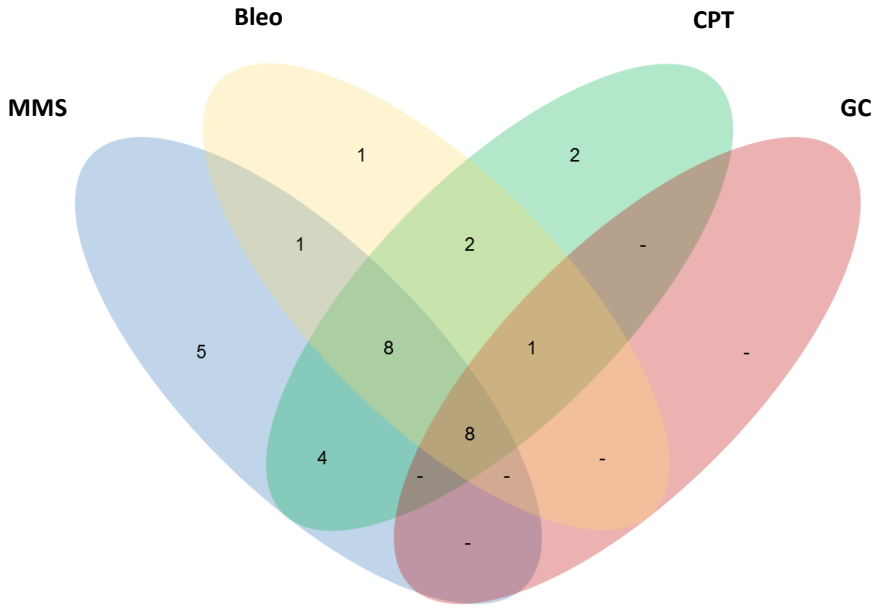


Figure 5.4: 4-set Venn diagram of sectoring cohort of genes. Sectoring cohort of gene deletions was grouped according to sensitivity to MMS, bleomycin (Bleo), camptothecin (CPT), as well as defective gene conversion (GC); intermediate or strong reduction.

5.2.4. Global analysis of DSB repair profiles of HR mutants

In an attempt to put the generated data in this part of the study in a wider context, the relationship between repair outcomes was analysed to gain insights into the mechanisms of failed HR repair. For this purpose, linear regression analysis was carried out, plotting GC versus failed repair events (Ch^{16} loss + LOH). As predicted, GC levels correlate inversely with combined failed repair events (Regression line: $y=-1.2105x+93.549$; $R^2=0.6531$) (**Figure 5.5A**): These findings are in agreement with prior studies of this lab (Cullen et al. 2007; Tinline-Purvis et al. 2009) (Moss, unpublished work), which established a role for HR genes in suppression of break-induced minichromosome loss, and LOH (**Figure 5.5B**).

Figure 5.5

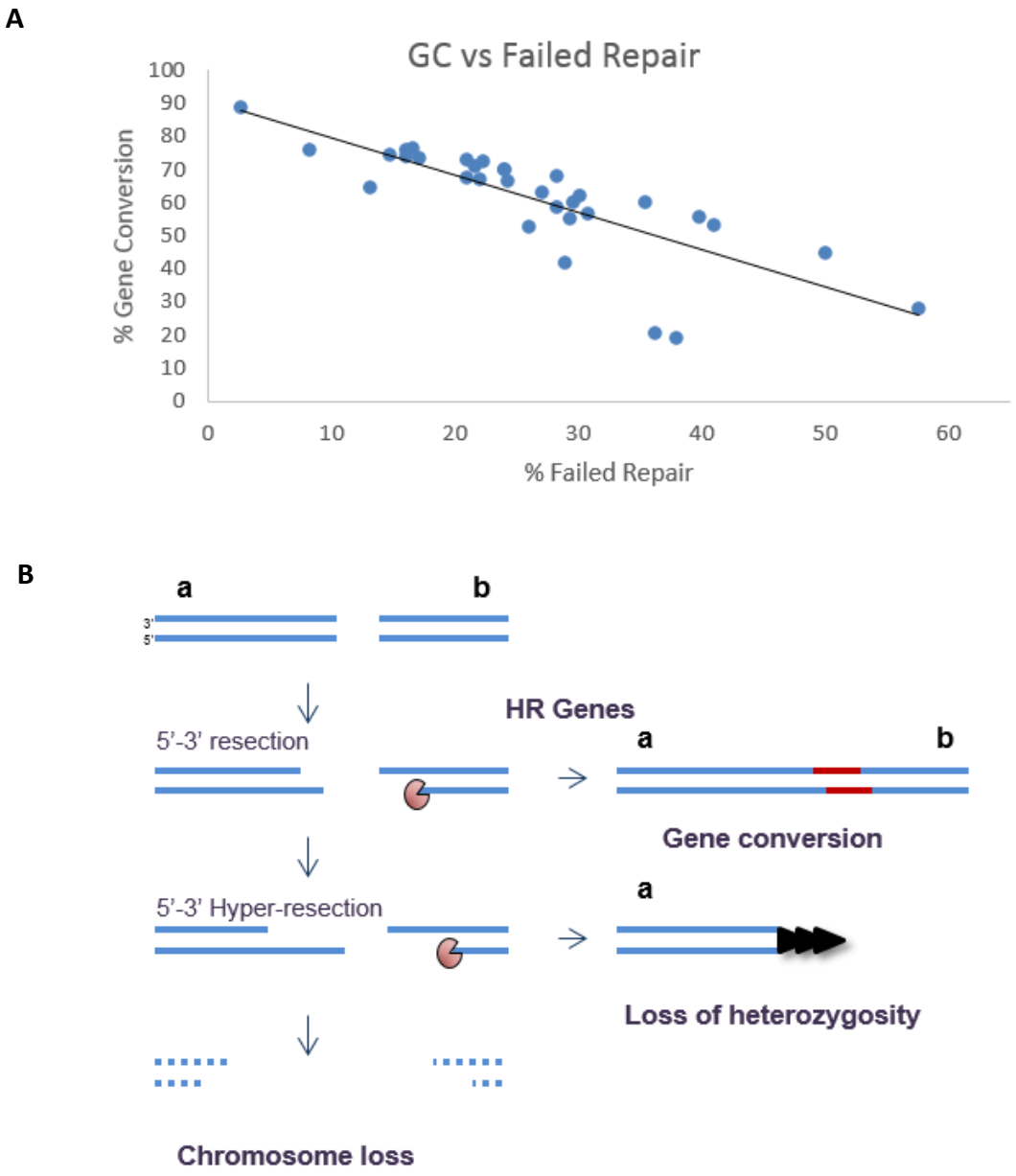


Figure 5.5: Linear regression analysis of Ch^{16}-*RMYAH* repair outcomes. (A) GC levels (y-axis) versus failed repair events (LOH+Ch^{16} loss) (x-axis). Regression line: y= -1.2105x + 93.549; R^2=0.6531. (B) Model. HR genes facilitating GC following a DSB suppress extensive end-processing leading to either LOH or minichromosome loss.

5.2.5 Novel factors in HR; A selection of hits

Further, a selection of mutants (*ago1*Δ, *arb2*Δ, *fkh2*Δ, *SPAC664.03*Δ, *est1*Δ, *atd1*Δ) exhibiting a reduction in GC and function in different cellular pathways, will be briefly discussed. In addition, *fbh1*Δ, displaying a strong increase in GC, will also be presented. The DSB repair profiles for all assayed deletion-strains can be found in **Appendix III**.

5.2.5.1 Ago1, Arb2, and the siRNA machinery

5.2.5.1.1 RNAi proteins Ago1 and Arb2

Strikingly, two factors involved in the fission yeast RNAi machinery (*arb2*Δ, *ago1*Δ), along with one putative member (*nrl1*Δ) were pulled out as part of this screen. Argonaute protein Ago1 is a central factor of the fission yeast siRNA machinery, and is evolutionary highly conserved from yeast to humans (Buhler and Moazed 2007). An *ago1*-deletion strain was found to be sensitive to bleomycin and camptothecin, but not to MMS at indicated concentrations (**Figure 5.6A**).

When assayed with Ch^{16}-*RMYAH*, it became apparent that Ago1 was required for efficient GC; *ago1*Δ: 55.6%, wt: 73%. Its disruption caused a concomitant increase in Ch^{16} loss; *ago1*Δ: 32.7%, wt: 15.6%, and a small increase in LOH; *ago1*Δ: 7.2%, wt: 5.5%, following a DSB (**Figure 5.6C**).

To examine HR defects in more detail, Rad51-eCFP foci formation was monitored in response to DNA damage. Rad51 is the central recombinase in HR repair and facilitates strand exchange. For this purpose, the deletion mutant and wild-type strains were subjected to 50 Gy of IR to induce DSBs, and Rad51-eCFP was monitored via fluorescence microscopy at indicated time-points (**Figure 5.6D**). As presented in **Figure 5.6E**, *ago1*Δ cells displayed attenuated localisation of Rad51-eCFP to sites of DNA damage, indicative of a pre-synaptical function in HR repair.

siRNA protein Arb2 was found to be very sensitive to all DNA damaging agents, and to facilitate DSB repair when tested with the Ch^{16}-*RMYAH* assay. Consistent with a stronger hypersensitivity to bleomycin (**Figure 5.7A**), the null mutant exhibited a bigger decrease in GC to 41.6%, with an accompanying increase in failed repair events LOH to 14.7%, and Ch^{16} loss to 23% (**Figure 5.7C**). In addition, spontaneous Ch^{16} loss without break-induction was very high (11%) in the mutant strain (**Appendix III**). Analogously to the Rad51-eCFP recruitment kinetics of the *ago1*Δ strain, Arb2-deficient cells also displayed loading defects of Rad51 (**Figure 5.7D** and **E**), consistent with a pre-synaptical role of Arb2 in HR repair.

Figure 5.6

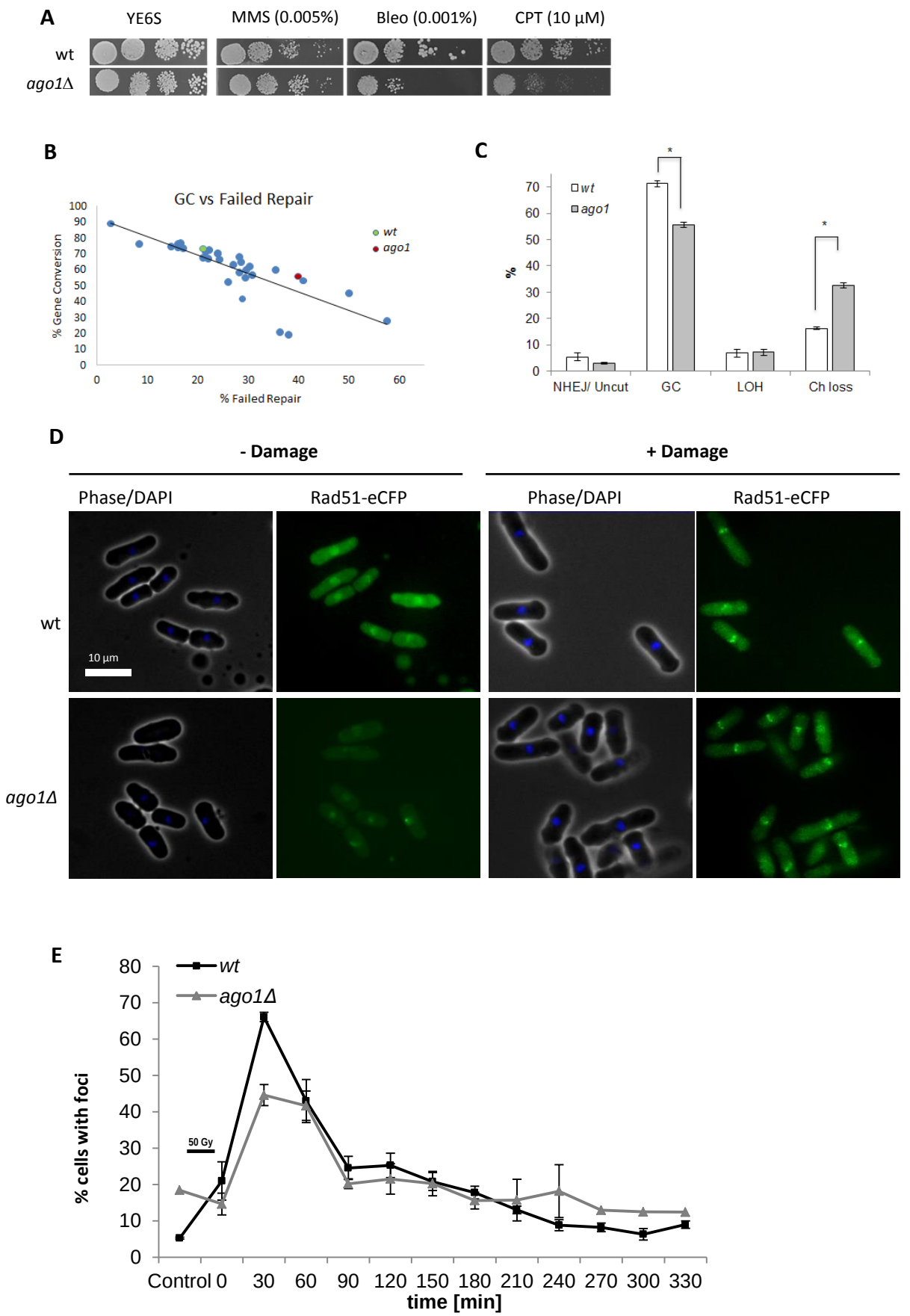

A
YE6S
MMS (0.005%)
Bleo (0.001%)
CPT (10 µM)
wt
ago1Δ
B
GC vs Failed Repair
% Gene Conversion
% Failed Repair
wt
ago1
C
wt
ago1
%
NHEJ/ Uncut
GC
LOH
Ch loss
D
- Damage
+ Damage
Phase/DAPI
Rad51-eCFP
wt
ago1Δ
10 µm
E
wt
ago1Δ
% cells with foci
50 Gy
Control 0 30 60 90 120 150 180 210 240 270 300 330
time [min]

Figure 5.6: Ago1 is a novel factor in HR. (A) Ago1 conferred sensitivity to bleomycin and CPT, but not MMS. (B) The Ch^{16}-*RMYAH* DSB repair profile of *ago1*Δ was similar to those of other HR mutants. (C) The *ago1*-null mutant displayed an intermediate reduction in GC, with a concomitant increase in Ch^{16} loss. Asterisks indicate statistical significance ($p<0.05$). (D) Wild-type and *ago1*Δ cells were treated with 50 Gy of IR (+ Damage), and Rad51-eCFP foci formation was monitored. (E) Quantitation of (D). Localisation of Rad51-eCFP to DNA damage sites was attenuated in *ago1*Δ cells. Error bars represent standard deviation of the mean of three experiments.

Figure 5.7

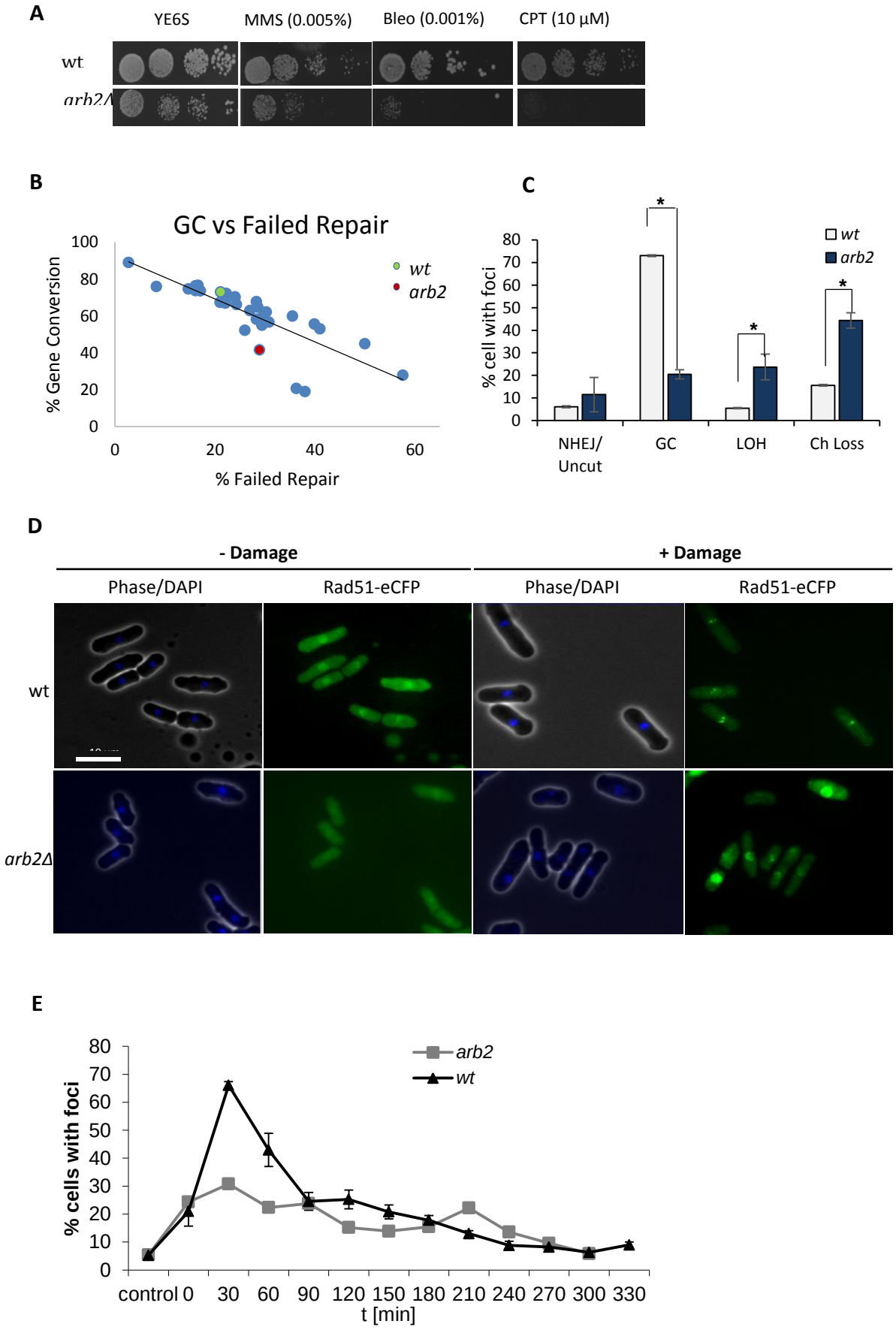

A
YE6S
MMS (0.005%)
Bleo (0.001%)
CPT (10 µM)
wt
arb2Δ
B
GC vs Failed Repair
% Gene Conversion
% Failed Repair
wt
arb2
C
% cell with foci
wt
arb2
NHEJ/ Uncut
GC
LOH
Ch Loss
D
- Damage
+ Damage
Phase/DAPI
Rad51-eCFP
wt
arb2Δ
E
% cells with foci
arb2
wt
control 0 30 60 90 120 150 180 210 240 270 300 330
t [min]

Figure 5.7: Arb2 is a novel factor in HR. (A) *arb2*Δ exhibited hypersensitivity to MMS, bleomycin, and CPT at indicated concentration. (B) The Ch^{16}-*RMYAH* DSB repair profile of *arb2*Δ is similar to those of other HR mutants. (C) The *arb2*-null mutant displayed an intermediate reduction in GC, with a concomitant increase in Ch^{16} loss, and LOH. Asterisks indicate statistical significance ($p<0.05$). (D) Wild-type and *ago1*Δ cells were treated with 50 Gy of IR (+ Damage), and Rad51-eCFP foci formation was monitored. (E) Quantitation of (D). Localisation of Rad51 to DNA damage sites was attenuated in *arb2*Δ cells. Error bars represent standard deviation of the mean of three experiments.

5.2.5.1.2 The siRNA machinery and DNA damage repair

Since accounts of an involvement of the siRNA machinery in DNA repair in mammalian cells are growing (Francia et al. 2012, Wei et al. 2012), a potential crosstalk of the RNAi machinery in DNA damage repair in fission yeast was further investigated. For this purpose, other participants in this pathway were examined. Strains with deletions of the siRNA core factors *arb1*, *arb2*, *dcr1*, *ago1*, *clr4*, *ers1*, *swi6,* and putative member *nrl1* were challenged with the DNA damaging agents MMS, bleocin, and UV at indicated concentrations (**Figure 5.8A**). While varying degrees of sensitivities could be observed for the different strains, only *ers1*Δ, *arb2*Δ, and *nrl1*Δ displayed high sensitivity to all agents; while *ers1*Δ and *arb2*Δ also exhibited growth defects on non-selective media. *ago1*Δ, *clr4*Δ and *dcr1*Δ were only sensitive to bleomycin, while *arb1*Δ was not sensitive at all. *swi6*Δ displayed mild sensitivity to all utilised agents. Further, quantifiable Ch^{16}-*RMYAH* DSB assays were carried out for *dcr1*, *arb1*, and *swi6* deletion mutants (**Appendix III**). While the *swi6*-null mutant exhibited slightly attenuated GC (61%) accompanied with 4.8% spontaneous Ch^{16} loss, Dcr1, and Arb1 were not required for efficient HR repair (**Appendix III**). Minichromosomes could not be stably introduced into *ers1*Δ.

To investigate a potential involvement of the siRNA machinery in checkpoint control, the siRNA deletion mutants were treated with 10 mM HU for 6 hours at 32ºC and imaged (**Figure 5.8B**). As presented, the vast majority of cells of all indicated deletion strains were elongated, indicative of functional cell cycle arrest in response to replication stress.

Taken together, these data indicate involvement in DNA repair of some (Ago1, Arb2, Nrl1, Swi6), but not all siRNA factors. Surprisingly, core factor Dcr1 was not found to confer resistance to DNA damaging agents, suggesting potentially siRNA-independent participation in DNA repair for other members of this pathway.

Figure 5.8

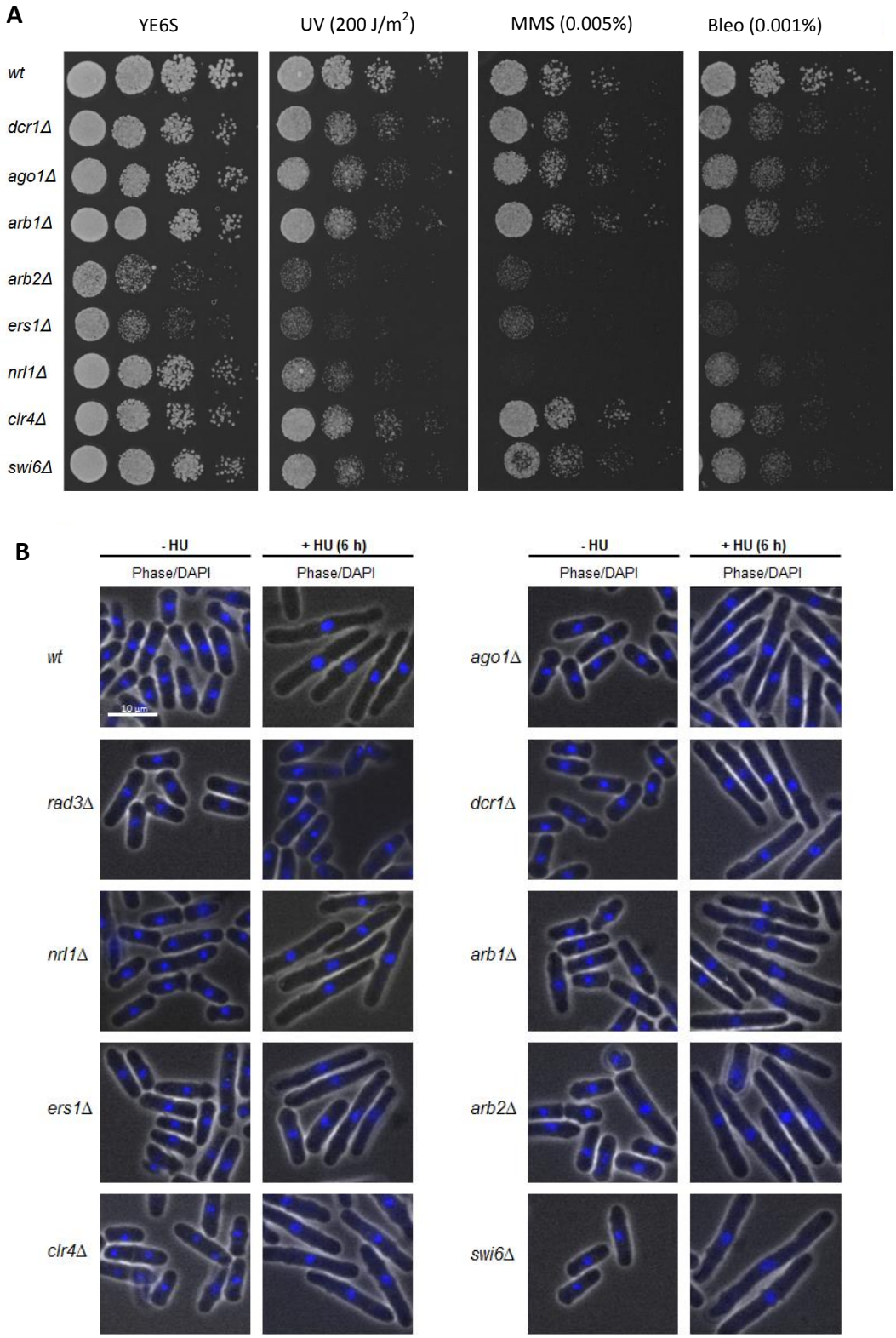


Figure 5.8: Examination of the siRNA pathway. (A) Spot-dilution assay of siRNA core components. Deletion strains were diluted five-fold and challenged with MMS, bleomycin, and UV at indicated concentrations/exposures. (B) Deletion strains were incubated for 6 h at 32°C with 10 mM HU and imaged using DAPI/Phase filters (100x).

5.2.5.2 Transcription factor Fkh2

As briefly described in **Chapter IV**, fission yeast forkhead transcription factor Fkh2 is homologous to human tumour suppressors of the FOXO family (Postnikoff et al. 2012). The *fkh2*-null mutant was acutely hypersensitive to MMS, bleomycin, and CPT at indicated concentrations (**Figure 5.9A**). *fkh2*Δ cells displayed a stark decrease in GC following a DSB in Ch^{16}-*RMYAH* to 20.7% (**Figure 5.9C**). *fkh2*Δ also exhibited an increase in LOH to 16% and Ch^{16} loss levels were elevated to 20.3%. Strikingly, and in contrast to other HR mutants as illustrated in **Figure 5.9B**, the null mutant maintained very high levels of NHEJ/Uncut/SCC; *fkh2*Δ: 43%, in comparison to wild type: 6.1%. The only other mutant in this study with a comparable phenotype, was the deletion mutant of helicase *rqh1*, placing near *fkh1*Δ on the linear regression plot (**Figure 5.9B**). Since Fkh2 is a transcription factor, it is tempting to speculate on a role in transcriptional regulation of helicases, such as Rqh1, in DNA damage repair.

Figure 5.9

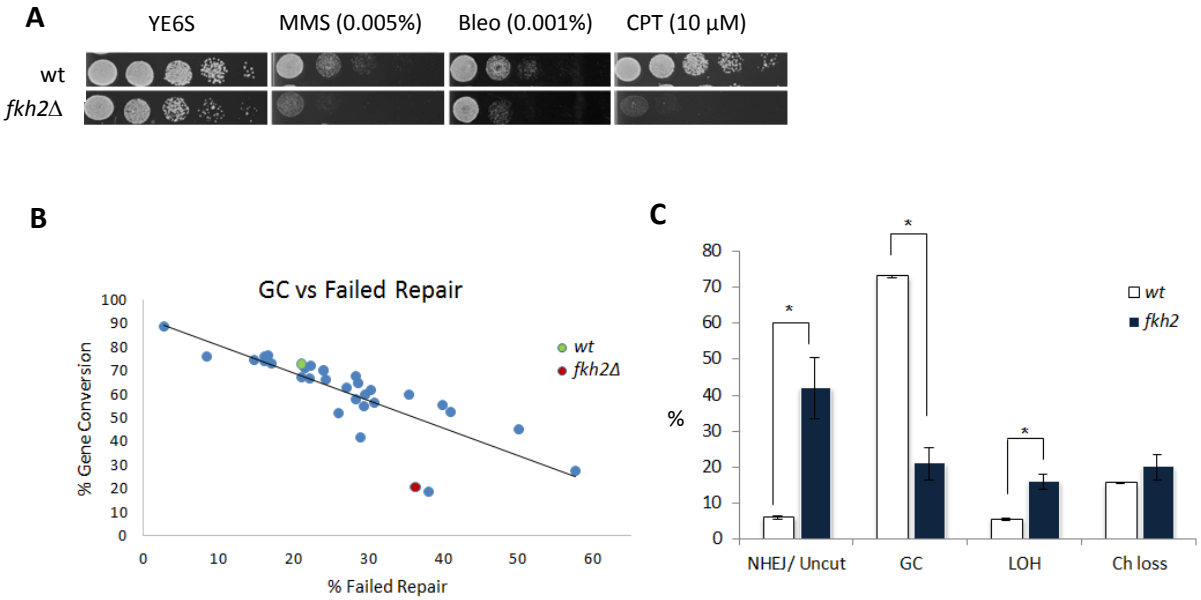


Figure 5.9: Fkh2 is conferring resistance to DNA damaging agents and facilitates efficient HR repair. (A) The *fkh2*-null mutant was sensitive to MMS, bleomycin, and CPT at indicated concentrations. (B) As illustrated in the global linear regression plot of GC levels and failed repair events, its DSB repair profile is an outlier (along with *rqh1*Δ) when compared to the other HR mutants. (C) The detailed DSB repair profile unveiled a stark increase in NHEJ/SCC/Uncut levels of *fkh2*Δ in comparison to wild-type levels, with a concomitant strong decrease in GC. While Ch^{16} loss levels remained close to wild-type levels, LOH was significantly increased in the null mutant. Error bars represent standard deviation of the mean of three experiments. Asterisks indicate statistical significance ($p<0.05$).

5.2.5.3 RNA biogenesis protein SPAC664.03 (Paf1 complex)

SPAC664.03 is predicted to be part of the fission yeast polymerase-associated factor 1 (Paf1) complex (Paf1C), and thus involved in RNA metabolism (Jaehning 2010). The null mutant displayed sensitivity to all three DNA damaging agents MMS, bleomycin, and CPT (**Figure 5.10A**). The Ch^{16}-*RMYAH* DSB repair profile was typical of an HR mutant (**Figure 5.10B**), with an intermediate decrease in GC to 51%, and concomitant increase in LOH to 13%, and Ch^{16} loss to 28%. The null mutant maintained the NHEJ/Uncut/SCC levels of wild type; 7% in *SPAC664.03*Δ, 8% in wild type **(Figure 5.10C**). While the Paf1 complex has been linked to NER (Tatum et al. 2011), its involvement in HR repair remains widely elusive. These data are supporting the emerging ties of RNA metabolism with DNA damage repair.

Figure 5.10

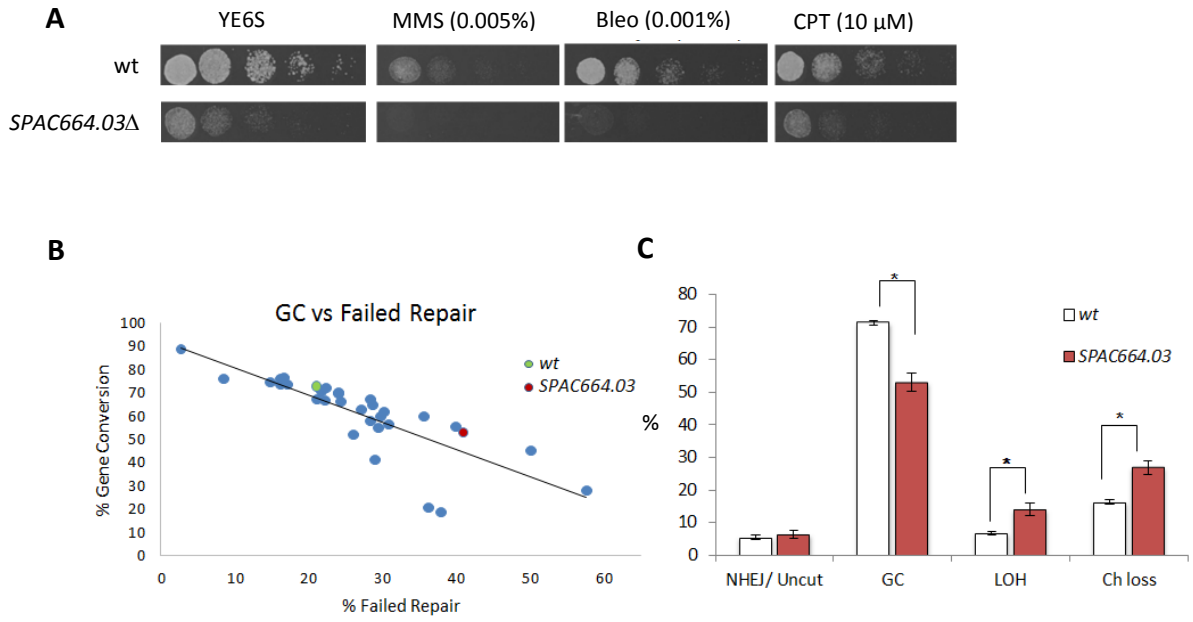


Figure 5.10: SPAC664.03 is a novel factor in HR. (A) *SPAC664.03*Δ exhibited hypersensitivity to MMS, bleomycin, and CPT at indicated concentration. (B) The Ch^{16}-*RMYAH* DSB repair profile of *SPAC664.03*Δ was similar to those of other HR mutants. (C) The *SPAC664.03*-null mutant displayed an intermediate reduction in GC, with a concomitant increase in Ch^{16} loss, and LOH. Error bars represent standard deviation of the mean of three experiments. Asterisks indicate statistical significance ($p<0.05$).

5.2.5.4 Telomere maintenance protein Est1

Telomere protein Est1 (Ever Shorter Telomeres 1) is a telomerase co-factor and required for the prevention of corrosion of chromosome ends during each cell division (Smogorzewska and de Lange 2004). As part of this study, the null mutant was found to be sensitive to all three DNA damaging agents MMS, bleomycin, and CPT (**Figure 5.11A**). The Ch^{16}-*RMYAH* profile is reminiscent of those of other HR mutants (**Figure 5.11B**). GC levels were reduced in the mutant to 55%, while Ch^{16} loss levels were elevated to 22.7%. LOH levels were not significantly increased; 6.7% in *est1*Δ. NHEJ levels were approximately the same as wild-type levels; *est1*Δ: 7.2% (**Figure 5.11C**). The role for Est1 in genomic stability was also supported by the very high levels (8%) of spontaneous Ch^{16} loss, which were observed in this study (**Appendix III**). Further, repair kinetics involving recruitment of Rad51-eCFP to DNA damage sites following 50 Gy of IR were comparable to wild type (**Figure 5.11D** and **E**), thus excluding a pre-synaptical role for Est1 in HR repair. However, even after 330 minutes, some *est1*Δ cells were strongly elongated, indicative of an arrested cell cycle resulting from failed repair of the IR-induced lesions (**Figure 5.11F**), consistent with slightly elevated background levels of Rad51 foci formation in the deletion mutant.

Finally, since spore viability of *est1*Δ cells was found to be very low, potential chromosome segregation effects due to chromosome end corrosion were examined. For this purpose, pictures of DAPI stains of resulting tetrads of an *est1*Δ *x* wt cross were taken. As presented with exemplary pictures in **Figure 5.11G**, meiotic defects of Est1-defective cells could be visualised, consistent with dysfunctional telomeres causing chromosome missegregation throughout meiosis (**Figure 5.11G**).

In conclusion, these findings are congruent with the reported role for Est1 in genome stability, and additionally hint at a more direct involvement for this telomeric factor in HR.

Figure 5.11

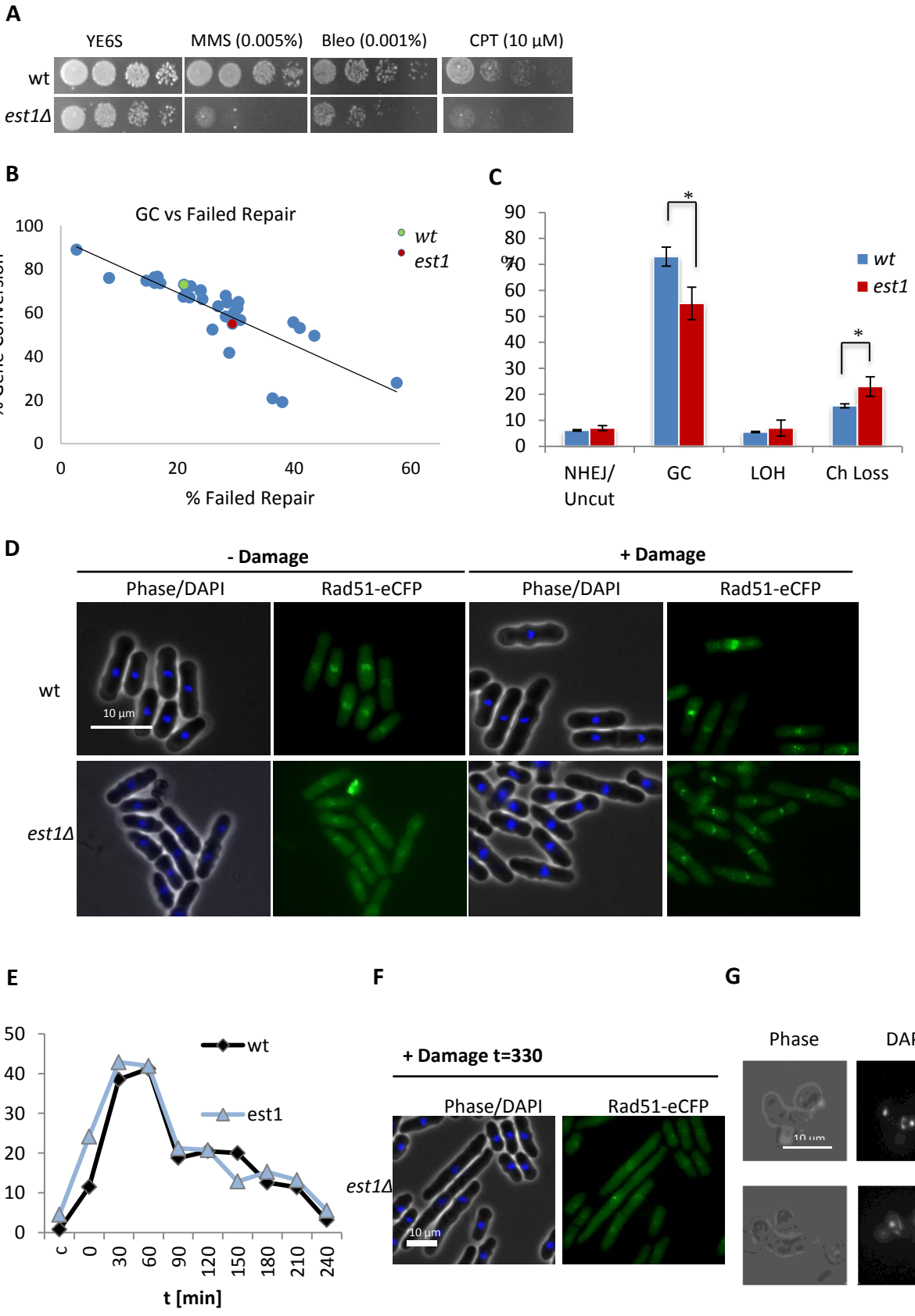

A
YE6S
MMS (0.005%)
Bleo (0.001%)
CPT (10 µM)
wt
est1Δ
B
GC vs Failed Repair
wt
est1
% Gene Conversion
% Failed Repair
C
%
wt
est1
NHEJ/ Uncut
GC
LOH
Ch Loss
D
- Damage
+ Damage
Phase/DAPI
Rad51-eCFP
wt
est1Δ
10 µm
E
% percentage cells with foci
wt
est1
t [min]
F
+ Damage t=330
Phase/DAPI
Rad51-eCFP
est1Δ
10 µm
G
Phase
DAPI
10 µm

Figure 5.11: Est1 is required for efficient HR. (A) *est1*Δ exhibited hypersensitivity to MMS, bleomycin, and CPT at indicated concentration. (B) The Ch^{16}-*RMYAH* DSB repair profile of *arb2*Δ was similar to those of other HR mutants. (C) The *est1*-null mutant displayed an intermediate reduction in GC, with a concomitant increase in Ch^{16} loss, and LOH. Error bars represent standard deviation of the mean of three experiments. Asterisks indicate statistical significance ($p<0.05$). (D) Wild-type and *ago1*Δ cells were treated with 50 Gy of IR (+ Damage), and Rad51-eCFP foci formation was monitored. (E) Quantitation of (D). Localisation of Rad51 to DNA damage sites was functional in *est1*Δ cells. (F) After 330 min, some proportion of *est1*Δ cells elongated, indicative of failed repair of the lesions, causing cell cycle arrest. (G) Bright-field microscopy (100x) of tetrads from a cross of *est1*Δxwild type. Dysfunctional spore formation can be observed with DAPI staining.

5.2.5.5 Anti-recombinogenic helicase Fbh1

The 3'-5' F-box helicase 1 (Fbh1) has been demonstrated to possess anti-recombinogenic activity, directly opposing Rad51 loading factor Rad22, primarily to attenuate hyper-recombination during recovery of stalled replication forks (Osman et al. 2005). Consequently, the *fbh1*-null mutant was highly sensitive to replication stress-inducing agents MMS and CPT, while only displaying very mild sensitivity to the radiomimetic drug bleomycin (**Figure 5.12A**). Further, the Ch^{16}-*RMYAH* DSB profile was unique when compared to those of other HR mutants (**Figure 5.12B**). GC levels in Fbh1-deficient cells actually surpassed wild-type levels; *fbh1*Δ: 89.1%, while LOH levels were significantly decreased to 2.7%. Strikingly, Ch^{16} loss was entirely absent (**Figure 5.12C**). The hyper-recombinogenic phenotype of the *fbh1*-null mutant as observed in this study is in good agreement with the published literature on Fbh1.

Figure 5.12

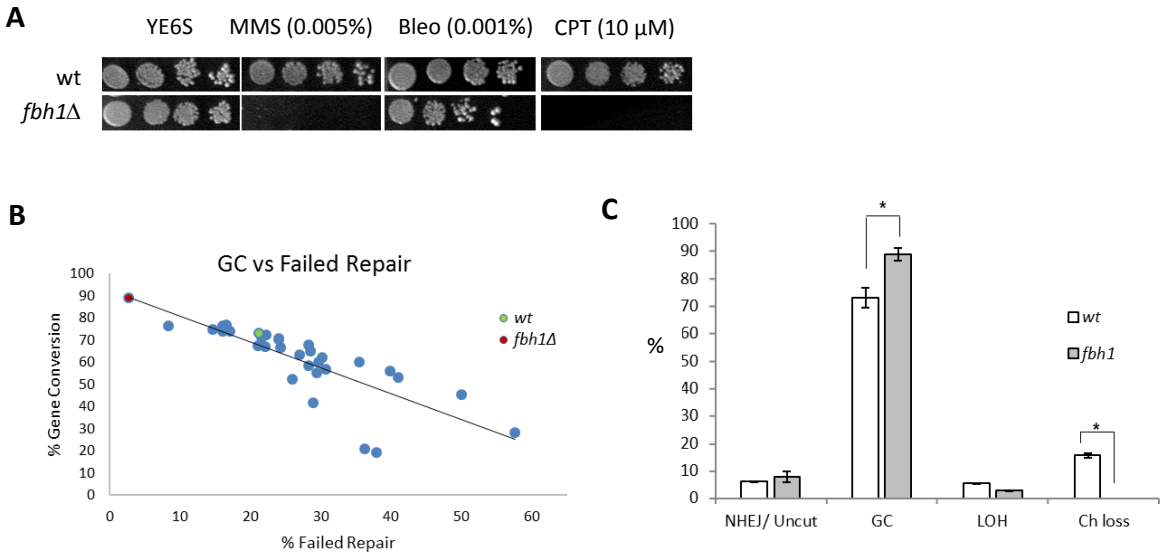


Figure 5.12: Fbh1 is a Rad51 disruptase. (A) *fbh1*Δ cells exhibited hypersensitivity to MMS, bleomycin, and CPT at indicated concentrations. (B) The Ch^{16}-*RMYAH* DSB repair profile of *fbh1*Δ was unique in comparison with the other assayed mutant strains (C) The *fbh1*-null mutant displayed an increase in GC following break-induction, with a complete lack of Ch^{16} loss. Error bars represent standard deviation of the mean of three experiments. Asterisks indicate statistical significance ($p<0.05$).

5.2.5.6 Cell metabolism protein Atd1

Aldehyde dehydrogenase (Atd1) is predicted to function in NADPH metabolism. As part of this study, Atd1 was found to confer resistance to the DNA damaging agents MMS, bleomycin, and CPT for the first time (**Figure 5.13A**). Atd1-deficient strains exhibited an intermediate decrease in GC to 52.3%, with an accompanying increase in both Ch^{16} loss; 23%, and NHEJ/Uncut/SCC; 21.7%, LOH levels were slightly decreased to 3% (**Figure 5.13C**). While it is tempting to speculate on potential functions for NADPH metabolism proteins in HR repair of DSBs, the data generated in this study, as well as published literature on Atd1 is too limited to support any hypothesis.

Figure 5.13

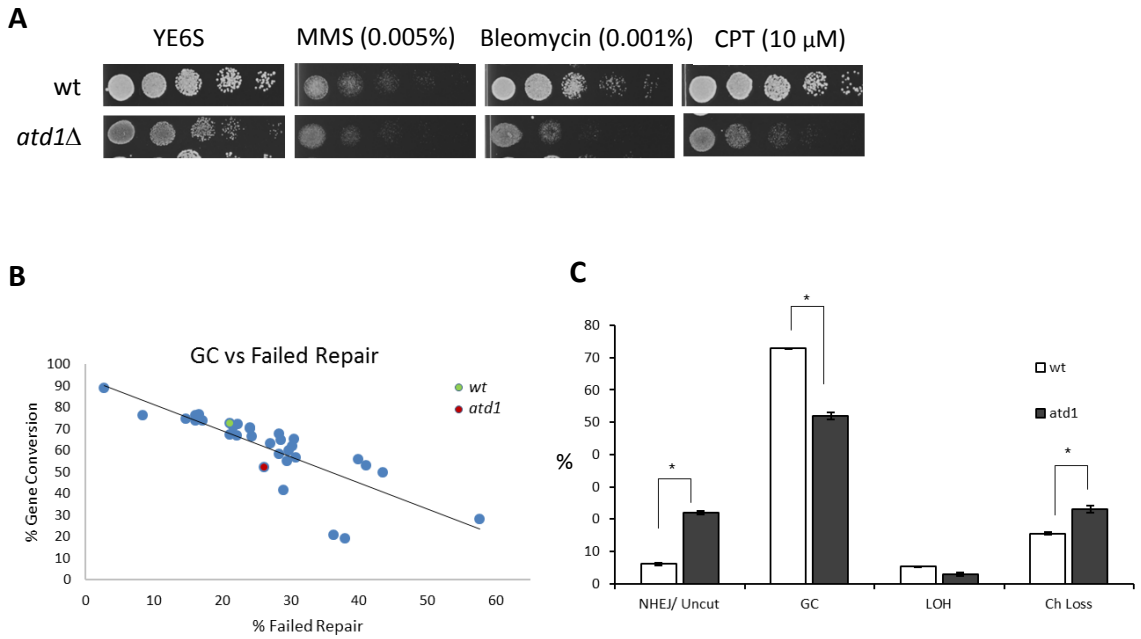


Figure 5.13: Atd1 is a novel factor in HR. (A) *atd1*Δ exhibited hypersensitivity to MMS, bleomycin, and CPT at indicated concentration. (B) The Ch^{16}-*RMYAH* DSB repair profile of *atd1*Δ was similar to those of other HR mutants. (C) The *atd1*-null mutant displayed an intermediate reduction in GC, with a concomitant increase in Ch^{16} loss, and NHEJ/Uncut/SCC, while LOH levels stayed similar to wild-type levels. Error bars represent standard deviation of the mean of three experiments. Asterisks indicate statistical significance ($p<0.05$).

5.3 Discussion

5.3.1 Colony sectoring is an intermediate predictor of DSB repair efficiency

Quantitative analysis of DNA damage repair in the derived set of sectoring mutants uncovered that not all deletion strains exhibited attenuated GC levels following break-induction. Many mutants displayed no significant, or only very mild, decreases in levels of GC. Since the sectoring hits also contain factors involved in genome stability and minichromosome maintenance, a colony sectoring phenotype does not necessarily translate to defects in mending of DSBs. Possible functions for these genes preventing colony sectoring, but not facilitation of DSB repair, include replication, prevention of non-disjunction in mitosis, chromosome segregation, and telomere maintenance. In addition, differences in experimental conditions might account for some of the false positive hits. Firstly, the gene encoding the HO endonuclease is present endogenously on the Ch^{16}-*LMYAU* minichromosome, utilised in the sectoring assay; hence, leaky expression under restrictive conditions is more common, leaving the cells longer periods of time exposed to DNA breaks when compared to the DSB assay. Secondly, cells undergoing the sectoring assay are incubated for more than 48 hours on plates at 4°C, being kept in stationary phase, which might affect retention of the minichromosome. Finally, subjective evaluation of experimental outcomes always leaves room for artefacts, potentially causing false assignment of a sectored phenotype. However, it must be considered, that known DNA repair factors were widely excluded from the sectoring analysis and onwards, already artificially selecting against very obvious phenotypes, leaving a pool of mutants with more subtle effects on DNA damage repair. Finally, since the minichomosomes were originally derived from chromosome III, one intrinsic experimental limitation was the complementation of gene deletions through the introduction of the minichromosomes,

when a functional copy of the deleted gene was present on Ch^{16}; thus, creating false negatives.

5.3.2 DNA damage sensitivities and HR proficiency

All of the deletion mutants with disrupted GC were hypersensitive to the radiomimetic agent bleomycin, consistent with inefficient HR repair of DSBs from both enzymatic and chemical origins. Interestingly, the reverse was not true; not all bleomycin-sensitive mutants exhibited inefficient GC in the DSB assay. This might be explained by a dosage effect, since the HO endonuclease only inflicts a single DSB, while bleomycin induces multiple (complex) DSBs with non-complementary overhangs as well as SSBs. In addition, the semi-quantitative nature of the spot-dilution assay might account for false sensitivity assignments, and thus experimental artefacts. Strikingly, all mutants, apart from *ago1*Δ, with strong or intermediate disruption of GC displayed sensitivity to all utilised DNA damaging agents MMS, CPT, and bleomycin. Consequently, defective HR repair is a very strong predictor for sensitivity to these three clastogens.

5.3.3 HR genes suppress Ch^{16} loss and LOH in response to a DSB

The data presented in this chapter are in good agreement with prior studies from the lab, suggesting a role for HR genes in suppression of minichromosome loss and LOH in response to a DSB. As supported by the linear regression analysis of the examined cohort of sectoring deletion mutants, disruption of GC facilitated by HR, leads to a concomitant increase in failed repair events, *i.e.* Ch^{16} loss and LOH. This model was originally established by Helen Tinline-Purvis (2009), confirming a role for a small number of HR factors in suppression of extensive end-processing of broken chromosome ends, giving rise to failed repair events. Subsequently, Jennifer Moss (unpublished work) carried out the first genome-wide study utilising the colony-sectoring assay in a DNA damage sensitive sub-set of the Bioneer-Version 1 deletion library, further underpinning and extending this

role for HR. As an extension of their work, an inverse correlation between GC and failed repair events was also uncovered in the selected group of genes, derived from this study.

5.3.3 Novel HR factors

As a result of this study, a number of novel factors, functioning in different biological processes, were associated with HR repair for the first time in fission yeast. These efforts underpin the complex mechanisms underlying the DNA damage response in fission yeast, and illustrate the requirements for finely-tuned orchestration of distinct pathways to warrant efficient DNA repair. To exemplify this, a small selection of hits were briefly presented, which function in RNAi (*arb2*, *ago1*), RNA metabolism (*SPAC664.03*), transcription (*fkh2*), telomere maintenance (*est1*), and cell metabolism (*atd1*). In addition, the helicase Fbh1 was discussed as an example for an anti-recombinogenic factor, contributing to genome stability, despite an increase in GC proficiency when disrupted. Finally, one hit of particular interest, putative RNA metabolism protein Nrl1, was characterised further, as presented in **Chapter VI**.

5.3.3.1 Ago1 and Arb2

The core members of the fission yeast siRNA machinery Ago1, Arb2 were identified as novel determinants of genome stability in response to a DSB. In a subsequent investigation, it was uncovered that HP-1 homolog Swi6 also contributes to efficient DSB repair, while most examined core genes conferred resistance to DNA damaging agents. Ago1 is known to be part of the RITS, and ARC complex (Buker et al. 2007) and the deletion mutant was found to be both sensitive to DNA damaging agents and displaying a reduction in HR repair. The human *ago1*-homologs *EIF2C1* and *EIFC2* have been linked to high-risk myeloma (Zhou et al. 2010), and epithelial skin cancer (Sand et al. 2012), and are thus of clinical interest. Arb2 is also part of the ARC complex (Buker et al. 2007);

however, its function remains widely elusive. No direct human homolog has been discovered yet.

Intriguingly, deletion mutants of both *ago1* and *arb2* exhibited defects in recruitment of Rad51-eCFP to DSBs, hinting at a pre-synaptical function for these two members of the siRNA machinery. As part of the characterisation of putative siRNA protein Nrl1, hypotheses regarding crosstalk between RNA metabolism and DNA repair are further discussed in **Chapter VI**. Interestingly, members of the siRNA machinery displayed very different phenotypes in regard to DNA damaging agents, as well as enzymatically-induced breaks. These data hint at a very complex involvement on multiple layers within DNA repair. While a more thorough investigation was out of the scope of this study, the generated preliminary findings, along with the growing amount of evidence for crosstalk of RNA metabolism and DNA repair, certainly warrant further investigation.

5.3.3.2 Fkh2

The deletion mutant of the transcription factor *fkh2* exhibited a very interesting and complex phenotype, mirroring the DSB profile of an *rqh1*-null mutant. The forkhead box family is evolutionary highly conserved from yeast to higher eukaryotes and has been associated with a number of cellular functions including apoptosis, DNA damage, metabolism, chromatin silencing, and cell aging (Laoukili et al. 2007; Tuteja and Kaestner 2007; van der Horst and Burgering 2007; Fu et al. 2008; Hannenhalli and Kaestner 2009; Sandri 2012). In addition, *fkh2*Δ cells have been found to display cell cycle progression defects in yeast (Linke et al. 2013). The human homologs FOXO and FOXM1 have been found to occupy pivotal roles in tumorigenesis and mediating response to chemotherapy (Myatt and Lam 2007), rendering Fkh2 a highly intriguing target with obvious clinical implications. Since Fkh2 has been associated with such a high number of cellular processes with possible entanglements with DNA repair pathways, further research is

required for robust hypotheses in this regard. Since Fkh2 regulates transcription, a microarray or RNAseq analysis of mutant cells with and without genotoxic stress would yield further insights into the mechanisms underlying the phenotype.

5.3.3.3 SPAC664.03 (Paf1 complex)

The pombe yeast factor SPAC664.03 is part of the polymerase-associated-factor 1 (Paf1) complex (Paf1C) in fission yeast. In *S. cerevisiae,* the Paf1 complex is composed of Paf1, Ctr9, Cdc73, Rtf1, and Lei1 and has been identified as an RNA polymerase II associated complex (Wade et al. 1996; Jaehning 2010). Paf1C fulfils multiple roles during transcription, via facilitation of Ser2-phosphorylation of RNAPII (Nordick et al. 2008) and has been associated with histone modifications (Oh et al. 2008). Strains lacking Paf1C have also been shown to exhibit telomeric silencing defects (Krogan et al. 2003), and alterations in mRNA maturation (Mueller et al. 2004). Paf1C-dependent histone modifications have been documented as being important for DNA repair in humans and yeast (Huyen et al. 2004; Wysocki et al. 2005); however, further research is needed to elucidate the contribution of Paf1C to HR repair to determine if its involvement is limited to its histone modification functions. Human Paf1C has been implicated in HIV and influenza susceptibility (Marazzi et al. 2012), as well as tumour progression in a variety of malignancies (Tomson and Arndt 2013). The findings generated as part of this study, along with the emerging evidence in the literature, further underpin the importance of RNA metabolism in the DNA damage response.

5.3.3.4 Est1

The telomerase co-factor Est1 (Ever Shorter Telomeres 1) exists in a wide range or organisms from yeast to humans. It is involved in the recruitment of telomerase to chromosome ends by interaction with Cdc13 (Evans and Lundblad 1999; Bianchi et al. 2004), or interaction with Rfa2 (Luciano et al. 2012). Dysfunctional telomeres are

associated with genome instability and chromosome end-fusion; thus, participants of the telomere maintenance machinery are determinants of genome stability. While telomerase is primarily involved in telomere maintenance at chromosome ends, preventing erosion of telomeric DNA at each cell division (Greider and Blackburn 1985; Greider and Blackburn 1987; Greider and Blackburn 1989), it has also been found to facilitate *de novo* telomere addition at DSBs (Kramer and Haber 1993; Diede and Gottschling 1999; Mangahas et al. 2001). However, *de novo* telomere addition is a very rare event and often associated with extensive LOH; thus, it cannot be considered a bona fide sub-pathway. Recent reports demonstrated an accumulation of Est1 and Est2 at non-telomeric DSBs in an Mre11-dependent way (Ribaud et al. 2012). Taken together with the data generated during this study, establishing Est1 as a facilitator of efficient HR, a direct role for Est1 in DSB repair represents an intriguing conjecture.

5.3.3.5 Fbh1

The 3'-5' F-box helicase 1 (Fbh1) is highly conserved from yeast to humans. Fbh1 has not only been shown to localise to sites of stalled replication sites, functioning in the cellular response to replication stress (Fugger et al. 2009; Fugger et al. 2013), but has also been demonstrated to operate as a modulator of Rad51 (Lorenz et al. 2009). In this function, Fbh1 is a direct antagonist of Rad22, curbing coating of ssDNA with Rad51 (Osman et al. 2005). This disruptive action is thought to attenuate spontaneous direct-repeat recombination, and is critical for preventing recombination at blocked replication forks (Lorenz et al. 2009). In line with these reports, Fbh1 was found to confer resistance to replication stress-inflicting agents MMS, and CPT. Further, its role as Rad51 disruptase was supported by the hyper-recombinogenic phenotype of the *fbh1*-null mutant when assayed with Ch^{16}-*RMYAH*. While the role of Fbh1 in HR is well studied, it has not yet been examined in this particular assay. GC levels in the mutant were, as predicted,

increased; however, the complete absence of Ch^{16} loss following a DSB presents a riveting yet enigmatic observation.

5.3.3.6 Atd1

Aldehyde dehydrogenase (Atd1) has been found to confer resistance to all three DNA damaging agents MMS, CPT, and bleomycin for the first time as part of this study. The protein is predicted to function in NADPH (Nicotinamide adenine dinucleotide phosphate) regeneration, based on sequence homology (http://www.pombase.org/). NADPH metabolism functions in protection against reactive oxygen species (ROS), and other biosynthetic reactions (Paravicini and Touyz 2008). Surprisingly, Atd1 facilitated efficient GC in response to a DSB, hinting at roles for metabolic factors in DNA repair. However, based on the limited data of this study and in the literature, no strong hypotheses regarding a function can be postulated, but further research is certainly warranted.

5.4 Summary

In this chapter, a list of previously derived deletion mutants, sensitive to DNA damaging agents, was enriched for novel factors functioning in HR repair. For this purpose, known HR mutants were excluded from the list, and two non-essential minichromosomes Ch^{16}-*LMYAU*, and Ch^{16}-*RMYAH* were utilised to select for genes facilitating efficient HR repair of DSBs. 39 deletion strains were found to exhibit colony sectoring as part of the Ch^{16}-*LMYAU* assay. Of those, 31 strains were assayed with Ch^{16}-*RMYAH*; 9 deletion strains displaying at least an intermediate reduction of GC levels were further identified. Finally, a selection of the most interesting hits was presented and discussed. The characterisation of the most interesting hit, Nrl1, is presented in the following **Chapter VI**.

CHAPTER VI

Nrl1 is part of the DNA damage response

6.1 Introduction

Having compiled a comprehensive list of genes functioning in homologous recombinational repair of DSBs in fission yeast, as described in **Chapter IV** and **V**, the objective of this chapter was the further characterisation of one putative novel DNA damage repair factor, Nrl1 (NRDE-2 like-1). Nrl1 was originally identified and characterised in *C. elegans* as NRDE-2 (Nuclear RNAi-defective), a required factor for nuclear RNA interference via inhibition of RNA polymerase II (RNAPII) transcription elongation (Guang et al. 2010; Burton et al. 2011). NRDE-2 is recruited to nascent transcripts by the siRNA machinery. In this context, non-coding RNAs (ncRNAs) direct NRDE factors to RNAPII, which inhibit RNAPII during transcription elongation, establishing RNAPII regulation and co-transcriptional silencing. In this chapter, its role in DSB repair is described.

6.2 Results

6.2.1 Phenotypic characterisation of Nrl1

6.2.1.1 Nrl1 confers resistance to DNA damaging agents and is localised to the nucleus

As described in **Chapter V**, *nrl1* was found as part of a genome-wide DNA damage screen. The deletion strain *nrl1*Δ displayed sensitivity to all used DNA damaging agents, MMS, CPT, and bleomycin at high concentrations (**Figure 6.1A**). As described in greater detail in **Chapter V**, bleomycin is a radiomimetic drug, inflicting DNA DSBs and SSBs; MMS as an alkylating agent causes adducts, leading to SSBs and replication fork stalling; camptothecin is a topoisomerase inhibitor, giving rise to S-phase specific DSBs. Typically, genes conferring resistance to all three agents function in either cell cycle control or DNA double-strand break repair (**Figure 6.1B)**. Utilising an YFP-tagged version of Nrl1, it became apparent that Nrl1 is localised to the nucleus (**Figure 6.1C**).

Figure 6.1

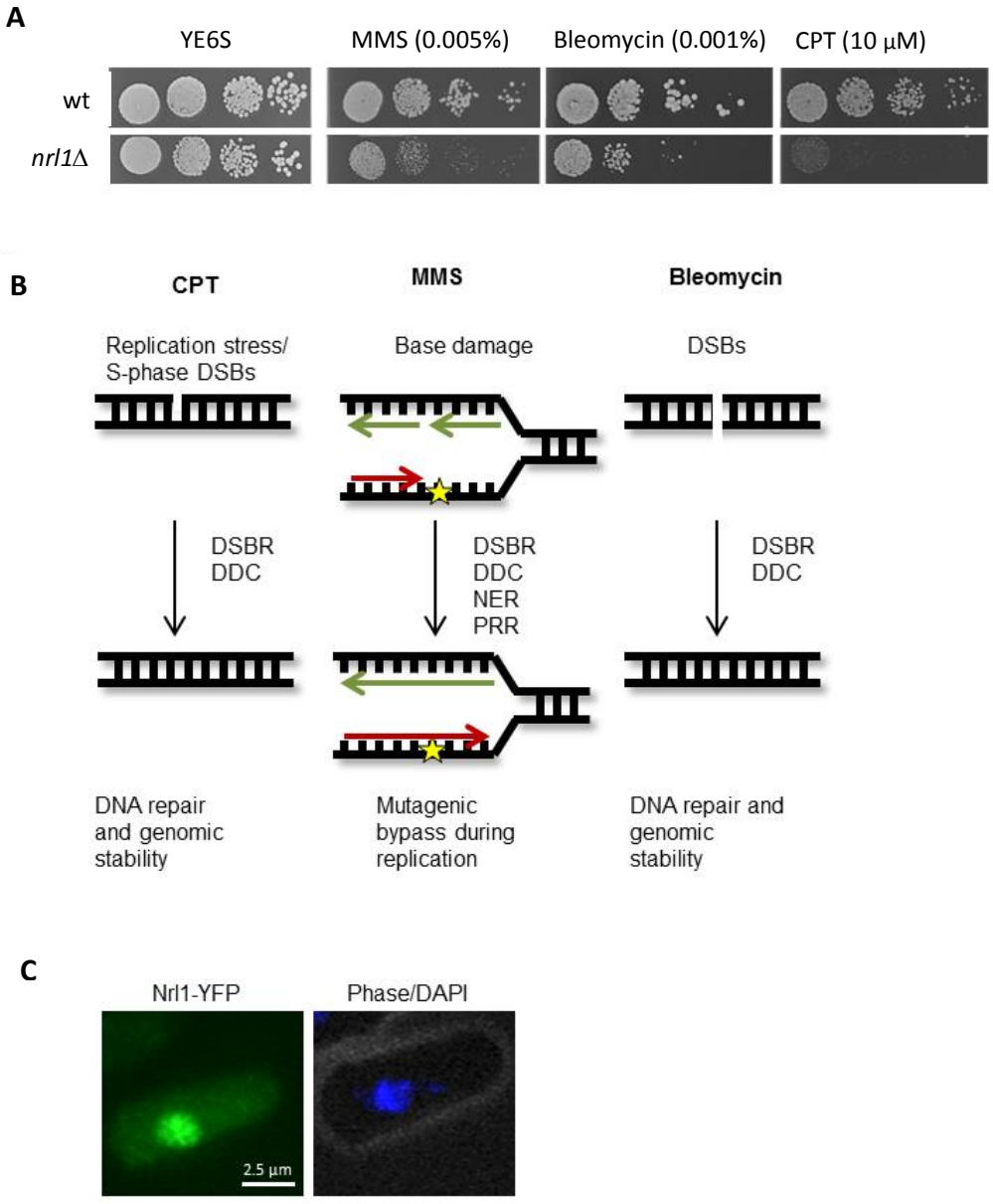


Figure 6.1: Nrl1 confers resistance to DNA damaging agents and is localised to the nucleus. (A) Spot-dilution of *nrl1*Δ and wild type on YE6S, MMS, bleomycin, and CPT at indicated concentrations. Strains were diluted five-fold and grown for 2-3 d at 32˚C. (B) DNA repair pathways required for resistance to mend inflicted lesions by the different drugs. (C) Fluorescence-microscopy of Nrl1-YFP (100x).

6.2.1.2 Nrl1 harbours evolutionary conserved functional domains

Nrl1 is evolutionary highly conserved and displays 23% identity and 36% similarity (*E-value* $3x10^{-12}$) with its human counterpart, *C14orf102*, a predicted but uncharacterised ORF (**Figure 6.2A**). One of the conserved domains, NRDE-2, formerly known as the DUF1740 domain, is hypothesised to be required for RNA interference in *C. elegans*. Nrl1 also contains 7 HAT (half a tetratricopeptide) domains, as opposed to 4 in *C. elegans* and 5 in humans, which are thought to function in RNA processing (**Figure 6.2B**). The HAT domain is characterised by a conserved repetitive pattern, containing three aromatic residues. The repeats are predicted to function in protein-protein interactions and are present in several RNA-binding proteins (Preker and Keller 1998).

Figure 6.2

A


NP_596369 1 M----------PSNHNT-------SVPKF--SSFNSVKAKKN----------PITKSNKKYRSSHDQVSS-------- 41
AAH98568 1 MALFPAFAGLSEAPDGGSSRKELDWLSNPSFCVGSITSLSQQTEAAPAHVSEGLPLTRSHLKSESSDESDTNKKLKQTSR 80
NP_596369 42 ----------NHAKSSFPSHRSIQSNFAVDTKGEKQNLLYGI---------- 73
AAH98568 81 KKKKEKKKKRKHQHHKKTKRKHGPSSSSRSETDTDSEKDKPSRGVGGSKKESEEPNQGNNAAADTGHRFVWLEDIQAVTG 160
NP_596369 74 -----NKRPVP----------KYHRSSSSVYGSAPLLRIVKESKEGITLNKKKSLEIKYDEERSFDEKEN------ 128
AAH98568 161 ETFRTDKKPDPANWEYKSLYRGDIARYKRKGDSCLGINPKKQCI--SWEGTSTEKKHS---RKQVERYFTKKSVGLMNID 235
NP_596369 129 ----------DESEFEDGQQGFIPLLVNRNSDPSEKSTFSLNI 161
AAH98568 236 GVAISSKTEPPSSEPISFIPVKDLEDAAPVTTWLNPLGIYDQSTTHWLQGQGPPEQESKQPDAQPDSESAA--------L 307
NP_596369 162 LKAIKETDEEIKKNPGKARLWIKMCEYQERLLFDEFRRSNSDDIKGKLKIE-NNSRSVKLSILEKALKEVKGCDHEILVS 240
AAH98568 308 KAKVEEFNRRVRENPRDTQLWMAFVAFQDEVMKSPGLYAIEEGEQEKRKRSLKLILEKKLAILERAIE--SNQSSVDLKL 385
NP_596369 241 YYLQLGSEEWSKEETNQKFEEVLIEHPGYLNLWMKYAEYFTG-ISEFTFNDCLNMFSKCFKFLKQKLSDRKSCKERESTD 319
AAH98568 386 AKLKLCTEFWEPSTLVKEWQKLIFLHPNNTALWQKYLLFCQSQFSTFSISKIHSLYGKCLSTLSAVKDGSI-------LS 458
NP_596369 320 VTSNFEVEEAILHLLIRLCDFLKNCGYYELAWSIFQANMELCYFYPRYLEKKLDSTFFESFSKFWNSDTPKFSEENARGW 399
AAH98568 459 HPALPGTEEAMFALFLQQCHFLRQAGHSEKAISLFQAMVDFTFFKPDSVKDLPTKGQVEFFEPFWDSGEPRAGEKGARGW 538
NP_596369 400 CNVLDD----------ESSQQNQNFSSEIG--IFQTVKLWYLNESKFDTNP--PPRSTMSCRKLS-GIDDPFRYIVFN 462
AAH98568 539 KAWMHQQERGGWVVINPDEDDDEPEEDDQEIKDKTLPRWQIWLAAERSRDQRHWRPWRPDKTKKQTEEDCEDPERQVLFD 61
NP_596369 463 DIQDFIVCFESETIAFAFKYKFFAFCGVPL-FPPGISTNSWFASYDKGIYNLLFGMASSESFINGQIAEKNSFQFPCSIL 541
AAH98568 619 DIGQSLIRLSSHDLQFQLVEAFLQFLGVPSGFTPPASC----------LYLAMDENSIFDNGLYDEK-----PLTFF 680
NP_596369 542 PSYIDLFISLMSFKNLNFKLFDYNLAHHVKESMERAFH----------QLVFSADDEYLASVYLIYLKQMETKNLSEE 609
AAH98568 681 NPLFSGASCVGRMDRLGYPRWTRGQNREGEEFIRNVFHLVMPLFSGKEKSQLCFSWLQYEIAKV-IWCLHTKNKKRLKSQ 759
NP_596369 610 KPQVNKIVKKILKKYDS--SVSVWNTYAQLEHLSGAFTMAETIFKTIFQIHAS-QLRYIDNLNVYKNWAFRKLLINDTEG 686
AAH98568 760 GKNCKKLAKNLLKEPENCNNFCLWKQYAHLEWLLGNTEDARKVFDTALGMAGSRELKDSDLCELSLLYAELEVELSPEVR 839
NP_596369 687 CLVIIKC--LLFPGDKSLTSDNNRASEMLFGMLENCASKEELLYVCLIYTIWTHCTDMDSMDNCVYL--CIQKF------ 756
AAH98568 840 RAATARAVHILTKLTESSPYGPYTGQVLAVHILKARKAYEHALQDCLGDSCVSNPAPTDSCSRLISLAKCFMLFQYLTIG 919
NP_596369 757 ----------ESYGWGASSEMECYFSYCSLIFYYQATTLQF------YNLPKVRPFFEKGVTLFSANTA 809
AAH98568 920 IDAAVQIYEQVFAKLNSSVFPEGSGEGDSASSQSWTSVLEAITLMHTSLLRFHMKVSVYPLAPLREALSQALKLYPGNQV 999
NP_596369 810 IWEVYIFFESKLRQENKPKIRAMKILKSASNAVVTACWYLFYVAVQQ----------IEPTNSQYFLRTL 869
AAH98568 1000 LWRSYVQIQNKSHSASKTRRFFDTITRSAKPLEP----WLFAIEAEKLRKRLVETVQRLDGREIHATIPETGLMHRIQAL 1075
NP_596369 870 -DITLNNEKLKSVAKFWRIYLKILNLRLNGTEWVSAITTKALASCPCNKGVCMD----------VIDLLLKKEMESRAI 937
AAH98568 1076 FENAMRSDSGSQCPLLWRMYLNFL-VSLGNKERSKGVFYKALQSCPWAKVLYLDAVEYFPDEMQEILDLMTEKELRVR-- 1152
NP_596369 938 ICYIIMLEKGFRVHNEIRRDVLKFERGDELILSPN 972
AAH98568 1153 ----LPLEEL----------ELLLED- 1164

B

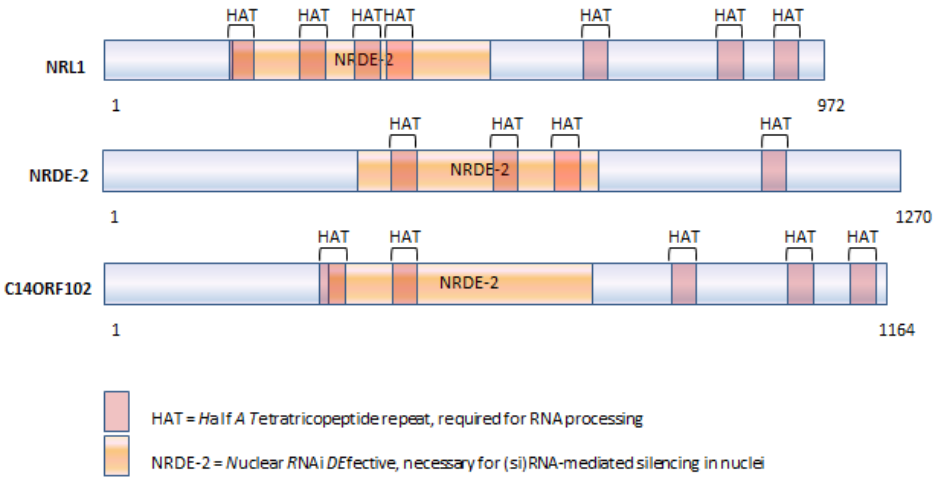


Figure 6.2: Nrl1 displays homology to human C14orf102. (A) Alignment of *S. pombe nrl1* (NP_596369) and *H. sapiens C14ORF102* (AAM98568. Red colour indicates conserved residues; blue colour indicates no gaps (COBALT tool, http://www.ncbi.nlm.nih.gov/tools/cobalt/). (B) Depiction of conserved function domains in *S. pombe* Nrl1, *C. elegans* NRDE-2, and *H. sapiens* C14ORF102.

Figure 6.3

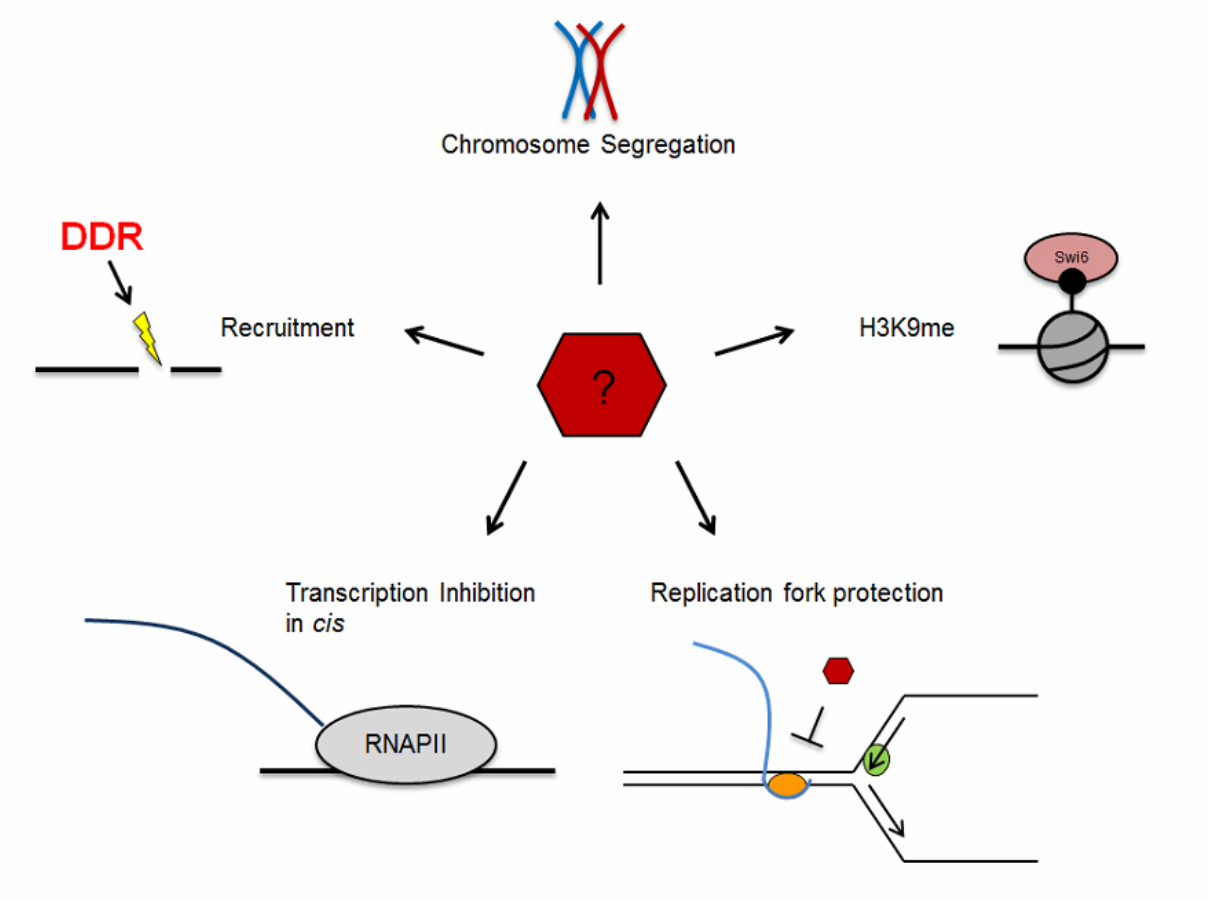


Figure 6.3: Proposed functions for Nrl1 at the interface of RNAi and DNA damage repair. Known functions of the fission yeast siRNA machinery include heterochromatisation by H3K9 methylation at four distinct genomic loci: subtelomeric regions, the centromeres, rDNA locus, and mating type locus. If compromised, cells display genomic instability due to chromosome segregation issues. Additionally, this pathway has also been implicated in protection of replication sites and recruitment of DNA damage factors (Zaratiegui et al. 2011), as well as transcription inhibition by functional modulation of RNAPII.

6.2.1.3 Proposed functions for Nrl1 in fission yeast

Based on data generated in *C. elegans* and functional predictions, the following non-exclusive hypotheses were postulated for a function of Nrl1 at the interface of RNA processing and DNA damage repair (**Figure 6.3**).

The siRNA machinery in fission yeast mainly functions in assembly of heterochromatin at three distinct loci in the genome: centromeres, subtelomeric regions, and the mating locus (Grewal 2000). Heterochromatin formation is guided by a number of factors, which are described in more detail in **Chapter I**, which generate sequence-dependent short inhibitory RNA fragments, to recruit the CLRC complex including Clr4 to methylate H3K9, which in turn binds human HP1 ortholog Swi6, resulting in transcriptional silencing of these regions. Disruption of RNAi genes typically results in silencing defects at these loci, as well as chromosome segregation errors, due to lack of heterochromatin around centromeres and telomeres.

A recent study reported the requirement of short non-coding RNA (ncRNA) fragments around a DNA break-site for activation of the DNA damage response in humans (Francia et al. 2012). Thus, it is tempting to speculate on a similar role for the fission yeast machinery. Although the mechanisms behind the crosstalk of these pathways remain elusive, potential roles for the ncRNAs in regard to DNA repair may lie within sequence-specific recruitment of DNA damage factors. Alternative options include protection of the break-site from the transcription machinery either via assembly of a heterochromatic roadblock, or via direct inhibition of RNAPII.

Since both MMS and camptothecin also apply replication stress, protection of replication-sites might also be carried out by Nrl1, since deficiency sensitised the cells to these agents by similar means.

6.2.1.4 Nrl1 is required for efficient homologous recombinational repair of DSBs

Having established that Nrl1 is conferring resistance to various DNA damaging agents, a more specific role in DSB repair was elucidated via utilisation of different non-essential minichromosomes. As described in **Chapter VI**, DSB repair in *nrl1*Δ was examined using the 'sectoring' assay, by crossing the non-essential minichromosome Ch^{16}-*LMYAU* into the deletion strain (**Figure 6.4A**). Levels of spontaneous colony sectoring were negligible in the null mutant when compared to wild type. Under break-inducing conditions, *nrl1*-deficient colonies displayed pink sectoring both on –L and +L plates, indicative of dysfunctional repair of the double-strand break and an increase in both failed repair events 'minichromosome loss' and 'LOH' (**Figure 6.4B**).

To derive a quantifiable DSB repair profile, the V2-Bioneer-deletion mutant *nrl1*Δ was back-crossed to auxotrophic wild type to lose its endogenous $arg3^+$ and $his3^+$ markers. Furthermore, a different non-essential minichromosome Ch^{16}-*RMYAH* was introduced (**Figure 6.4C**). In contrast to Ch^{16}-*LMYAU*, Ch^{16}-*RMYAH* harbours a different set of markers, and is lacking an endogenous inducible HO-endonuclease, preventing background cutting from leakage of the promoter. For break-induction, wild-type and *nrl1*Δ strains carrying Ch^{16}-*RMYAH,* were transformed with an exogenous copy of the HO-endonuclease under control of an *nmt* promoter on a plasmid (pREP81x), and expression was induced by thiamine depletion.

The DSB repair profile revealed a significant decrease of GC in the *nrl1*-null mutant (49%) from wild-type levels (72%, $p<0.05$). Concomitantly, when compared **to** wild type, failed repair events Ch^{16} loss and LOH were more prevalent in the *nrl1*-deletion mutant (Ch^{16} loss; wt: 18%, *nrl1*Δ: 29% and LOH; wt: 5% to *nrl1*Δ*:* 12%). NHEJ/Uncut levels were observed to be not significantly changed (8% in wt, 10% in *nrl1*Δ) (**Figure 6.4D**). In comparison to the DSB repair profiles of the set of sectoring mutants derived from the

genome-wide HR screen (**Chapter VI**) in a linear regression model, the phenotype of the *nrl1*-null mutant is comparable with those of other HR mutants, resulting from relatively low levels of GC, and relatively high levels of failed repair (**Figure 6.4E**). The DSB repair profile is consistent with a function in HR and further confirms the relationship between HR and Ch^{16} loss and LOH (**Figure 6.4F)**.

Figure 6.4

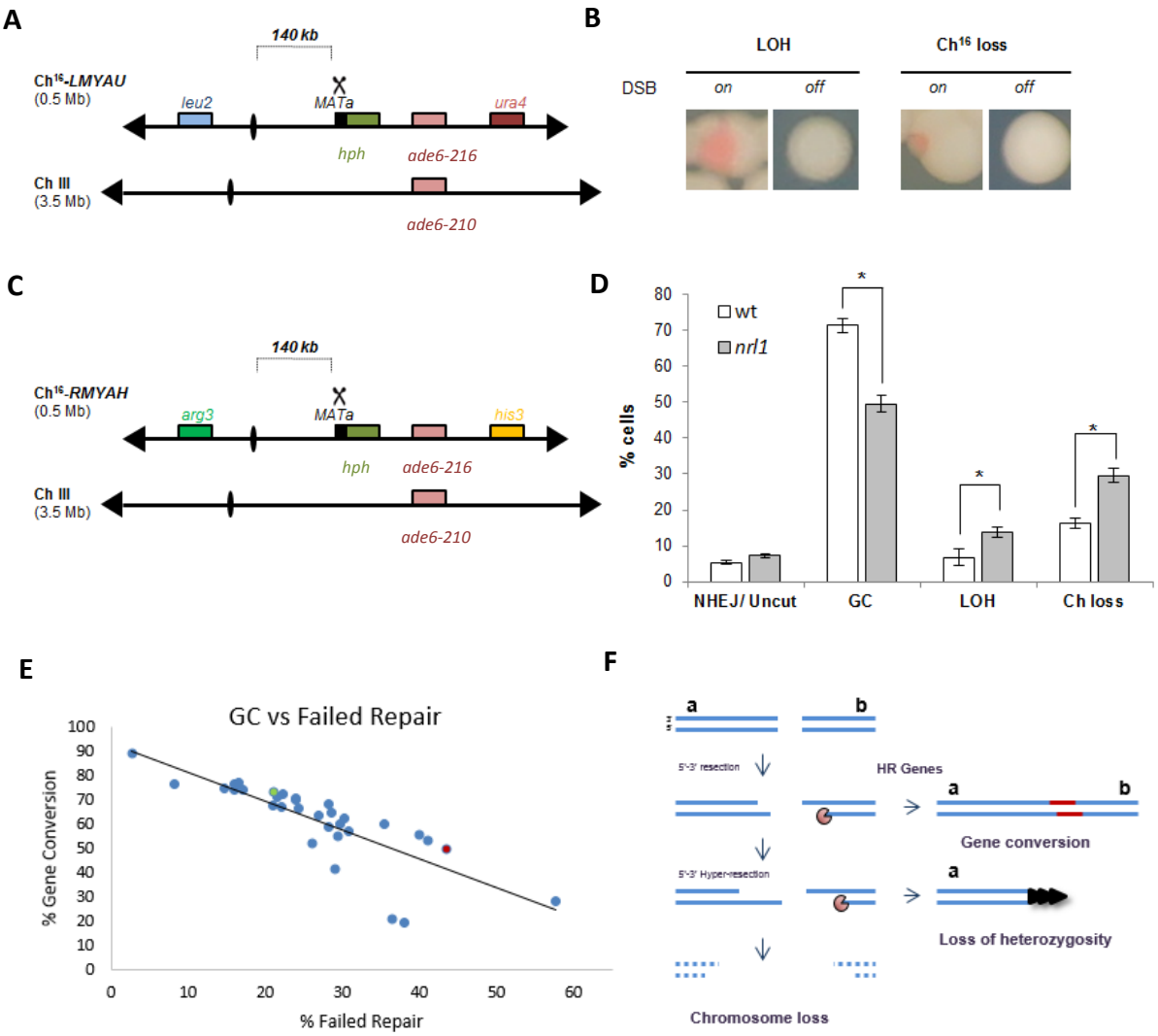


Figure 6.4: Further characterisation of Nrl1 in DSB repair. (A) Depiction of Ch^{16}-*LMYAU*, the non-essential minichromosome utilised for the 'sectoring' assay, described in Chapter V. (B) Sectoring of Nrl1 with and without break-induction; *nrl1*Δ colonies displayed sectoring both in an LOH and Ch^{16} loss context. (C) Depiction of Ch^{16}-*RMYAH*, the non-essential minichromosome utilised for the DSB assay, described in Chapter V. (D) Detailed DSB repair assay. Error bars represent standard deviation of the mean of three experiments. **(p<0.05)* (E) Linear regression analysis of the HR set defined in Chapter V. (F) Global model of HR genes function in context of the utilised assay.

6.2.1.5 Nrl1 is dispensable for checkpoint arrest following replication stress

A failure to arrest the DNA damage checkpoint in response to a DSB can potentially lead to mitotic catastrophe and cell death. Hence, many cell cycle factors are considered tumour-suppressor genes and confer resistance to DNA damaging agents by augmentation of DNA repair pathways. Thus, checkpoint deficiency can lead to disrupted DSB repair. Having established flawed DSB repair in an *nrl1*-null mutant, a potential involvement of Nrl1 in checkpoint control following DNA damage was investigated. For this purpose, wild-type and *nrl1*-deficient cells were challenged with 10 mM of HU for 6 h, causing replication fork stalling by depletion of dNTP pools, and cell length was measured (**Figure 6.5A**). Cells which fail to arrest the cell cycle will enter mitosis without a full round of replication, leading to a '*cut*' (cell untimely torn) phenotype. As presented in **Figure 6.5B,** wild-type and *nrl1*Δ cells displayed an elongated phenotype, indicative of an activated G2/M checkpoint. Consequently, Nrl1 was hypothesised to play a more direct role in HR repair of DSBs.

Figure 6.5

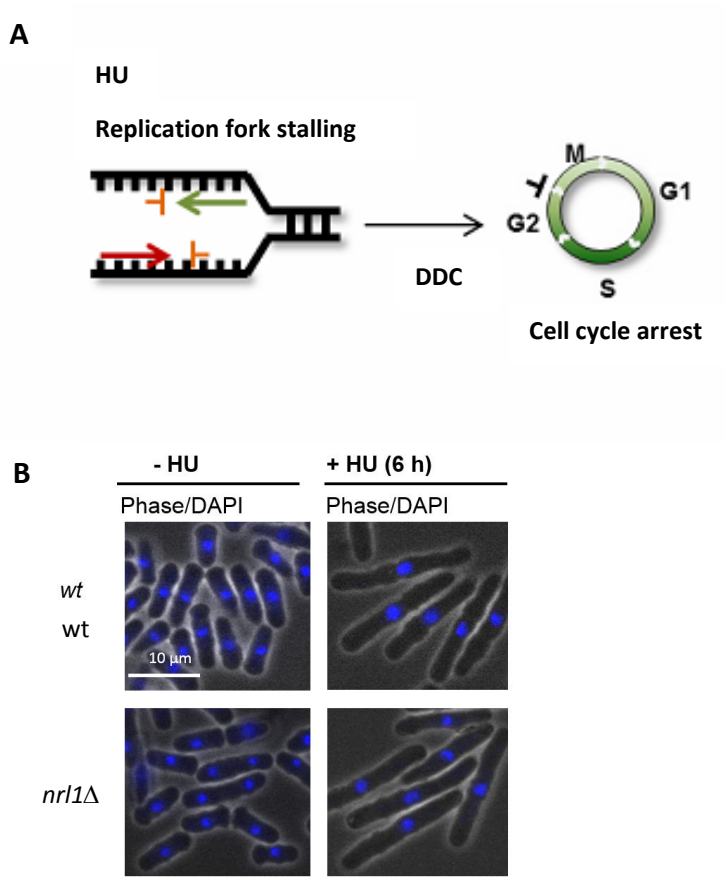


Figure 6.5: Nrl1 is not required for cell cycle arrest following replication stress. (A) Schematic: Incubation with hydroxyurea (HU) leads to replication fork stalling and activation of the G2/M checkpoint. (B) Microscopy Phase/DAPI (100x) images of wild-type and *nrl1*Δ cells before and after 6 h treatment with 10 mM HU.

6.2.1.6 Nrl1 displays defects in RPA unloading following IR

In the early stages of HR repair, the break-site is subjected to 5'-3' resection, exposing stretches of ssDNA, which are then coated and stabilised by RPA. Rad11 is the yeast homolog of the large subunit of human replication protein A (RPA). For further investigation of a potential role for Nrl1 in HR, it was sought to examine potential loading defects of upstream factor RPA onto ssDNA. To determine the kinetics of RPA recruitment and unloading, Rad11-GFP foci formation was monitored utilising fluorescence microscopy at different time points in response to 50 Gy of IR. While in *nrl1*Δ cells Rad11-GFP was accumulated as efficiently as in wild-type cells, peaking at the 30 min time point, the kinetics of the two strains diverged 90 min after irradiation (**Figure 6.6**). Wild-type cells' Rad11 foci tailed off, while *nrl1*Δ cells exhibited high levels of Rad11 foci (around 50% of cells) up to 5 hours after irradiation, indicative of failed repair. Performing microscopy of cells 5 hours after exposure of 50 Gy, it became apparent that most wild-type cells repaired the inflicted damage and underwent mitosis, as cells were no longer elongated. In stark contrast, *nrl1*Δ still displayed Rad11 foci and were elongated, consistent with inefficient mending of DNA lesions (**Figure 6.7**).

These data indicate that Nrl1 does not function upstream of RPA loading, since recruitment to the resected ssDNA stretches was functional. However, downstream processes seem to be affected, as expressed by defective unloading of RPA for further processing of the DNA-protein intermediates.

Figure 6.6

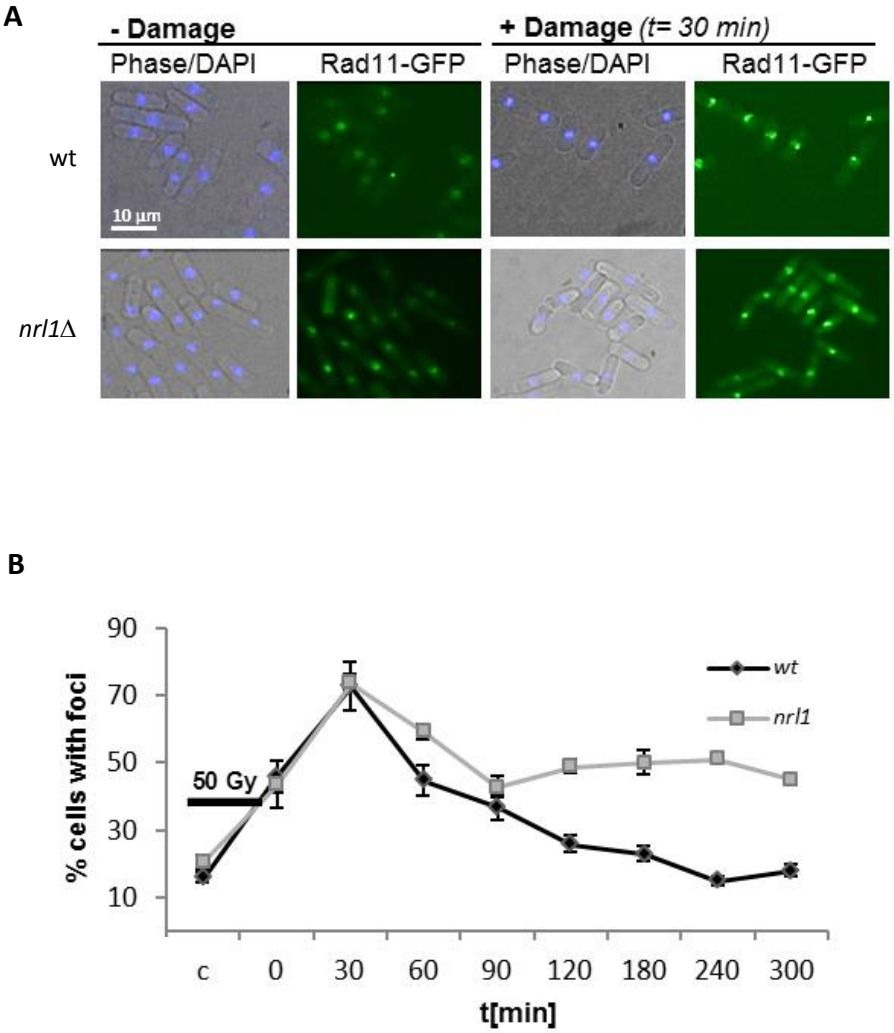


Figure 6.6: Nrl1 is required for efficient unloading of RPA following IR treatment. (A) Microscopy (100x) images of wt and *nrl1*Δ cells after treatment with 50 Gy of IR. Cells with more than 1 Rad11-GFP focus were scored. (B) Quantitation of (A). Error bars represent standard deviation of the mean of three experiments.

Figure 6.7

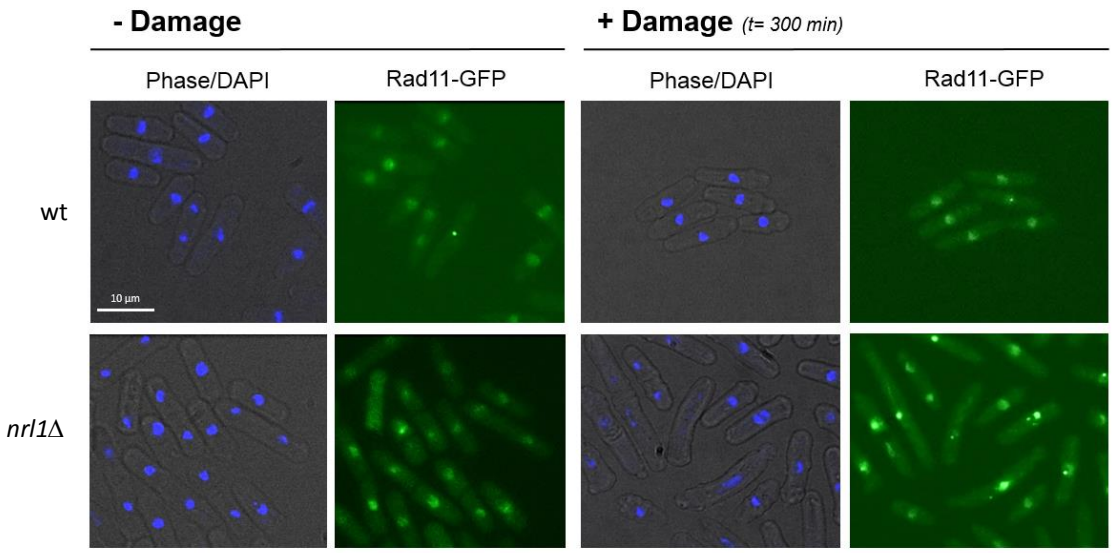


Figure 6.7: Nrl1 displays Rad11-GFP foci 5 h after irradiation. Microscopy (100x) images (Phase/DAPI and GFP) of wild-type and *nrl1*Δ cells after treatment with 50 Gy of IR. Right panel shows cells 5 h after irradiation.

6.2.1.7 Nrl1 is required for efficient Rad51 loading following IR

Rad51 is the central recombinase of HR repair and is functioning downstream of RPA. Replacement of RPA with Rad51 is facilitated by a number of loading factors, *i.e*. Rad55-Rad57 complex, Swi5-Sfr1, and Rad22 (Sugawara et al. 2003). The ssDNA-Rad51 nucleoprotein filament then mediates strand-invasion of the template strand and facilitates recombination. To investigate efficient loading of Rad51-CFP, foci formation was monitored via fluorescence microscopy (**Figure 6.8A**) and scored following 50 Gy of IR. Strikingly, Rad51 foci formation peaked at 30 min following treatment in both wild-type and *nrl1*Δ cells, but considerably lower overall formation was observed in the deletion mutant (65% in wild type to 35% in *nrl1*Δ) (**Figure 6.8B**). These findings are consistent with either defective unloading of RPA from ssDNA stretches, or defective loading of/replacement with Rad51. To investigate whether the observed phenotype was due to globally depleted cellular protein levels of Rad51, a Western Blot was carried out. As shown in **Figure 6.8C**, expression levels of Rad51-eCFP were comparable between wild type and *nrl1*Δ. These data are strongly suggestive of a role for Nrl1 in facilitating efficient Rad51 loading following a DSB, which would explain the reduced levels of GC observed in the null mutant. However, the mechanisms behind this function remain elusive.

Figure 6.8

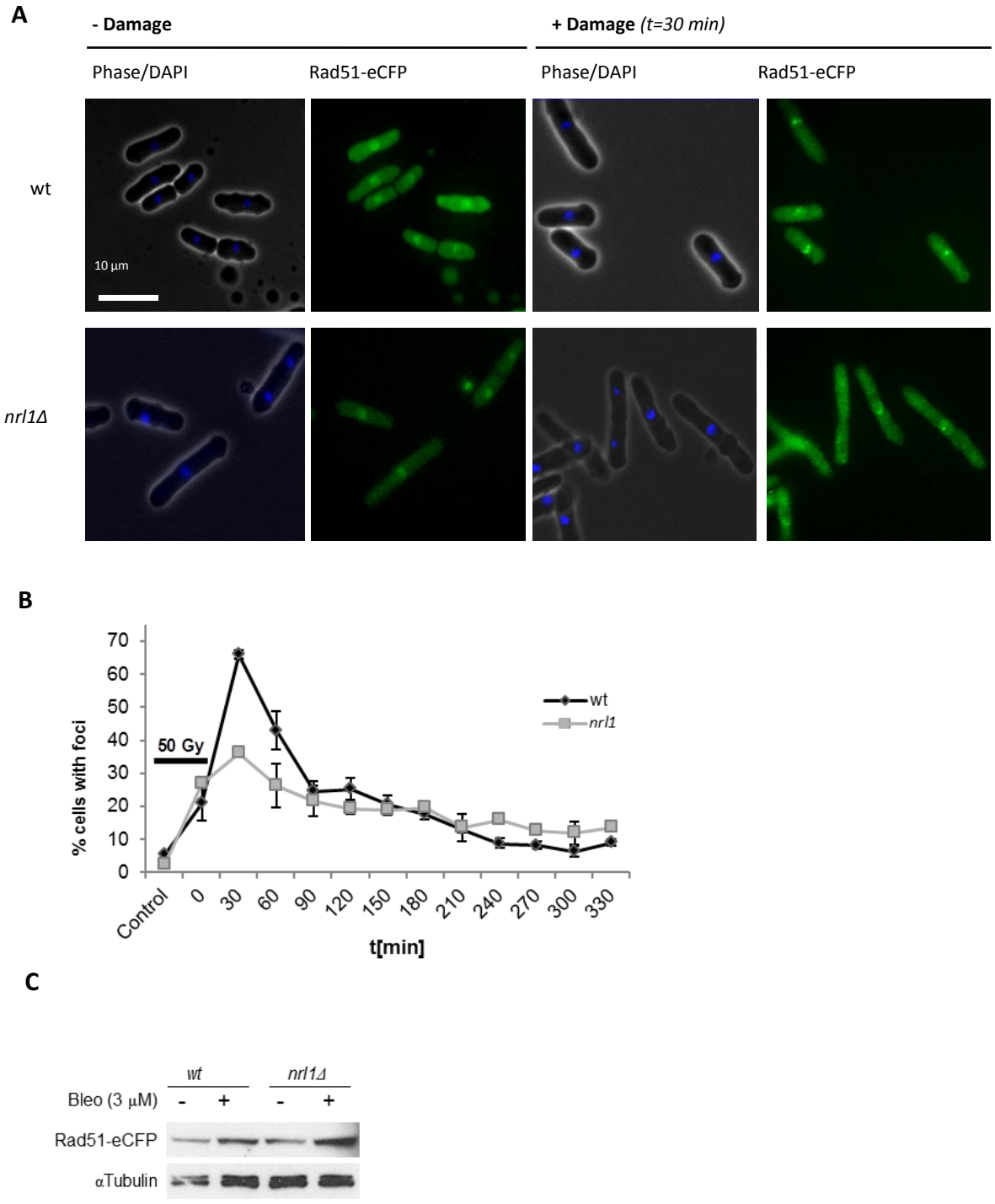


Figure 6.8: Defective loading of Rad51 in Nrl1-deficient cells. (A) Microscopy images (100x; Phase/DAPI and GFP) of wild-type and *nrl1*Δ cells after treatment with 50 Gy of IR (B) Quantitation of cells with Rad51-GFP foci (>1) at indicated time points. Error bars represent standard deviation of the mean of three experiments. (C) Western Blot of global Rad51-GFP levels with and without treatment with 3 µM bleocin.

6.2.1.8 *nrl1*Δ displays mild silencing defects

Having demonstrated a role for Nrl1 in HR repair of DSBs, a potential function in transcriptional silencing was investigated. In fission yeast, three distinct genomic loci are subjected to transcriptional silencing by the siRNA machinery via methylation of H3K9. These three loci are the centromeres, subtelomeric regions, and the mating type locus (Grewal 2000). In the context of genome stability, heterochromatised/silenced centromeres and telomeres are of vital importance, and strains lacking functional silencing often exhibit segregation defects, and dysfunctional telomeres respectively. Initially, a Western Blot of nuclear extracts was carried out to investigate proficiency of *nrl1*-null mutants to methylate H3K9. As presented in **Figure 6.9**, no global differences in H3K9me2 levels between *nrl1*-null and wild-type cells could be observed using this assay.

For a more sensitive and locus-specific investigation of silencing defects, strains with an *ura4* gene at silenced loci at the centromere (*otr1*), and telomere (*tlh1*) were utilised. Depictions of the assays are presented in (**Figure 6.10A**, and **Figure 6.11A**). The *nrl1*-null mutant was crossed with *otr1::ura4*, or *tlh1::ura4*, tetrads dissected, and double-mutants selected. To semi-quantitatively determine expression of *ura4* at these loci, a five-fold dilution series was spotted onto selective plates lacking uracil and plates containing the counter-selecting agent 5-FOA, and grown 3-4 d at 32˚C. Cells with inefficient silencing were thus expected to grow better than wild type on –uracil plates, but less well on 5-FOA plates. As presented in **Figure 6.10B,** expression levels of *ura4* at the centromere were higher in the *nrl1*-null mutant, as indicated by slightly better growth than wild-type cells on –uracil plates. However, differences in growth on 5-FOA plates were negligible. Analogously, subtle silencing defects were also observed around telomeres when tested on –uracil plates, while no difference was observed on 5-FOA plates (**Figure 6.11B**).

Figure 6.9

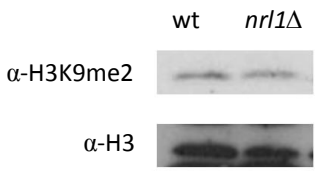


Figure 6.9: Efficient H3K9 methylation in *nrl1*Δ cells. Histones of wild-type and *nrl1*Δ cells were extracted and H3K9me2 levels determined using Western Blot. AB: α-H3K9me2 (1:1000), α -H3 (1:1000), α-Goat (1:10000).

Figure 6.10

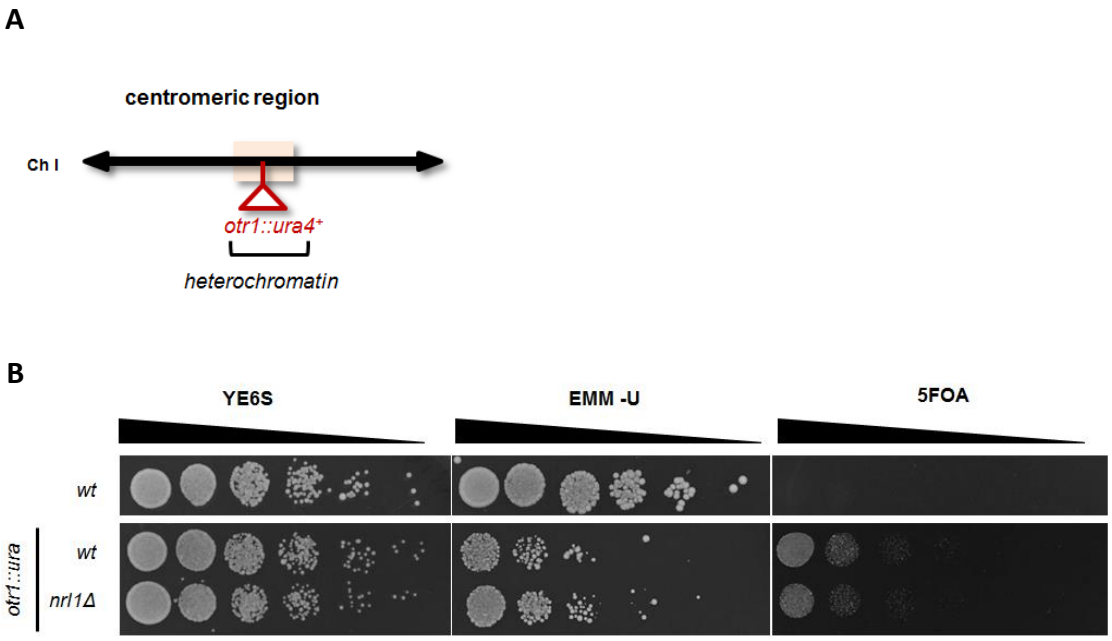


Figure 6.10: *nrl1*Δ exhibits mild silencing defects at centromeric regions. (A) Schematic of the silencing assay. Centromeric silenced gene *otr1* was replaced with an *ura4* marker to monitor gene expression. (B) For semi-quantitation, a five-fold dilution series of the following strains were spotted onto –Uracil and 5-FOA plates: wild type *ura4+*, wild type *otr1::ura4*, *nrl1*Δ *otr1::ura4.*

Figure 6.11

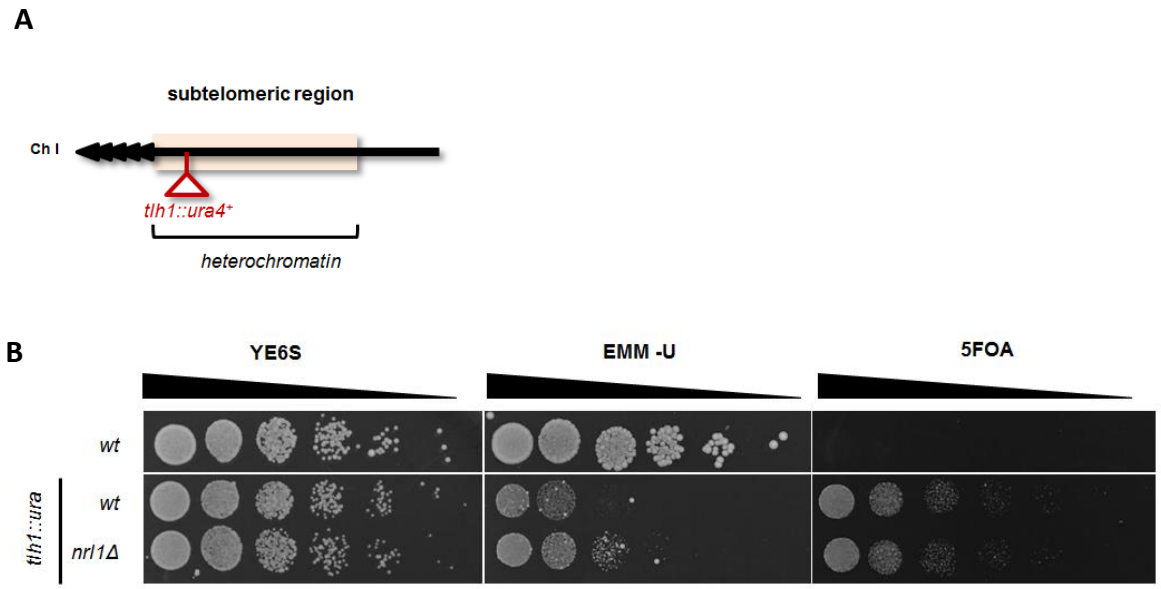


Figure 6.11: *nrl1*Δ exhibits mild silencing defects at subtelomeric regions. (A) Schematic of the silencing assay. Telomeric silenced gene *tlh1* was replaced with an *ura4* marker to monitor gene expression. (B) For semi-quantitation, a five-fold dilution series of the following strains were spotted onto –Uracil and 5-FOA plates: wild type *ura4+*, wild type *tlh1::ura4*, *nrl1*Δ *tlh1::ura4.*

6.2.2 Genetic characterisation of Nrl1

6.2.2.1 *nrl1*Δ is not synthetically lethal with *rad2*Δ

Having examined the phenotype of an *nrl1*-null mutant, and confirmed a role for Nrl1 in HR repair, subsequently genetic interactions were investigated based on these findings. Typically, deletions of genes involved in HR are synthetically lethal with deletions of fission yeast *rad2*, the ortholog of human Fen1, a flap endonuclease (Cao and Kogoma 1995; Symington 1998). Rad2 functions in Okazaki fragment processing in replication and Holliday junction resolution during mitosis (Sharma et al. 2008). If its function is impaired or absent, unprocessed Okazaki fragments lead to DSBs during replication, which are then resolved by HR. Hence, additional disruption of HR in a *rad2*Δ drives the cells into cell death due to the inability to mend the genetic lesions imposed by *rad2* deletion.

To investigate whether deletion of *nrl1* would display a similar phenotype, *rad2::ura4* was crossed with *nrl1::KanMX*, tetrads dissected, the formed colonies replica-plated onto selective plates, and the resulting genotypes scored and evaluated according to their expected Mendelian inheritance. As presented in **Figure 6.12A** and **Figure 6.12B**, *rad2*Δ was not synthetically lethal with *nrl1*Δ, as scored genotypes of the F1 were in accordance with predicted segregation of two non-lethal traits.

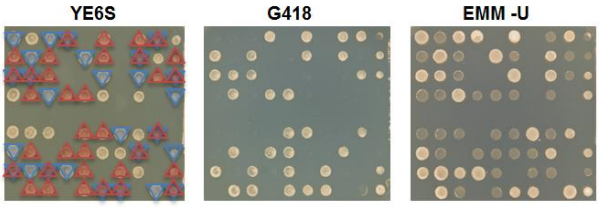
Subsequently, a potential synthetic sickness was examined by monitoring OD_{600} values of wild type, *nrl1*Δ, *rad2*Δ, and *nrl1*Δ *rad2*Δ when grown in liquid non-selective YE6S media at 32˚C. While the strains harbouring a *rad2* deletion were growing slightly slower than wild type and *nrl1*Δ, an additional deletion of *nrl1* in *rad2*Δ did not decrease fitness (**Figure 6.12C**).

When this set of strains was challenged with DNA damaging agents, it became apparent that Rad2 was dispensable for bleocin-induced DSBs, and the double-mutant *rad2*Δ *nrl1*Δ

displayed the same sensitivity to bleocin as *nrl1*Δ. However, when drugs were administered that impose additional replication stress, as MMS and CPT, *nrl1*Δ *rad2*Δ appeared to be slightly sicker than the respective single mutants, indicative of functions in parallel pathways, rather than the same pathway, to confer resistance to these drugs (**Figure 6.12D**). As Rad2 is not required for DSB repair, the epistatic relationship of *rad2*Δ and *nrl1*Δ, when challenged with bleomycin-induced DSBs was expected. The lack of synthetic sickness/lethality in a non-challenging context might be due to the intermediate attenuation of HR in an *nrl1*-null mutant, as quantified in the DSB assay.

Figure 6.12

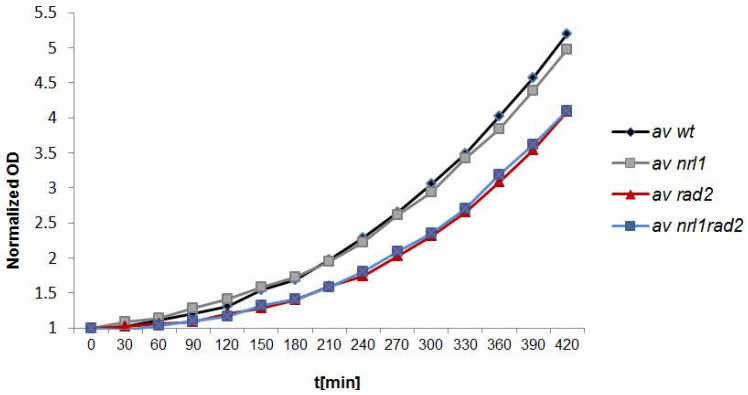
A



B

Genotype	Exp. Freq.	Obs. Freq.
wt	60/240 (.25)	53/240 (.22)
rad2Δnrl1Δ	60/240 (.25)	56/240 (.23)
rad2Δ	60/240 (.25)	65/240 (.27)
nrl1Δ	60/240 (.25)	66/240 (.28)

C



D

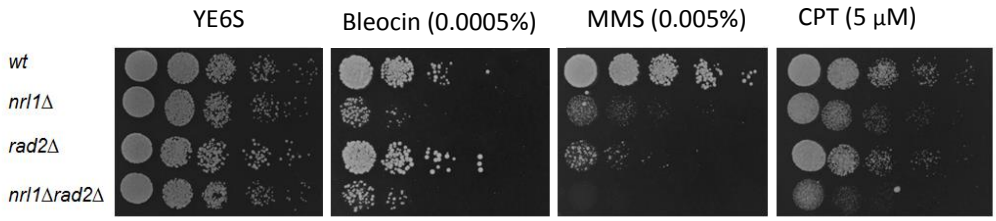


Figure 6.12: Epistasis analysis of Nrl1 and Rad2. (A) Depiction of spore-colonies formed of 20 dissected tetrads of an *nrl1::KanMR* x *rad2::ura4* cross. Nrl1-null colonies are marked with red triangles; Rad2-null mutants are marked with blue triangles. (B) Quantitation of observed genotypes of the F1. Exp.Freq: Expected frequency; Obs. Freq: Observed frequency. (C) Growth curve, derived from OD_{600} values of indicated strains, grown in non-selective YE6S media at 32˚C. (D) Spot-dilution assay: a five-fold dilution series was spotted onto indicated plates.

6.2.2.2 *nrl1*Δ is synthetically sick with Ku70 and Rad3 deletions when challenged with DNA damaging agents

To examine a potential role for Nrl1 in NHEJ, *nrl1*Δ was crossed to a *ku70* deletion. Ku70 is a central factor in NHEJ, the second major pathway to mend DSBs in eukaryotic organisms. In response to a DSB, the highly abundant Ku70/Ku80 duplex binds the DNA ends, and protects them of resection, which is required for HR repair. Furthermore the Ku70/80 complex functions as a nexus for other NHEJ core proteins, such as DNA-PK, Artemis, and Lig4 (Lieber 2010). Due to the competitive nature of NHEJ with HR, disruption of NHEJ will lead to more HR repair (described in **Chapter I**). While the double-mutant *nrl1*Δ *ku70*Δ did not exhibit a decrease in fitness on non-selective media, synthetic sickness was increased on CPT and MMS plates when compared with the respective single mutants. When challenged with bleomycin, *nrl1*Δ *ku70*Δ displayed a similar phenotype to *nrl1*Δ, while the *ku70*Δ single-mutant appeared to be even more resistant than wild type. NHEJ appears to be dispensable for repair of bleomycin-induced DSBs. Due to the error-prone nature of NHEJ in DSB repair, driving the cells into HR repair by deletion of the end-protecting Ku protein, potentially gives rise to the increased resistance to bleomycin.

Analogously, to test the relationship between Nrl1 and the DNA integrity checkpoint, a potential genetic interaction with Rad3, ortholog of human ATR was investigated. DNA repair pathways are augmented by the checkpoint machinery, arresting the cell cycle in response to DNA lesions to provide ample time for repair before mitosis is entered. Typically, gene-deletions of HR factors display synthetic sickness with checkpoint gene-deletions when challenged with DNA damaging factors. Rad3 is the major checkpoint kinase, activating an abundance of downstream factors in response to stretches of single-stranded DNA, emerging during the resection step of HR repair (see **Chapter I**). As

presented in **Figure 6.13**, *nrl1*Δ *rad3*Δ was acutely sensitive to very low levels of bleocin and CPT, which is in accordance with the postulated role for Nrl1 in HR repair. The data presented here are in accordance with a role for Nrl1 in HR repair, causing ineffective loading of Rad51 in response to a DSB, thus exhibiting synthetic sickness under damage conditions when *rad3* is deleted in addition to an *nrl1* deletion.

Figure 6.13

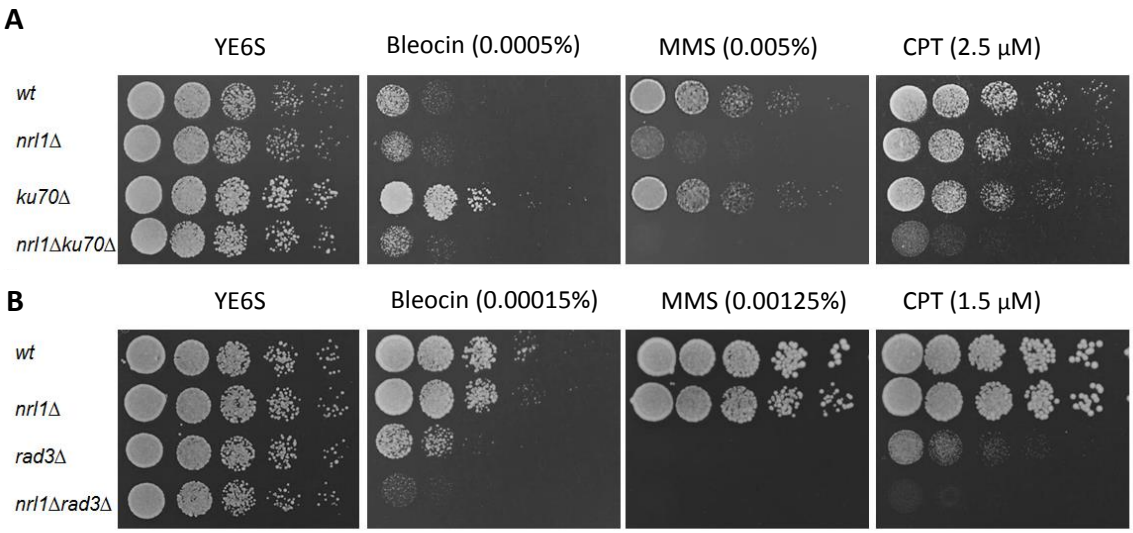


Figure 6.13: Epistasis analysis with Ku70 and Rad3. To examine potential genetic interaction with NHEJ factor Ku70 and checkpoint kinase Rad3, double-mutants with *nrl1*Δ were generated and subjected to five-fold spot-dilution onto DNA damage plates at indicated concentrations, and grown for 2-3 d, at 32˚C. (A) Epistasis analysis with Ku70. (B) Epistasis analysis with Rad3.

6.2.2.3 Nrl1 interacts negatively with Sen1

To examine genetic epistatic relationships of *nrl1*, the *Krogan Lab Interactome Database* (http://interactome-cmp.ucsf.edu/) has been searched for predicted interactors with Nrl1, which were ranked according to their correlation coefficient, which measures the strength of their predicted interaction. As presented in **Table 6.1**, the top hits were mainly enriched for factors functioning in 'Homologous Recombination', 'Chromatin Dynamics', 'RNAPII Modulation', and 'mRNA Processing', while no genetic interaction was predicted with any siRNA factors. Genetic interaction with 10 of those hits, present in the V2 deletion library (*mrc1*Δ, *cds1*Δ, *rtt109*Δ, *arp42*Δ, *sty1*Δ, *sen1*Δ, *knd1*Δ, *duf1716*Δ, *SPAC23h4.08*Δ, *sdh4*Δ) was investigated by spot-dilution of respective single- and double mutants onto DNA damage plates (**Appendix V**). As presented in **Figure 6.14**, the Nrl1-deficient strain displayed a strong synthetic sickness with an additional *sen1* deletion, even under non-genotoxic conditions. Sen1 is a RNA/DNA helicase which restricts transcription-linked RNA-DNA hybrids, and has been demonstrated to interact genetically with DNA repair genes (Mischo et al. 2011; Yuce and West 2013). These data are consistent with a role for Nrl1 in HR, as well as a role in prevention of RNA-DNA hybrids in a parallel pathway to Sen1.

Table 6.1

Sys. Name	Name	Int. Score	Corr.	Function
Chromatin dynamics				
SPAC2F3.15	lsk1	1.381	0.334	Kinase, RNAPII phosphorylation
SPBC530.13	lsc1	0.574	0.325	Lsk1 associated cyclin
SPCC4B3.08	lsg1		0.319	Lsk1 complex gamma subunit
SPBC609.05	pob3		0.311	FACT, chromatin silencing, RNAPII regulation
SPAC24B11.06c	sty1	1.069	0.31	RNAPII regulation
SPBC1289.10c	adn2		0.293	TF, RNAPII regulation
SPAC23D3.09	arp42	1.018	0.285	SWI/SNF, RSC, RNAPII regulation, chromatin rmd
SPAC3G9.04	ssu72	-0.497	0.257	RNAPII transcription termination
SPAC16C9.05	cph1	1.376	0.257	RNAPII transcription elongation
SPCC1494.10	adn3		0.253	TF, RNAPII regulation
Homologous recombination				
SPAC11E3.08c	nse6		0.361	SMC5/6 Complex; Replication fork protection
SPAC644.14c	rad51	-0.704	0.284	HR, Recombinase
SPAC14C4.13	rad17	-0.453	0.258	Checkpoint/HR
SPAC1952.07	rad1	0.359	0.253	Checkpoint/HR
SPCC23B6.05c	ssb3	-0.507	0.253	Rpa3
SPBC342.05	crb2	-1.033	0.247	53BP1
RNAPII Modulation				
SPBC609.05	pob3		0.311	FACT, chromatin silencing, RNAPII regulation
SPBC342.06c	rtt109	-0.508	0.305	HAT, H3K56Ac
SPAC23D3.09	arp42	1.018	0.285	SWI/SNF, RSC, RNAPII regulation, chromatin rmd
SPBC365.06	pmt3		0.276	Negative regulation of H3-K9/K4Me and H3K14Ac
SPAC16C9.05	cph1	1.376	0.257	RNAPII transcription elongation
SPCC70.08c			0.252	Methyltransferase

mRNA processing				
SPCC777.14	prp4	1.234	0.329	Pre-mrna splicing
SPBC336.14c	ppk26		0.293	mRNA processing
SPBC4B4.07c	usp102		0.289	Splicing
SPCC1281.02c	spf30	1.024	0.275	Splicing

Table 6.1: Predicted interaction partners of Nrl1 based on *Krogan Lab Interactome Database.* Top hits, when ranked by 'Correlation Coefficient', were assigned to four super-groups 'RNAPII Regulation', 'HR Genes', 'Histone Modifiers', and 'mRNA Processing' based on gene ontologies.

Figure 6.14

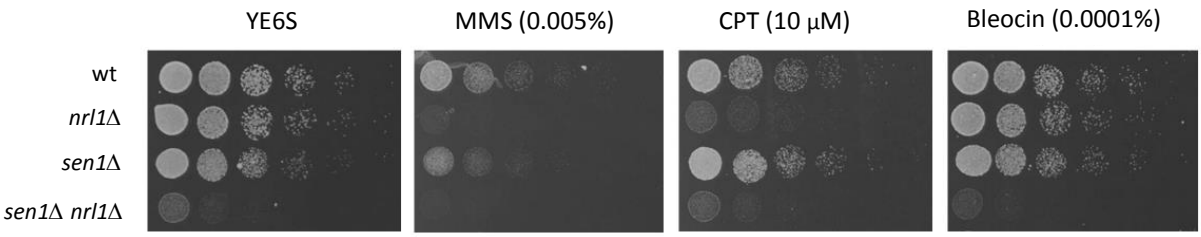


Figure 6.14: Epistasis analysis of Nrl1 and Sen1. Strains were derived using tetrad dissection, subsequently subjected to a five-fold dilution series, and challenged with DNA damaging agents MMS, CPT, and bleocin at indicated concentrations. Pictures were taken after 2 d of incubation at 32˚C.

6.3 Discussion

6.3.1 Nrl1 is a novel determinant of genome stability

In this chapter, the role of Nrl1 in DSB repair was characterised. Prior to this study, *nrl1*Δ has been identified as sensitive to CPT and UV (Han et al. 2010); the sensitivity to DSB-inducing agents bleocin and bleomycin was first described in this study. However, a role for Nrl1 in DNA damage has not been established. The data presented here suggest a complex involvement of Nrl1 in maintenance of genome stability in response to DNA damage.

Firstly, it was shown that Nrl1 is required to confer resistance to a variety of DNA damaging agents inflicting different types of lesions, *i.e.* MMS, bleocin/bleomycin, and CPT. Furthermore, utilising different non-essential minichromosomes, it became apparent that Nrl1 ensures efficient HR repair of DSBs. Since error-free NHEJ or sister-chromatid conversion (SCC) repair of the induced DSB in Ch^{16}-*RMYAH* will lead to re-cutting of the restored break-site, the assay selects for repair by gene-conversion and, if defective, for the failed repair events LOH and Ch^{16} loss. Data of this study, and prior data from the lab, support a global model in which HR genes facilitate GC in this context. If HR repair is defective or attenuated, either hyper-resection will lead to loss of the entire mini-chromosome, or LOH is realised by isochromosome formation, *de-novo* telomere addition, or break-induced replication (Tinline-Purvis et al. 2009).

Imaging experiments unveiled an attenuation of Rad51 loading onto RPA-coated ssDNA, following 5'-3' resection of an IR-induced DSB site. Concomitantly, unloading of upstream factor RPA was found to be defective; Rad11-GFP foci were found in *nrl1*Δ cells up to 5 hours after treatment with IR. These data present the first account of a critical, yet enigmatic involvement of Nrl1 in this regard.

Having characterised the phenotype of the *nrl1*-null mutant, efforts were made to unveil the genetic mechanism underlying the phenotype. Epistasis studies with null mutants of *rad2* and *rad3*, uncovered negative genetic interactions with *nrl1*. Furthermore, *nrl1*Δ also displayed a negative genetic interaction with NHEJ key player Ku70. Strikingly, effects were amplified when the respective double-mutants were challenged with MMS and CPT, two damaging agents known to apply replication stress. These findings are consistent with a role of Nrl1 in facilitating efficient HR repair, as well as protecting replication sites. Subsequently, epistasis analysis with a selection of *in-silico* predicted interactors were carried out. However, the attempts were inconclusive.

Finally, since the *C. elegans* homolog NRDE-2 is firmly implicated in RNAPII co-transcriptional silencing, a role for Nrl1 in this context was investigated. Transcription is highly regulated around DSB sites and replication forks, ensuring protection of these fragile loci from the transcription machinery. Silencing at centromeres and subtelomeric loci by heterochromatisation via the siRNA machinery, essential for genome stability in fission yeast, was demonstrated to be mildly disrupted, although it must be noted that *nrl1*-null mutants still exhibit H3K9-dimethylation. However, Western Blot might be too limited to expose subtle attenuation of histone methylation, and expression studies on selective plates are a more suitable tool to investigate deleterious effects. It became apparent, that the growth difference of wild-type and *nrl1*Δ cells on –uracil plates was bigger when compared to the growth on 5-FOA plates. The reason for this effect might be that positive selection on –uracil plates is more detectable, since every surviving cell results in a visible colony, especially when the phenotype is very subtle. While disruption of silencing at centromeres and subtelomeric regions was only mild in an *nrl1*-null mutant, these findings still hint at an involvement of Nrl1 in the siRNA pathway. However, no genetic interaction could be found using epistasis analysis of double-mutants, nor was an

siRNA factor found to interact physically with Nrl1 in purification experiments (Dr. Lucia Aronica, private correspondence).

6.3.2 Nrl1 physically interacts with splicing factors and affects splicing of Swi5 and RPA

Data from our collaborator Dr. Lucia Aronica (University of Vienna), confirmed physical interaction of tagged-Nrl1 with splicing proteins, and other factors involved in mRNA metabolism. Furthermore, utilising RT-PCR of candidate genes, it has been found that splicing of Swi5, as well as Rad55, and Rad57 was mildly affected in an *nrl1*-null mutant, which is in accordance with the observed phenotype in regard to faulty RPA unloading and defective Rad51 loading of ssDNA following DSB induction. Swi5 was first identified as a determinant of efficient mating type switching (Egel et al. 1984), and was further implicated in mediating Rad51-DNA nucleofilament formation by displacing RPA from ssDNA, functioning in a heteroduplex with Sfr1 (Haruta et al. 2006; Akamatsu et al. 2007). Similarly, the Rad55-Rad57 heterodimer has been described as recombination mediator, assisting loading of Rad51 onto ssDNA, by displacement of RPA (Sung 1997).

While these mediators are required for full activity of Rad51, Rad55-Rad57 and Sw5-Sfr1 process Rad51-dependent recombination events differently in response to a DSB (Akamatsu et al. 2007).

Utilising a tagged version of Nrl1 and subsequent mass-spectrometry of pull-downs, it was found that Nrl1 co-purifies with various factors of the Prp19/Nineteen Complex (Prp19C/NTC) and most of the Prp19 binding proteins, such as Ntr1 (Ohi and Gould 2002; Carnahan et al. 2005; Ren et al. 2011).

Intriguingly, Prp19 (precursor RNA processing protein 19) is functioning at the interface of mRNA processing and DNA damage repair, providing a putative link between these

pathways (Chanarat and Strasser 2013), and supporting the hypothesis of a function for Nrl1 in this regard.

Specifically, Prp19 has been reported as being a part of the spliceosome (Cheng et al. 1993), it plays a role in transcription elongation, (Chanarat et al. 2012) and DNA damage repair, in particular DNA strand break repair, and transcription-coupled repair (Yonemasu et al. 2005; Fousteri et al. 2006; Kuraoka et al. 2008). In addition, Prp19 has been found to be a member of the evolutionary conserved RAD52 epistasis group (de Morais et al. 1996).

The findings of this study are consistent with a role Nrl1 in splicing or transcription regulation. To further investigate potential splicing defects of DNA damage factors, genome-wide RNA-Seq experiments will be carried out.

6.3.3 RNA-DNA hybrids

Previous studies in *Saccharomyces cerevisiae* as well as mammalian cells revealed that DNA lesions emerging from fragile RNA-DNA hybrids can cause genome instability (Huertas and Aguilera 2003; Li and Manley 2005; Kim and Jinks-Robertson 2009; Paulsen et al. 2009; Wahba et al. 2011; Stirling et al. 2012). While the mechanics underlying RNA-DNA hybrid-inflicted genome instability remain obscure, it has recently been demonstrated that the HR machinery, in particular Rad51 and Rad52, promote RNA-DNA hybrid formation in mutants with defective RNA biogenesis, such as faulty transcription repression and mRNA degradation (Wahba et al. 2013). To prevent these detrimental lesions, many RNA processing and transcription factors co-transcriptionally bind to RNA polymerase to restrict access of nascent RNA stretches to the spatially close DNA template at the transcription site (Aguilera and Garcia-Muse 2012).

Sen1 is a helicase and has been demonstrated to resolve genetically fragile RNA-DNA hybrids, which naturally arise during transcription (Porrua and Libri 2013), thus placing it at the interface of transcription regulation and DNA damage repair (Yuce and West 2013). HR factors have been found to possess dual roles in R-loop metabolism: Rad51 and Rad52 were shown to promote R-loop formation in the absence of budding yeast Srs2 by potentially mediating strand invasion of the RNA stretch, and deletion of these genes in an *sae2*-null background was found to abrogate emergence of R-loops (Wahba et al. 2013). In contrast, HR was demonstrated to be required for resolving RNA-DNA hybrids, and mutants carrying deletions of *sen1* and HR factors (*rad52*) were found to be synthetically sick (Mischo et al. 2011).

Since a *sen1*-deletion has been found to be by synthetically sick with an additional Nrl1 deletion, it is thus tempting to speculate on a possible role for Nrl1 in this context, and this conjecture certainly warrants further investigation. To test an involvement of Nrl1 in R-loop prevention or resolution, immuno-staining of chromosome spreads for RNA-DNA hybrids will be carried out in different genetic backgrounds.

6.3.4 Predicted model

Based on the data presented here, the following preliminary model is presented for functions of Nrl1. While genetic mechanisms and requirements of its action still remain elusive, the following phenotypic observations could be made (**Figure 6.15**). Based on the presented data in this chapter, it is proposed that Nrl1 is functioning at the interface of RNA processing (splicing and transcription elongation) and DNA repair. This could be realised either by protection of sites of DNA damage and replication sites from the transcription machinery, or (non-exclusively) ensuring accurate splicing of Rad51 loading factors, such as Swi5, Rad55, and Rad57. Furthermore, a role for Nrl1 in prevention of

fragile RNA-DNA hybrid sites, causing genome instability, presents an intriguing corollary, and is further underpinned by its strong genetic interaction with Sen1, but requires further examination.

Figure 6.15

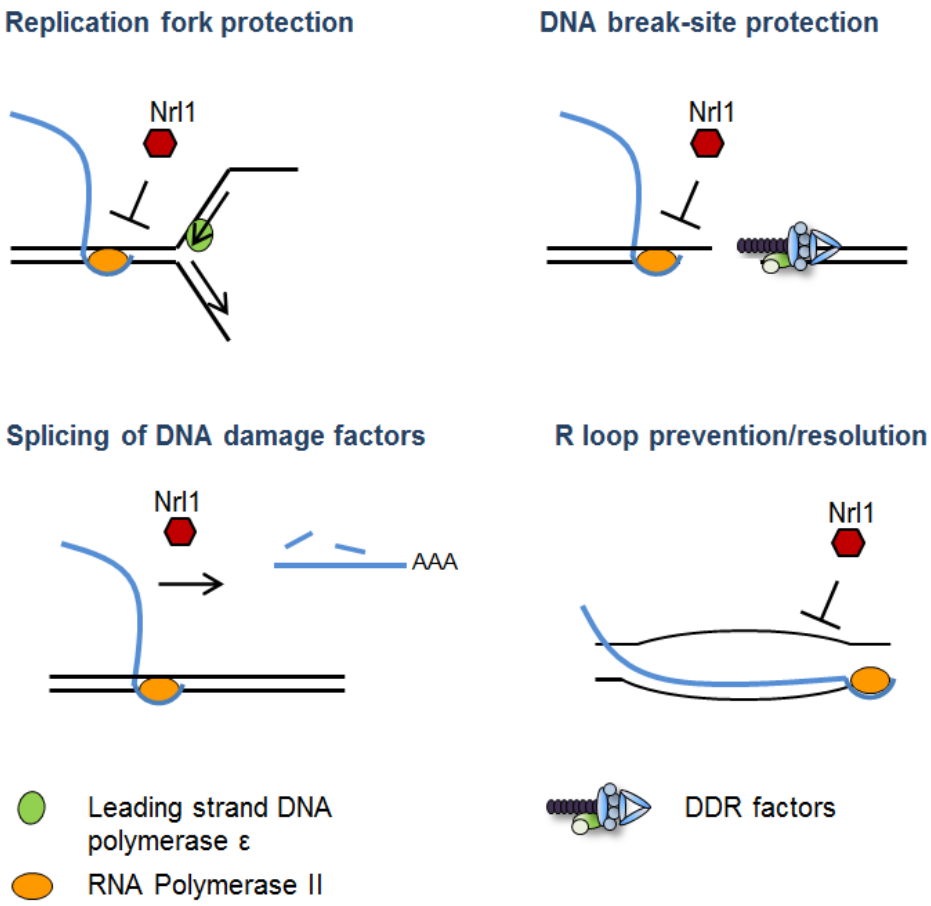


Figure 6.15: Model. Hypothesised involvement of Nrl1 in protecting DNA break-sites, replication forks, prevention of RNA-DNA hybrids, and splicing of DNA damage factors.

6.4 Summary

In this chapter, efforts have been described to characterise a putative novel factor, Nrl1, in DNA damage repair. For the first time, sensitivity to DSB-inducing agents was reported, and a role for Nrl1 in enabling efficient HR repair of DSBs was demonstrated. In addition, evidence for an involvement of Nrl1 in facilitating transcriptional silencing of centromeres and subtelomeric sites was presented. Finally, preliminary genetic studies were carried out, and negative genetic interactions with key players of the checkpoint response Rad3, NHEJ repair protein Ku70, and helicase Sen1 were revealed. The data presented here will be used towards a manuscript, complemented by data from our collaborator Dr. Lucia Aronica.

CHAPTER VII

General Discussion

This study describes the efforts to identify and characterise novel determinants of genome stability in response to a DSB. For this purpose, *S. pombe* mutants previously derived from a forward genetic screen by Helen Tinline-Purvis were identified by classical complementation as well as whole-genome sequencing, as described in **Chapter III**. Further, an *S. pombe* deletion library was screened for null mutants displaying hypersensitivity to the DNA damaging agents MMS, bleymycin, and CPT, which is presented in **Chapter IV**. The enrichment of the list of sensitive hits for novel participants in DSB repair, as well as preliminary characterisation utilising non-essential minichromosomes, are presented in **Chapter V**. A more detailed characterisation of one of the novel putative factors in HR, Nrl1, is described in **Chapter VI**. The data presented in this thesis further push the envelope in regard to inclusion of novel factors and pathways contributing to the maintenance of genome stability in eukaryotic cells.

7.1 A role for Rad17 in Resection

As presented in **Chapter III**, one of the '*loh mutants*' *loh-6,* was found to harbour a functionally disruptive point mutation in the checkpoint gene *rad17*, rendering the mutant strain sensitive to DNA damaging agents and deficient in efficient GC following a DSB. Intriguingly, the Ch^{16}-*RMGAH* DSB assay revealed a requirement for Rad17 (along with

members of the 9-1-1 complex) for efficient minichromosome removal in response to a DSB. While the crosstalk of cell cycle checkpoints with DNA damage repair pathways is extensively characterised, these data prompted the hypothesis for a direct role for checkpoint proteins in Ch^{16} loss by means of facilitating extensive resection. While this study could not settle this controversial conjecture, the data generated in this context were used to complement an existing project by Helen Tinline-Purvis, and will be used towards a manuscript (Tinline-Purvis et *al*., *submitted*).

Finally, the other '*loh mutants*' *loh-2*, *loh-5*, and *loh-7* were identified as mutants of Rad3, and Rad57 respectively; which is line with both the literature and prior data from the lab, characterising both genes and their human homologs as tumour-suppressors.

7.2 Genome-wide sensitivity screens in *S. pombe*

For many years, model organisms like yeast, worms, and mice have been utilised to understand the complex biology underlying sub-cellular systems, including the DNA damage response and cell cycle control (Hariharan and Haber 2003). Prior studies have used *S. pombe* deletion libraries to identify novel factors in DNA damage repair (Deshpande et al. 2009; Han et al. 2010), in addition to a study by Dr. Jennifer Moss in this lab (2011, unpublished). This study extends this line of enquiry and demonstrates that differences in the selection of agents, their used concentrations, as well as follow-up experiments, yield a slightly different cluster of hits. This further illustrates, that large-scale studies of deletion-libraries are not collectively exhaustive and more novel factors in the DDR remain to be identified. Since deletion-library screens are limited to the assessment of non-essential genes, there is merit to other approaches, such as temperature-sensitive libraries, synthetic lethality, or over-expression screens (Collavoli et al. 2008; Li

et al. 2011; Douglas et al. 2012; Guenole et al. 2013). Further, novel technology now also enables RNAi-based, pan-genomic, high-throughput screens in mammalian cell culture to screen for novel DDR factors, based on sensitivity (Bartz et al. 2006; Hurov et al. 2010), differential H2AX phosphorylation (Paulsen et al. 2009), or DR-GFP repair constructs (Slabicki et al. 2010; Adamson et al. 2012). Taken together, these studies are suggestive of a wide range of factors collectively functioning in maintenance of genome stability, and many factors at the interfaces of different pathways remain to be identified.

The study presented here made efforts to further extend the cohort of known genes and pathways, participating in suppression of genome instability. While the aim of the study was reached and novel genes in HR were identified (*nrl1*, *arb2*, *ago1*, *atd1*, *paf1*, *fkh2*, *est1*), the screen was limited by a number of factors and thus not considered exhaustive. Firstly, since a deletion-library was utilised, only non-essential genes were assessed, excluding all potential players in the DDR with essential functions for cell viability. Further, subsequent characterisation involved minichromosomes, carrying a 530 kb stretch of active genetic material of ChIII, causing partial diploidy; thus, wild-type copies of candidate genes were introduced into some of the deletion strains and copy numbers of some genes in the cell were altered. Further, the sectoring assay itself required stable retention of the utilised non-essential chromosome; its accuracy in regard to HR proficiency of the tested mutants might get compromised by relying on subjective assignement of sectoring status.

For a more thorough characterisation, a genetic interaction network of all hits with attenuated GC would further elucidate the complex HR network and its interdependencies. Additionally, it would be interesting to transfer the findings in yeast to a human cell system, given that approximately 70% of *S. pombe* genes have human orthologues.

7.3 RNA metabolism and DNA damage repair

As part of this study, the putative RNA biogenesis protein Nrl1 was found to confer resistance to DNA damaging agents and facilitate HR repair. The deletion mutant exhibited faulty recruitment kinetics of DDR factors RPA and Rad51. Further, genetic interactions with Rad3, Ku70, Rad2, and Sen1 were demonstrated. While preliminary, these findings, taken together with data from our collaborator and the literature, hint at a complex involvement of Nrl1 in genome stability. The synthetic sickness of the *nrl1*-null mutant with the additional deletion of *sen1* was of particular interest. The negative interaction of Sen1 and Nrl1 is consistent with a role for Nrl1 in HR; deletion of *sen1* causes an abundance of R-loops, while the deletion of *nrl1* leads to inefficient HR, thus causing a decrease in fitness. In addition, the negative genetic interaction could also suggest analogous functions for the two genes involved, but in parallel pathways. Nrl1 in worms has been shown to inhibit RNAPII transcription (Burton et al. 2011), and growth defects in *sen1* mutants have been shown to be exacerbated by faster RNAPII transcription (Hazelbaker et al. 2013). Hence, in a double mutant, an increase in R-loops due to unattenuated transcription could cause its poor viability.

These findings open the door to further investigation. First of all, direct evidence for increased R-loop formation in an *nrl1*-null strain needs to be acquired; for example by immunostaining for RNA-DNA hybrids. Also, it would be interesting to uncover the genetic requirements of R-loop formation and elucidating the complex and opaque role for the HR machinery in this regard.

To characterise the role of Nrl1 in HR, double mutants with deletions of HR key genes (*rad51*, *rad52*) will be examined. To test whether the attenuated Rad51 recruitment to DSB sites is caused by splicing defects of loading factors such as Swi5, Nrl1-deficient

cells could be complemented by ectopic expression of cDNA of candidate recombination mediators.

In addition, the potential role for Nrl1 in transcription regulation warrants an investigation of changes in transcription levels, as well as splicing of core DNA damage factors. To examine the need for inhibition of the transcription machinery around sites of DNA damage for protection, a novel Ch^{16}-based DSB assay could be made, placing the inducible MATa break-site close to an *nmt*-promoter. Transcription levels of the locus adjacent to the break-site can be modulated via thiamine concentration, and its impact on DSB repair could be studied in various genetic backgrounds.

Finally, to investigate a requirement for short non-coding RNAs for an efficient DDR along with potential participants, analogously to mammalian cells, various experiments could be carried out. Transient inhibition of transcription, following break induction, could be achieved either via chemical agents such as 6-Azauracil, or temperature-sensitive RNAPII mutants and DNA repair proficiency tested. However, altering transcription of a cell, even transiently, will impact the biology of the cell globally, potentially introducing many imponderables. Alternatively, Southern blot could be utilised to probe directly for ncRNAs around a defined DSB site.

The data generated as part of this study further illustrate the complexity and scale of the cellular response to DNA damage, justifying the efforts of this and similar studies.

References

Abraham, R. T. (2001). "Cell cycle checkpoint signaling through the ATM and ATR kinases." Genes Dev **15**(17): 2177-2196.

Adamson, B., A. Smogorzewska, F. D. Sigoillot, R. W. King and S. J. Elledge (2012). "A genome-wide homologous recombination screen identifies the RNA-binding protein RBMX as a component of the DNA-damage response." Nat Cell Biol **14**(3): 318-328.

Aguilera, A. and T. Garcia-Muse (2012). "R loops: from transcription byproducts to threats to genome stability." Mol Cell **46**(2): 115-124.

Aguilera, A. and B. Gomez-Gonzalez (2008). "Genome instability: a mechanistic view of its causes and consequences." Nat Rev Genet **9**(3): 204-217.

Akamatsu, Y., Y. Tsutsui, T. Morishita, M. S. Siddique, Y. Kurokawa, M. Ikeguchi, F. Yamao, B. Arcangioli and H. Iwasaki (2007). "Fission yeast Swi5/Sfr1 and Rhp55/Rhp57 differentially regulate Rhp51-dependent recombination outcomes." EMBO J **26**(5): 1352-1362.

Alcasabas, A. A., A. J. Osborn, J. Bachant, F. Hu, P. J. Werler, K. Bousset, K. Furuya, J. F. Diffley, A. M. Carr and S. J. Elledge (2001). "Mrc1 transduces signals of DNA replication stress to activate Rad53." Nat Cell Biol **3**(11): 958-965.

Ashton, T. M., H. W. Mankouri, A. Heidenblut, P. J. McHugh and I. D. Hickson (2011). "Pathways for Holliday Junction Processing during Homologous Recombination in Saccharomyces cerevisiae." Molecular and Cellular Biology **31**(9): 1921-1933.

Aylon, Y. and M. Kupiec (2003). "The checkpoint protein Rad24 of Saccharomyces cerevisiae is involved in processing double-strand break ends and in recombination partner choice." Mol Cell Biol **23**(18): 6585-6596.

Aylon, Y. and M. Kupiec (2004). "New insights into the mechanism of homologous recombination in yeast." Mutat Res **566**(3): 231-248.

Aylon, Y., B. Liefshitz and M. Kupiec (2004). "The CDK regulates repair of double-strand breaks by homologous recombination during the cell cycle." EMBO J **23**(24): 4868-4875.

Bao, X., J. Tang, V. Lopez-Pajares, S. Tao, K. Qu, G. R. Crabtree and P. A. Khavari (2013). "ACTL6a enforces the epidermal progenitor state by suppressing SWI/SNF-dependent induction of KLF4." Cell Stem Cell **12**(2): 193-203.

Bartek, J., C. Lukas and J. Lukas (2004). "Checking on DNA damage in S phase." Nat Rev Mol Cell Biol **5**(10): 792-804.

Bartz, S. R., Z. Zhang, J. Burchard, M. Imakura, M. Martin, A. Palmieri, R. Needham, J. Guo, M. Gordon, N. Chung, P. Warrener, A. L. Jackson, M. Carleton, M. Oatley, L. Locco, F. Santini, T. Smith, P. Kunapuli, M. Ferrer, B. Strulovici, S. H. Friend and P. S. Linsley (2006). "Small interfering RNA screens reveal enhanced cisplatin cytotoxicity in tumor cells having both BRCA network and TP53 disruptions." Mol Cell Biol **26**(24): 9377-9386.

Bentley, N. J., D. A. Holtzman, G. Flaggs, K. S. Keegan, A. DeMaggio, J. C. Ford, M. Hoekstra and A. M. Carr (1996). "The Schizosaccharomyces pombe rad3 checkpoint gene." EMBO J **15**(23): 6641-6651.

Beretta, G. L., L. Gatti, M. D. Cesare, E. Corna, S. Tinelli, N. Carenini, F. Zunino and P. Perego (2008). "The human homolog of fission yeast Rad17 is implicated in tumor growth." Cancer Lett **266**(2): 194-202.

Bermudez, V. P., L. A. Lindsey-Boltz, A. J. Cesare, Y. Maniwa, J. D. Griffith, J. Hurwitz and A. Sancar (2003). "Loading of the human 9-1-1 checkpoint complex onto DNA by the checkpoint clamp loader hRad17-replication factor C complex in vitro." Proc Natl Acad Sci U S A **100**(4): 1633-1638.

Bianchi, A., S. Negrini and D. Shore (2004). "Delivery of yeast telomerase to a DNA break depends on the recruitment functions of Cdc13 and Est1." Mol Cell **16**(1): 139-146.

Bokel, C. (2008). "EMS screens : from mutagenesis to screening and mapping." Methods Mol Biol **420**: 119-138.

Bosch, E., M. E. Hurles, A. Navarro and M. A. Jobling (2004). "Dynamics of a human interparalog gene conversion hotspot." Genome Res **14**(5): 835-844.

Bosco, G. and J. E. Haber (1998). "Chromosome break-induced DNA replication leads to nonreciprocal translocations and telomere capture." Genetics **150**(3): 1037-1047.

Bothmer, A., D. F. Robbiani, N. Feldhahn, A. Gazumyan, A. Nussenzweig and M. C. Nussenzweig (2010). "53BP1 regulates DNA resection and the choice between classical and alternative end joining during class switch recombination." J Exp Med **207**(4): 855-865.

Boulton, S. J. and S. P. Jackson (1996). "Saccharomyces cerevisiae Ku70 potentiates illegitimate DNA double-strand break repair and serves as a barrier to error-prone DNA repair pathways." EMBO J **15**(18): 5093-5103.

Broustas, C. G., A. Zhu and H. B. Lieberman (2012). "Rad9 protein contributes to prostate tumor progression by promoting cell migration and anoikis resistance." J Biol Chem **287**(49): 41324-41333.

Budman, J. and G. Chu (2005). "Processing of DNA for nonhomologous end-joining by cell-free extract." EMBO J **24**(4): 849-860.

Buhler, M. and D. Moazed (2007). "Transcription and RNAi in heterochromatic gene silencing." Nat Struct Mol Biol **14**(11): 1041-1048.

Buker, S. M., T. Iida, M. Buhler, J. Villen, S. P. Gygi, J. Nakayama and D. Moazed (2007). "Two different Argonaute complexes are required for siRNA generation and heterochromatin assembly in fission yeast." Nat Struct Mol Biol **14**(3): 200-207.

Burton, N. O., K. B. Burkhart and S. Kennedy (2011). "Nuclear RNAi maintains heritable gene silencing in Caenorhabditis elegans." Proc Natl Acad Sci U S A **108**(49): 19683-19688.

Cao, Y. and T. Kogoma (1995). "The mechanism of recA polA lethality: suppression by RecA-independent recombination repair activated by the lexA(Def) mutation in Escherichia coli." Genetics **139**(4): 1483-1494.

Cappelli, E., S. Townsend, C. Griffin and J. Thacker (2011). "Homologous recombination proteins are associated with centrosomes and are required for mitotic stability." Exp Cell Res **317**(8): 1203-1213.

Carnahan, R. H., A. Feoktistova, L. Ren, S. Niessen, J. R. Yates, 3rd and K. L. Gould (2005). "Dim1p is required for efficient splicing and export of mRNA encoding lid1p, a component of the fission yeast anaphase-promoting complex." Eukaryot Cell **4**(3): 577-587.

Caspari, T. and A. M. Carr (2002). "Checkpoints: how to flag up double-strand breaks." Curr Biol **12**(3): R105-107.

Cavenee, W. K., M. F. Hansen, M. Nordenskjold, E. Kock, I. Maumenee, J. A. Squire, R. A. Phillips and B. L. Gallie (1985). "Genetic origin of mutations predisposing to retinoblastoma." Science **228**(4698): 501-503.

Cejka, P., J. L. Plank, C. Z. Bachrati, I. D. Hickson and S. C. Kowalczykowski (2010). "Rmi1 stimulates decatenation of double Holliday junctions during dissolution by Sgs1-Top3." Nat Struct Mol Biol **17**(11): 1377-1382.

Chambers, A. L. and J. A. Downs (2012). "The RSC and INO80 chromatin-remodeling complexes in DNA double-strand break repair." Prog Mol Biol Transl Sci **110**: 229-261.

Chanarat, S., C. Burkert-Kautzsch, D. M. Meinel and K. Strasser (2012). "Prp19C and TREX: interacting to promote transcription elongationand mRNA export." Transcription **3**(1): 8-12.

Chanarat, S. and K. Strasser (2013). "Splicing and beyond: the many faces of the Prp19 complex." Biochim Biophys Acta **1833**(10): 2126-2134.

Chaurushiya, M. S. and M. D. Weitzman (2009). "Viral manipulation of DNA repair and cell cycle checkpoints." DNA Repair (Amst) **8**(9): 1166-1176.

Chen, J. M., D. N. Cooper, N. Chuzhanova, C. Ferec and G. P. Patrinos (2007). "Gene conversion: mechanisms, evolution and human disease." Nat Rev Genet **8**(10): 762-775.

Chen, X., H. Niu, W. H. Chung, Z. Zhu, A. Papusha, E. Y. Shim, S. E. Lee, P. Sung and G. Ira (2011). "Cell cycle regulation of DNA double-strand break end resection by Cdk1-dependent Dna2 phosphorylation." Nat Struct Mol Biol **18**(9): 1015-1019.

Cheng, S. C., W. Y. Tarn, T. Y. Tsao and J. Abelson (1993). "PRP19: a novel spliceosomal component." Mol Cell Biol **13**(3): 1876-1882.

Chiarle, R., Y. Zhang, R. L. Frock, S. M. Lewis, B. Molinie, Y. J. Ho, D. R. Myers, V. W. Choi, M. Compagno, D. J. Malkin, D. Neuberg, S. Monti, C. C. Giallourakis, M. Gostissa and F. W. Alt (2011). "Genome-wide translocation sequencing reveals mechanisms of chromosome breaks and rearrangements in B cells." Cell **147**(1): 107-119.

Chini, C. C. and J. Chen (2003). "Human claspin is required for replication checkpoint control." J Biol Chem **278**(32): 30057-30062.

Chini, C. C. and J. Chen (2004). "Claspin, a regulator of Chk1 in DNA replication stress pathway." DNA Repair (Amst) **3**(8-9): 1033-1037.

Christmann, M., M. T. Tomicic, W. P. Roos and B. Kaina (2003). "Mechanisms of human DNA repair: an update." Toxicology **193**(1-2): 3-34.

Chun, J., E. S. Buechelmaier and S. N. Powell (2013). "Rad51 paralog complexes BCDX2 and CX3 act at different stages in the BRCA1-BRCA2-dependent homologous recombination pathway." Mol Cell Biol **33**(2): 387-395.

Chung, W. H., Z. Zhu, A. Papusha, A. Malkova and G. Ira (2010). "Defective resection at DNA double-strand breaks leads to de novo telomere formation and enhances gene targeting." PLoS Genet **6**(5): e1000948.

Ciccia, A. and S. J. Elledge (2010). "The DNA damage response: making it safe to play with knives." Mol Cell **40**(2): 179-204.

Collavoli, A., L. Comelli, G. Rainaldi and A. Galli (2008). "A yeast-based genetic screening to identify human proteins that increase homologous recombination." FEMS Yeast Res **8**(3): 351-361.

Costa, R. M., V. Chigancas, S. Galhardo Rda, H. Carvalho and C. F. Menck (2003). "The eukaryotic nucleotide excision repair pathway." Biochimie **85**(11): 1083-1099.

Creighton, H. B. and B. McClintock (1931). "A Correlation of Cytological and Genetical Crossing-Over in Zea Mays." Proc Natl Acad Sci U S A **17**(8): 492-497.

Cuadrado, M., B. Martinez-Pastor, M. Murga, L. I. Toledo, P. Gutierrez-Martinez, E. Lopez and O. Fernandez-Capetillo (2006). "ATM regulates ATR chromatin loading in response to DNA double-strand breaks." J Exp Med **203**(2): 297-303.

Cullen, J. K., S. P. Hussey, C. Walker, J. Prudden, B. Y. Wee, A. Dave, J. S. Findlay, A. P. Savory and T. C. Humphrey (2007). "Break-induced loss of heterozygosity in fission yeast: dual roles for homologous recombination in promoting translocations and preventing de novo telomere addition." Mol Cell Biol **27**(21): 7745-7757.

de Morais, M. A., Jr., E. J. Vicente, J. Brozmanova, A. C. Schenberg and J. A. Henriques (1996). "Further characterization of the yeast pso4-1 mutant: interaction with rad51 and rad52 mutants after photoinduced psoralen lesions." Curr Genet **29**(3): 211-218.

Deem, A., A. Keszthelyi, T. Blackgrove, A. Vayl, B. Coffey, R. Mathur, A. Chabes and A. Malkova (2011). "Break-induced replication is highly inaccurate." PLoS Biol **9**(2): e1000594.

Deshpande, G. P., J. Hayles, K. L. Hoe, D. U. Kim, H. O. Park and E. Hartsuiker (2009). "Screening a genome-wide S. pombe deletion library identifies novel genes and pathways involved in genome stability maintenance." DNA Repair (Amst) **8**(5): 672-679.

Diede, S. J. and D. E. Gottschling (1999). "Telomerase-mediated telomere addition in vivo requires DNA primase and DNA polymerases alpha and delta." Cell **99**(7): 723-733.

Difilippantonio, M. J., S. Petersen, H. T. Chen, R. Johnson, M. Jasin, R. Kanaar, T. Ried and A. Nussenzweig (2002). "Evidence for replicative repair of DNA double-strand breaks leading to oncogenic translocation and gene amplification." J Exp Med **196**(4): 469-480.

Difilippantonio, M. J., J. Zhu, H. T. Chen, E. Meffre, M. C. Nussenzweig, E. E. Max, T. Ried and A. Nussenzweig (2000). "DNA repair protein Ku80 suppresses chromosomal aberrations and malignant transformation." Nature **404**(6777): 510-514.

Dimitrova, N., Y. C. Chen, D. L. Spector and T. de Lange (2008). "53BP1 promotes non-homologous end joining of telomeres by increasing chromatin mobility." Nature **456**(7221): 524-528.

Douglas, A. C., A. M. Smith, S. Sharifpoor, Z. Yan, T. Durbic, L. E. Heisler, A. Y. Lee, O. Ryan, H. Gottert, A. Surendra, D. van Dyk, G. Giaever, C. Boone, C. Nislow and B. J. Andrews (2012). "Functional analysis with a barcoder yeast gene overexpression system." G3 (Bethesda) **2**(10): 1279-1289.

Egel, R., D. H. Beach and A. J. Klar (1984). "Genes required for initiation and resolution steps of mating-type switching in fission yeast." Proc Natl Acad Sci U S A **81**(11): 3481-3485.

Evans, S. K. and V. Lundblad (1999). "Est1 and Cdc13 as comediators of telomerase access." Science **286**(5437): 117-120.

Ferguson, D. O., J. M. Sekiguchi, S. Chang, K. M. Frank, Y. Gao, R. A. DePinho and F. W. Alt (2000). "The nonhomologous end-joining pathway of DNA repair is required for genomic stability and the suppression of translocations." Proc Natl Acad Sci U S A **97**(12): 6630-6633.

Fire, A., S. Xu, M. K. Montgomery, S. A. Kostas, S. E. Driver and C. C. Mello (1998). "Potent and specific genetic interference by double-stranded RNA in Caenorhabditis elegans." Nature **391**(6669): 806-811.

Fisher, C. R. (1969). "Enzymology of the pigmented adenine-requiring mutants of Saccharomyces and Schizosaccharomyces." Biochem Biophys Res Commun **34**(3): 306-310.

Fishman-Lobell, J., N. Rudin and J. E. Haber (1992). "Two alternative pathways of double-strand break repair that are kinetically separable and independently modulated." Mol Cell Biol **12**(3): 1292-1303.

Fortini, P. and E. Dogliotti (2007). "Base damage and single-strand break repair: mechanisms and functional significance of short- and long-patch repair subpathways." DNA Repair (Amst) **6**(4): 398-409.

Fousteri, M., W. Vermeulen, A. A. van Zeeland and L. H. Mullenders (2006). "Cockayne syndrome A and B proteins differentially regulate recruitment of chromatin remodeling and repair factors to stalled RNA polymerase II in vivo." Mol Cell **23**(4): 471-482.

Francia, S., F. Michelini, A. Saxena, D. Tang, M. de Hoon, V. Anelli, M. Mione, P. Carninci and F. d'Adda di Fagagna (2012). "Site-specific DICER and DROSHA RNA products control the DNA-damage response." Nature **488**(7410): 231-235.

Friedberg, E. C., A. Aguilera, M. Gellert, P. C. Hanawalt, J. B. Hays, A. R. Lehmann, T. Lindahl, N. Lowndes, A. Sarasin and R. D. Wood (2006). "DNA repair: from molecular mechanism to human disease." DNA Repair (Amst) **5**(8): 986-996.

Fu, L., J. E. Girling and P. A. Rogers (2008). "Expression of Fox head protein 1 in human eutopic endometrium and endometriosis." Reprod Sci **15**(3): 243-252.

Fugger, K., W. K. Chu, P. Haahr, A. N. Kousholt, H. Beck, M. J. Payne, K. Hanada, I. D. Hickson and C. S. Sorensen (2013). "FBH1 co-operates with MUS81 in inducing DNA double-strand breaks and cell death following replication stress." Nat Commun **4**: 1423.

Fugger, K., M. Mistrik, J. R. Danielsen, C. Dinant, J. Falck, J. Bartek, J. Lukas and N. Mailand (2009). "Human Fbh1 helicase contributes to genome maintenance via pro- and anti-recombinase activities." J Cell Biol **186**(5): 655-663.

Fujiwara, Y. (1975). "Postreplication repair of alkylation damage to DNA of mammalian cells in culture." Cancer Res **35**(10): 2780-2789.

Furnari, B., N. Rhind and P. Russell (1997). "Cdc25 mitotic inducer targeted by chk1 DNA damage checkpoint kinase." Science **277**(5331): 1495-1497.

Gan, W., Z. Guan, J. Liu, T. Gui, K. Shen, J. L. Manley and X. Li (2011). "R-loop-mediated genomic instability is caused by impairment of replication fork progression." Genes Dev **25**(19): 2041-2056.

Gomez-Gonzalez, B., I. Felipe-Abrio and A. Aguilera (2009). "The S-phase checkpoint is required to respond to R-loops accumulated in THO mutants." Mol Cell Biol **29**(19): 5203-5213.

Goodarzi, A. A., P. Jeggo and M. Lobrich (2010). "The influence of heterochromatin on DNA double strand break repair: Getting the strong, silent type to relax." DNA Repair (Amst) **9**(12): 1273-1282.

Grandin, N. and M. Charbonneau (2007). "Mrc1, a non-essential DNA replication protein, is required for telomere end protection following loss of capping by Cdc13, Yku or telomerase." Mol Genet Genomics **277**(6): 685-699.

Greider, C. W. and E. H. Blackburn (1985). "Identification of a specific telomere terminal transferase activity in Tetrahymena extracts." Cell **43**(2 Pt 1): 405-413.

Greider, C. W. and E. H. Blackburn (1987). "The telomere terminal transferase of Tetrahymena is a ribonucleoprotein enzyme with two kinds of primer specificity." Cell **51**(6): 887-898.

Greider, C. W. and E. H. Blackburn (1989). "A telomeric sequence in the RNA of Tetrahymena telomerase required for telomere repeat synthesis." Nature **337**(6205): 331-337.

Grewal, S. I. (2000). "Transcriptional silencing in fission yeast." J Cell Physiol **184**(3): 311-318.

Guang, S., A. F. Bochner, K. B. Burkhart, N. Burton, D. M. Pavelec and S. Kennedy (2010). "Small regulatory RNAs inhibit RNA polymerase II during the elongation phase of transcription." Nature **465**(7301): 1097-1101.

Guenole, A., R. Srivas, K. Vreeken, Z. Z. Wang, S. Wang, N. J. Krogan, T. Ideker and H. van Attikum (2013). "Dissection of DNA damage responses using multiconditional genetic interaction maps." Mol Cell **49**(2): 346-358.

Guirouilh-Barbat, J., S. Huck, P. Bertrand, L. Pirzio, C. Desmaze, L. Sabatier and B. S. Lopez (2004). "Impact of the KU80 pathway on NHEJ-induced genome rearrangements in mammalian cells." Mol Cell **14**(5): 611-623.

Han, T. X., X. Y. Xu, M. J. Zhang, X. Peng and L. L. Du (2010). "Global fitness profiling of fission yeast deletion strains by barcode sequencing." Genome Biol **11**(6): R60.

Hannenhalli, S. and K. H. Kaestner (2009). "The evolution of Fox genes and their role in development and disease." Nat Rev Genet **10**(4): 233-240.

Hariharan, I. K. and D. A. Haber (2003). "Yeast, flies, worms, and fish in the study of human disease." N Engl J Med **348**(24): 2457-2463.

Harper, J. W. and S. J. Elledge (2007). "The DNA damage response: ten years after." Mol Cell **28**(5): 739-745.

Harrison, J. C. and J. E. Haber (2006). "Surviving the breakup: the DNA damage checkpoint." Annu Rev Genet **40**: 209-235.

Hartlerode, A. J. and R. Scully (2009). "Mechanisms of double-strand break repair in somatic mammalian cells." Biochem J **423**(2): 157-168.

Haruta, N., Y. Kurokawa, Y. Murayama, Y. Akamatsu, S. Unzai, Y. Tsutsui and H. Iwasaki (2006). "The Swi5-Sfr1 complex stimulates Rhp51/Rad51- and Dmc1-mediated DNA strand exchange in vitro." Nat Struct Mol Biol **13**(9): 823-830.

Hazelbaker, D. Z., S. Marquardt, W. Wlotzka and S. Buratowski (2013). "Kinetic competition between RNA Polymerase II and Sen1-dependent transcription termination." Mol Cell **49**(1): 55-66.

Heyer, W. D., K. T. Ehmsen and J. Liu (2010). "Regulation of homologous recombination in eukaryotes." Annu Rev Genet **44**: 113-139.

Holliday, R. (2007). "Evolution of optimal accuracy and stability in biological systems." Chem Biodivers **4**(9): 1972-1978.

Hsiang, Y. H., R. Hertzberg, S. Hecht and L. F. Liu (1985). "Camptothecin induces protein-linked DNA breaks via mammalian DNA topoisomerase I." J Biol Chem **260**(27): 14873-14878.

Hsiang, Y. H. and L. F. Liu (1988). "Identification of mammalian DNA topoisomerase I as an intracellular target of the anticancer drug camptothecin." Cancer Res **48**(7): 1722-1726.

Huertas, P. and A. Aguilera (2003). "Cotranscriptionally formed DNA:RNA hybrids mediate transcription elongation impairment and transcription-associated recombination." Molecular cell **12**(3): 711-721.

Hurov, K. E., C. Cotta-Ramusino and S. J. Elledge (2010). "A genetic screen identifies the Triple T complex required for DNA damage signaling and ATM and ATR stability." Genes Dev **24**(17): 1939-1950.

Huyen, Y., O. Zgheib, R. A. Ditullio, Jr., V. G. Gorgoulis, P. Zacharatos, T. J. Petty, E. A. Sheston, H. S. Mellert, E. S. Stavridi and T. D. Halazonetis (2004). "Methylated lysine 79 of histone H3 targets 53BP1 to DNA double-strand breaks." Nature **432**(7015): 406-411.

Iftode, C., Y. Daniely and J. A. Borowiec (1999). "Replication protein A (RPA): the eukaryotic SSB." Crit Rev Biochem Mol Biol **34**(3): 141-180.

Iiizumi, S., A. Kurosawa, S. So, Y. Ishii, Y. Chikaraishi, A. Ishii, H. Koyama and N. Adachi (2008). "Impact of non-homologous end-joining deficiency on random and targeted DNA integration: implications for gene targeting." Nucleic Acids Res **36**(19): 6333-6342.

Ip, S. C., U. Rass, M. G. Blanco, H. R. Flynn, J. M. Skehel and S. C. West (2008). "Identification of Holliday junction resolvases from humans and yeast." Nature **456**(7220): 357-361.

Ira, G., A. Pellicioli, A. Balijja, X. Wang, S. Fiorani, W. Carotenuto, G. Liberi, D. Bressan, L. Wan, N. M. Hollingsworth, J. E. Haber and M. Foiani (2004). "DNA end resection, homologous recombination and DNA damage checkpoint activation require CDK1." Nature **431**(7011): 1011-1017.

Ivanov, E. L., N. Sugawara, J. Fishman-Lobell and J. E. Haber (1996). "Genetic requirements for the single-strand annealing pathway of double-strand break repair in Saccharomyces cerevisiae." Genetics **142**(3): 693-704.

Jackson, S. P. (2002). "Sensing and repairing DNA double-strand breaks." Carcinogenesis **23**(5): 687-696.

Jackson, S. P. and J. Bartek (2009). "The DNA-damage response in human biology and disease." Nature **461**(7267): 1071-1078.

Jacob, S., C. Miquel, A. Sarasin and F. Praz (2005). "Effects of camptothecin on double-strand break repair by non-homologous end-joining in DNA mismatch repair-deficient human colorectal cancer cell lines." Nucleic Acids Res **33**(1): 106-113.

Jaehning, J. A. (2010). "The Paf1 complex: platform or player in RNA polymerase II transcription?" Biochim Biophys Acta **1799**(5-6): 379-388.

Jasin, M. (2000). "Chromosome breaks and genomic instability." Cancer Invest **18**(1): 78-86.

Jeffreys, A. J., J. K. Holloway, L. Kauppi, C. A. May, R. Neumann, M. T. Slingsby and A. J. Webb (2004). "Meiotic recombination hot spots and human DNA diversity." Philos Trans R Soc Lond B Biol Sci **359**(1441): 141-152.

Jeggo, P. and M. Lobrich (2006). "Radiation-induced DNA damage responses." Radiat Prot Dosimetry **122**(1-4): 124-127.

Jia, X., T. Weinert and D. Lydall (2004). "Mec1 and Rad53 inhibit formation of single-stranded DNA at telomeres of Saccharomyces cerevisiae cdc13-1 mutants." Genetics **166**(2): 753-764.

Jiang, M., L. Zhao, M. Gamez and M. J. Imperiale (2012). "Roles of ATM and ATR-mediated DNA damage responses during lytic BK polyomavirus infection." PLoS Pathog **8**(8): e1002898.

Judd, S. R. and T. D. Petes (1988). "Physical lengths of meiotic and mitotic gene conversion tracts in Saccharomyces cerevisiae." Genetics **118**(3): 401-410.

Kabotyanski, E. B., L. Gomelsky, J. O. Han, T. D. Stamato and D. B. Roth (1998). "Double-strand break repair in Ku86- and XRCC4-deficient cells." Nucleic Acids Res **26**(23): 5333-5342.

Karras, G. I., M. Fumasoni, G. Sienski, F. Vanoli, D. Branzei and S. Jentsch (2013). "Noncanonical role of the 9-1-1 clamp in the error-free DNA damage tolerance pathway." Mol Cell **49**(3): 536-546.

Kasparek, T. R. and T. C. Humphrey (2011). "DNA double-strand break repair pathways, chromosomal rearrangements and cancer." Semin Cell Dev Biol **22**(8): 886-897.

Kass, E. M. and M. Jasin (2010). "Collaboration and competition between DNA double-strand break repair pathways." FEBS Lett **584**(17): 3703-3708.

Kemp, M. and A. Sancar (2009). "DNA distress: just ring 9-1-1." Curr Biol **19**(17): R733-734.

Kent, N. A., A. L. Chambers and J. A. Downs (2007). "Dual chromatin remodeling roles for RSC during DNA double strand break induction and repair at the yeast MAT locus." J Biol Chem **282**(38): 27693-27701.

Khursheed, M., J. N. Kolla, V. Kotapalli, N. Gupta, S. Gowrishankar, S. G. Uppin, R. A. Sastry, S. Koganti, C. Sundaram, J. R. Pollack and M. D. Bashyam (2013). "ARID1B, a member of the human SWI/SNF chromatin remodeling complex, exhibits tumour-suppressor activities in pancreatic cancer cell lines." Br J Cancer **108**(10): 2056-2062.

Kim, D. U., J. Hayles, D. Kim, V. Wood, H. O. Park, M. Won, H. S. Yoo, T. Duhig, M. Nam, G. Palmer, S. Han, L. Jeffery, S. T. Baek, H. Lee, Y. S. Shim, M. Lee, L. Kim, K. S. Heo, E. J. Noh, A. R. Lee, Y. J. Jang, K. S. Chung, S. J. Choi, J. Y. Park, Y. Park, H. M. Kim, S. K. Park, H. J. Park, E. J. Kang, H. B. Kim, H. S. Kang, H. M. Park, K. Kim, K. Song, K. B. Song, P. Nurse and K. L. Hoe (2010). "Analysis of a genome-wide set of gene deletions in the fission yeast Schizosaccharomyces pombe." Nat Biotechnol **28**(6): 617-623.

Kim, N. and S. Jinks-Robertson (2009). "dUTP incorporation into genomic DNA is linked to transcription in yeast." Nature **459**(7250): 1150-1153.

Klein, I. A., W. Resch, M. Jankovic, T. Oliveira, A. Yamane, H. Nakahashi, M. Di Virgilio, A. Bothmer, A. Nussenzweig, D. F. Robbiani, R. Casellas and M. C. Nussenzweig (2011). "Translocation-capture sequencing reveals the extent and nature of chromosomal rearrangements in B lymphocytes." Cell **147**(1): 95-106.

Knudson, A. G., Jr. (1971). "Mutation and cancer: statistical study of retinoblastoma." Proc Natl Acad Sci U S A **68**(4): 820-823.

Kobayashi, Y., S. Saitoh, Y. Ogiyama, S. Soejima and K. Takahashi (2007). "The fission yeast DASH complex is essential for satisfying the spindle assembly checkpoint induced by defects in the inner-kinetochore proteins." Genes Cells **12**(3): 311-328.

Kosho, T., N. Okamoto, H. Ohashi, Y. Tsurusaki, Y. Imai, Y. Hibi-Ko, H. Kawame, T. Homma, S. Tanabe, M. Kato, Y. Hiraki, T. Yamagata, S. Yano, S. Sakazume, T. Ishii, T. Nagai, T. Ohta, N. Niikawa, S. Mizuno, T. Kaname, K. Naritomi, Y. Narumi, K. Wakui, Y. Fukushima, S. Miyatake, T. Mizuguchi, H. Saitsu, N. Miyake and N. Matsumoto (2013). "Clinical correlations of mutations affecting six components of the SWI/SNF complex: detailed description of 21 patients and a review of the literature." Am J Med Genet A **161**(6): 1221-1237.

Kowalczykowski, S. C., D. A. Dixon, A. K. Eggleston, S. D. Lauder and W. M. Rehrauer (1994). "Biochemistry of homologous recombination in Escherichia coli." Microbiol Rev **58**(3): 401-465.

Kramer, K. M. and J. E. Haber (1993). "New telomeres in yeast are initiated with a highly selected subset of TG1-3 repeats." Genes Dev **7**(12A): 2345-2356.

Krogan, N. J., J. Dover, A. Wood, J. Schneider, J. Heidt, M. A. Boateng, K. Dean, O. W. Ryan, A. Golshani, M. Johnston, J. F. Greenblatt and A. Shilatifard (2003). "The Paf1 complex is required for histone H3 methylation by COMPASS and Dot1p: linking transcriptional elongation to histone methylation." Mol Cell **11**(3): 721-729.

Krogh, B. O. and L. S. Symington (2004). "Recombination proteins in yeast." Annu Rev Genet **38**: 233-271.

Kumagai, A. and W. G. Dunphy (2000). "Claspin, a novel protein required for the activation of Chk1 during a DNA replication checkpoint response in Xenopus egg extracts." Mol Cell **6**(4): 839-849.

Kumagai, A. and W. G. Dunphy (2003). "Repeated phosphopeptide motifs in Claspin mediate the regulated binding of Chk1." Nat Cell Biol **5**(2): 161-165.

Kumar, M. S., J. Lu, K. L. Mercer, T. R. Golub and T. Jacks (2007). "Impaired microRNA processing enhances cellular transformation and tumorigenesis." Nature genetics **39**(5): 673-677.

Kuppers, R. and R. Dalla-Favera (2001). "Mechanisms of chromosomal translocations in B cell lymphomas." Oncogene **20**(40): 5580-5594.

Kuraoka, I., S. Ito, T. Wada, M. Hayashida, L. Lee, M. Saijo, Y. Nakatsu, M. Matsumoto, T. Matsunaga, H. Handa, J. Qin, Y. Nakatani and K. Tanaka (2008). "Isolation of XAB2 complex involved in pre-mRNA splicing, transcription, and transcription-coupled repair." J Biol Chem **283**(2): 940-950.

Laoukili, J., M. Stahl and R. H. Medema (2007). "FoxM1: at the crossroads of ageing and cancer." Biochim Biophys Acta **1775**(1): 92-102.

Lavin, M. F. (2007). "ATM and the Mre11 complex combine to recognize and signal DNA double-strand breaks." Oncogene **26**(56): 7749-7758.

Lee, J., X. Lu, E. S. Shin, W. F. Kern, J. J. Mulvihill and S. Li (2008). "A novel subtelomeric translocation t(5;9) and a deletion of the RB1 gene in a patient with acute myeloid leukemia (AML-M0)." Cancer Genet Cytogenet **181**(1): 36-39.

Lee, J. H. and T. T. Paull (2004). "Direct activation of the ATM protein kinase by the Mre11/Rad50/Nbs1 complex." Science **304**(5667): 93-96.

Lee, K. K., S. K. Swanson, L. Florens, M. P. Washburn and J. L. Workman (2009). "Yeast Sgf73/Ataxin-7 serves to anchor the deubiquitination module into both SAGA and Slik(SALSA) HAT complexes." Epigenetics Chromatin **2**(1): 2.

Lee, W. R., D. T. Beranek and B. J. Byrne (1989). "Dosage-response relationships for methyl methanesulfonate in Drosophila melanogaster spermatozoa: DNA methylation per nucleotide vs. sex-linked recessive lethal frequency." Mutat Res **211**(2): 243-257.

Lejeune, E. and R. C. Allshire (2011). "Common ground: small RNA programming and chromatin modifications." Curr Opin Cell Biol **23**(3): 258-265.

Li, G. M. (2008). "Mechanisms and functions of DNA mismatch repair." Cell Res **18**(1): 85-98.

Li, X. and J. L. Manley (2005). "New talents for an old acquaintance: the SR protein splicing factor ASF/SF2 functions in the maintenance of genome stability." Cell Cycle **4**(12): 1706-1708.

Li, X., C. M. Stith, P. M. Burgers and W. D. Heyer (2009). "PCNA Is Required for Initiation of Recombination-Associated DNA Synthesis by DNA Polymerase delta." Molecular Cell **36**(4): 704-713.

Li, Z., F. J. Vizeacoumar, S. Bahr, J. Li, J. Warringer, F. S. Vizeacoumar, R. Min, B. Vandersluis, J. Bellay, M. Devit, J. A. Fleming, A. Stephens, J. Haase, Z. Y. Lin, A. Baryshnikova, H. Lu, Z. Yan, K. Jin, S. Barker, A. Datti, G. Giaever, C. Nislow, C. Bulawa, C. L. Myers, M. Costanzo, A. C. Gingras, Z. Zhang, A. Blomberg, K. Bloom, B. Andrews and C. Boone (2011). "Systematic exploration of essential yeast gene function with temperature-sensitive mutants." Nat Biotechnol **29**(4): 361-367.

Lieber, M. R. (2010). "The mechanism of double-strand DNA break repair by the nonhomologous DNA end-joining pathway." Annu Rev Biochem **79**: 181-211.

Lilley, C. E., R. A. Schwartz and M. D. Weitzman (2007). "Using or abusing: viruses and the cellular DNA damage response." Trends Microbiol **15**(3): 119-126.

Linke, C., E. Klipp, H. Lehrach, M. Barberis and S. Krobitsch (2013). "Fkh1 and Fkh2 associate with Sir2 to control CLB2 transcription under normal and oxidative stress conditions." Front Physiol **4**: 173.

Liu, J., L. Renault, X. Veaute, F. Fabre, H. Stahlberg and W. D. Heyer (2011). "Rad51 paralogues Rad55-Rad57 balance the antirecombinase Srs2 in Rad51 filament formation." Nature **479**(7372): 245-248.

Liu, P., A. Erez, S. C. Nagamani, S. U. Dhar, K. E. Kolodziejska, A. V. Dharmadhikari, M. L. Cooper, J. Wiszniewska, F. Zhang, M. A. Withers, C. A. Bacino, L. D. Campos-Acevedo, M. R. Delgado, D. Freedenberg, A. Garnica, T. A. Grebe, D. Hernandez-Almaguer, L. Immken, S. R. Lalani, S. D. McLean, H. Northrup, F. Scaglia, L. Strathearn, P. Trapane, S. H. Kang, A. Patel, S. W. Cheung, P. J. Hastings, P. Stankiewicz, J. R. Lupski and W. Bi (2011). "Chromosome catastrophes involve replication mechanisms generating complex genomic rearrangements." Cell **146**(6): 889-903.

Liu, Y. and X. Lu (2012). "Non-coding RNAs in DNA damage response." Am J Cancer Res **2**(6): 658-675.

Ljungman, M. (2010). "The DNA damage response--repair or despair?" Environ Mol Mutagen **51**(8-9): 879-889.

Llorente, B., C. E. Smith and L. S. Symington (2008). "Break-induced replication: what is it and what is it for?" Cell Cycle **7**(7): 859-864.

Long, D. T., M. Raschle, V. Joukov and J. C. Walter (2011). "Mechanism of RAD51-dependent DNA interstrand cross-link repair." Science **333**(6038): 84-87.

Lopez-Girona, A., B. Furnari, O. Mondesert and P. Russell (1999). "Nuclear localization of Cdc25 is regulated by DNA damage and a 14-3-3 protein." Nature **397**(6715): 172-175.

Lorenz, A., F. Osman, V. Folkyte, S. Sofueva and M. C. Whitby (2009). "Fbh1 limits Rad51-dependent recombination at blocked replication forks." Molecular and cellular biology **29**(17): 4742-4756.

Loveday, C., C. Turnbull, E. Ramsay, D. Hughes, E. Ruark, J. R. Frankum, G. Bowden, B. Kalmyrzaev, M. Warren-Perry, K. Snape, J. W. Adlard, J. Barwell, J. Berg, A. F. Brady, C. Brewer, G. Brice, C. Chapman, J. Cook, R. Davidson, A. Donaldson, F. Douglas, L. Greenhalgh, A. Henderson, L. Izatt, A. Kumar, F. Lalloo, Z. Miedzybrodzka, P. J. Morrison, J. Paterson, M.

Porteous, M. T. Rogers, S. Shanley, L. Walker, D. Eccles, D. G. Evans, A. Renwick, S. Seal, C. J. Lord, A. Ashworth, J. S. Reis-Filho, A. C. Antoniou and N. Rahman (2011). "Germline mutations in RAD51D confer susceptibility to ovarian cancer." Nat Genet **43**(9): 879-882.

Luciano, P., S. Coulon, V. Faure, Y. Corda, J. Bos, S. J. Brill, E. Gilson, M. N. Simon and V. Geli (2012). "RPA facilitates telomerase activity at chromosome ends in budding and fission yeasts." EMBO J **31**(8): 2034-2046.

Lydeard, J. R., Z. Lipkin-Moore, S. Jain, V. V. Eapen and J. E. Haber (2010). "Sgs1 and exo1 redundantly inhibit break-induced replication and de novo telomere addition at broken chromosome ends." PLoS Genet **6**(5): e1000973.

Mack, G. S. (2007). "MicroRNA gets down to business." Nat Biotechnol **25**(6): 631-638.

Mahaney, B. L., K. Meek and S. P. Lees-Miller (2009). "Repair of ionizing radiation-induced DNA double-strand breaks by non-homologous end-joining." Biochem J **417**(3): 639-650.

Mahowald, G. K., J. M. Baron and B. P. Sleckman (2008). "Collateral damage from antigen receptor gene diversification." Cell **135**(6): 1009-1012.

Malkova, A., E. L. Ivanov and J. E. Haber (1996). "Double-strand break repair in the absence of RAD51 in yeast: a possible role for break-induced DNA replication." Proc Natl Acad Sci U S A **93**(14): 7131-7136.

Mangahas, J. L., M. K. Alexander, L. L. Sandell and V. A. Zakian (2001). "Repair of chromosome ends after telomere loss in Saccharomyces." Mol Biol Cell **12**(12): 4078-4089.

Manthey, G. M. and A. M. Bailis (2010). "Rad51 inhibits translocation formation by non-conservative homologous recombination in Saccharomyces cerevisiae." PLoS One **5**(7): e11889.

Marazzi, I., J. S. Ho, J. Kim, B. Manicassamy, S. Dewell, R. A. Albrecht, C. W. Seibert, U. Schaefer, K. L. Jeffrey, R. K. Prinjha, K. Lee, A. Garcia-Sastre, R. G. Roeder and A. Tarakhovsky (2012). "Suppression of the antiviral response by an influenza histone mimic." Nature **483**(7390): 428-433.

Matsuoka, S., B. A. Ballif, A. Smogorzewska, E. R. McDonald, 3rd, K. E. Hurov, J. Luo, C. E. Bakalarski, Z. Zhao, N. Solimini, Y. Lerenthal, Y. Shiloh, S. P. Gygi and S. J. Elledge (2007). "ATM and ATR substrate analysis reveals extensive protein networks responsive to DNA damage." Science **316**(5828): 1160-1166.

Mazon, G., E. P. Mimitou and L. S. Symington (2010). "SnapShot: Homologous recombination in DNA double-strand break repair." Cell **142**(4): 646, 646 e641.

McClintock, B. (1941). "The Stability of Broken Ends of Chromosomes in Zea Mays." Genetics **26**(2): 234-282.

McVey, M. and S. E. Lee (2008). "MMEJ repair of double-strand breaks (director's cut): deleted sequences and alternative endings." Trends Genet **24**(11): 529-538.

Mischo, H. E., B. Gomez-Gonzalez, P. Grzechnik, A. G. Rondon, W. Wei, L. Steinmetz, A. Aguilera and N. J. Proudfoot (2011). "Yeast Sen1 helicase protects the genome from transcription-associated instability." Mol Cell **41**(1): 21-32.

Mitelman, F., B. Johansson and F. Mertens (2007). "The impact of translocations and gene fusions on cancer causation." Nat Rev Cancer **7**(4): 233-245.

Moazed, D. (2009). "Small RNAs in transcriptional gene silencing and genome defence." Nature **457**(7228): 413-420.

Monahan, B. J., J. Villen, S. Marguerat, J. Bahler, S. P. Gygi and F. Winston (2008). "Fission yeast SWI/SNF and RSC complexes show compositional and functional differences from budding yeast." Nat Struct Mol Biol **15**(8): 873-880.

Moore, E. C. and R. B. Hurlbert (1985). "The inhibition of ribonucleoside diphosphate reductase by hydroxyurea, guanazole and pyrazoloimidazole (IMPY)." Pharmacol Ther **27**(2): 167-196.

Moore, J. K. and J. E. Haber (1996). "Cell cycle and genetic requirements of two pathways of nonhomologous end-joining repair of double-strand breaks in Saccharomyces cerevisiae." Mol Cell Biol **16**(5): 2164-2173.

Morrison, A. J., J. Highland, N. J. Krogan, A. Arbel-Eden, J. F. Greenblatt, J. E. Haber and X. Shen (2004). "INO80 and gamma-H2AX interaction links ATP-dependent chromatin remodeling to DNA damage repair." Cell **119**(6): 767-775.

Mortensen, U. H., C. Bendixen, I. Sunjevaric and R. Rothstein (1996). "DNA strand annealing is promoted by the yeast Rad52 protein." Proc Natl Acad Sci U S A **93**(20): 10729-10734.

Moss, J., H. Tinline-Purvis, C. A. Walker, L. K. Folkes, M. R. Stratford, J. Hayles, K. L. Hoe, D. U. Kim, H. O. Park, S. E. Kearsey, O. Fleck, C. Holmberg, O. Nielsen and T. C. Humphrey (2010). "Break-induced ATR and Ddb1-Cul4(Cdt)(2) ubiquitin ligase-dependent nucleotide synthesis promotes homologous recombination repair in fission yeast." Genes Dev **24**(23): 2705-2716.

Mueller, C. L., S. E. Porter, M. G. Hoffman and J. A. Jaehning (2004). "The Paf1 complex has functions independent of actively transcribing RNA polymerase II." Mol Cell **14**(4): 447-456.

Myatt, S. S. and E. W. Lam (2007). "The emerging roles of forkhead box (Fox) proteins in cancer." Nat Rev Cancer **7**(11): 847-859.

Myung, K., C. Chen and R. D. Kolodner (2001). "Multiple pathways cooperate in the suppression of genome instability in Saccharomyces cerevisiae." Nature **411**(6841): 1073-1076.

Negrini, S., V. Ribaud, A. Bianchi and D. Shore (2007). "DNA breaks are masked by multiple Rap1 binding in yeast: implications for telomere capping and telomerase regulation." Genes Dev **21**(3): 292-302.

Nickoloff, J. A., J. D. Singer and F. Heffron (1990). "In vivo analysis of the Saccharomyces cerevisiae HO nuclease recognition site by site-directed mutagenesis." Mol Cell Biol **10**(3): 1174-1179.

Nicolas, E., T. Yamada, H. P. Cam, P. C. Fitzgerald, R. Kobayashi and S. I. Grewal (2007). "Distinct roles of HDAC complexes in promoter silencing, antisense suppression and DNA damage protection." Nat Struct Mol Biol **14**(5): 372-380.

Niida, H. and M. Nakanishi (2006). "DNA damage checkpoints in mammals." Mutagenesis **21**(1): 3-9.

Nimonkar, A. V. and S. C. Kowalczykowski (2009). "Second-end DNA capture in double-strand break repair: how to catch a DNA by its tail." Cell Cycle **8**(12): 1816-1817.

Niwa, O., T. Matsumoto, Y. Chikashige and M. Yanagida (1989). "Characterization of Schizosaccharomyces pombe minichromosome deletion derivatives and a functional allocation of their centromere." EMBO J **8**(10): 3045-3052.

Nordick, K., M. G. Hoffman, J. L. Betz and J. A. Jaehning (2008). "Direct interactions between the Paf1 complex and a cleavage and polyadenylation factor are revealed by dissociation of Paf1 from RNA polymerase II." Eukaryot Cell **7**(7): 1158-1167.

Nowell, P. C. and D. A. Hungerford (1960). "Chromosome studies on normal and leukemic human leukocytes." J Natl Cancer Inst **25**: 85-109.

Nussenzweig, A. and M. C. Nussenzweig (2010). "Origin of chromosomal translocations in lymphoid cancer." Cell **141**(1): 27-38.

Oh, S., S. Park and S. van Nocker (2008). "Genic and global functions for Paf1C in chromatin modification and gene expression in Arabidopsis." PLoS Genet **4**(8): e1000077.

Ohi, M. D. and K. L. Gould (2002). "Characterization of interactions among the Cef1p-Prp19p-associated splicing complex." RNA **8**(6): 798-815.

Osman, F., J. Dixon, A. R. Barr and M. C. Whitby (2005). "The F-Box DNA helicase Fbh1 prevents Rhp51-dependent recombination without mediator proteins." Mol Cell Biol **25**(18): 8084-8096.

Pandita, R. K., G. G. Sharma, A. Laszlo, K. M. Hopkins, S. Davey, M. Chakhparonian, A. Gupta, R. J. Wellinger, J. Zhang, S. N. Powell, J. L. Roti Roti, H. B. Lieberman and T. K. Pandita (2006).

"Mammalian Rad9 plays a role in telomere stability, S- and G2-phase-specific cell survival, and homologous recombinational repair." Mol Cell Biol **26**(5): 1850-1864.

Paques, F. and J. E. Haber (1999). "Multiple pathways of recombination induced by double-strand breaks in Saccharomyces cerevisiae." Microbiol Mol Biol Rev **63**(2): 349-404.

Paravicini, T. M. and R. M. Touyz (2008). "NADPH oxidases, reactive oxygen species, and hypertension: clinical implications and therapeutic possibilities." Diabetes Care **31 Suppl 2**: S170-180.

Pascucci, B., M. T. Russo, M. Crescenzi, M. Bignami and E. Dogliotti (2005). "The accumulation of MMS-induced single strand breaks in G1 phase is recombinogenic in DNA polymerase beta defective mammalian cells." Nucleic Acids Res **33**(1): 280-288.

Paulsen, R. D., D. V. Soni, R. Wollman, A. T. Hahn, M. C. Yee, A. Guan, J. A. Hesley, S. C. Miller, E. F. Cromwell, D. E. Solow-Cordero, T. Meyer and K. A. Cimprich (2009). "A genome-wide siRNA screen reveals diverse cellular processes and pathways that mediate genome stability." Mol Cell **35**(2): 228-239.

Petermann, E., M. L. Orta, N. Issaeva, N. Schultz and T. Helleday (2010). "Hydroxyurea-stalled replication forks become progressively inactivated and require two different RAD51-mediated

Peterson, C. L. and J. Cote (2004). "Cellular machineries for chromosomal DNA repair." Genes Dev **18**(6): 602-616.

Pfeiffer, P., W. Goedecke and G. Obe (2000). "Mechanisms of DNA double-strand break repair and their potential to induce chromosomal aberrations." Mutagenesis **15**(4): 289-302.

Plasterk, R. H. (2006). "Micro RNAs in animal development." Cell **124**(5): 877-881.

Porrua, O. and D. Libri (2013). "A bacterial-like mechanism for transcription termination by the Sen1p helicase in budding yeast." Nat Struct Mol Biol **20**(7): 884-891.

Postnikoff, S. D., M. E. Malo, B. Wong and T. A. Harkness (2012). "The yeast forkhead transcription factors fkh1 and fkh2 regulate lifespan and stress response together with the anaphase-promoting complex." PLoS Genet **8**(3): e1002583.

Povirk, L. F. (1996). "DNA damage and mutagenesis by radiomimetic DNA-cleaving agents:

Prado, F. and A. Aguilera (2005). "Impairment of replication fork progression mediates RNA polII transcription-associated recombination." EMBO J **24**(6): 1267-1276.

Preker, P. J. and W. Keller (1998). "The HAT helix, a repetitive motif implicated in RNA processing." Trends Biochem Sci **23**(1): 15-16.

Prudden, J., J. S. Evans, S. P. Hussey, B. Deans, P. O'Neill, J. Thacker and T. Humphrey (2003). "Pathway utilization in response to a site-specific DNA double-strand break in fission yeast." EMBO J **22**(6): 1419-1430.

Raji, H. and E. Hartsuiker (2006). "Double-strand break repair and homologous recombination in Schizosaccharomyces pombe." Yeast **23**(13): 963-976.

Ren, L., J. R. McLean, T. R. Hazbun, S. Fields, C. Vander Kooi, M. D. Ohi and K. L. Gould (2011). "Systematic two-hybrid and comparative proteomic analyses reveal novel yeast pre-mRNA splicing factors connected to Prp19." PLoS One **6**(2): e16719.

Rhind, N., B. Furnari and P. Russell (1997). "Cdc2 tyrosine phosphorylation is required for the DNA damage checkpoint in fission yeast." Genes Dev **11**(4): 504-511.

Rhind, N. and P. Russell (2000). "Chk1 and Cds1: linchpins of the DNA damage and replication checkpoint pathways." J Cell Sci **113 (Pt 22)**: 3889-3896.

Ribaud, V., C. Ribeyre, P. Damay and D. Shore (2012). "DNA-end capping by the budding yeast transcription factor and subtelomeric binding protein Tbf1." EMBO J **31**(1): 138-149.

Ribeyre, C. and D. Shore (2013). "Regulation of telomere addition at DNA double-strand breaks." Chromosoma **122**(3): 159-173.

Rich, T., R. L. Allen and A. H. Wyllie (2000). "Defying death after DNA damage." Nature **407**(6805): 777-783.

Roos-Mattjus, P., K. M. Hopkins, A. J. Oestreich, B. T. Vroman, K. L. Johnson, S. Naylor, H. B. Lieberman and L. M. Karnitz (2003). "Phosphorylation of human Rad9 is required for genotoxin-activated checkpoint signaling." J Biol Chem **278**(27): 24428-24437.

Rouse, J. and S. P. Jackson (2002). "Interfaces between the detection, signaling, and repair of DNA damage." Science **297**(5581): 547-551.

Saini, N., S. Ramakrishnan, R. Elango, S. Ayyar, Y. Zhang, A. Deem, G. Ira, J. E. Haber, K. S. Lobachev and A. Malkova (2013). "Migrating bubble during break-induced replication drives conservative DNA synthesis." Nature.

Saka, Y., F. Esashi, T. Matsusaka, S. Mochida and M. Yanagida (1997). "Damage and replication checkpoint control in fission yeast is ensured by interactions of Crb2, a protein with BRCT motif, with Cut5 and Chk1." Genes Dev **11**(24): 3387-3400.

Saleh-Gohari, N., H. E. Bryant, N. Schultz, K. M. Parker, T. N. Cassel and T. Helleday (2005). "Spontaneous homologous recombination is induced by collapsed replication forks that are caused by endogenous DNA single-strand breaks." Mol Cell Biol **25**(16): 7158-7169.

San Filippo, J., P. Sung and H. Klein (2008). "Mechanism of eukaryotic homologous recombination." Annu Rev Biochem **77**: 229-257.

Sand, M., D. Sand, P. Altmeyer and F. G. Bechara (2012). "MicroRNA in non-melanoma skin cancer." Cancer Biomark **11**(6): 253-257.

Sandri, M. (2012). "FOXOphagy path to inducing stress resistance and cell survival." Nat Cell Biol **14**(8): 786-788.

Schildkraut, E., C. A. Miller and J. A. Nickoloff (2005). "Gene conversion and deletion frequencies during double-strand break repair in human cells are controlled by the distance between direct repeats." Nucleic Acids Res **33**(5): 1574-1580.

Sharma, S., J. A. Sommers and R. M. Brosh, Jr. (2008). "Processing of DNA replication and repair intermediates by the concerted action of RecQ helicases and Rad2 structure-specific nucleases." Protein Pept Lett **15**(1): 89-102.

Shim, E. Y., J. L. Ma, J. H. Oum, Y. Yanez and S. E. Lee (2005). "The yeast chromatin remodeler RSC complex facilitates end joining repair of DNA double-strand breaks." Mol Cell Biol **25**(10): 3934-3944.

Shinohara, A., H. Ogawa and T. Ogawa (1992). "Rad51 protein involved in repair and recombination in S. cerevisiae is a RecA-like protein." Cell **69**(3): 457-470.

Shinohara, M., K. Sakai, T. Ogawa and A. Shinohara (2003). "The mitotic DNA damage checkpoint proteins Rad17 and Rad24 are required for repair of double-strand breaks during meiosis in yeast." Genetics **164**(3): 855-865.

Shrivastav, M., L. P. De Haro and J. A. Nickoloff (2008). "Regulation of DNA double-strand break repair pathway choice." Cell Res **18**(1): 134-147.

Shrivastav, N., D. Li and J. M. Essigmann (2010). "Chemical biology of mutagenesis and DNA repair: cellular responses to DNA alkylation." Carcinogenesis **31**(1): 59-70.

Sikora, A., D. Mielecki, A. Chojnacka, J. Nieminuszczy, M. Wrzesinski and E. Grzesiuk (2010). "Lethal and mutagenic properties of MMS-generated DNA lesions in Escherichia coli cells deficient in BER and AlkB-directed DNA repair." Mutagenesis **25**(2): 139-147.

Slabicki, M., M. Theis, D. B. Krastev, S. Samsonov, E. Mundwiller, M. Junqueira, M. Paszkowski-Rogacz, J. Teyra, A. K. Heninger, I. Poser, F. Prieur, J. Truchetto, C. Confavreux, C. Marelli, A. Durr, J. P. Camdessanche, A. Brice, A. Shevchenko, M. T. Pisabarro, G. Stevanin and F. Buchholz (2010). "A genome-scale DNA repair RNAi screen identifies SPG48 as a novel gene associated with hereditary spastic paraplegia." PLoS Biol **8**(6): e1000408.

Smith, C. E., B. Llorente and L. S. Symington (2007). "Template switching during break-induced replication." Nature **447**(7140): 102-105.

Smith, J., L. M. Tho, N. Xu and D. A. Gillespie (2010). "The ATM-Chk2 and ATR-Chk1 pathways in DNA damage signaling and cancer." Adv Cancer Res **108**: 73-112.

Smogorzewska, A. and T. de Lange (2004). "Regulation of telomerase by telomeric proteins." Annu Rev Biochem **73**: 177-208.

Sobol, R. W., M. Kartalou, K. H. Almeida, D. F. Joyce, B. P. Engelward, J. K. Horton, R. Prasad, L. D. Samson and S. H. Wilson (2003). "Base excision repair intermediates induce p53-independent cytotoxic and genotoxic responses." J Biol Chem **278**(41): 39951-39959.

Song, B. and P. Sung (2000). "Functional interactions among yeast Rad51 recombinase, Rad52 mediator, and replication protein A in DNA strand exchange." J Biol Chem **275**(21): 15895-15904.

Soulas-Sprauel, P., P. Rivera-Munoz, L. Malivert, G. Le Guyader, V. Abramowski, P. Revy and J. P. de Villartay (2007). "V(D)J and immunoglobulin class switch recombinations: a paradigm to study the regulation of DNA end-joining." Oncogene **26**(56): 7780-7791.

Soutoglou, E., J. F. Dorn, K. Sengupta, M. Jasin, A. Nussenzweig, T. Ried, G. Danuser and T. Misteli (2007). "Positional stability of single double-strand breaks in mammalian cells." Nat Cell Biol **9**(6): 675-682.

Stephens, P. J., C. D. Greenman, B. Fu, F. Yang, G. R. Bignell, L. J. Mudie, E. D. Pleasance, K. W. Lau, D. Beare, L. A. Stebbings, S. McLaren, M. L. Lin, D. J. McBride, I. Varela, S. Nik-Zainal, C. Leroy, M. Jia, A. Menzies, A. P. Butler, J. W. Teague, M. A. Quail, J. Burton, H. Swerdlow, N. P. Carter, L. A. Morsberger, C. Iacobuzio-Donahue, G. A. Follows, A. R. Green, A. M. Flanagan, M. R. Stratton, P. A. Futreal and P. J. Campbell (2011). "Massive genomic rearrangement acquired in a single catastrophic event during cancer development." Cell **144**(1): 27-40.

Stirling, P. C., Y. A. Chan, S. W. Minaker, M. J. Aristizabal, I. Barrett, P. Sipahimalani, M. S. Kobor and P. Hieter (2012). "R-loop-mediated genome instability in mRNA cleavage and polyadenylation mutants." Genes Dev **26**(2): 163-175.

Stros, M., D. Launholt and K. D. Grasser (2007). "The HMG-box: a versatile protein domain occurring in a wide variety of DNA-binding proteins." Cell Mol Life Sci **64**(19-20): 2590-2606.

Su, T. T. (2006). "Cellular responses to DNA damage: one signal, multiple choices." Annu Rev Genet **40**: 187-208.

Sugawara, N., X. Wang and J. E. Haber (2003). "In vivo roles of Rad52, Rad54, and Rad55 proteins in Rad51-mediated recombination." Mol Cell **12**(1): 209-219.

Sung, P. (1997). "Function of yeast Rad52 protein as a mediator between replication protein A and the Rad51 recombinase." J Biol Chem **272**(45): 28194-28197.

Sung, P. (1997). "Yeast Rad55 and Rad57 proteins form a heterodimer that functions with replication protein A to promote DNA strand exchange by Rad51 recombinase." Genes Dev **11**(9): 1111-1121.

Sung, P. and H. Klein (2006). "Mechanism of homologous recombination: mediators and helicases take on regulatory functions." Nat Rev Mol Cell Biol **7**(10): 739-750.

Svejstrup, J. Q., K. Christiansen, Gromova, II, A. H. Andersen and O. Westergaard (1991). "New technique for uncoupling the cleavage and religation reactions of eukaryotic topoisomerase I. The mode of action of camptothecin at a specific recognition site." J Mol Biol **222**(3): 669-678.

Svendsen, J. M. and J. W. Harper (2010). "GEN1/Yen1 and the SLX4 complex: Solutions to the problem of Holliday junction resolution." Genes Dev **24**(6): 521-536.

Symington, L. S. (1998). "Homologous recombination is required for the viability of rad27 mutants." Nucleic Acids Res **26**(24): 5589-5595.

Tatum, D., W. Li, M. Placer and S. Li (2011). "Diverse roles of RNA polymerase II-associated factor 1 complex in different subpathways of nucleotide excision repair." J Biol Chem **286**(35): 30304-30313.

Taub, R., I. Kirsch, C. Morton, G. Lenoir, D. Swan, S. Tronick, S. Aaronson and P. Leder (1982). "Translocation of the c-myc gene into the immunoglobulin heavy chain locus in human Burkitt lymphoma and murine plasmacytoma cells." Proc Natl Acad Sci U S A **79**(24): 7837-7841.

Tercero, J. A. and J. F. Diffley (2001). "Regulation of DNA replication fork progression through damaged DNA by the Mec1/Rad53 checkpoint." Nature **412**(6846): 553-557.

Tinline-Purvis, H., A. P. Savory, J. K. Cullen, A. Dave, J. Moss, W. L. Bridge, S. Marguerat, J. Bahler, J. Ragoussis, R. Mott, C. A. Walker and T. C. Humphrey (2009). "Failed gene conversion leads to extensive end processing and chromosomal rearrangements in fission yeast." EMBO J **28**(21): 3400-3412.

Toczyski, D. P. (2006). "Methods for studying adaptation to the DNA damage checkpoint in yeast." Methods Enzymol **409**: 150-165.

Tomson, B. N. and K. M. Arndt (2013). "The many roles of the conserved eukaryotic Paf1 complex in regulating transcription, histone modifications, and disease states." Biochim Biophys Acta **1829**(1): 116-126.

Tsukuda, T., A. B. Fleming, J. A. Nickoloff and M. A. Osley (2005). "Chromatin remodelling at a DNA double-strand break site in Saccharomyces cerevisiae." Nature **438**(7066): 379-383.

Tuteja, G. and K. H. Kaestner (2007). "Forkhead transcription factors II." Cell **131**(1): 192.

Uziel, T., Y. Lerenthal, L. Moyal, Y. Andegeko, L. Mittelman and Y. Shiloh (2003). "Requirement of the MRN complex for ATM activation by DNA damage." EMBO J **22**(20): 5612-5621.

van Attikum, H. and S. M. Gasser (2005). "ATP-dependent chromatin remodeling and DNA double-strand break repair." Cell Cycle **4**(8): 1011-1014.

van der Horst, A. and B. M. Burgering (2007). "Stressing the role of FoxO proteins in lifespan and disease." Nat Rev Mol Cell Biol **8**(6): 440-450.

Ventura, A. and T. Jacks (2009). "MicroRNAs and cancer: short RNAs go a long way." Cell **136**(4): 586-591.

Verdel, A., S. Jia, S. Gerber, T. Sugiyama, S. Gygi, S. I. Grewal and D. Moazed (2004). "RNAi-mediated targeting of heterochromatin by the RITS complex." Science **303**(5658): 672-676.

Verdin, H., B. D'Haene, D. Beysen, Y. Novikova, B. Menten, T. Sante, P. Lapunzina, J. Nevado, C. M. Carvalho, J. R. Lupski and E. De Baere (2013). "Microhomology-mediated mechanisms underlie non-recurrent disease-causing microdeletions of the FOXL2 gene or its regulatory domain." PLoS Genet **9**(3): e1003358.

Verdun, R. E. and J. Karlseder (2006). "The DNA damage machinery and homologous recombination pathway act consecutively to protect human telomeres." Cell **127**(4): 709-720.

Volpe, T. A., C. Kidner, I. M. Hall, G. Teng, S. I. Grewal and R. A. Martienssen (2002). "Regulation of heterochromatic silencing and histone H3 lysine-9 methylation by RNAi." Science **297**(5588): 1833-1837.

Wade, P. A., W. Werel, R. C. Fentzke, N. E. Thompson, J. F. Leykam, R. R. Burgess, J. A. Jaehning and Z. F. Burton (1996). "A novel collection of accessory factors associated with yeast RNA polymerase II." Protein Expr Purif **8**(1): 85-90.

Wahba, L., J. D. Amon, D. Koshland and M. Vuica-Ross (2011). "RNase H and multiple RNA biogenesis factors cooperate to prevent RNA:DNA hybrids from generating genome instability." Molecular cell **44**(6): 978-988.

Wahba, L., S. K. Gore and D. Koshland (2013). "The homologous recombination machinery modulates the formation of RNA-DNA hybrids and associated chromosome instability." Elife **2**: e00505.

Wahba, L. and D. Koshland (2013). "The Rs of biology: R-loops and the regulation of regulators." Mol Cell **50**(5): 611-612.

Wan, S., H. Capasso and N. C. Walworth (1999). "The topoisomerase I poison camptothecin generates a Chk1-dependent DNA damage checkpoint signal in fission yeast." Yeast **15**(10A): 821-828.

Wang, X. and P. Baumann (2008). "Chromosome fusions following telomere loss are mediated by single-strand annealing." Mol Cell **31**(4): 463-473.

Wei, W., Z. Ba, M. Gao, Y. Wu, Y. Ma, S. Amiard, C. I. White, J. M. Rendtlew Danielsen, Y. G. Yang and Y. Qi (2012). "A role for small RNAs in DNA double-strand break repair." Cell **149**(1): 101-112.

Weinstock, D. M., E. Brunet and M. Jasin (2007). "Formation of NHEJ-derived reciprocal chromosomal translocations does not require Ku70." Nat Cell Biol **9**(8): 978-981.

Weiss, R. S., S. Matsuoka, S. J. Elledge and P. Leder (2002). "Hus1 acts upstream of chk1 in a mammalian DNA damage response pathway." Curr Biol **12**(1): 73-77.

Wheeler, B. S., J. A. Blau, H. F. Willard and K. C. Scott (2009). "The impact of local genome sequence on defining heterochromatin domains." PLoS Genet **5**(4): e1000453.

Whitehall, S., P. Stacey, K. Dawson and N. Jones (1999). "Cell cycle-regulated transcription in fission yeast: Cdc10-Res protein interactions during the cell cycle and domains required for regulated transcription." Mol Biol Cell **10**(11): 3705-3715.

Wold, M. S. (1997). "Replication protein A: a heterotrimeric, single-stranded DNA-binding protein required for eukaryotic DNA metabolism." Annu Rev Biochem **66**: 61-92.

Wu, L. and I. D. Hickson (2006). "DNA helicases required for homologous recombination and repair of damaged replication forks." Annu Rev Genet **40**: 279-306.

Wysocki, R., A. Javaheri, S. Allard, F. Sha, J. Cote and S. J. Kron (2005). "Role of Dot1-dependent histone H3 methylation in G1 and S phase DNA damage checkpoint functions of Rad9." Mol Cell Biol **25**(19): 8430-8443.

Yang, X. H. and L. Zou (2006). "Recruitment of ATR-ATRIP, Rad17, and 9-1-1 complexes to DNA damage." Methods Enzymol **409**: 118-131.

Yarbro, J. W. (1992). "Mechanism of action of hydroxyurea." Semin Oncol **19**(3 Suppl 9): 1-10.

Yonemasu, R., M. Minami, Y. Nakatsu, M. Takeuchi, I. Kuraoka, Y. Matsuda, Y. Higashi, H. Kondoh and K. Tanaka (2005). "Disruption of mouse XAB2 gene involved in pre-mRNA splicing, transcription and transcription-coupled DNA repair results in preimplantation lethality." DNA Repair (Amst) **4**(4): 479-491.

You, Z., L. Kong and J. Newport (2002). "The role of single-stranded DNA and polymerase alpha in establishing the ATR, Hus1 DNA replication checkpoint." J Biol Chem **277**(30): 27088-27093.

Yuce, O. and S. C. West (2013). "Senataxin, defective in the neurodegenerative disorder ataxia with oculomotor apraxia 2, lies at the interface of transcription and the DNA damage response." Mol Cell Biol **33**(2): 406-417.

Zaratiegui, M., S. E. Castel, D. V. Irvine, A. Kloc, J. Ren, F. Li, E. de Castro, L. Marin, A. Y. Chang, D. Goto, W. Z. Cande, F. Antequera, B. Arcangioli and R. A. Martienssen (2011). "RNAi promotes heterochromatic silencing through replication-coupled release of RNA Pol II." Nature **479**(7371): 135-138.

Zeng, Y., K. C. Forbes, Z. Wu, S. Moreno, H. Piwnica-Worms and T. Enoch (1998). "Replication checkpoint requires phosphorylation of the phosphatase Cdc25 by Cds1 or Chk1." Nature **395**(6701): 507-510.

Zeng, Y. and H. Piwnica-Worms (1999). "DNA damage and replication checkpoints in fission yeast require nuclear exclusion of the Cdc25 phosphatase via 14-3-3 binding." Mol Cell Biol **19**(11): 7410-7419.

Zhang, F., M. Khajavi, A. M. Connolly, C. F. Towne, S. D. Batish and J. R. Lupski (2009). "The DNA replication FoSTeS/MMBIR mechanism can generate genomic, genic and exonic complex rearrangements in humans." Nat Genet **41**(7): 849-853.

Zhao, H. and H. Piwnica-Worms (2001). "ATR-mediated checkpoint pathways regulate phosphorylation and activation of human Chk1." Mol Cell Biol **21**(13): 4129-4139.

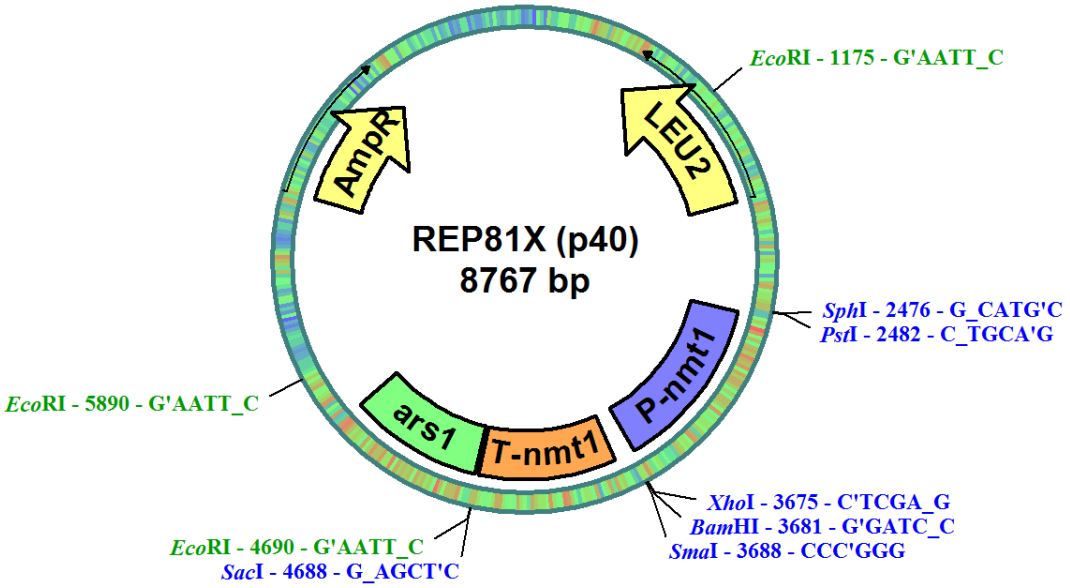
Zhou, B. B. and S. J. Elledge (2000). "The DNA damage response: putting checkpoints in perspective." Nature **408**(6811): 433-439.

Zhou, Y., L. Chen, B. Barlogie, O. Stephens, X. Wu, D. R. Williams, M. A. Cartron, F. van Rhee, B. Nair, S. Waheed, M. Pineda-Roman, Y. Alsayed, E. Anaissie and J. D. Shaughnessy, Jr. (2010). "High-risk myeloma is associated with global elevation of miRNAs and overexpression of EIF2C2/AGO2." Proc Natl Acad Sci U S A **107**(17): 7904-7909.

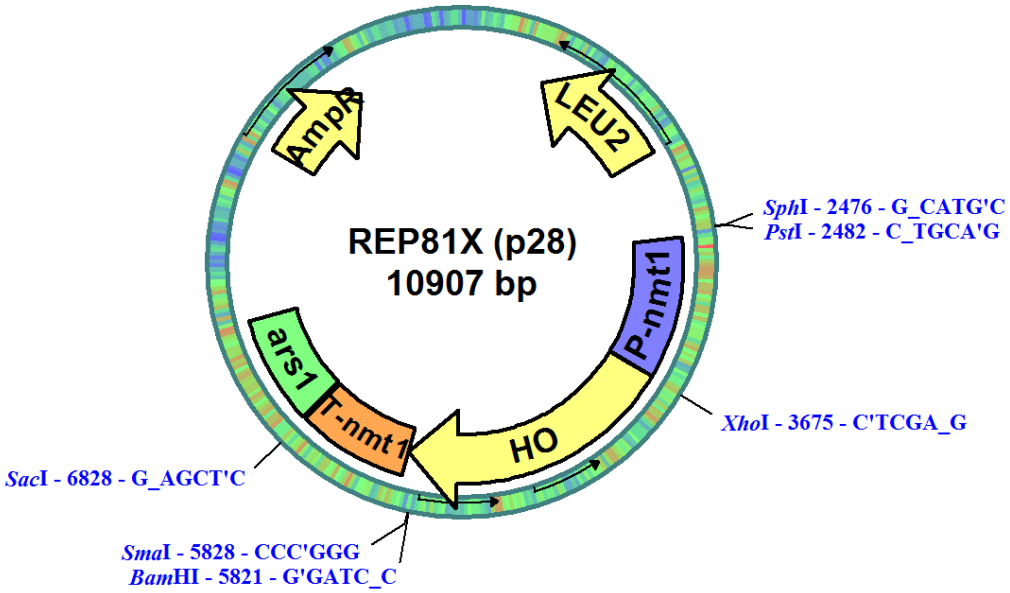
Zhu, Y., T. Takeda, S. Whitehall, N. Peat and N. Jones (1997). "Functional characterization of the fission yeast Start-specific transcription factor Res2." EMBO J **16**(5): 1023-1034.

Zou, L., D. Cortez and S. J. Elledge (2002). "Regulation of ATR substrate selection by Rad17-dependent loading of Rad9 complexes onto chromatin." Genes Dev **16**(2): 198-208.

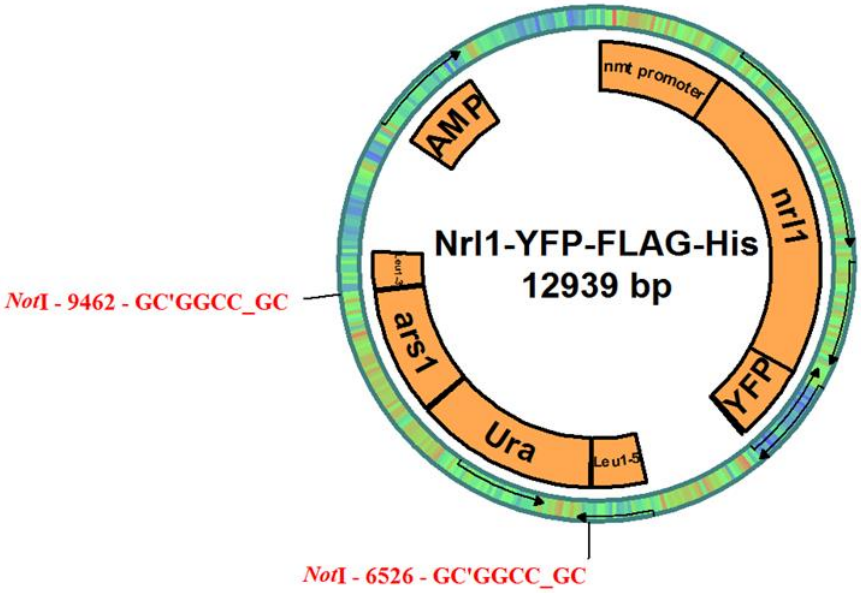
Appendix I: Plasmids used in this study



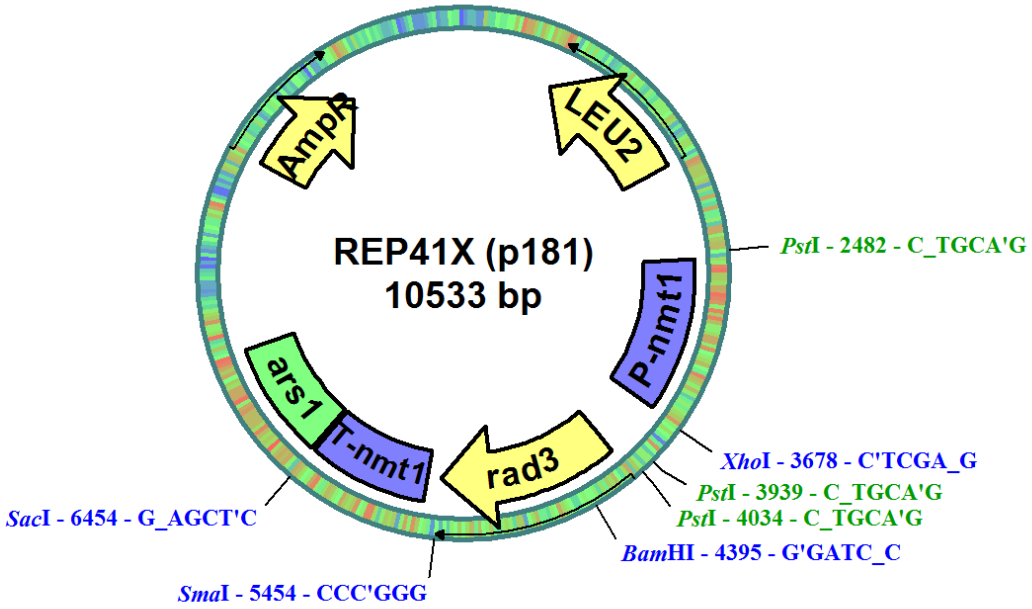
pREP81X (p40); this *LEU2* multi-copy plasmid contains the thiamine-repressible *nmt* promoter. A kind gift from Fekret Osman (Osman et al., 1996).



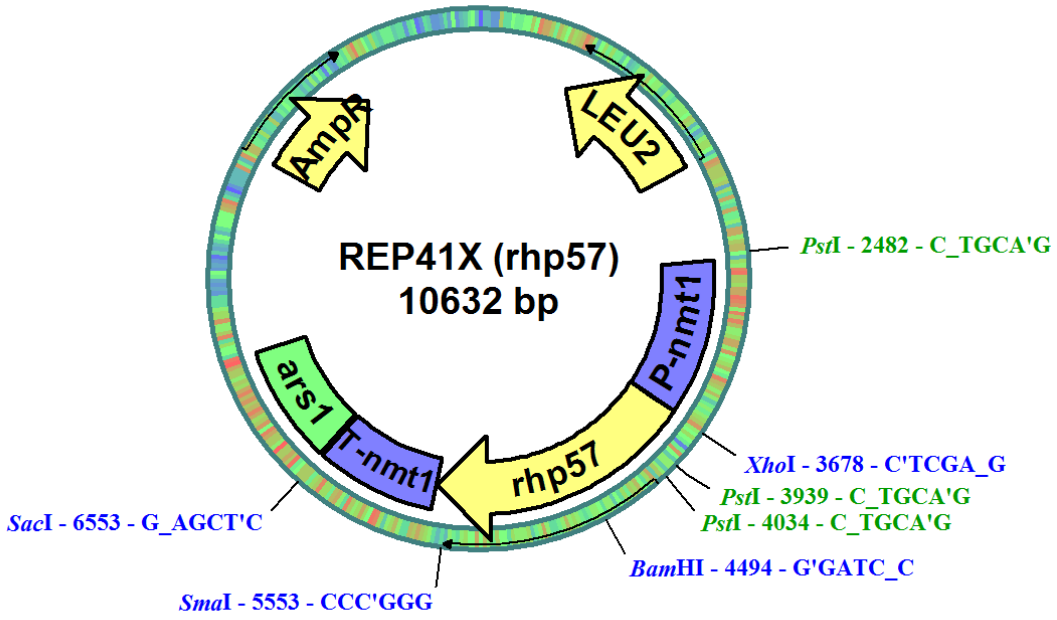
pREP81X-*HO* (p28) contains the *S. cerevisiae* HO-endonuclease ORF under control of the thiamine repressible-*nmt* promoter. A kind gift from Fekret Osman (Osman et al., 1996).



SpYFH47G01 (Nrl1-YFP) contains the Nrl1 ORF under control of the thiamine-repressible-*nmt* promoter. Purchased from RIKEN BioResource Center (http://dna.brc.riken.jp/index.html).



pREP41X-*HO* (p181) contains Rad3 ORF under control of the thiamine repressible-*nmt* promoter. (Helen Tinline-Purvis)



pREP41X-*HO* (prhp57) contains Rad57 ORF under control of the thiamine repressible-*nmt* promoter.

Appendix II Oligonucleotide primers used in this study

Systematic Name	Gene	Primer- F	Primer- R
SPBC16G5.15c	*fkh2*	CGTGAGTAA ACAGTTGAGC G	
SPBC29A10.05	*exo1*	CCAGTAACGC AGTTACGCTT	
SPBC11B10.10c	*pht1*	TG ACATAGGATT TTGTTCAAGA	
SPBC342.01c	*alg6*	AATGGGCTAG TATCACTGAA AC	
SPAC9E9.09c		GTAGAACAGC ACGGTCTTTT	
SPBC215.03c	*csn1*	G TCATTGGGAG GACAAAGTAG	
SPAC17C9.15c		C CAAGCGTTTG ATTGTTAATC	
SPAC23C11.02c	*rps23*	GGATGGGACT TGTAGATGG	
SPAC13G7.07	*Arb2*	GGCTCGGAA TTTATAAGTT CAG	
SPBC20F10.05	*nrl1*	GCT TAAATATTAC ACACCAAACC	
SPAC57A7.04c	*pabp*	GACTA AATATCTTGG AAGTATTCC	
SPBC2G2.03c	*sbh1*	CAGTTATTGA CATTTCTCAG TGAT	
SPAC1556.05c	*cgr1*	GCTAATGGCA TGGGATTC	
SPAC22F3.09c	*res2*	AAGCAAGACA GCGTGGTC	
SPBC660.14	*mik1*	C TTGGAGAATT GGATTAGGAG	
SPBC2D10.13	*est1*	GAGTACAGGG TTGCTCCGAG	
SPBC30D10.04	*swi3*	TGTAACATGA GCCTTCTGAA	
SPAC664.03	*paf1*	AACATCCATA ATGATGCATG	
SPAC1556.01c	*rad50*	CTAGTATTTG TAATCCTTGG GC	
SPBC119.14	*rad22*	GAGGCACGAT CAAGTTCCTA	
SPAC2G11.12	*rqh1*	ATACCTCGAA AGCACAGGTG	
SPBC336.01	*fbh1*	ACGTGGCATTT ATAGTGTCTA A	
SPAC16C9.05	*cph1*	GCTCCATGT TCCATCAAAT	
SPCC1919.15	*brl1*	G CCTCGAACAA ACTTAGTTATT	
SPAC1D4.06c	*csk1*	CATCATGCGA GATCACAGTT	
SPBC16C6.02c	*vps1302*	CGTTCACG TCATGCTCTG	
SPBC660.09	*mug168*	TGGCGAGCC ATCCTTAAT	
SPBC3D6.10	*apn2*	GCATTTTATT TTCCATCAGAT	
SPCC126.07c		AACCGTCGTA CGACCGTAC	
SPAC521.04c		GAAGGTTGAC GACCCAACTC	
SPAC2G11.13	*atg22*	GGCTCAGT TCCTAAGCGT	
SPBC3E7.08c	*rad13*	AGACGTCTCG TTCACCAATG	
SPAC140.03	*Arb1*	GGTTGCGATTA TTTTAAGCAA	
SPCC736.11	*Ago1*	GCGTGCTCAG AGAAGTATAGA	
SPBC23E6.09	*ssn6*	CCGCTCAA CCCAAGTACA	
SPBC119.08	*pmk1*	CGCTCAA CCCAAGTACA AA	
SPBC18H10.19	*atg14*	GGACGAGGTTC AGTTGTTCTC	
SPBC1778.02	*rap1*	AACCGATTGTA AATTGCATAT	
SPBC216.05	*rad3_1*	AAGATGCCCTCACCAAT	CCACTTTAAGAATAATTTGACAAG
SPBC216.05	*rad3_2*	GGGTAGCATATTTTACCAATACC	CCCTGGCATAAAGCCTTG
SPAC20H4.07	*rhp57*	GTAGTCAAAGTGAGTTATTACA	CTTATCAGCTTTGGGATACC
SPAC14C4.13	*rad17*	GCGACAGTTGTCGTTTCAT	CCTCTTTACGTAGAATAGAGCC
SPBC20F10.05	*nrl1 clone*	GAGGTTAGATACGCTATTGG	CAATCAATTTTGTGCATACTC

Appendix III: Genetic determinants of site-specific DSB-induced marker loss

Genetic background	NHEJ/ Uncut	p value	GC	p value	LOH	p value	Ch Loss	p value	Sp. loss
wt RMYAH	6 ± 0.75	-	73 ± 0.58	-	5.5 ± 0.5	-	15 ± 0.7	-	
wt RMGAH	21 ± 2.61	-	53 ± 3.2	-	10 ± 1.6	-	16 ± 3.5	-	
*atg22*Δ	7 ± 2	0.38	76 ± 2.6	0.12	5 ± 1.6	0.63	11 ± 0.6	0.01	
*mik1*Δ	9 ± 2.2	0.27	66 ± 6.9	0.15	6 ± 2.2	0.72	19 ± 3	0.08	
*csk1*Δ	10 ± 6.1	0.09	74 ± 4.9	0.74	8 ± 0.7	0.01	9 ± 0.3	<0.01	
*pht1*Δ	8 ± 3.5	0.65	75 ± 4.7	0.5	4 ± 1	0.08	11 ± 0.6	0.01	
*cph1*Δ	15 ± 5.1	0.05	76 ± 2.2	0.08	1 ± 3.4	0.08	7 ± 4.4	0.03	
*exo1*Δ	12 ± 5.5	0.19	57 ± 7.5	0.02	10 ± 2	0.01	21 ± 1	<0.01	
*apn2*Δ	9 ± 5.7	0.54	74 ± 2.7	0.56	5 ± 1.2	0.54	13 ± 5.9	0.59	
*rad13*Δ	5 ± 0.4	<0.01	70 ± 2.2	0.08	11 ± 2	0.01	14 ± 2.1	0.47	
*rad50*Δ	7 ± 0.58	1	71 ± 2.6	0.26	10 ± 1.2	0	11 ± 3.2	0.1	
*rad22*Δ	14 ± 4.2	0.04	28 ± 3.1	<0.01	3 ± 3.1	0.24	55 ± 3.6	<0.01	
*rqh1*Δ	43 ± 6	<0.01	19 ± 6	<0.01	5 ± 5	0.87	33 ± 1.5	<0.01	
*fbh1*Δ	8 ± 2	0.65	89 ± 2.3	<0.01	3 ± 0.3	<0.01	0 ± 0	<0.01	
*csn1*Δ	9. ± 0.9	0.01	67 ± 3.1	0.03	5 ± 3.1	0.79	18 ± 5.9	0.43	
*SPCC126.07c*Δ	7 ± 2.6	0.85	65 ± 3.2	0.01	8 ± 0.6	<0.01	20 ± 4.9	0.15	
*alg6*Δ	9 ± 1	0.07	60 ± 0.5	<0.01	6 ± 0.6	0.32	24 ± 1.1	<0.01	
*atd1*Δ	22 ± 0.57	<0.01	52 ± 0.58	<0.01	3 ± 1.1	0.02	23 ± 1	<0.01	
*SPAC521.04c*Δ	5 ± 0.4	0.02	70 ± 2.3	0.09	11 ± 2.1	0.01	14 ± 2.1	0.47	
*swi3*Δ	10 ± 2.3	0.12	63 ± 2.3	<0.01	15 ± 4.4	0.02	12 ± 3.1	0.17	
*rps23*Δ	7 ± 4.4	0.79	77 ± 6	0.31	8 ± 1	0.01	9 ± 1.3	0.01	
*cgr1*Δ	5 ± 2.1	0.09	65 ± 6	0.08	6 ± 1.1	0.51	25 ± 4.9	<0.01	
*arb2*Δ	11 ± 4.5	0.22	42 ± 5.1	<0.01	14.7 ± 4	0.07	23 ± 2.5	<0.01	11
*nrl1*Δ	5 ± 1.3	0.05	50 ± 3.5	<0.01	14 ± 2	<0.01	30 ± 3.2	<0.01	
*ago1*Δ	4 ± 0.5	<0.01	56 ± 1.7	<0.01	7 ± 1.9	0.25	33 ± 1.15	<0.01	
*est1*Δ	7 ± 1	0.89	55 ± 6.2	<0.01	7 ± 3	0.44	23 ± 3.8	<0.01	8

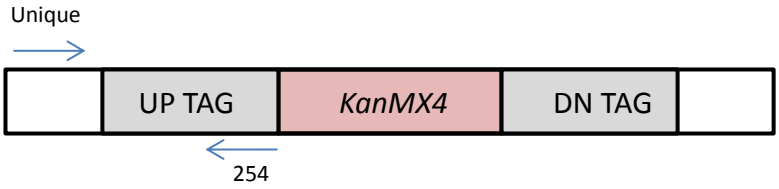
Genetic background	NHEJ/ Uncut	p value	GC	p value	LOH	p value	Ch Loss	p value	Sp. loss
*fkh2*Δ	42 ± 8.5	<0.01	21 ± 4.5	<0.01	16 ± 1.2	<0.01	20 ± 3.1	0.05	
*res2*Δ	14 ± 0.6	<0.01	58 ± 2.5	<0.01	5 ± 1.2	0.54	23 ± 3.5	<0.01	
*paf1*Δ	6 ± 1	0.28	53 ± 1	<0.01	14 ± 1.8	<0.01	27 ± 1	<0.01	
*sbh1*Δ	5 ± 0.9	0.21	69 ± 1.7	0.02	6 ± 0.8	0.41	19 ± 1.8	0.02	
*mug168*Δ	8 ± 1	0.38	62 ± 7.2	0.05	7 ± 3.8	0.53	23 ± 4.1	<0.01	
*pmk1*Δ	5 ± 1.1	0.03	72 ± 1.1	0.24	8 ± 1.6	0.06	15 ± 0.7	<0.01	
*rtt109*Δ	12 ± 1.4	0.01	67 ± 0.1	<0.01	8 ± 3.4	0.27	13 ± 4.7	0.73	
*swi6*Δ	8 ± 2.6	0.26	61 ± 0.4	<0.01	10.2 ± 1	<0.01	18 ± 1.67	0.03	4.8
*arb1*Δ	6 ± 1.1	1	75 ± 1	0.04	7 ± 1.3	0.13	12 ± 0.5	<0.01	
*L5-rad17*Δ[a]	11 ± 2.2	0.14	35 ± 3.5	0.68	52 ± 2.7	0.8	1 ± 2.2	0.29	
wt L5[b]	19 ± 2.1	0.36	49 ± 3.3	0.2	15 ± 2.7	0.05	17 ± 1.9	0.69	
loh-2	27 ± 3.6	0.08	2 ± 0.67	<0.01	40 ± 1.65	<0.01	28 ± 4.83	<0.01	
loh-5	22 ± 4.3	0.75	13 ± 4.23	<0.01	28 ± 6.04	<0.01	34 ± 6	<0.01	
loh-6	8 ± 1.7	<0.01	34 ± 1.8	<0.01	53 ± 6.82	<0.01	4 ± 3.56	<0.01	
loh-7	20 ± 0.98	0.56	19 ± 0.37	<0.01	29 ± 2.24	<0.01	31 ± 2.65	<0.01	
*dcr1*Δ	13 ± 1.7	<0.01	71 ± 2.5	0.25	6.3 ± 1.7	0.49	9 ± 1.2	<0.01	

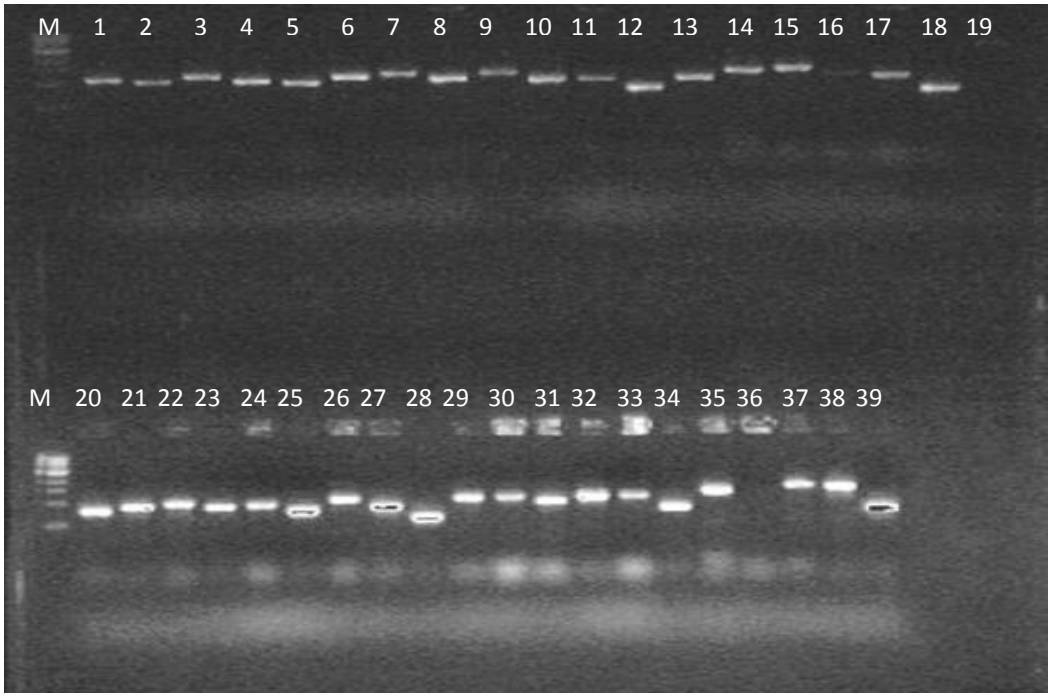
For each genetic background the assay was repeated three times, to score >600 colonies. Mean ± the standard deviation of the 3 experiments are shown. A single blank vector control was also analysed in each genetic background to give a spontaneous level of Ch_{16} loss, which was subtracted to calculate the break-induced values shown above. P values are calculated against wild-type Ch_{16}-RMYAH unless otherwise stated:

[a] compared to *loh-6* Ch_{16}-RMYAH,

[b] compared to wild-type Ch_{16}-RMYAH,

Appendix IV: Confirmation of deletion library mutant identities

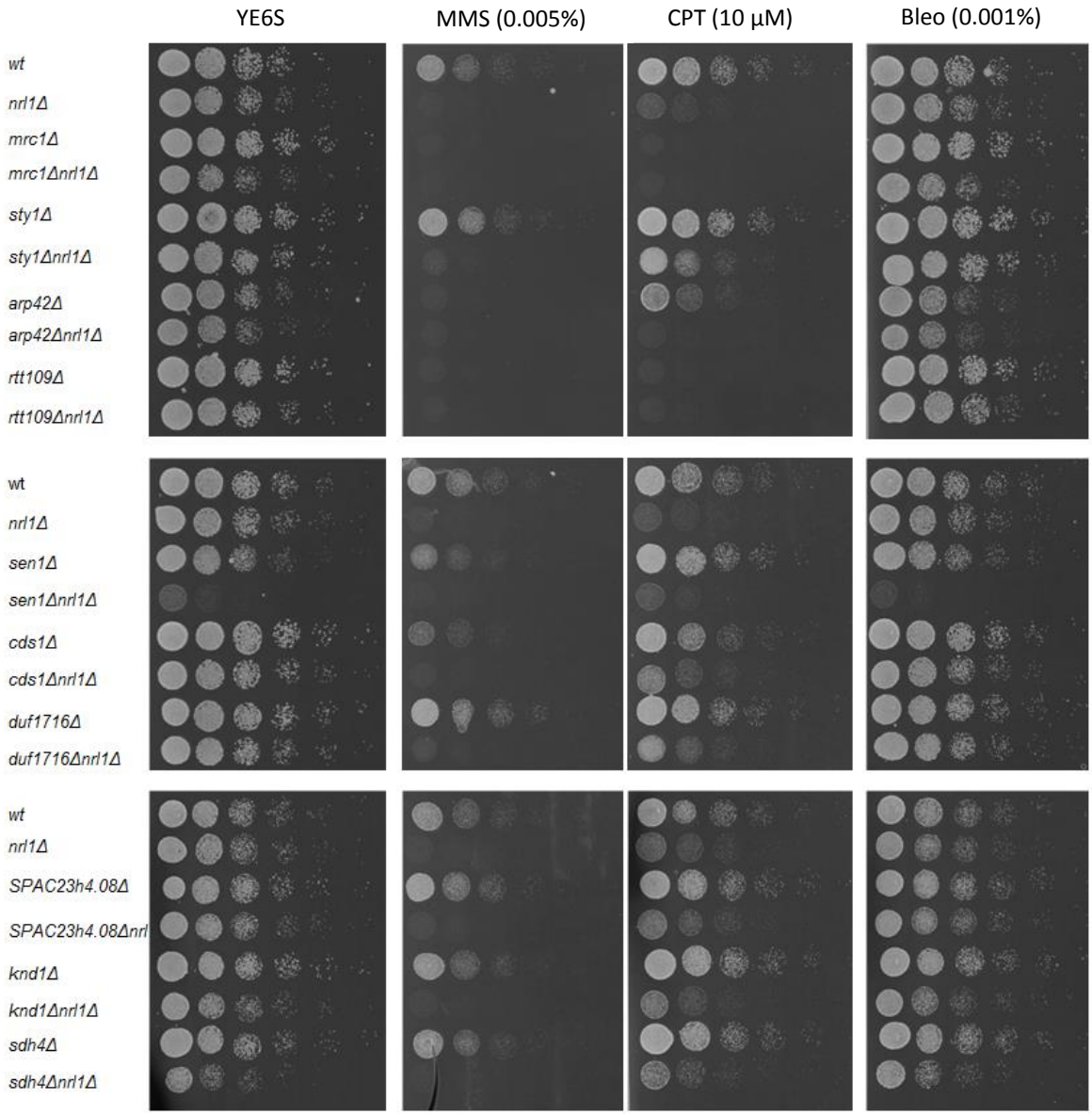




PCR	Gene	PCR	Gene	PCR	Gene
1	*pht1*	14	*res2*	27	*mug168*
2	*alg6*	15	*mik1*	28	*apn2*
3	*csn1*	16	*est1*	29	*SPCC126.07c*
4	*SPAC17C9.15c*	17	*paf1*	30	*SPAC521.04c*
6	*fkh2*	18	*rad50*	31	*atg22*
5	*rps23*	19	*cgr1*	32	*rad13*
7	*exo1*	20	*rad22*	33	*Arb1*
8	*SPAC9E9.09c*	21	*rqh1*	34	*Ago1*
9	*Arb2*	22	*fbh1*	35	*ssn6*
10	*nrl1*	23	*cph1*	36	*pmk1*
11	*pabp*	24	*brl1*	37	*atg14*
12	*sbh1*	25	*csk1*	38	*rap1*
13	*swi3*	26	*vps1302*	39	*mcl1*

PCR was carried out with forward primers specific to the flanking sequence of the gene deletion; reverse primer was specific to the deletion cassette.

Appendix V: Nrl1 epistasis analysis



Epistasis analysis of Nrl1 with a selection of predicted interactors.

Appendix VI: List of publications

Torben R. Kasparek, Timothy C. Humphrey, DNA double-strand break repair pathways, chromosomal rearrangements and cancer, Seminars in Cell & Developmental Biology, Volume 22, Issue 8, October 2011, Pages 886-897, ISSN 1084-9521, http://dx.doi.org/10.1016/j.semcdb.2011.10.007.
(http://www.sciencedirect.com/science/article/pii/S1084952111001868)

Helen Tinline-Purvis, Elizabeth J. Blaikley, **Torben R. Kasparek**, Samuel Marguerat, Lydia Hulme, Sharon Hussey, Boon-Yu Wee, Rachel S. Deegan, Carol A. Walker, Chen-Chun Pai, Jürg Bähler, Takuro Nakagawa, and Timothy C. Humphrey, The DNA damage checkpoint pathway promotes extensive resection and nucleotide synthesis to facilitate homologous recombination repair and genome stability in fission yeast (s*ubmitted*).

Torben R. Kasparek et *al.*, (manuscript in preparation).